IMPROVEMENT OF GEOTECHNICAL SITE INVESTIGATIONS VIA STATISTICAL ANALYSES AND SIMULATION

A Dissertation
Presented to
The Academic Faculty

by

Jong Hee Kim

In Partial Fulfillment
of the Requirements for the Degree
Doctor of Philosophy in the
School of Civil and Environmental Engineering

Georgia Institute of Technology
August 2011

IMPROVEMENT OF GEOTECHNICAL SITE INVESTIGATIONS VIA STATISTICAL ANALYSES AND SIMULATION

Approved by:

Dr. Glenn J. Rix, Advisor
School of Civil & Environmental Engineering
Georgia Institute of Technology

Dr. Paul W. Mayne
School of Civil & Environmental Engineering
Georgia Institute of Technology

Dr. J. Carlos Santamarina
School of Civil & Environmental Engineering
Georgia Institute of Technology

Dr. Seong-Hee Kim
School of Industrial & Systems Engineering
Georgia Institute of Technology

Dr. Nelson C. Baker
School of Civil & Environmental Engineering
Georgia Institute of Technology

Date Approved: July 07, 2011

ACKNOWLEDGMENTS

Among many peoples who have been helpful in the preparation of this dissertation, I am especially thankful to Dr. Glenn J. Rix. If he had not served as my advisor and had not encouraged me throughout this dissertation process, this dissertation could not have been completed. I thank him for providing me with the opportunity to pursue this research.

I wish to express my sincere gratitude to the following committee members for providing guidance and suggestions for me to prepare this dissertation: Dr. J. Carlos Santamarina, Dr. Nelson C. Baker, Dr. Paul W. Mayne, and Dr. Seong-Hee Kim.

I would also like to warmly acknowledge Dr. Lee Young for his editing and recommendations.

I would like to extend a hearty thanks to my friends: Jong Wan Hu, Duhwan Kim, Dongha Kim, Sihyun Kim, Xiyan Zhang, Bo Gao, Jiewu Meng, Miguel Roca, Robert Young, Hosung Shin, Sungsoo Yoon, Jongwon Choi, Hyunki Kim, and Alec McGillvray. In particular, a special thanks to Wonyong Jang.

Mr. Jim Sailors and my companions, Lee Schuman, Mike Federer, Nick Rudolph, and Greg Webb, in Sailors Engineering Associates are specially appreciated for their consideration and friendship.

I dedicate this dissertation to my parents and in-law, my wife, Minhye Lee, and the remainder of my family. You all were always on my side with your unconditional love and support in whichever situations I faced.

TABLE OF CONTENTS

LIST OF TABLES

LIST OF FIGURES

SUMMARY

The purpose of this study is to improve site investigation in geotechnical engineering via the evaluation and development of statistical approaches for characterizing the spatial variability of soil properties and the development of site investigation simulation software for educational use.

This study consists of four components: statistical characteristics, data measurement, simulation, and educational training. Statistical measures of spatial variability of soil properties were examined for three different geographical areas where soil formation processes differ to assess the influence on the spatial variability of soils. Statistical measures of spatial variability were also calculated for a case history where blasting was used as a method of soil improvement to evaluate the effects of man-made changes to soil structure.

The concept of spatial aliasing was employed to estimate the maximum allowable sampling interval for field data as a function of the spatial correlation properties. Once a maximum statistically allowable sampling interval is determined for a specific soil property, the minimum statistically required number of soundings / borings is calculated to perform an economical site investigation at a specific site.

A simple and efficient simulation technique was proposed to generate correlated, multi-dimensional simulations of soil properties. Based on limited data, the proposed simulation technique generated accurate and correlated simulations of soil properties that are consistent with the observed or proposed correlation structures of soil properties.

Lastly, a geotechnical site investigation simulation program with a wide variety of in situ and laboratory tests was developed to allow students to plan and perform a comprehensive site investigation program. The simulation generates an input file based partly on the statistical characteristics of the spatial variability of soil properties analyzed in this study and partly on traditional values. Spatial variability in soil properties is modeled via correlated random fields, interpolation, and a decomposition method to yield realistic geotechnical data. Via the simulation, students are able to obtain experience and judgment in an essential component of geotechnical engineering practice.

The four components of this research (statistical characteristics, data measurement, simulation, and educational training) focus on the improvement of site investigation performance in geotechnical engineering, thereby improving reliability analysis in geotechnical practice.

CHAPTER 1

INTRODUCTION

1.1. Objectives of study

In geotechnical engineering practice, the determination of soil properties at a specific site depends on tests performed in the laboratory based on a limited number of field specimens, as well as tests performed in the field. As the constrained budget of a typical construction project results in limitations on the ability to acquire data, the exact spatial variability of soil properties remain largely undetermined. In actuality, geotechnical design has traditionally been based on a deterministic (or trend-based) approach associated with the identification of soil types and the use of representative soil properties regardless of the spatial variability within each soil layer. The simplified estimates of soil properties do not sufficiently supply valuable information for performing reliability analysis in geotechnical practice In this dissertation, the statistical characteristics of spatial variability were more closely examined based on stochastic (or statistics-based) methods.

Soils are heterogeneous materials generated by natural geologic, environmental, and physical-chemical processes, all of which have an influence on the properties of in situ soil. In other words, the properties of in situ soil undergo changes over both time and space. Thus, measured soil properties can present considerable spatial variation even within relatively homogeneous layers (i.e., the same soil type). The use of statistical

analyses allows one to determine the spatial variability of soil property from a data set in a more logical and accurate manner than otherwise determined. Moreover, statistical analysis allows designers to rely more heavily on stochastic methods for geotechnical design. When dealing with various uncertainties related to soil properties, the use of stochastic methods makes better geotechnical designs possible by virtue of accurately assessing the influence of spatial variability of various soil properties on structure behavior, and achievable through the use of spatial statistical structures such as trend and correlation structure analyses. These methods, when used to analyze the spatial variability of soil properties, quantify unknown soil property variations at a site, offer better estimates for unsampled locations, and provide valuable information for systematically treating the sources of uncertainty of soil property measurements in reliability analyses. In this connection, Baecher (1986) indicated that when quantitative estimates of variation are not available, geotechnical design may tend to be conservative with respect to the estimates of soil properties. As a result, there is a poor understanding of the possible range of performance of the structure or system, and it is difficult to use reliability-based design methods in geotechnical practice.

Soil properties in themselves may be regarded as random variables owing to the uncertainties associated with inherent spatial variability and to the limited obtainable data. Additionally, uncertainties inherent in the quality and quantity of soil samples, the characteristics of the testing device, and the operator's experience may have a significant effect on the measured geotechnical properties. In order, then, to adequately and logically determine the appropriate parameters for engineering analysis and design, these uncertainties in the soil properties should be recognized and quantified.

Over the past decades, significant advances have been made at a variety of geotechnical facilities by the application of stochastic methods for analyzing the spatial variability of soil properties and by reliability analysis. However, the overall assessment of complex soil conditions at a site through the application of stochastic methods on a limited number of samples remains a challenge in spite of the recent contributions of stochastic methods that have attempted to overcome this dilemma. As a rule, the robustness of statistical characteristics of soil increases with the volume of available field data, and the limited availability of field data, in turn, is usually handled by means of various methods of interpolation. In order to obtain reliable estimates of soil properties at unsampled locations, it is necessary to account for the degree of spatial correlation exhibited by soil properties. In fact, achieving this would require a comprehensive database of the general statistical characteristics of spatial variability for various soil type layers.

In this dissertation, it is anticipated that (1) an effort to characterize the spatial variability of soil properties based on the geological nature of deposits and the material composition of the formations, (2) the estimation of the maximum statistically allowable sampling interval and the minimum statistically required number of borings/soundings based on the correlation structures of soil properties, (3) the effect of dynamic loadings on the spatial variability of soil properties, and (4) the development of a simple and efficient technique for more accurate multi-dimensional simulations of soil properties will contribute to the improvement of the characterization of geotechnical uncertainties and, consequently, to better geotechnical designs. In addition, a geotechnical site investigation simulation program was developed to help students connect basic

theoretical principles and concepts of geotechnical site investigation with their use in practice as well as to complement the traditional education methods of site investigation. The statistical characteristics of the spatial variability of soil properties were not only estimated as an objective in the educational simulation, but also for improving site investigation performance in geotechnical engineering. The educational simulation in geotechnical engineering employed representative statistical values of soil properties to satisfy both statistical values obtained from this study and the existing known statistical values for input data. A student's performance is assessed and quantified based on the cost, boring plan, subsurface conditions, and soil parameters determined by the student. According to the evaluation of the effectiveness of the simulation program, the simulation program overall improved students' understanding level of entire aspects of site investigation in geotechnical engineering. The simulation program will promote self-directed learning, engineering intuition, and skills in decision-making and resource management, thereby leading students to become well-trained engineers with sound education in both theory and practice in geotechnical engineering.

1.2. Research scope

This dissertation endeavored to make a contribution to general statistical characteristics of spatial variability for various types of soil layers according to processes of soil formation. This undertaking requires statistical analyses of data based on test results obtained from general in situ tests. A first step in such analyses is an assessment of stationarity; when the mean and the variance of a field data set is independent of

absolute location but dependent only on relative distance and the covariance should depend only on the spatial separation between two points, the field data are said to be stationary. Stationarity is acquired through standardization of the data. Then, statistical structures (i.e., coefficient of variation and correlation coefficient function) are estimated.

Furthermore, the concept of the maximum statistically allowable sampling interval of data obtained in the field was employed, thus determining the minimum statistically required number of soundings/borings needed to perform an initial site investigation. The aliasing concept was applied to estimate the maximum statistically allowable sampling interval and the minimum statistically required number of borings/soundings.

Existing granular soil structures are broken and rearranged by the dynamic loadings such as earthquakes and blasts. The spatial rearrangement of soil structures resulting from dynamic loadings was observed to cause a change in the statistics of soil properties within the same soil layer. This dissertation contributed to some extent to the study on how changes in the structure of soils are reflected in the statistical structures.

Using procured statistical structures, a technique was utilized to perform realizations of multi-dimensional random fields in the vertical and horizontal directions. Since the random process representing the variation of soil properties with depth has the same joint distribution at any horizontal location, various soundings are merely expressed as different realizations of this process. Thus, based on limited data in geotechnical engineering, a simple and efficient technique to generate more accurate multi-dimensional simulations of soil properties that are consistent with the observed or proposed correlation structures of soil properties was developed.

Today's educational simulations in geotechnical engineering focused primarily on basic soil behavior and laboratory testing and did not afford students significant opportunities to acquire the judgment and experience involved in the practice of comprehensive site investigation engineering. To provide students with an opportunity to plan, conduct, evaluate, and refine their own comprehensive site investigations, a simulation program was developed. The effectiveness of the simulation program was evaluated in a geotechnical course.

1.3. Organization

The issues to be handled within this study are theoretically supported and formulated as a general theoretical background to spatial variability of soil properties in the context of geotechnical field tests in Chapter 2. The existing works on the spatial variability of soil properties are reviewed and the statistical characterization of soil properties of interest is presented in detail.

Chapter 3 describes the effects of soil composition and formation processes on soil properties. According to the processes of soil formation, areas of interest are categorized into three representative zones for study, including the Upper Mississippi Embayment, the Atlantic Coastal Plain Province, and the Piedmont Province. Soil properties of each soil type obtained from each area were used to estimate correlation structures pertaining to the spatial variability of soil properties. While these three regions may not be sufficient to obtain a comprehensive database, they are each quite different region and provide a diversity of soil property data.

Chapter 4 introduces the aliasing concept to estimate the maximum statistically allowable sampling intervals of data obtained from the above three areas as a function of spatial equivalent wavelength. How to estimate the minimum statistically required number of soundings/borings needed to perform an initial site investigation is described by use of estimated equivalent wavelengths.

In Chapter 5, the effects of dynamic loadings such as earthquakes and blasting with accompanying strong impacts on the statistical structures of soil properties are highlighted via a case study. Even though dynamic loadings do not cause a change in soil composition within a specific soil layer, spatial rearrangement of soil structures resulting from dynamic loadings led to a change in the soil properties within the same soil layer. This chapter aims to incrementally improve the understanding level of the statistical characteristics of soil properties.

Chapter 6 describes a method for simulation of random fields using the characteristics of the spatial variability of soil properties obtained in advance by means of stochastic methods.

Chapter 7 introduces a site investigation simulation program for undergraduates as an educational tool for students in civil engineering, who understand theory but remain unprepared for the actual practice of site investigation in geotechnical engineering. The effectiveness of the simulation program is discussed.

Overall conclusions and recommendations for future research are presented in Chapter 8.

CHAPTER 2

STATISTICAL ANALYSES OF SPATIAL VARIABILITY OF SOILS

2.1. Introduction

Geotechnical engineers have traditionally favored deterministic (or trend-based) methods for characterizing the spatial variability of soil properties because of their simplicity. The most common method may be subjectively representing the trend of a particular soil property with depth by drawing a line or curve. In some cases, more formal linear or nonlinear regression methods may be used to determine the trend. In subsequent analyses, the variability of the soil property about the trend is ignored. As a result, there is a poor understanding of the possible range of performance of the structure or system, and it is difficult to use reliability-based design methods in geotechnical practice.

In recent decades, there has been a shift in favor of utilizing stochastic (or statistics-based) methods. These new methods resulted in increased cost savings that are cumulative in nature and therefore considerable for very large projects in particular (Hicks, 2005; Parsons and Frost, 2002). Statistical characteristics of spatial variability of soil properties obtained from high-quality investigations are obviously useful in performing a site investigation program with similar soil types because the statistical characteristics of spatial variability of soil properties do not so much depend on the site for similar soil types (Soulie et al., 1990; Vanmarcke, 1977); that is, stochastic methods enable geotechnical engineers to acquire a better understanding from limited data; this has led to improvements in site investigation, thereby making geotechnical designs and

analyses more efficient (Lacasse and Nadim, 1996). The statistical characteristics of soil properties are not completely, but to a considerable extent, independent of space for the same or similar soil types in the same or similar areas.

Modern stochastic methods of data analysis are more rational in their approach to geotechnical design in relation to various uncertainties in soil properties. Therefore, the statistical characterization of spatial variability is a major contributor to spatial analysis in geotechnical engineering. Thus, the spatial variability of soil properties in geotechnical engineering should be taken into consideration in the performance of geotechnical practice. Trend lines in deterministic approaches represent the mean of the data using linear or nonlinear regression models; that is, they offer a limited view of spatial variability. The variable features of soil properties may cause inaccuracy in the estimates of soil properties implemented by deterministic approaches. Therefore, geotechnical engineers have judged and analyzed soil properties in a somewhat conservative way due to the limited ability of deterministic approaches to analyze variable features of the data; they have estimated soil properties in a simple way using regression models without treating the spatial variability of soil properties in a rigorous way. The simplified estimates of soil properties do not sufficiently supply valuable information for performing reliability analysis in geotechnical practice; these simplified methods brought in the performance of relatively more site investigation than stochastic methods to supplement the spatial variability of soil properties disregarded by deterministic approaches, thereby giving rise to extra cost.

This realization has provoked researchers to improve trend-based methods and develop more sophisticated statistical methods to better estimate the spatial variability of

soil properties. Statistical approaches can be usefully applied to interpreting and representing the spatial variability of such field tests as cone penetration tests (CPT) and shear velocity (*Vs*) tests using autocovariance functions.

2.2. Uncertainties in geotechnical engineering

In general, the uncertainties associated with geotechnical properties can be divided into the following three main sources (Baecher, 1982; Baecher, 1986; Baecher and Christian, 2003; Kulhawy et al., 1992; Phoon and Kulhawy, 1999a, 1999b). Although this distinction is useful as a conceptual framework, it is difficult in practice to isolate and quantify each individual source of uncertainty (Jaksa et al., 1997).

2.2.1. Inherent variability

Soil properties at a single location change with time by means of random geologic, environmental, and physical-chemical processes. Soil properties at a single time vary with spatial location due to these same processes. That is, soil properties vary in both time and space. This feature is defined as inherent soil variability or natural variability. The inherent soil variability can be represented using statistical parameters such as the mean, variance, and covariance. This study concentrates on methods to characterize the inherent variability of soil properties.

2.2.2. Measurement error

Measurement error is attributed to a variety of factors including the human error, equipment error, test imperfections, and soil disturbance during the measurement process. In general, measurement error is considered independent of individual tests performed at different locations. The measurement error can have both random and systematic components. In situ tests with good-quality equipment and systematic procedural control are likely to have relatively small measurement errors (Kulhawy and Trautmann, 1996).

2.2.3. Transformation uncertainty (model uncertainty)

Transformation uncertainty, arising from transforming reality into simplified models for convenience of measurement or understanding, occurs during the process of transforming in situ and laboratory measurements into mathematical models. It is associated with the accuracy of mathematical models used to represent soil behavior. Due to the difference between theories and natural physical behavior, the efforts to use high-quality data may not decrease transformation uncertainty. In other words, transformation uncertainty exists as an independent uncertainty in geotechnical engineering. For example, when measured cone tip resistance is transformed into undrained shear strength using an existing correlation equation, the transformation uncertainty depends on the accuracy of the correlation equation. Efforts to reduce transformation uncertainty are made employing better fitting models to create more accurate estimates regarding the statistical characteristics of soil properties.

2.2.4. Models of spatial variability

In a probabilistic framework, we can characterize the variability of soil properties as follows (Soulié et al., 1990):

$$\theta(x,y,z) = \mu_\theta + \varepsilon_s(x,y,z) + \varepsilon_b(x,y,z) + \varepsilon_m(x,y,z) \qquad (2.2.1)$$

where μ_θ is the expected value of the soil property θ, $\varepsilon_s(x,y,z)$ is the random variable describing the inherent spatial variability, $\varepsilon_b(x,y,z)$ is the random variable describing possible constant bias in horizontal direction between observations, and $\varepsilon_m(x,y,z)$ is the random variable describing random measurement errors.

We generally assume that the three random variables above are independent and that the expected values of the spatial variability and random errors are equal to zero:

$$E[\varepsilon_s] = E[\varepsilon_m] = 0 \qquad (2.2.2)$$

The expected value of the soil property is

$$E[\theta] = \mu_\theta + E[\varepsilon_b] \qquad (2.2.3)$$

and the variance is

$$\mathrm{Var}[\theta] = \mathrm{Var}[\varepsilon_s] + \mathrm{Var}[\varepsilon_b] + \mathrm{Var}[\varepsilon_m] \qquad (2.2.4)$$

Note that this differs somewhat from the model used by Baecher and Christian (2003) who consider the bias term to be a multiplicative factor rather than an additive factor.

Phoon and Kulhawy (1999a) and Baecher and Christian (2003) choose an alternative form of Eq. 2.2.1 in which the spatial variation of the soil property is split into

two components – a *trend* and a *residual* – rather than a single component. Thus they write:

$$\theta(x,y,z) = \mu_\theta(x,y,z) + \varepsilon_s(x,y,z) + \varepsilon_b(x,y,z) + \varepsilon_m(x,y,z) \qquad (2.2.5)$$

where $\mu_\theta(x,y,z)$ describes the *trend* of the observations. In this context, the term $\varepsilon_s(x,y,z)$ is called the *residual*. The advantage of this form is that the residual can be modeled by a homogeneous random variable in which (1) the mean and variance are independent of spatial position, i.e., ε_s is constant, and (2) the covariance or correlation between observations at two different positions is a function only of their separation distance rather than their absolute spatial coordinates. We may also say that partitioning the variance into two components yields a deterministic component (i.e., the trend) and a stochastic component (i.e., the residuals). Note that this division is arbitrary and depends on the function used to characterize the trend.

2.3. Characterization of Spatial Variability

Figure 2.1 presents a flow chart of procedures for estimating the statistical characteristics of soil properties in geotechnical engineering. Each of the following sections summarizes methods employed in each step. Examples using a CPT data set are presented to facilitate the understanding of methods in each step.

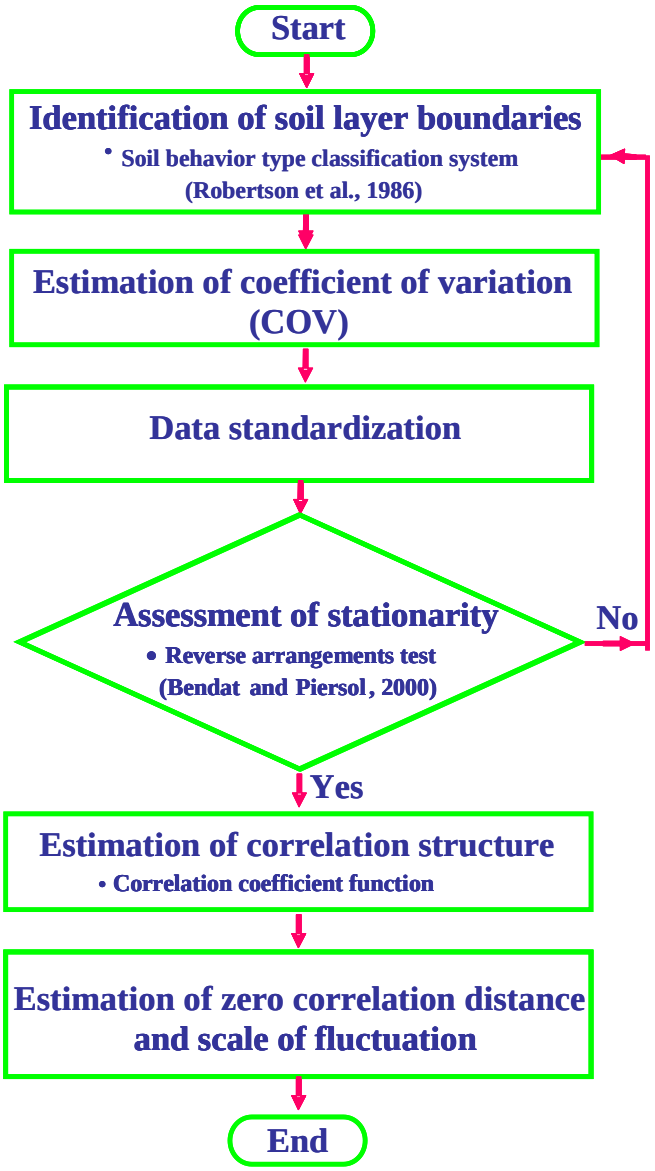

Figure 2.1 Procedures for estimating statistical characteristics of soil properties in geotechnical engineering

2.3.1. Identification of statistically homogeneous soil layers

When statistical characteristics of soil properties are constant, depending only on the relative distance between data points not spatial location, these are statistically homogeneous. The initial step in methods to characterize the inherent spatial variability

of soil properties is to identify statistically homogeneous subsets of the soil property data. Frequently, this is achieved by interpreting the available data to determine subsurface layers in which the soil type is reasonably homogeneous. When the data include the results of visual soil classifications performed on disturbed or undisturbed specimens of soil, identifying layers with the same soil type is straightforward. For in situ tests such as the cone penetration test (CPT) where no samples are obtained, the identification of layers with similar soil types must be based on indirect means.

Robertson et al. (1986) introduced a chart for soil behavioral classification based on the tip resistance and sleeve friction measurements obtained in the CPT test that is shown in Figure 2.2 (a). The chart was created mainly using CPT data obtained from the ground surface to a depth of 30 m, and thus its use for depths greater than 30 m may lead to some error (Robertson et al., 1986). However, the chart for soil behavioral classification allows geotechnical engineers to easily estimate soil types.

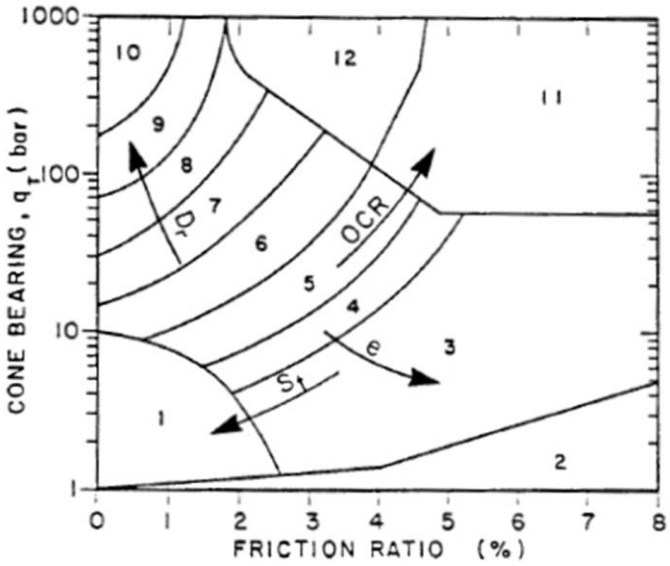

Zone	Soil Behavior Type
1	Sensitive fine grained
2	Organic material
3	Clay
4	Silty clay to clay
5	Clayey silt to silty clay
6	Sandy silt to clayey silt
7	Silty sand to sandy silt
8	Sand to silty sand
9	Sand
10	Gravelly sand to sand
11	Very stiff fine grained
12	Sand to clayey sand

(a)

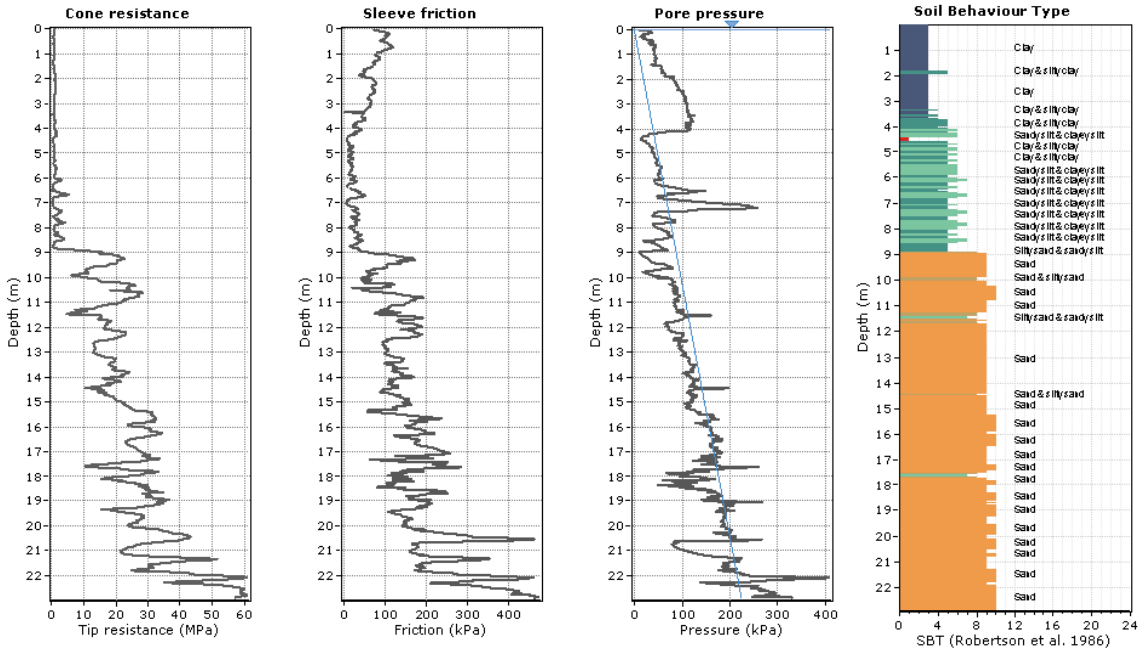

(b)

Figure 2.2 Soil classification: (a) soil behavioral classification system (Robertson et al., 1986); (b) CPT-90 raw data with soil profile obtained from Wyatt, Missouri (reference: http://geosystems.ce.gatech.edu/Faculty/Mayne/Research/index.html)

Statistical tests may also be used to identify boundaries between layers, including the modified Bartlett test and two-dimensional cluster analysis introduced by Phoon et al. (2003) and Hegazy and Mayne (2002), respectively. In the modified Bartlett test, a Bartlett statistic profile is generated by applying a moving window to detrended CPT data or residuals. Where the Bartlett statistic profile exceeds an estimated critical value is a boundary between soil types. The cluster analysis binds data points with similar parameter values in main clusters (i.e., soil layers) and classifies the measurement errors, irregularities, and transitional layers as small clusters. The soil-behavior type classification system introduced by Robertson et al. (1986) is more widely used than the modified Bartlett test and two-dimensional cluster analysis in geotechnical practice due to its relative simplicity. However, these two methods can complement the soil-behavior type classification system.

The soil-behavior type classification system was used in this dissertation to subdivide CPT profiles into layers with similar soil types. *CPeT-IT,* a commercial software program developed by the *Geologismiki* was used to determine soil profile. Figure 2.2 (b) shows an example of the output of the *CPeT-IT* software using the soil-behavior type classification system introduced by Robertson et al. (1986).

2.3.2. Coefficient of variation (COV)

The standard deviation for a raw data set is defined as

$$\sigma_\theta = \sqrt{\frac{1}{n-1} \cdot \sum_{k=1}^{n} [\theta(x,y,z_k) - \mu_\theta]^2} \qquad (2.3.1)$$

where μ_θ is the expected value of the soil property θ, n is total data number of the data set, and $n - 1$ is used instead of n as the denominator to avoid a statistical bias. When the standard deviation, σ_θ, is divided by the mean of soil property, μ_θ, a dimensionless value is obtained. It is the coefficient of variation, COV_θ, defined as

$$\mathrm{COV}_\theta = \frac{\sigma_\theta}{\mu_\theta} \tag{2.3.2}$$

When comparing one raw data set with another raw data set, where individual raw data sets have different means, the coefficient of variation for the comparison is generally more useful rather than the standard deviation. This makes it possible to measure the relative deviation between individual data sets with different means. When the mean of a raw data set is near zero, however, the coefficient of variation is infinite so that individual raw data sets can not be efficiently compared with each other.

The COVs of soil properties in a variety of soil types are tabulated in Table 2.1. Many researchers have made significant efforts on estimating COVs of soil properties as a descriptor of uncertainties of geotechnical data mentioned in previous section.

Table 2.1 COV of soil properties in various soil types

Soil Property	Soil	Direction	COV (%)	Reference
SPT N value	Clay and sand	Vertical	25 ~ 50	Phoon and Kulhawy (1996)
CPT cone resistance	River sand	Vertical	25 ~ 43	Reyna and Chameau (1991)
	River sand	Vertical	25 ~ 43	Reyna and Chameau (1991)
	Clay	Vertical	20 ~ 40	Phoon and Kulhawy (1996)
	Clay	Vertical	20 ~ 40	Phoon and Kulhawy (1996)
	Sand	Vertical	20 ~ 60	Phoon and Kulhawy (1996)
CPT sleeve friction	River sand	Vertical	26 ~ 43	Reyna and Chameau (1991)
DMT A reading	Clay	Vertical	10 ~ 35	Phoon and Kulhawy (1996)
	Sand	Vertical	20 ~ 50	Phoon and Kulhawy (1996)
DMT B reading	Clay	Vertical	10 ~ 35	Phoon and Kulhawy (1996)
	Sand	Vertical	20 ~ 50	Phoon and Kulhawy (1996)
DMT dilatometer modulus	Sand	Vertical	15 ~ 65	Phoon and Kulhawy (1996)
	River sand	Vertical	25 ~ 42	Reyna and Chameau (1991)
DMT material index	Sand	Vertical	20 ~ 60	Phoon and Kulhawy (1996)
	River sand	Vertical	22 ~ 37	Reyna and Chameau (1991)
DMT horizontal stress index	Sand	Vertical	20 ~ 60	Phoon and Kulhawy (1996)
	River sand	Vertical	28 ~ 39	Reyna and Chameau (1991)
PMT limit pressure	Clay	Vertical	10 ~ 35	Phoon and Kulhawy (1996)
	Sand	Vertical	20 ~ 50	Phoon and Kulhawy (1996)
PMT Young's modulus	Sand	Vertical	15 ~ 65	Phoon and Kulhawy (1996)
Vane test undrained shear strength	Clay	Vertical	18 ~ 30	Asaoka and A-Grivas (1982)
	Clay	Vertical	10 ~ 40	Phoon and Kulhawy (1996)
Laboratory relative density	Sand	---	11 ~ 36	Haldar and Tang (1979)
Laboratory natural water content	All soil types	---	9 ~ 32	Kulhawy et al. (1991)
Laboratory liquid limit	All soil types	---	3 ~ 19	Kulhawy et al. (1991)
Laboratory plastic limit	All soil types	---	7 ~ 17	Kulhawy et al. (1991)
Laboratory void ratio	All soil types	---	13 ~ 26	Kulhawy et al. (1991)
Laboratory total unit weight	All soil types	---	2 ~ 12	Kulhawy et al. (1991)
Laboratory effective friction angle	All soil types	---	6 ~ 21	Kulhawy et al. (1991)
Laboratory undrained shear strength	All soil types	---	16 ~ 61	Kulhawy et al. (1991)
Laboratory compression index	All soil types	---	26 ~ 48	Kulhawy et al. (1991)

Kulhawy et al. (1991) estimated the coefficients of variation of soil index properties (natural water content, liquid limit, plastic limit, unit weight, initial void ratio) and soil performance properties (effective friction angle, undrained shear strength, and

compression index) via extensive literature review and illustrated that the mean COVs of soil performance properties are larger than that of soil index properties. They argued that the relatively high mean COVs of soil performance properties are attributed to indirect estimation of soil performance properties from several soil index properties; that is, the mean COV of a soil performance property is the combination of the mean COVs of several soil index properties.

Reyna and Chameau (1991) compared COVs of DMT data in loose silty sand obtained at a normal penetration rate with those in the same soil layer obtained at a slow penetration rate. As a result, lift-off pressure was decreased as penetration rate was decreased because lift-off pressure is directly related to excess pore water pressure; that is, the variability level in lift-off pressure decreased with decrease in penetration rate.

Haldar and Miller (1984) suggested a correlation equation of relative dry density associated with parameters such as *N* value, maximum dry density, minimum dry density, and effective vertical stress using the regression analysis. As a result, the COV of in situ relative density decreased as the mean relative density increased.

Kulatilake and Um (2003) studied the effect of trend removal on the variability level of cone tip resistance in clayey soil layers at Texas A & M University. When the trend is not removed, the variance of spatial variability is larger than that at the same sounding locations when the trend is removed. They found that the trend removal decreases the variation of spatial variability of soil properties.

Phoon and Kulhawy (1996) evaluated the COV of inherent spatial variability of soil properties obtained from a variety of field tests in geotechnical engineering via a broad literature review. Overall, the COVs of inherent spatial variability of soil properties

obtained from the Dilatometer test (DMT) were high due to relatively small amount of available data. The COVs of inherent spatial variability in sandy soil layers were overall higher than those in clayey soil layers due to the relatively high variation of soil properties in sandy soil layers. In practice, the standard deviation and mean of the sandy soil layer ranging from 11.5 m to 17.5 m from the CPT-90 data in Wyatt, Missouri were estimated to be 5.99 and 21.98 MPa, respectively. Therefore, COV was calculated to be 27.2% by using the above equation.

2.3.3. Stationarity and normalization

Once subsets of the data that are nominally homogeneous with respect to soil type have been identified, one should check that the data are statistically homogeneous or stationary to assure that any subsequent statistical analyses are meaningful. Stationarity may be defined in either a strict (or strong) sense or a wide (or weak) sense. Brockwell and Davis (1987), Jaksa (1995), and Jaksa et al. (1997) define stationarity in a strict sense as data for which the joint probability density function is independent of the spatial location and/or time. For most analyses, it is sufficient to consider only wide-sense stationarity, which requires that the mean and the variance be independent of spatial location and the covariance depend only on the spatial separation between two points. Thus, strict-sense stationarity is a subset of wide-sense stationarity. For the purpose of this dissertation, the wide-sense definition of stationary as defined by Jaksa (1995) will be used.

It is important to note that even though soil data are determined to be stationary, the soil data may not be isotropic. In other words, the vertical statistical structure such as

the covariance function of soil in a homogenous soil layer is usually not equal to the horizontal statistical structure.

Bendat and Piersol (1986) introduced the reverse arrangements test to determine the stationarity of a set of data. The procedure to estimate the total number of reverse arrangements A is as follows:

1) Calculate h_{ij} from data sequence $x_1, x_2, \ldots, x_n$.

$$h_{ij} = \begin{cases} 1 & \text{if } x_i > x_j \\ 0 & \text{otherwise} \end{cases} \tag{2.3.3}$$

2) Calculate A using

$$A = \sum_{i=1}^{n-1} A_i \tag{2.3.4}$$

where

$$A_i = \sum_{j=i+1}^{n} h_{ij} \tag{2.3.5}$$

As illustrated in Figure 2.3, when the total number of reverse arrangements estimated from a given data set is within the 5% level of significance, the data set is considered stationary.

In general, a data set is transformed prior to statistical analysis. The transformation consists of removing trends from the measured raw data and normalizing the resulting residual values.

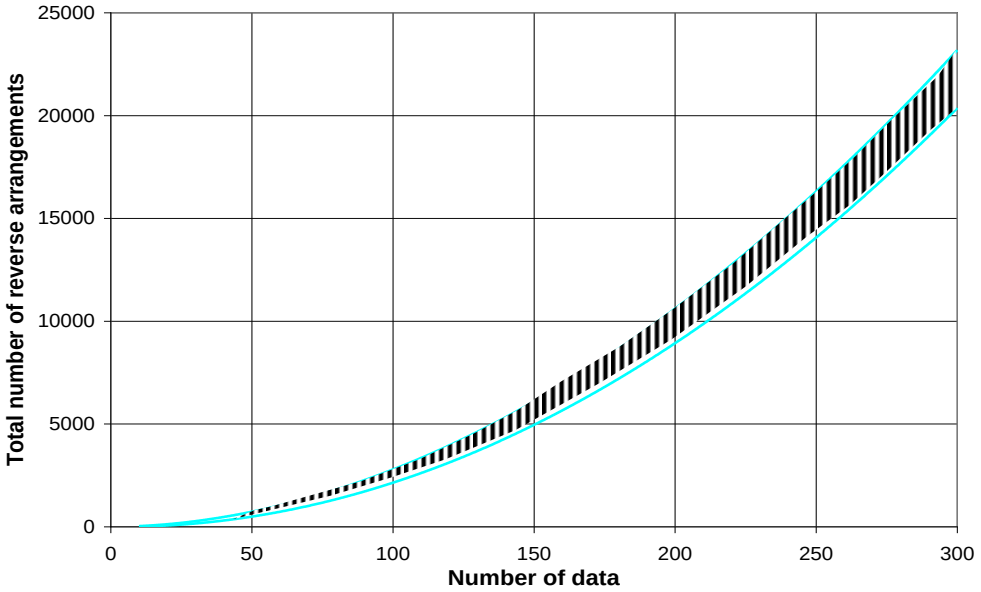

Figure 2.3 Reverse arrangements test with 5% level of significance for assessment of stationarity (Bendat and Piersol, 1986)

Figure 2.4 shows a linear regression analysis applied to the CPT tip resistance in a sand layer ranging from 11.5 m to 17.5 m from the CPT-90 data. Residual values are calculated by subtracting the linear trend as a best fit from the raw data. The residuals are subsequently normalized by the standard deviation of the residuals, thereby bringing about zero-mean, unit-variance, homogeneous random field. Alternatively, Uzielli et al. (2005) used vertical stresses to normalize residuals of cone resistance instead of the standard deviation of residuals. A representative total unit weight of the sand layer was assumed to be 20 kN/m^3 in order to normalize the CPT-90 data by the stress-normalization technique. Figure 2.5 presents the profiles of normalized CPT-90 tip resistance data by the two techniques. When the reverse arrangements test is applied to the CPT data normalized by the standard deviation of residuals and the vertical stress, the two normalized CPT data sets are stationary as shown in Figure 2.6.

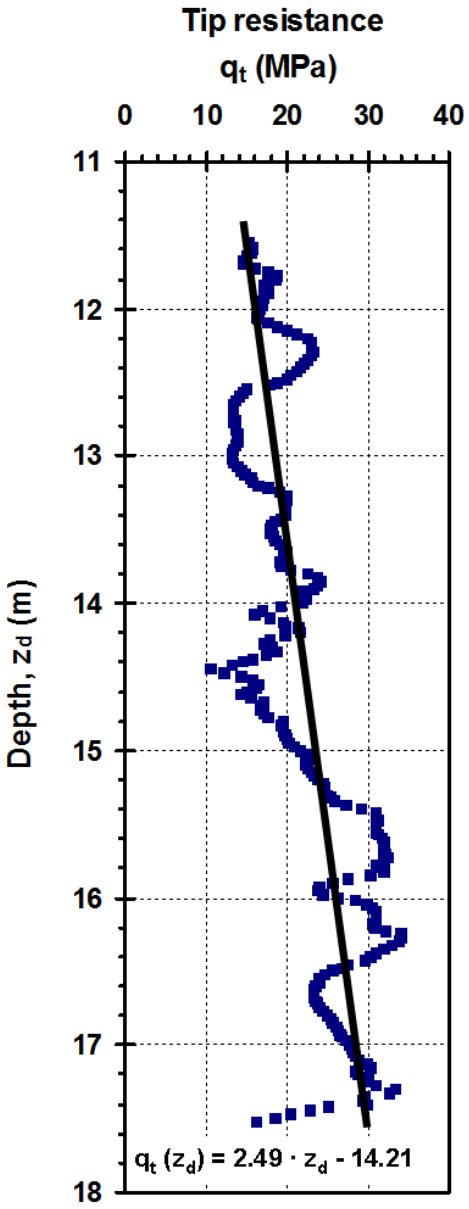

Figure 2.4 Application of linear regression analysis to CPT-90 data

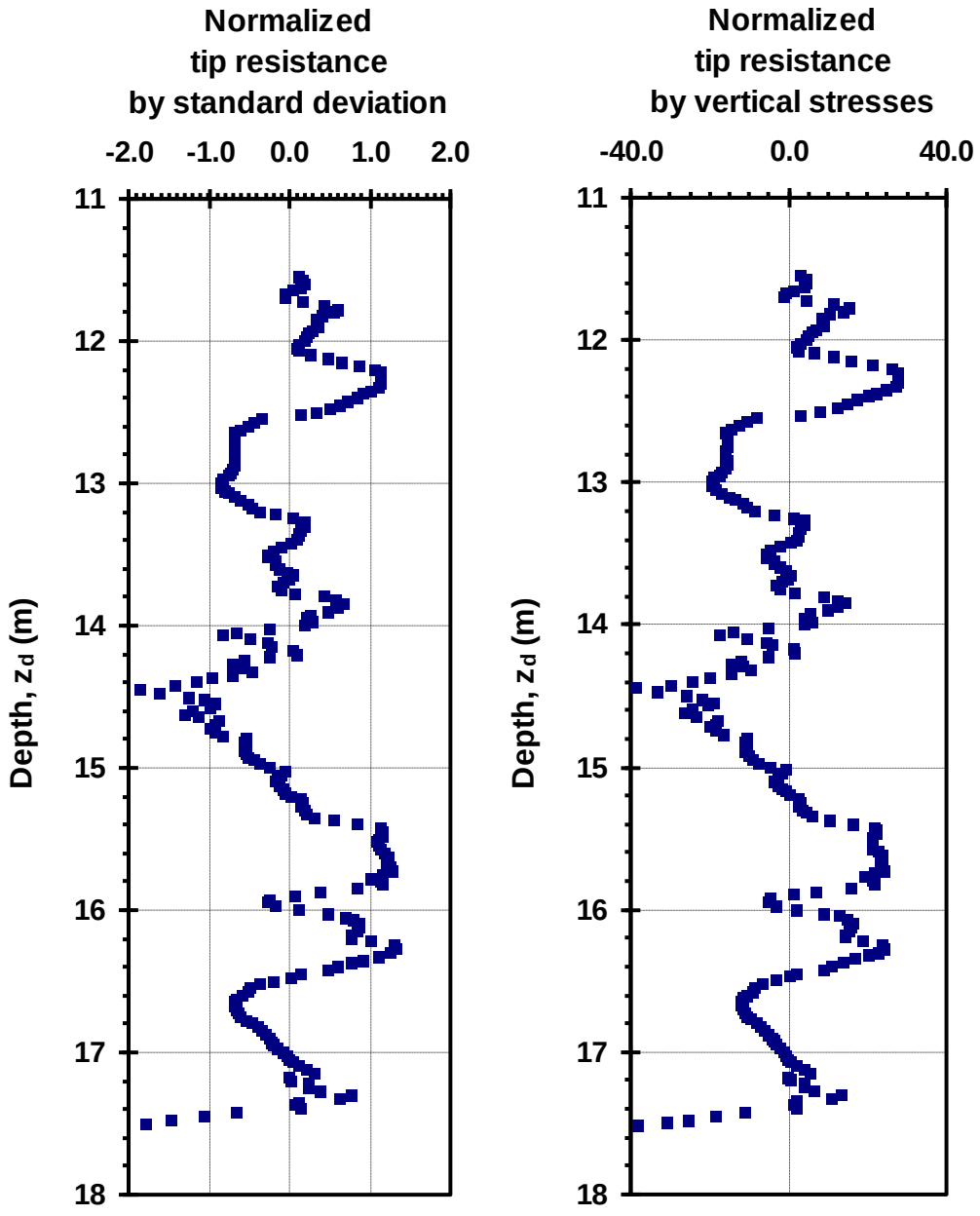

(a) (b)

Figure 2.5 Normalization of CPT-90 data by (a) standard deviation and (b) the vertical stress

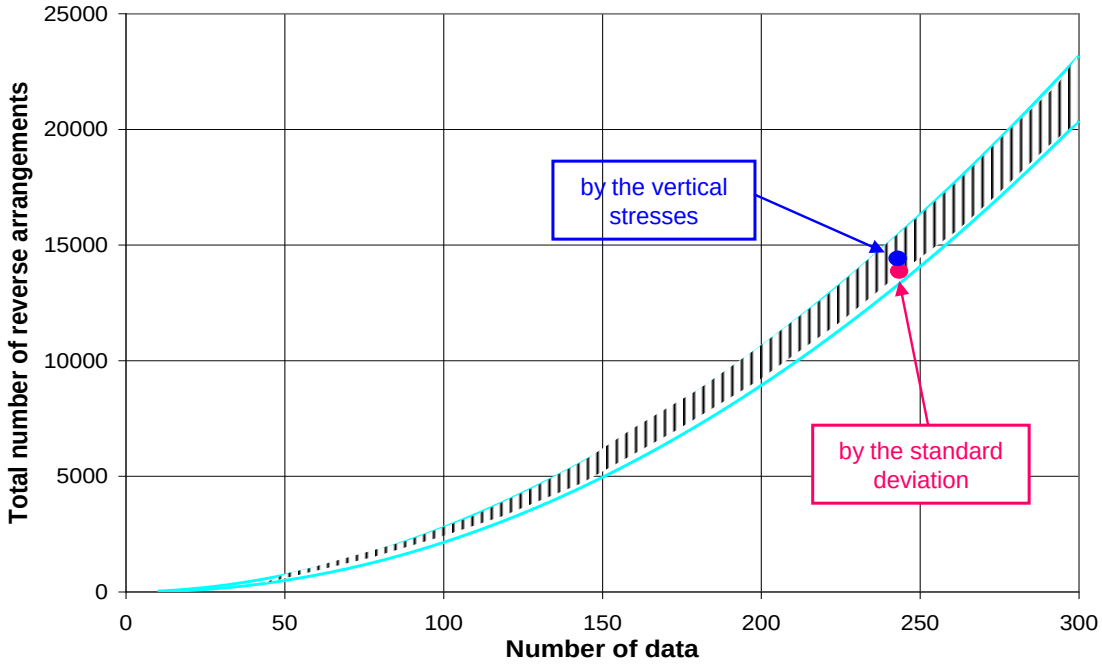

Figure 2.6 Reverse arrangements test with 5% level of significance for assessment of stationarity of CPT-90 data normalized by the standard deviation and by the vertical stresses (Bendat and Piersol, 1986)

2.4. Statistical characterization of spatial variability

2.4.1. One-dimensional correlation structures

2.4.1.1. With uniform lag (relative) distance in the vertical and the horizontal directions

One-dimensional correlation structures include the autocovariance function and the autocorrelation function. The autocovariance function is a mathematical model to describe the correlation of residuals with relative distance estimated by removing a trend from a given raw data set. When residuals are stationary, the autocovariance function of residuals is defined as (Baecher and Christian (2003):

$$C_\lambda(k) = \frac{1}{n-k} \cdot \sum_{i=1}^{n-k} \left[\lambda_i - \overline{\lambda_i}\right] \cdot \left[\lambda_{i+k} - \overline{\lambda_{i+k}}\right] \qquad (2.4.1)$$

where subscript *i* is a point number of *n* raw data, *k* is the lag index, and $\overline{\lambda}$ is the mean of a set of residuals, λ. In addition, when the autocovariance function is divided by the variance of a sequence of given residuals, the autocorrelation function, $\rho_\lambda(k)$, is estimated as follows:

$$\rho_\lambda(k) = \frac{C_\lambda(k)}{\sigma_\lambda{}^2} \qquad (2.4.2)$$

where the variance σ_λ^2 is the square of the standard deviation of a set of residuals. Figure 2.7 presents correlation coefficient functions of CPT-90 data in Wyatt, Missouri estimated by the standard deviation of the raw CPT-90 data sequence and by the vertical stresses.

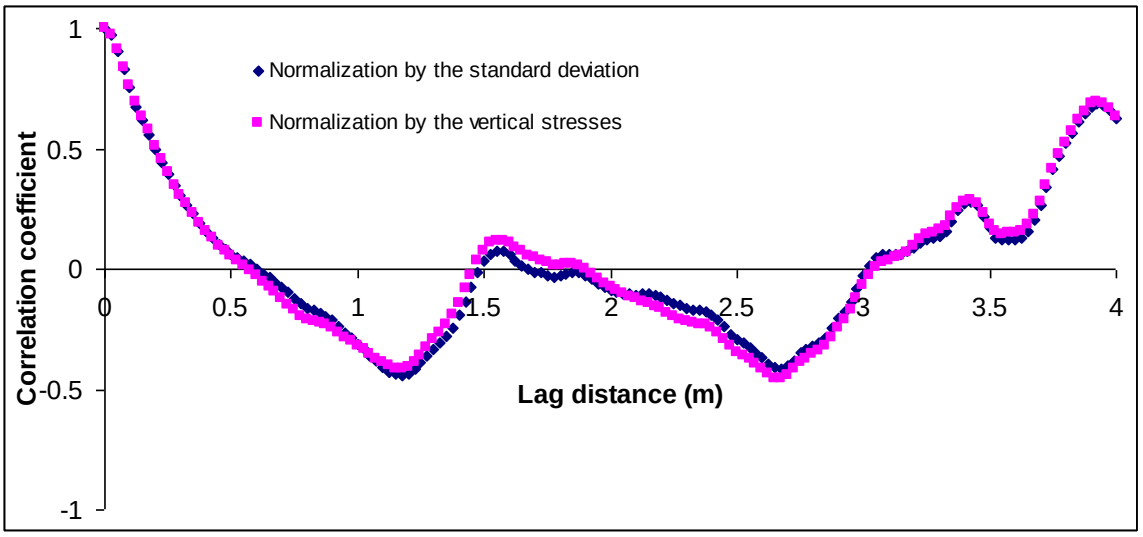

Figure 2.7 Correlation coefficient functions of CPT-90 data in Wyatt, Missouri normalized by the standard deviation and by the vertical stresses

2.4.1.2. With non-uniform lag (or relative) distance in the horizontal direction

As shown in the previous section, the autocovariance function is a mathematical model to describe the correlation of residuals with relative distance. Lag distance or relative distance should have a constant interval to estimate the autocovariance function of field data in geotechnical engineering; that is, data point locations are separated from each other in a line to estimate autocovariance function values at each multiple of a separation distance. However, most site investigation programs have the spatial locations of borings with an irregular pattern, rather than a systematic pattern, with a limited number of borings. This increases the difficulty in analyzing correlation structures with the traditional methods mentioned previously because data to be grouped based on uniform separation distances are limited in number. A new technique is proposed to satisfy both conditions above to analyze correlation structures of data with non-uniform separation distance that are limited in number. With the traditional methods, it is difficult to analyze correlation structures of soil properties with non-uniform separation distance and a limited number of borings as shown in Figure 2.8. A new technique is needed to overcome this issue related to the analysis of covariance function with non-uniform separation. Possible solutions include:

(1) Put each boring into bins with the same or similar separation distances. Bind each boring within each bin with the other borings within the same bin into one pair.

(2) Determine the range of the stationary and common soil type layers of each boring pair.

(3) Each point in a boring is correlated with a corresponding point in a coupled boring. Then, the value of horizontal covariance function for each separation

distance can be calculated. For example, assume that "C" boring has detrended data or residuals of (c_1, c_2, c_3, . . . , c_n), and "D" boring paired with "C" boring has detrended data or residuals of (d_1, d_2, d_3, . . . , d_n). The residuals of both borings all are assumed to be stationary and should be standardized by normalizing the residuals of each boring by the standard deviation of the residuals. Then, "C" boring has standardized residuals of (c_1', c_2', c_3', . . . , c_n'), and "D" boring paired with "C" boring has residuals of (d_1', d_2', d_3', . . . , d_n'). It is assumed that the coupled borings are separated with distance. A method for covariance function is

$$C_z = \frac{1}{n} \cdot \sum_{i=1}^{n} c_i' \cdot d_i' \qquad (2.4.3)$$

This equation can be applied to the other pairs of borings within the same bin. Therefore, the average value of the horizontal covariance function within each bin for the mean value of similar separation distances within the same bin can be calculated.

(4) Repeat steps (1)–(3) for the other coupled borings with different separation distances within other bins.

(5) Plot the average values of covariance function at the mean value of the separation distances within each bin.

A practice performed using CPT data obtained from the site of Bridge A-1700, Caruthersville, Missouri is described in Section 3.5 following the above procedures.

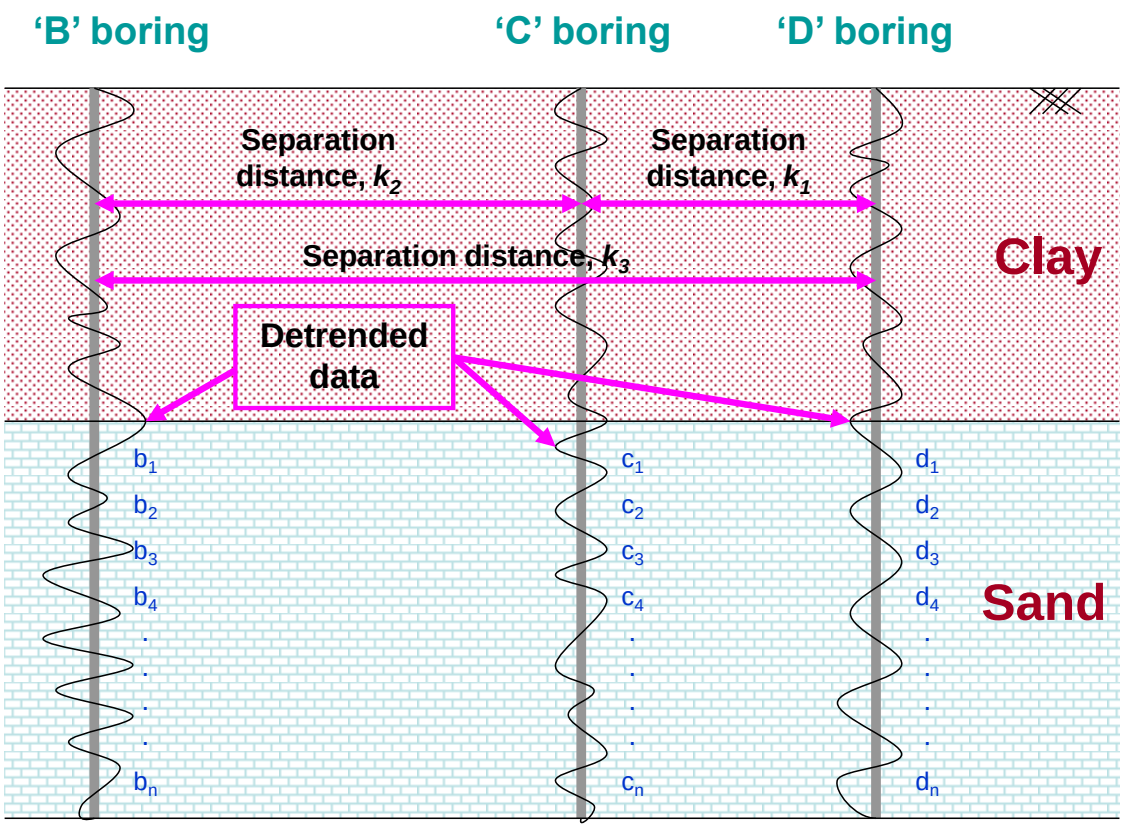

Figure 2.8 Detrended data of each boring with a lag, *k*, in sand layer

2.4.2. Scale of fluctuation

The scale of fluctuation is the distance within which two values of a given soil property show relatively strong spatial correlation. When the relative distance between two values of a given soil property is smaller than the scale of fluctuation, the two values are considered strongly correlated; when the relative distance is greater, the two values are considered less correlated. As summarized in Table 2.2, Vanmarcke (1977, 1983) approximated correlation functions and the scales of fluctuation of residuals by use of such common models as the exponential model, the squared exponential model, the triangular model, and the cosine decaying model. For example, DeGroot and Baecher (1993) employed the exponential model to estimate the horizontal scale of fluctuation of

undrained shear strength in a soft marine clay layer; this was estimated to be 46 m. With the squared exponential model, Tang (1979) estimated the horizontal scale of fluctuation of cone resistance of CPT data in a marine clay layer as 60 m.

Table 2.2 Correlation structures for common correlation models (after Vanmarcke, 1977)

Correlation model	**Correlation coefficient function, $\rho_x(k)$**	**Scale of fluctuation, δ**
Exponential	$e^{\frac{-\lvert k\rvert}{\alpha}}$	$2 \cdot \alpha$
Squared exponential	$e^{-\left(\frac{k}{\alpha}\right)^2}$	$\alpha \cdot \sqrt{\pi}$
Triangular	$\begin{cases} 1-\frac{\lvert k\rvert}{\alpha}, & \lvert k\rvert \le \alpha \\ 0, \text{ otherwise} \end{cases}$	α
Cosine Exponential decaying	$e^{\frac{-\lvert k}{\alpha_1}} \cdot \cos(k/\alpha_2)$	$\frac{2 \cdot \alpha_1 \cdot \alpha_2^2}{\alpha_1^2 + \alpha_2^2}$

Note: α, α_1, and α_2 are constants and k is lag distance of correlation coefficient function.

In a study of the effect of trend removal on estimating statistics of cone tip resistance in clay soil layers at Texas A & M University, Kulatilake and Um (2003) found that the trend removal decreases the scale of fluctuation of spatial variability. Phoon and Kulhawy (1999b) concluded via a broad literature review that the horizontal scale of fluctuation of soil properties is more than one order of magnitude larger than vertical scale of fluctuation due to larger variation in the vertical direction than in the horizontal direction.

As mentioned before, the scale of fluctuation is an indicator of correlation level. For example, large scales of fluctuation indicate high correlation. DeGroot (1996) summarized the scales of fluctuation obtained from a variety of in situ tests in geotechnical engineering as shown in Table 2.3.

Table 2.3 Scale of fluctuation of soil properties in various in situ tests (after DeGroot, 1996)

Soil Property	**Soil**	**Direction**	**Scale of fluctuation, m**	**Reference**
SPT N value	Dune sand	Horizontal	40.0	Hilldale-Cunningham (1971)
	Alluvial sand	Horizontal	33.4	DeGroot (1996)
DMT P_0	Varved clay	Vertical	2.28	DeGroot (1996)
CPT cone resistance	Sea clay	Horizontal	60.0	Hoeg and Tang (1976); Tang (1979)
	Silty clay	Horizontal	10.0 ~ 24.0	Lacasse and de Lamballerie (1995)
	Copper tailings	Vertical	1.0	Baecher (1987)
	Sensitive clay	Vertical	4.0 for q_c, f_s, and u_2	Chiasson et al. (1995)
	Silty clay	Vertical	2.0	Lacasse and de Lamballerie (1995)
	Clay	Vertical	2.0	Vanmarcke (1977)
	Mexico clay	Vertical	2.0	Alonzo and Krizek (1975)
	Clean sand	Vertical	6.0	Alonzo and Krizek (1975)
	Clean sand	Vertical	3.2	Kulatilake and Ghosh (1988)
	North sea sand	Horizontal	28.0 ~ 76.0	Keaveny et al. (1989)
Vane shear test undrained shear strength	Clay	Vertical	2.0 ~ 6.0	Asaoka and A-Grivas (1982)
	Sensitive clay	Vertical	2.0	Baecher (1982)
	Sensitive clay	Horizontal	46.0	DeGroot and Baecher (1993)
Laboratory undrained shear strength	Chicago clay	Vertical	1.0 (Unconfined compression test)	Wu (1974)
	Offshore sites	Vertical	0.6 ~ 7.2 (Triaxial and DSS)	Keaveny et al. (1989)
Hydraulic conductivity	Compacted clay	Horizontal	1.0 ~ 4.0	Benson (1991)

As observed by Phoon and Kulhawy (1999b), Table 2.3 shows that the scales of fluctuation of each soil type in the horizontal direction are larger than those in the vertical direction. This means that each soil layer is more correlated in the horizontal direction than in the vertical direction. This is attributed to anisotropy of soils.

As an exercise, the correlation coefficient functions of CPT-90 data normalized by the standard deviation and the vertical stresses were estimated in Figure 2.9. In Figure 2.9, the regression analysis was also applied to obtain the exponential model to best fit the correlation coefficient function of CPT-90 data normalized by the standard deviation. The parameter, *a*, of the exponential model was estimated to be 0.25. The scale of fluctuation of the CPT-90 data is estimated to be 0.5 by the correlation equation suggested by Vanmarcke (1977, 1983) in Table 2.2.

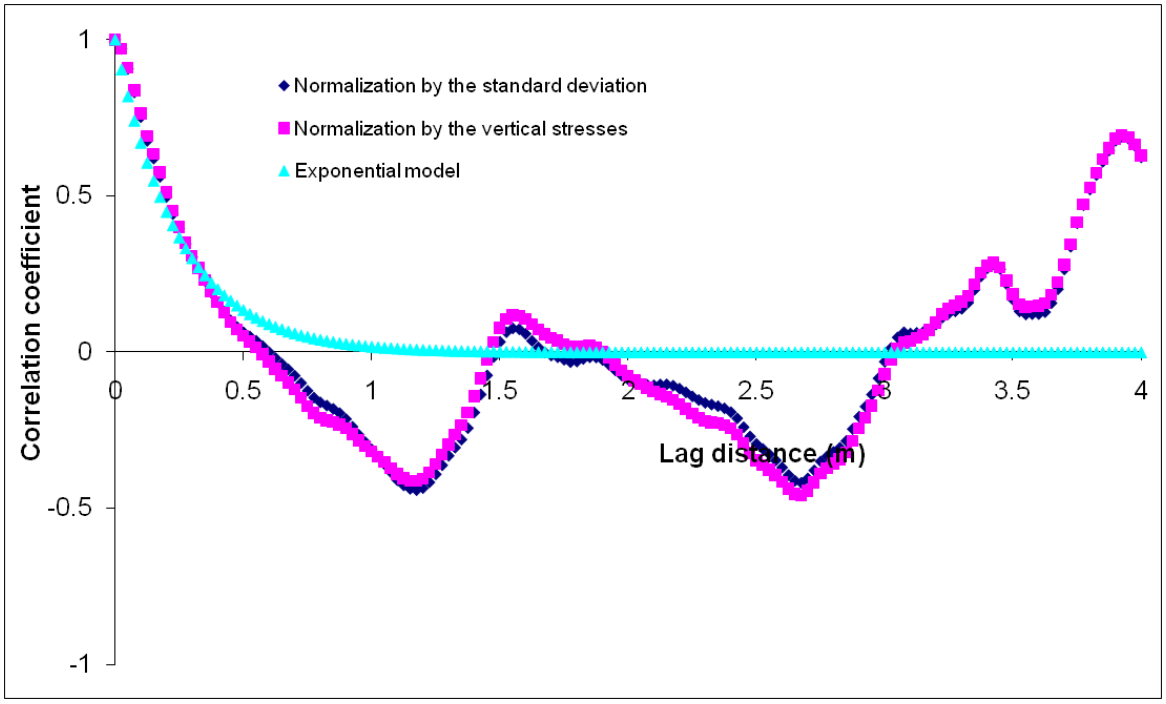

Figure 2.9 Modeling of the correlation coefficient function of normalized CPT-90 data in Wyatt, Missouri using the exponential model

2.4.3. Zero-correlation distance

The zero-correlation distance is the lag distance at which a correlation coefficient function of a given soil property approaches zero as illustrated in Figure 2.10. The zero-correlation distance has characteristics similar to those of the scale of fluctuation.

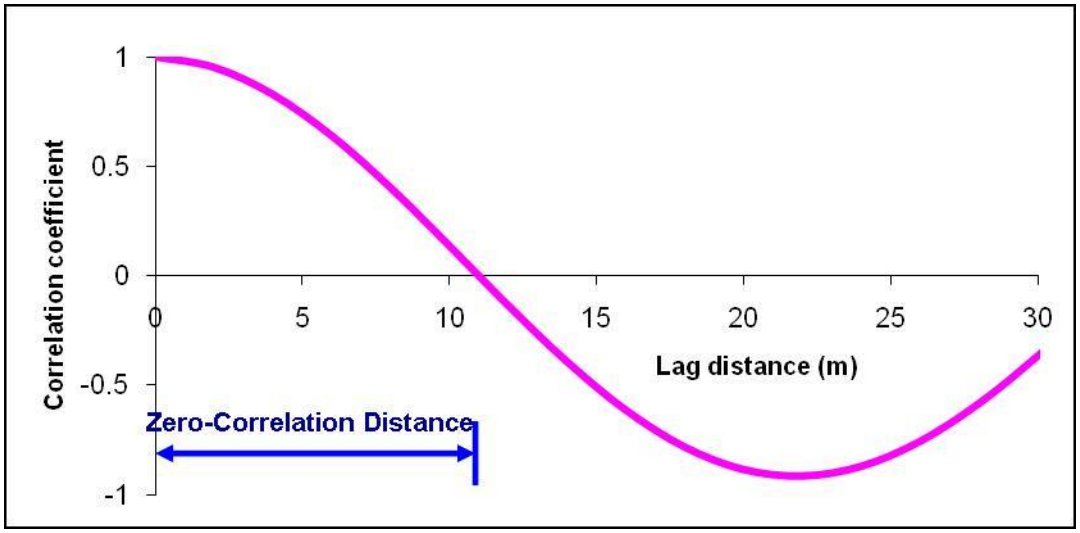

Figure 2.10 Concept of zero-correlation distance in the correlation coefficient function

As mentioned in the scale of fluctuation, if a relative distance between two points of a given soil property is smaller than the zero-correlation distance, the two points are considered to be strongly correlated. If not, the two points are considered less correlated. However, the scale of fluctuation is a correlation distance in the wide sense and the zero-correlation distance is a correlation distance in the strict sense. As an exercise, the zero correlation distances of CPT-90 data in Wyatt, Missouri were estimated in Figures 2.7 and 2.9. The zero correlation distances of the normalized CPT-90 data by the standard deviation and by the vertical stresses were estimated to be 0.63 m and 0.56 m,

respectively. As indicated by Uzielli et al. (2005), the stress-normalization led to a relative decrease in the scale of fluctuation for cone resistances in comparison to the normalization of the standard deviation.

CHAPTER 3

EFFECT OF COMPOSITION AND FORMATION PROCESS OF SOIL ON STATISTICAL STRUCTURES OF SOIL PROPERTIES

3.1. Introduction

As described in Chapter 2, stochastic methods may be used to characterize the inherent spatial variability of soils, thus allowing the effects of spatial variability to be more accurately incorporated into reliability-based geotechnical design approaches. Furthermore, estimates of soil properties at unsampled or undersampled locations can be obtained. That is, stochastic methods help geotechnical engineers handle uncertainties in soil properties in a rational manner.

The inherent spatial variability of soil properties depends on soil type and the process of soil formation. Nevertheless, relatively few quantitative estimates of the spatial variability of soil properties linked to soil composition and the process of soil formation have been reported. In this chapter, three areas of the Eastern United States with different geologic characteristics—the Upper Mississippi Embayment, the Atlantic Coastal Plain Province, and the Piedmont Province—are examined to investigate how the process of soil formation influences the stochastic properties of the soils. These three areas were chosen in part due to the availability of plentiful data from specific sites to use in evaluating the stochastic soil properties.

3.2. Description of sites

3.2.1. Upper Mississippi Embayment

As illustrated in Figure 3.1, the Mississippi Embayment is located in the Mississippi Valley. The Embayment extends from southern Illinois to the Gulf of Mexico southward along the Mississippi River (Rix and Romero-Hudock, 2006). In the past, numerous layers of soil sediments were deposited in the Embayment when the Mississippi River flooded. The soil sediment depth ranges from a depth of a few meters in southern Illinois to a depth of more than 1000 meters near western Tennessee (Rix and Romero-Hudock, 2006; Ng et al., 1989). The portion of the Mississippi Embayment studied in this dissertation is the Upper Mississippi Embayment.

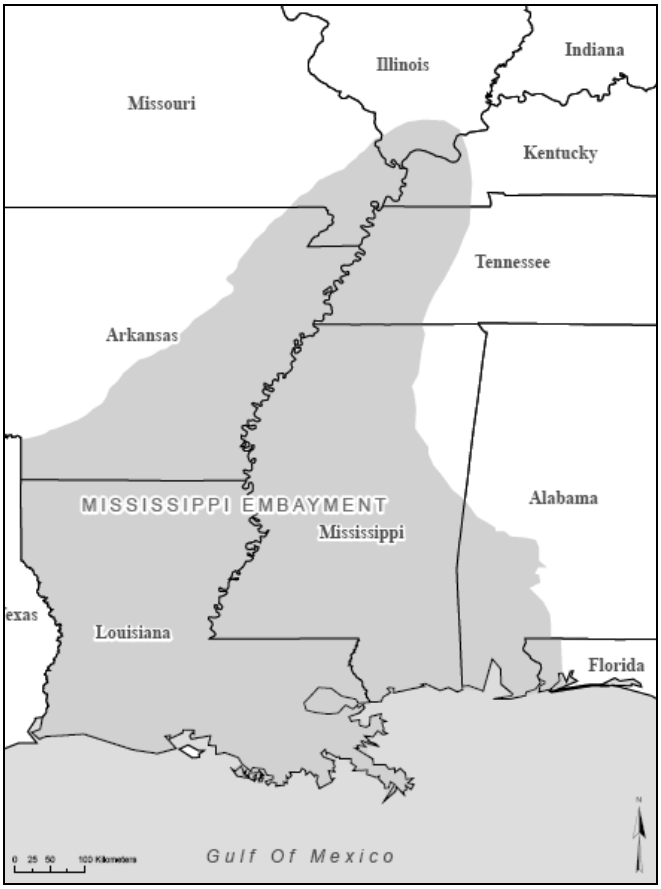

Figure 3.1 Map of the Mississippi Embayment

Figure 3.2 shows the thickness of the Upper Mississippi Embayment sediments overlying Paleozoic bedrock (Ng et al., 1989). The Upper Mississippi Embayment includes the New Madrid seismic zone, which is considered to be an area with significant seismic hazard. The soil formation process or sedimentation in the Embayment resulted in thick layers of coarse-grained soil.

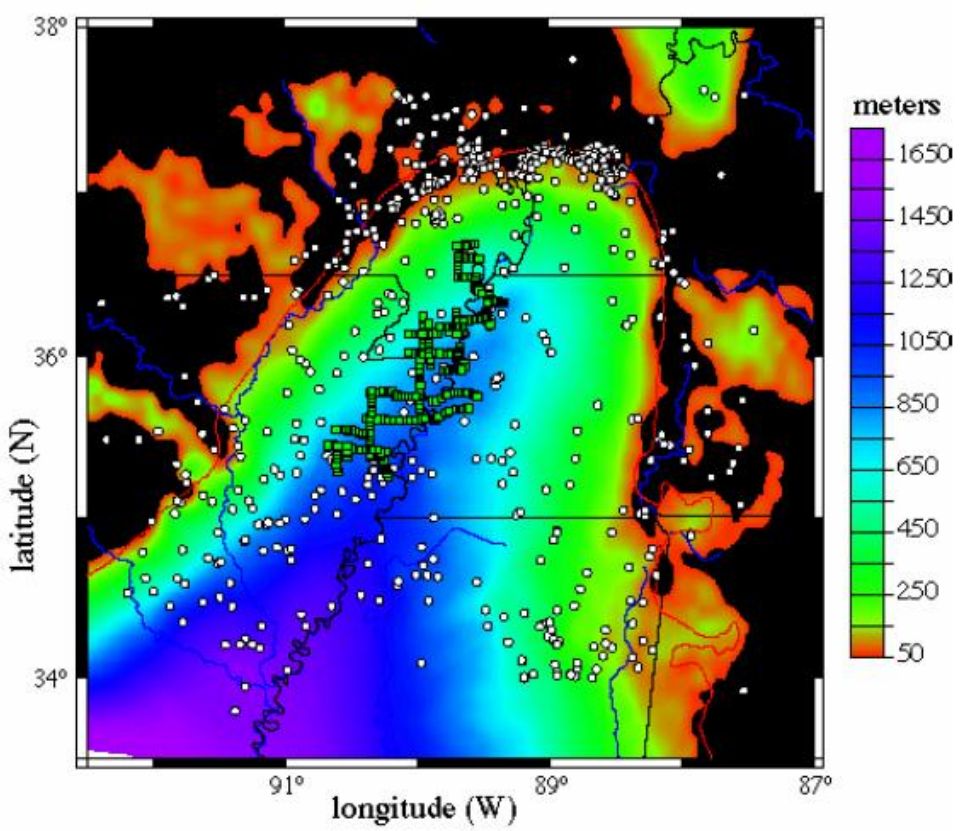

Figure 3.2 Thickness of Mississippi Embayment sediments
(reference: http://www.ceri.memphis.edu/usgs/model/sedthick.shtml)

Statistical characteristics of cone tip resistance and sleeve friction in the Upper Mississippi Embayment were estimated using cone penetration test (CPT) data of 90 soundings obtained from the web site (http://geosystems.ce.gatech.edu/Faculty/Mayne /Research/index.html) of Dr. Paul W. Mayne's group at Georgia Tech. The sounding locations are shown in Figure 3.3. Statistical analysis of the CPT data was performed for five soil types including sand, silty sand, sandy silt, clayey silt, and clay, which were classified using the empirical chart developed by Robertson et al. (1986) as discussed in Chapter 2.

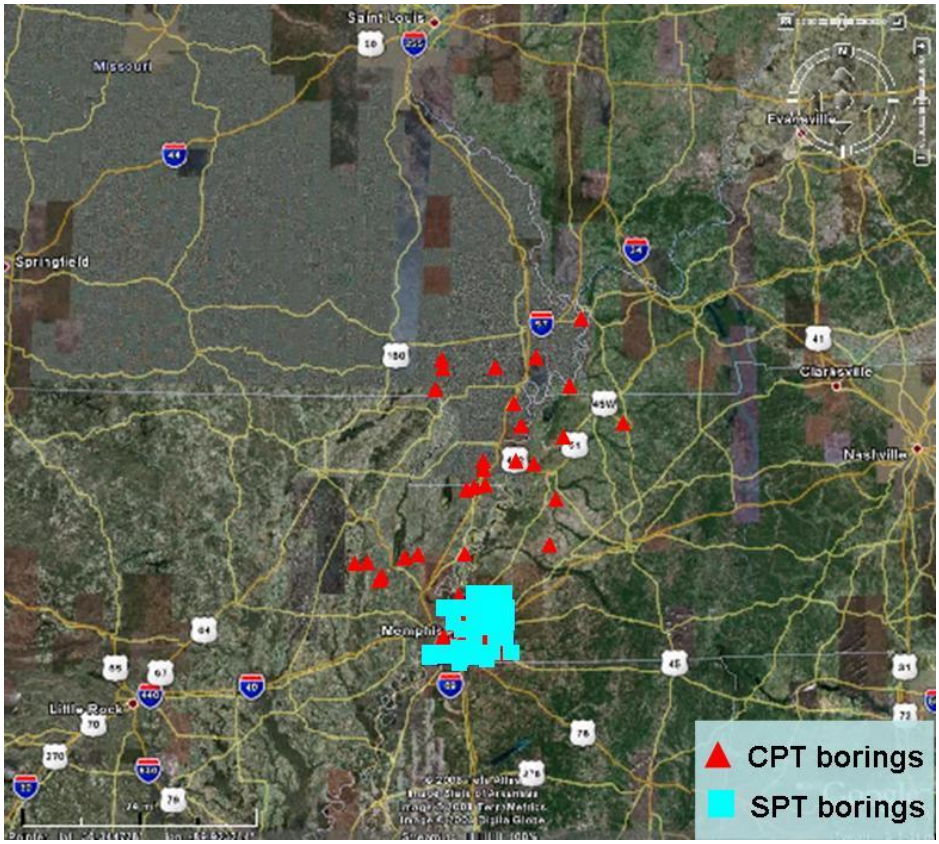

Figure 3.3 CPT and SPT locations in the Upper Mississippi Embayment

Statistical analysis of CPT data was performed for soil layers greater than 2 m in thickness on the assumption that a thickness of 2 m or greater is sufficient to avoid potential statistical error or measurement error that may be occurred when soil layers with thickness less than their zero-correlation distance or scale of fluctuation are analyzed. The CPT soundings were performed to depths between approximately 9 and 39 m, with a sampling interval of 2.5 cm. Figure 3.4 shows the results of a representative CPT performed in the Upper Mississippi Embayment. The remainder of the CPT profiles is included in Appendix A-1.

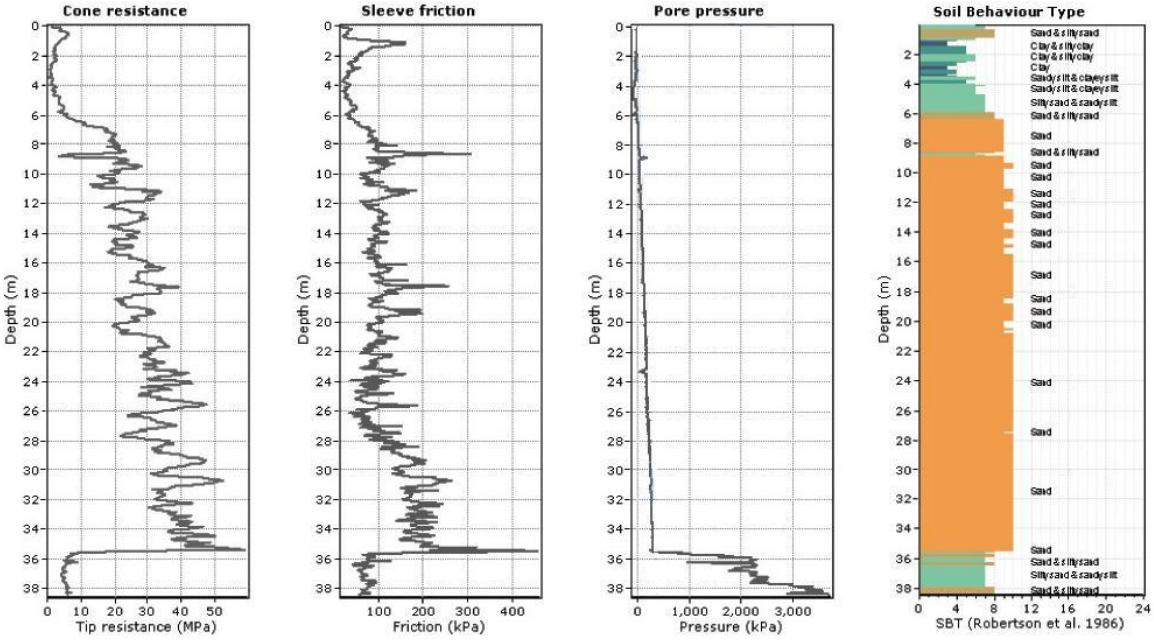

Figure 3.4 Result of CPT-4 performed in Blytheville, Arkansas in the Upper Mississippi Embayment

(reference: http://geosystems.ce.gatech.edu/Faculty/Mayne/Research/index.html)

Statistical analysis of Standard Penetration Test (SPT) *N* values in the Memphis subregion of the Upper Mississippi Embayment was performed using 623 SPT profiles collected by Ng et al. (1989) and additional 894 SPT profiles collected by Hwang et al. (1999). The SPT boring locations are shown in Figure 3.3. Unfortunately, some SPT profiles among the SPT profiles collected by Ng et al. (1989) and Hwang et al. (1999) have been lost. In the present study, 1420 SPT profiles were used to perform statistical analyses of *N* values. These SPT profiles constitute a considerable amount of data, but soil type, surface elevation, ground water table, and *N* values are occasionally absent. The SPT data in the Memphis subregion of the Upper Mississippi Embayment were obtained with a sampling interval of 2 feet (0.6 m). Considering the depth to drive a split-spoon sampler during *N* value measurement, the 2.0-foot sampling interval indicates subsequent measurements of *N* value with depth. Statistical characteristics of nine soil types including SP, SP-SM, SM, SM-SC, SC, ML, ML-CL, CL, and CH based on the Unified Soil Classification System (USCS) were estimated. Statistical analysis was focused on soil type layers with thickness of more than 16 feet (4.8 m). Figure 3.5 shows the results of a representative SPT performed in the Memphis subregion of the Upper Mississippi Embayment. The rest of the SPT boring logs are provided in Appendix A-2.

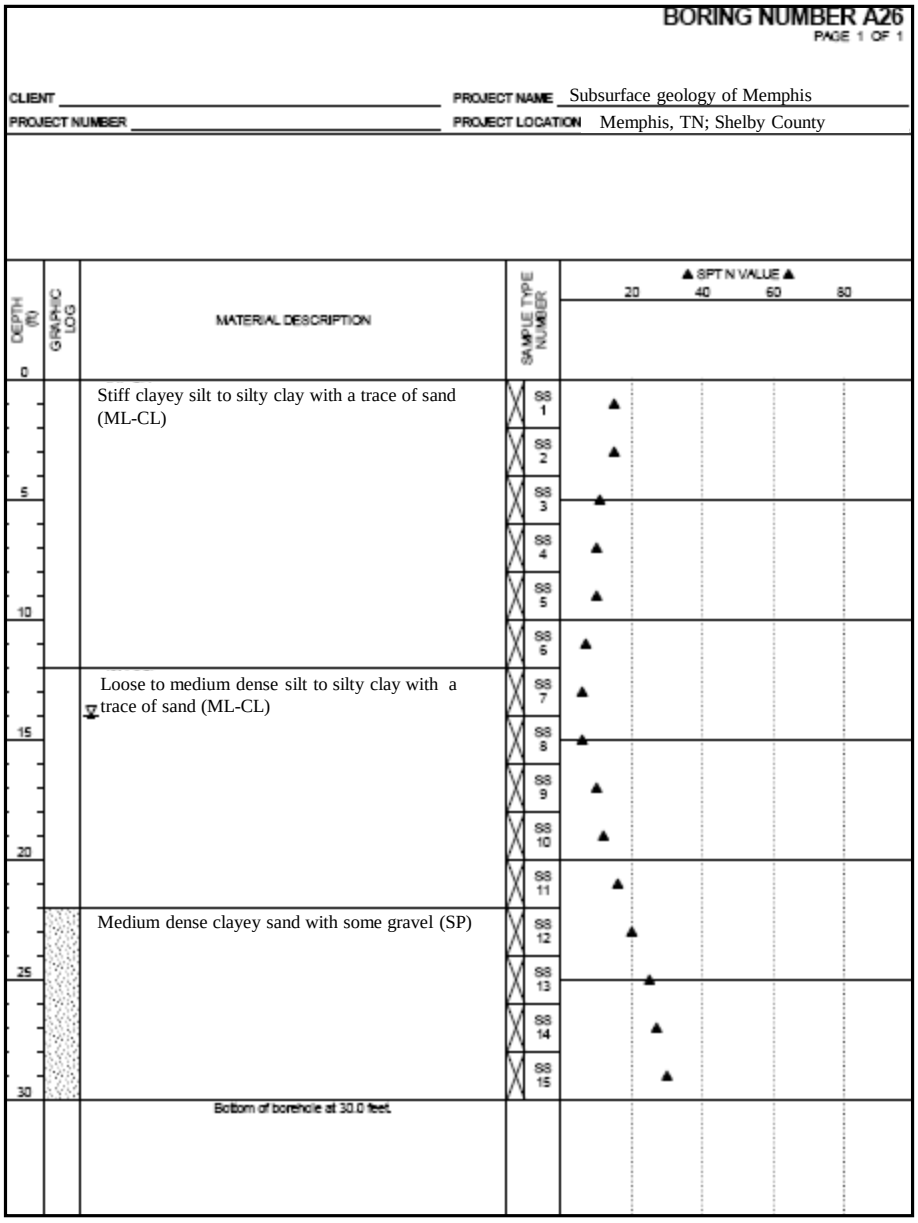

Figure 3.5 Result of a representative SPT boring log performed in the Memphis subregion (Upper Mississippi Embayment)

3.2.2. Piedmont Province

The Piedmont Province is located in the southeastern United States. It measures 161 km wide and 1290 km long, lying between the Blue Ridge Mountains to the west and the Coastal Plain to the east, as illustrated in Figure 3.6.

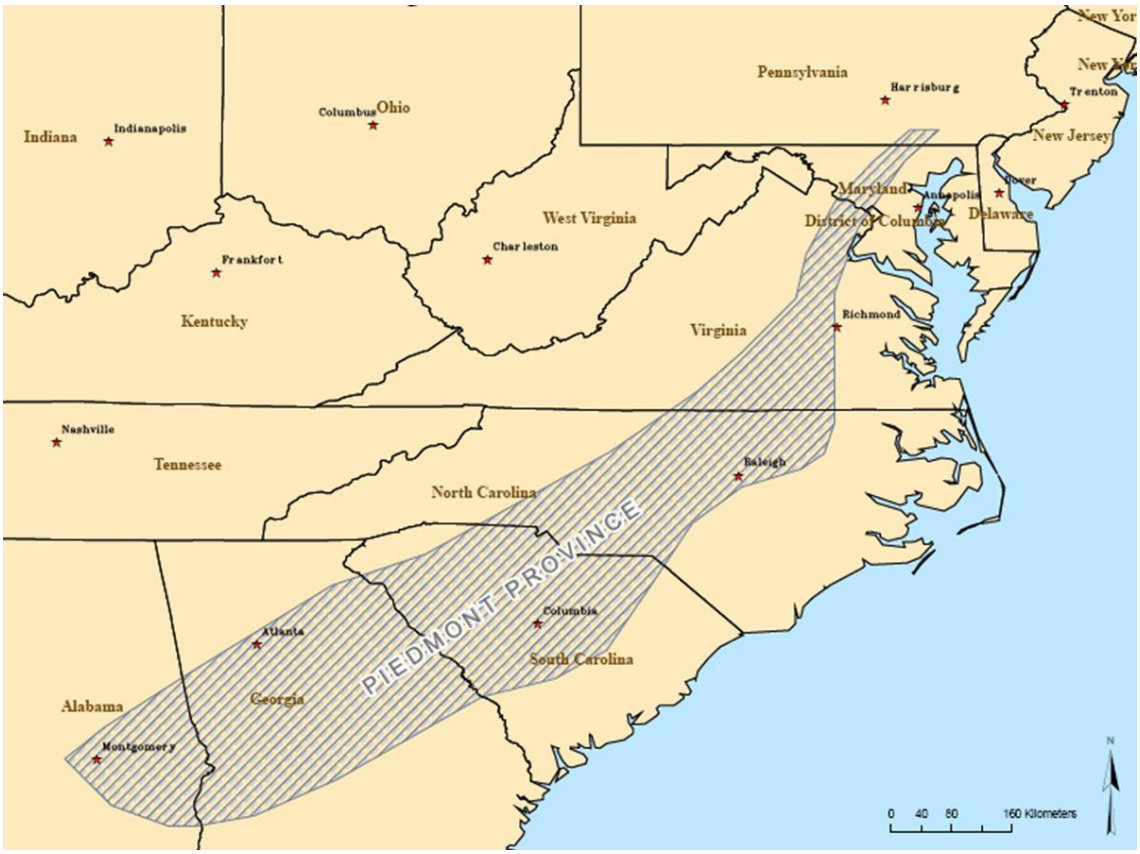

Figure 3.6 Map of Piedmont Province

Piedmont residual soils, found across the Piedmont Province, are formed by the chemical weathering of various complex aluminum silicate minerals of original rock. The Southeastern Piedmont residuum is mainly kaolinite, commonly termed saprolite; chemically weathered from original rock, it is prone to contain montmorillonites (Sowers, 1963; Sowers and Richardson, 1983). Piedmont residual soils are categorized typically as silty sands (SM) to sandy silts (ML) according to the USCS. Generally, the Piedmont residual soils feature red or reddish brown coloration found in the feldspar and mica due to oxidation of iron and aluminum (Gidigasu, 1976; Sowers, 1963; Willmer et al., 1982; Blight, 1997). The temperate and warm temperatures, abundant moisture, and well-

established vegetation result in rapid weathering. Weathering profiles from the Piedmont Province vary significantly due to local variations seen in rock mineralogy, rock structure, topography, erosion rates, and regional variations in temperature and rainfall (Gidigasu, 1976; Townsend, 1985).

As shown in Figure 3.7, the following describes the general weathering profiles in the Piedmont Province with increasing depth:

(1) Upper zone

The upper zone is completely weathered to a depth of about 3 meters (Sowers, 1963). This zone is typically composed of residual soils (Petersen et al., 1999; Sowers, 1963; Sowers and Richardson, 1983). According to USCS, this zone consists of CL or CL-ML materials.

(2) Intermediate zone

The soils of the intermediate zone are typically termed saprolite because the clay minerals are largely composed of kaolintes such as kaolinte and halloysite. Its thickness is 6.1 m to 24 m, and its soil texture shows relict structure of the original rock with *N* values of less than 50–70 (Petersen et al., 1999). This zone also is classified as residual soils (Sowers, 1963; Sowers and Richardson, 1983).

(3) Partly weathered zone

The partly weathered zone is a zone having less weathering than the saprolite zone with *N* values greater than 50–70 (Petersen et al., 1999). This zone contains seams of

hard-weathered rock and soil of coarser grain as compared to the saprolite zone (Sowers, 1963).

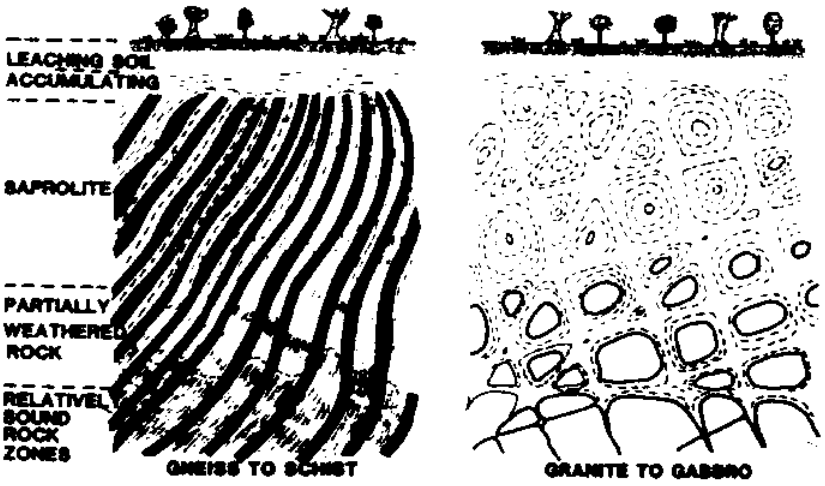

Figure 3.7 Weathering Profile of Crystalline Rocks in Humid Temperature Region (Sowers and Richardson, 1983)

The statistical characteristics of cone tip resistance and sleeve friction in the Piedmont Province were estimated using CPT data of 85 soundings obtained from the web site (http://geosystems.ce.gatech.edu/Faculty/Mayne/Research/index.html) of Dr. Paul W. Mayne's group at Georgia Tech. The locations of the soundings are shown on the map in Figure 3.8.

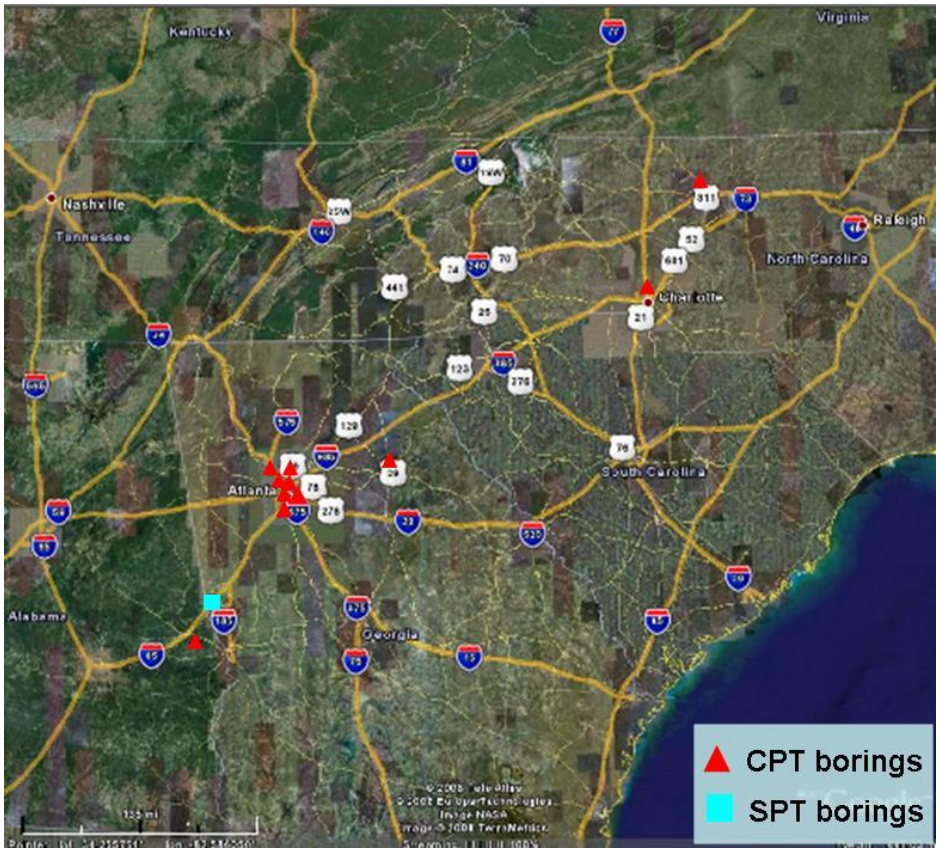

Figure 3.8 CPT and SPT boring locations in the Piedmont Province

Statistical characteristics were estimated from CPT data in five soil type layers including sand, silty sand, sandy silt, clayey silt, and clay, which were classified via the soil classification system introduced by Robertson et al. (1986). As noted earlier, statistical analyses of CPT data in each soil type layer were performed for layers greater than 2 m in thickness. The CPT soundings were terminated at depths between approximately 1.4 and 30 m and were measured with a sampling interval of 2.5 cm. Figure 3.9 shows the results of a representative CPT performed in the Piedmont Province. The rest of the CPT profiles are presented in Appendix B-1.

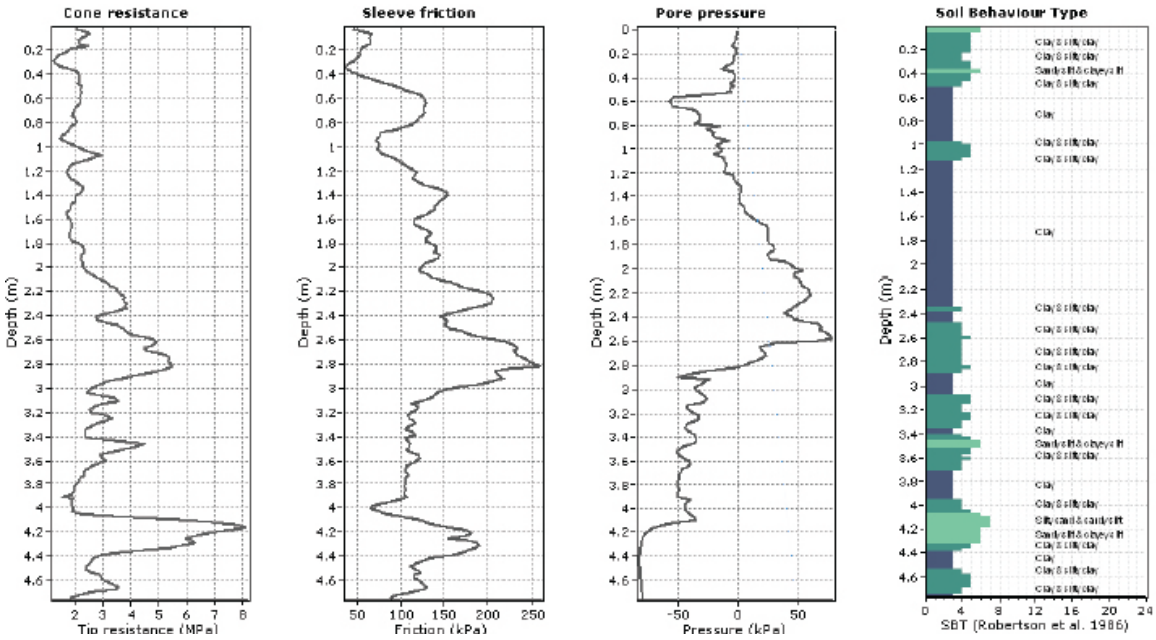

Figure 3.9 Result of CPT-1 performed in Atlanta, Georgia in the Piedmont Province (reference: http://geosystems.ce.gatech.edu/Faculty/Mayne/Research/index.html)

Statistical analysis of SPT data in the Piedmont Province was performed using 115 SPT profiles provided by Mr. Douglas Gilmore of S&ME, Inc., Kennesaw, Georgia. These SPT profiles provide soil classification, surface elevation, ground water table, and *N* value. The SPT boring locations in the Piedmont Province are shown in Figure 3.8. The SPT data in the Piedmont Province were measured with a sampling interval of 5 feet (1.5 m). Statistical characteristics of SM and ML soil types were estimated. Statistical analysis focused on soil type layers with thickness of more than 25.0 feet (7.5 m). Figure 3.10 shows the results of a representative SPT boring performed in the Piedmont Province. The remainder of the SPT boring logs is attached in Appendix B-2.

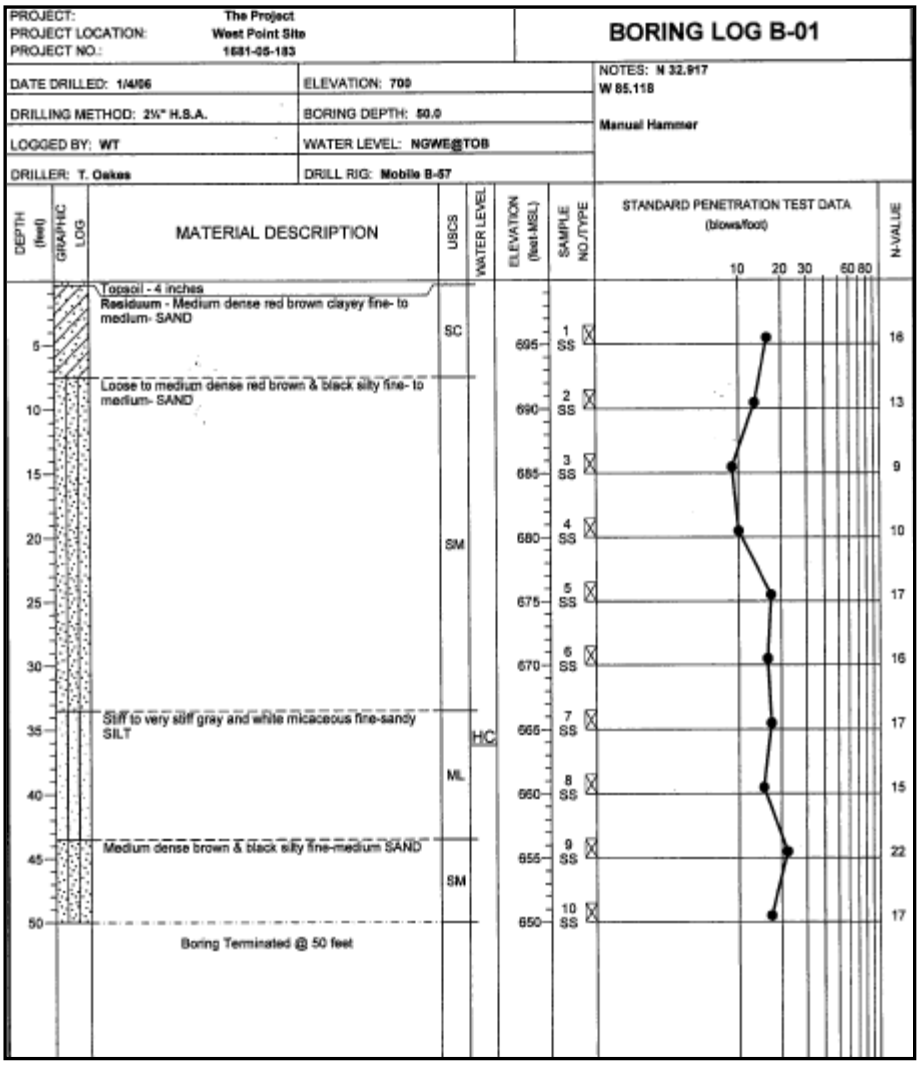

Figure 3.10 Result of a representative SPT boring performed in the Piedmont Province

3.2.3. Coastal Plain Province

The third study area is located in the Atlantic Coastal Plain of South Carolina. Two-thirds of South Carolina falls within the Coastal Plain area, which is nearly flat and mainly consists of sediments of sand, silt, and clay (Olsen et al., 1991; South Carolina Emergency Preparedness Division, 2007). The area extends from the southeast shoreline to the northwest about 70 miles (South Carolina Emergency Preparedness Division, 2007). The boundary of the Atlantic Coastal Plain of South Carolina is a discontinuity

called the Fall Line that extends in a northeast-southwest direction bisecting the state into two major soil provinces. There is a third zone, the Blue Ridge Province, in the extreme northwest. The Atlantic Coastal Plain of South Carolina is located in the southeastern portion of the state. Stratigraphy of this state consists, in order of decreasing depth, of Paleozoic crystalline rock as a bedrock, a Mesozoic basin with Pre-Cretaceous hard sedimentary and igneous rock, and loosely-deposited recent sediments as the top part as shown in Figure 3.11. Sediments in the Atlantic Coastal Plain of South Carolina consist of marine deposits formed during periods of high sea level. The sedimentation process resulted in relatively thick layers of coarse-grained soil.

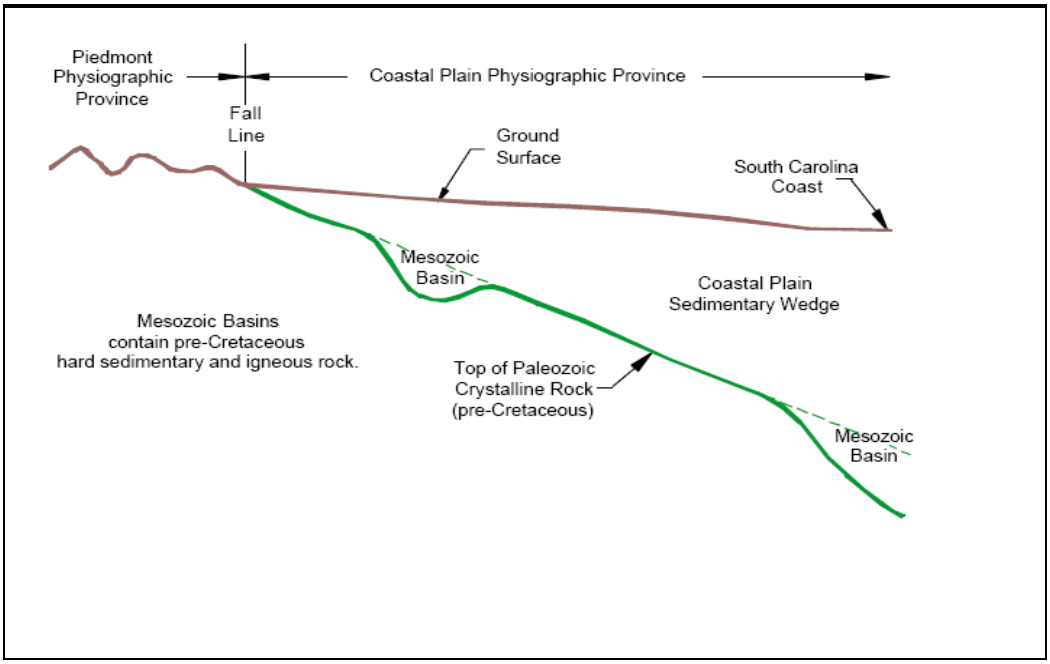

Figure 3.11 Conceptual profile of the Coastal Plain Province in South Carolina (South Carolina Emergency Preparedness Division, 2001)

Figure 3.12 shows the thickness of sediments of the Coastal Plain Province in South Carolina. As one can see, the contour lines show that the thickness of sediments in the east-west section ranges from zero on the Fall Line to approximately 1,250 m at the southernmost corner of South Carolina; the thickness of sediments decreases along the northeastern coastline.

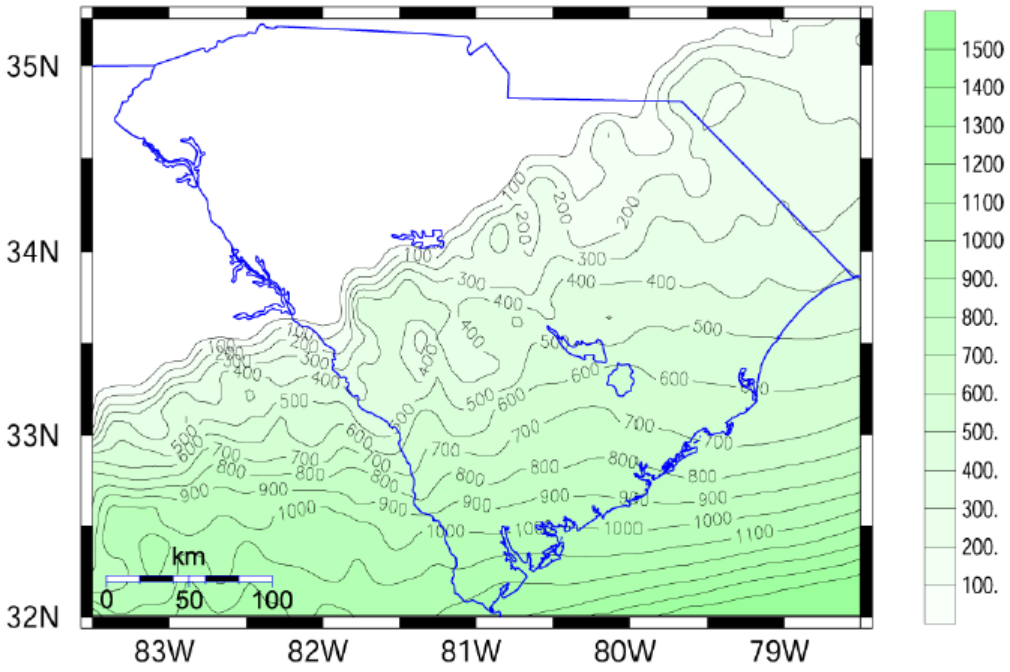

Figure 3.12 Sediment thickness of the Coastal Plain Province in South Carolina (unit of depth: meter) (reference: http://www.scdot.org/doing/pdfs/Reporttxt.pdf)

Statistical analysis of CPT data obtained from the Atlantic Coastal Plain of South Carolina was performed using CPT data of 22 soundings obtained from the web site (http://geosystems.ce.gatech.edu/Faculty/Mayne/Research/index.html) of Dr. Paul W. Mayne's group at Georgia Tech. The sounding locations are shown in Figure 3.13. The CPT soundings were terminated at depths between approximately 7 and 35.5 m, and were

sampled at intervals of 2.5 cm. Statistical characteristics of CPT data in silty sand, sandy silt, and clay deposits exceeding 2 m in thickness were estimated. Figure 3.14 shows the results of a representative CPT performed in the Atlantic Coastal Plain. The rest of the CPT soundings are included in Appendix C-1.

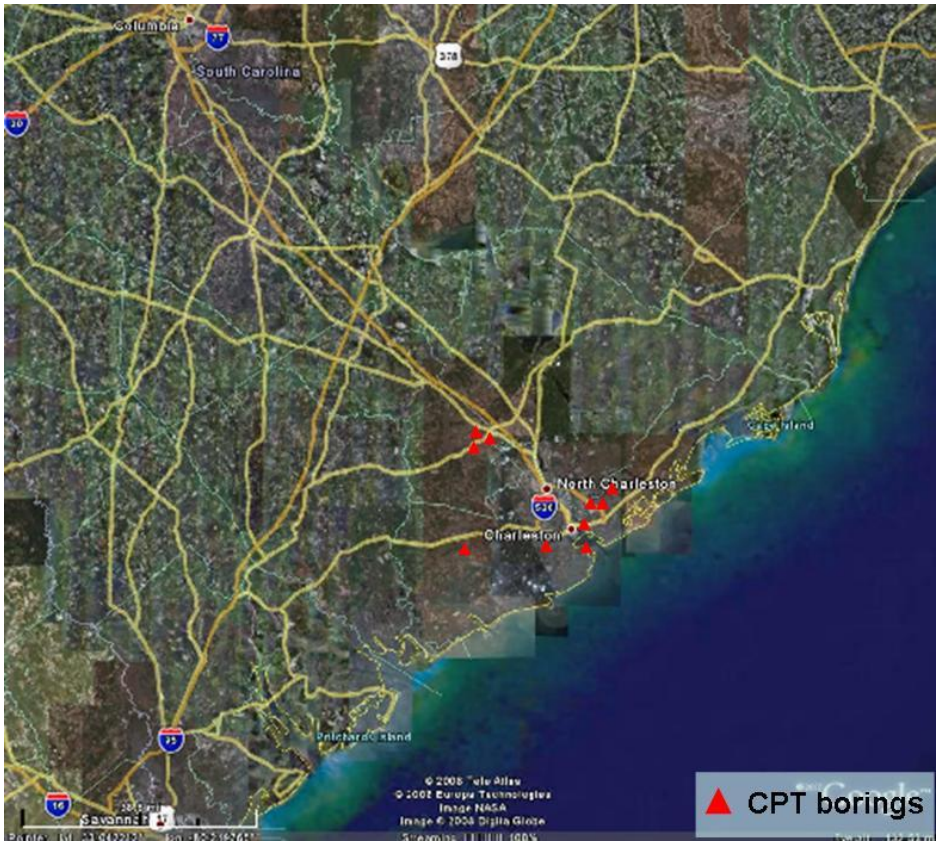

Figure 3.13 CPT boring locations in the Coastal Plain Province

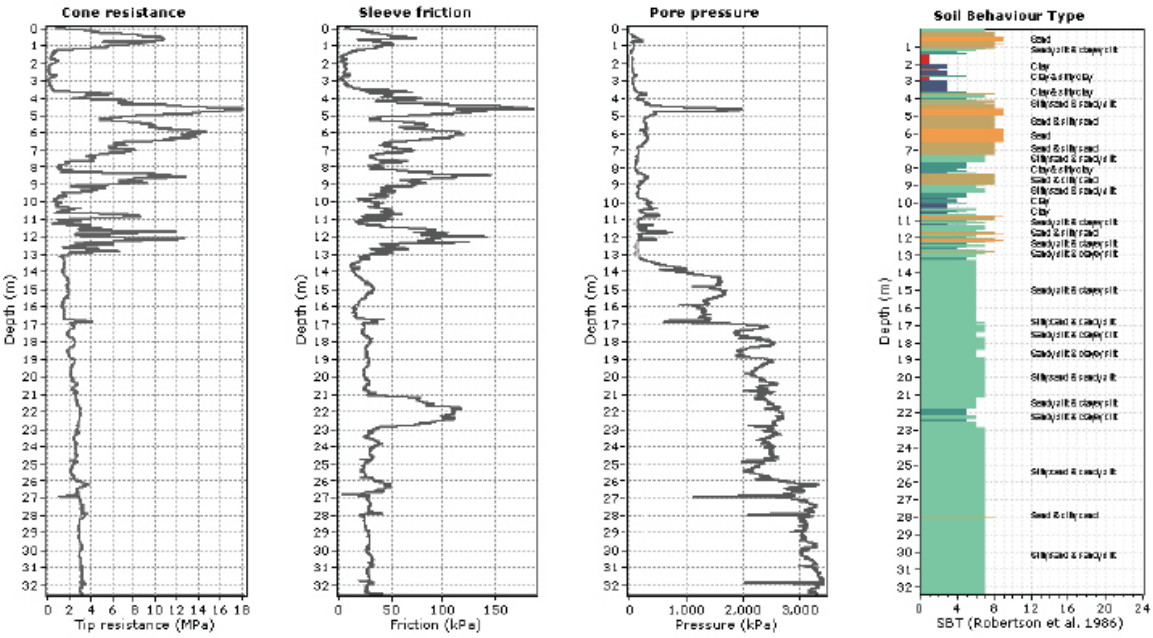

Figure 3.14 Result of CPT-2 performed in Mt. Pleasant, SC in the Coastal Plain Province (reference: http://geosystems.ce.gatech.edu/Faculty/Mayne/Research/index.html)

3.3. Coefficient of variation (COV) in vertical direction

3.3.1. CPT

In this section, using data from sublayers that are identified as spatially homogeneous by the soil-behavior-type classification system suggested by Robertson et al. (1986), and verified as statistically homogeneous by the method of reverse arrangements (Bendat and Piersol, 1986), the coefficients of variation of the CPT data in the Upper Mississippi Embayment, the Atlantic Coastal Plain Province, and the Piedmont Province were estimated.

Tables 3.1 to 3.3 summarize the average values of COV of each soil layer for CPT data including cone resistance and sleeve friction in the Upper Mississippi Embayment, the Atlantic Coastal Plain Province, and the Piedmont Province.

Table 3.1 Results of average values of COV of each soil layer for CPT data in the Upper Mississippi Embayment

Area	Soil Property	COV	Soil Type				
			Sand	Silty Sand	Clayey Silt	Silty Clay	Clay
Upper Mississippi Embayment	Cone Resistance	Average (%)	23	21	23	26	26
		Standard Deviation (%)	9	11	14	12	14
		No. of Samples	66	11	9	9	20
	Sleeve Friction	Average (%)	33	29	31	41	38
		Standard Deviation (%)	11	12	19	16	16
		No. of Samples	66	11	9	9	20

Table 3.2 Results of average values of COV of each soil layer for CPT data in Piedmont Province

Area	Soil Property	COV	Soil Type				
			Sand	Silty Sand	Sandy Silt	Clayey Silt	Clay
Piedmont Province	Cone Resistance	Average (%)	21	20	18	16	15
		Standard Deviation (%)	7	8	8	6	10
		No. of Samples	10	13	11	11	66
	Sleeve Friction	Average (%)	32	26	23	20	19
		Standard Deviation (%)	14	13	11	7	10
		No. of Samples	10	13	11	11	66

Table 3.3 Results of average values of COV of each soil layer for CPT data in the Coastal Plain Province

Area	Soil Property	COV	Soil Type		
			Silty Sand	Sandy Silt	Clay
Coastal Plain Province	Cone Resistance	Average (%)	22	15	28
		Standard Deviation (%)	12	10	14
		No. of Samples	13	12	10
	Sleeve Friction	Average (%)	29	26	32
		Standard Deviation (%)	16	19	11
		No. of Samples	13	12	10

Figures 3.15 to 3.16 illustrate the first quartile, the third quartile, median, maximum, and minimum values of COV of cone resistance and sleeve friction for coarse-grained and fine-grained soils of each area.

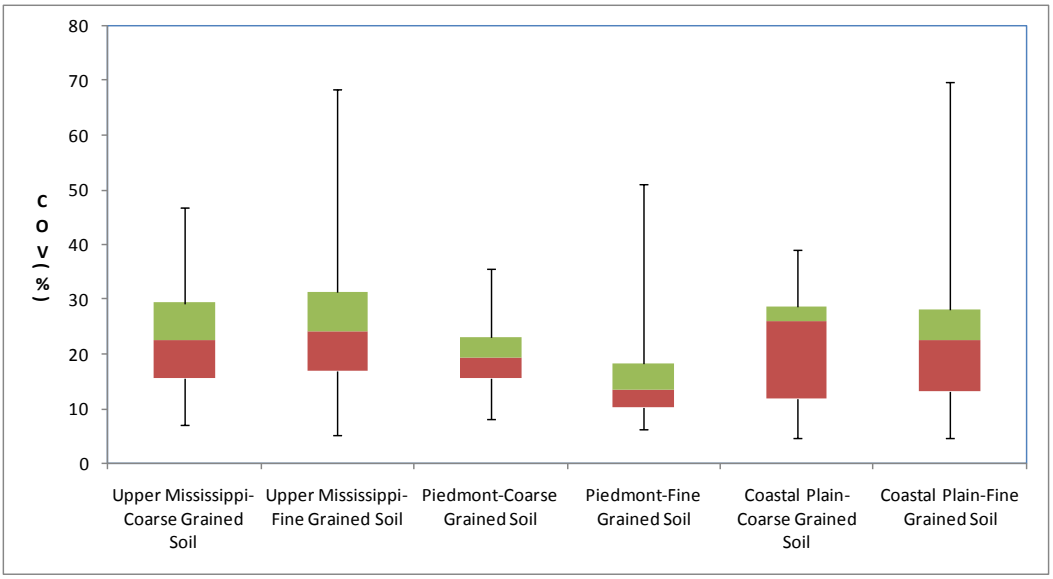

Figure 3.15 The first quartile, the third quartile, median, maximum, and minimum values of COV of cone resistance for soil type of each area

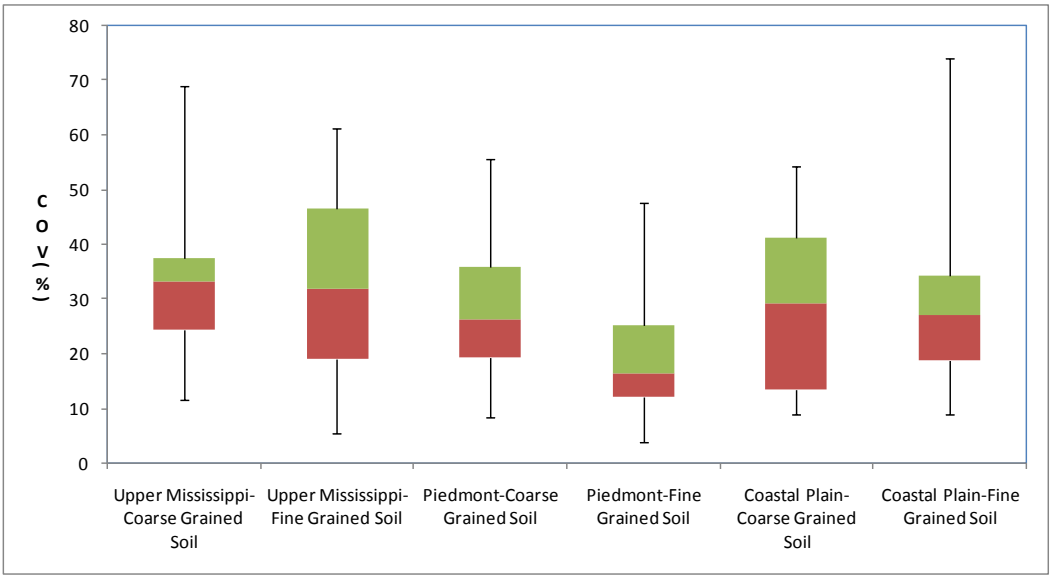

Figure 3.16 The first quartile, the third quartile, median, maximum, and minimum values of COV of sleeve friction for soil type of each area

Hypothesis testing was employed to interpret the results of data analysis in a statistical sense. An emphasis was put on the statistical differences between granular soil layer (i.e., sand layer) and fine soil layer (i.e., clay layer). It was assumed that COVs of each soil layer are independent normal distributions and have different sample numbers, and the unknown population variances of COV of each soil layer are not necessarily equal. The *t* test on two samples was employed to satisfy these conditions. For the null hypothesis, it was assumed that the population mean values of COV of the two soil type layers are equal to each other: $\mu_1 = \mu_2$. A 10% level of significance (α) for this hypothesis testing was applied to make a valid statistical conclusion on the assumption that a 10% level of significance is sufficiently high for this hypothesis testing. The *t* test statistic is

$$t_{\text{statistic}} = \frac{\bar{x}_1 - \bar{x}_2}{\sqrt{\frac{\bar{s}_1^2}{n_1} + \frac{\bar{s}_2^2}{n_2}}} \qquad (3.3.1)$$

where $\bar{x}_1$ and $\bar{x}_2$ are the sample means, $\bar{s}_1$ and $\bar{s}_2$ are the sample standard deviations, and n_1 and n_2 are sample numbers.

The degrees of freedom (D_F) are calculated by

$$D_F = \frac{\left(\frac{\bar{s}_1^2}{n_1} + \frac{\bar{s}_2^2}{n_2}\right)^2}{\frac{\left(\bar{s}_1^2 / n_1\right)^2}{n_1 + 1} + \frac{\left(\bar{s}_2^2 / n_2\right)^2}{n_2 + 1}} - 2 \qquad (3.3.2)$$

The null hypothesis is rejected if $t_{statistic} > t_{\alpha / 2, D_F}$ and accepted if $t_{statistic} < t_{\alpha / 2, D_F}$.

Table 3.4 shows the statistically meaningful soil types for the average COV values of cone resistance and sleeve friction in each subregion.

Table 3.4 Statistically meaningful soil types for the average COV values of cone resistance and sleeve friction in each subregion

	Cone Resistance	Sleeve Friction
Upper Mississippi Embayment	None	COV of Clay ≠ COV of Silty Sand where ≠ : statistically different from each other
Piedmont Province	COV of Sand ≠ COV of Clayey Silt COV of Sand ≠ COV of Clay COV of Clay ≠ COV of Silty Sand	COV of Sand ≠ COV of Clayey Silt COV of Sand ≠ COV of Clay COV of Clay ≠ COV of Silty Sand
Coastal Plain Province	COV of Clay ≠ COV of Sandy Silt	None

The null hypotheses for the average COV values of all cone resistance and sleeve friction for each soil type layer except for sleeve friction between clay and silty sand layers in the Upper Mississippi Embayment can not been rejected as shown in Appendix D. This indicates that the differences between the average COV values of cone resistance and sleeve friction for each soil type layer (except for sleeve friction between clay and silty sand layers in the Upper Mississippi Embayment) are not statistically significant.

The average COV values for the Piedmont Province provided the following results:

- Statistically meaningful results:
  - Cone resistance between sand and clayey silt layers, sand and clay layers, and clay and silty sand layers.
  - Sleeve friction between sand and clayey silt layers, sand and clay layers, and clay and silty sand layers.
- No statistically significant differences (thus the values for these soil layers appear to be statistically equal to each other):

- Cone resistance and sleeve friction of the sand layer versus the silty sand and sandy silt layers.
- Clay layer versus the clayey silt and sandy silt layers.

The average COV values of the cone resistance between clay and sandy silt layers in the Coastal Plain Province presented statistically meaningful results. That is, the COV values of cone resistance between clay and sandy silt layers in the Coastal Plain Province were statistically different from each other.

Not a few geotechnical engineers denominate soil type by combining a major grain size component with minor grain size components in suffixes [i.e., *trace* (0 to 15%), *some* (16 to 30%), *-y* (31 to 45%), and *and* (46 to 49%)] based on the portion of grain size components (Sowers, 1979). However, the sandy silt layers (consisting 45 to 49% sand and 51 to 55% silt) still have a lower average COV value of cone resistance than the clay layers (consisting of 0 to 14% sand and 86 to 100% clay). Taking portions of grain size components of each soil type into account, in general, it is correct to conclude that granular soil layers in the Atlantic Coastal Plain Province are associated with lower levels of variation of soil properties than do very fine soil layers.

At least from the above evidence in the Upper Mississippi Embayment and the Coastal Plain Province, it may be concluded that an area with sedimentary, granular soil layers have lower levels of variation of soil property than do very fine soil layers. In the Piedmont Province, which is governed by a process of the chemical weathering of intact rock, very fine soil layers tend to have soil properties with lower variation than do granular soil layers, consistent with this conclusion. Figures 3.17 to 3.19 illustrate the

average values of COV of each soil layer for cone resistance and sleeve friction in these zones. From Figures 3.17 to 3.19, one can see that cone resistance and sleeve friction of granular soil layers and fine soil layers are in a trend depending on the soil formation processes: in the sleeve friction of the Upper Mississippi Embayment, silty sand layers have a lower average COV value than clay layers; in the cone resistance and sleeve friction of the Piedmont Province, the more granular a soil layer becomes, the higher average COV value it has; in the cone resistance of the Coastal Plain Province, the sandy silt layers have a lower average COV value than the clay layers. Taking into account the processes of soil formation, it is observed that the process of soil formation is to some extent associated with the level of variation of soil properties.

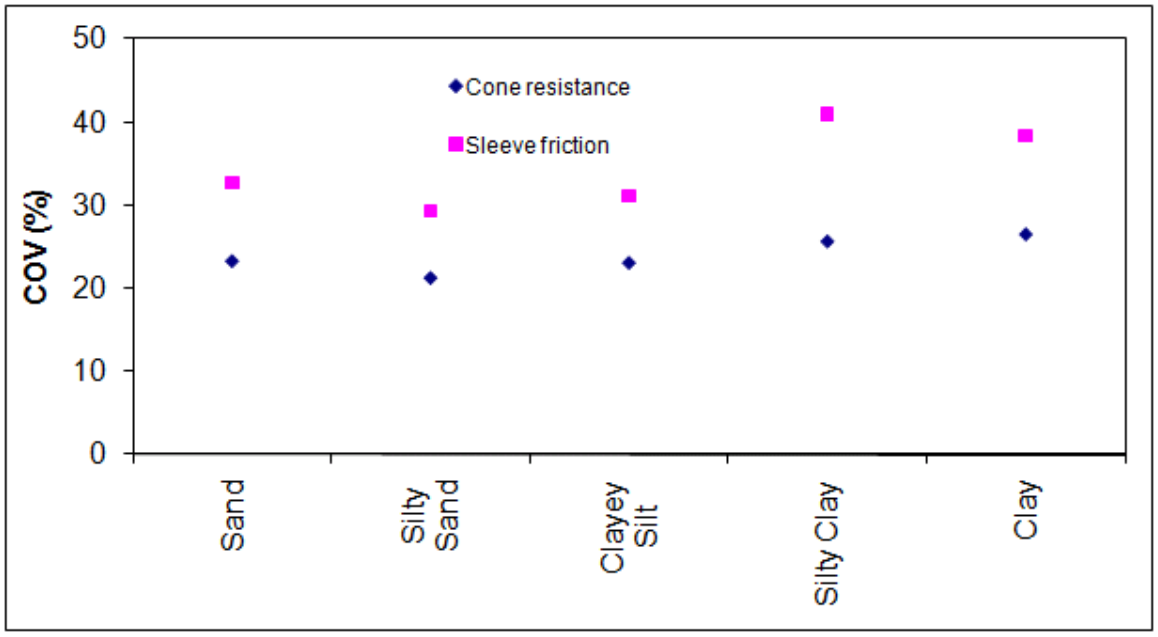

Figure 3.17 Average COV values of each soil layer for cone resistance and sleeve friction in the Upper Mississippi Embayment

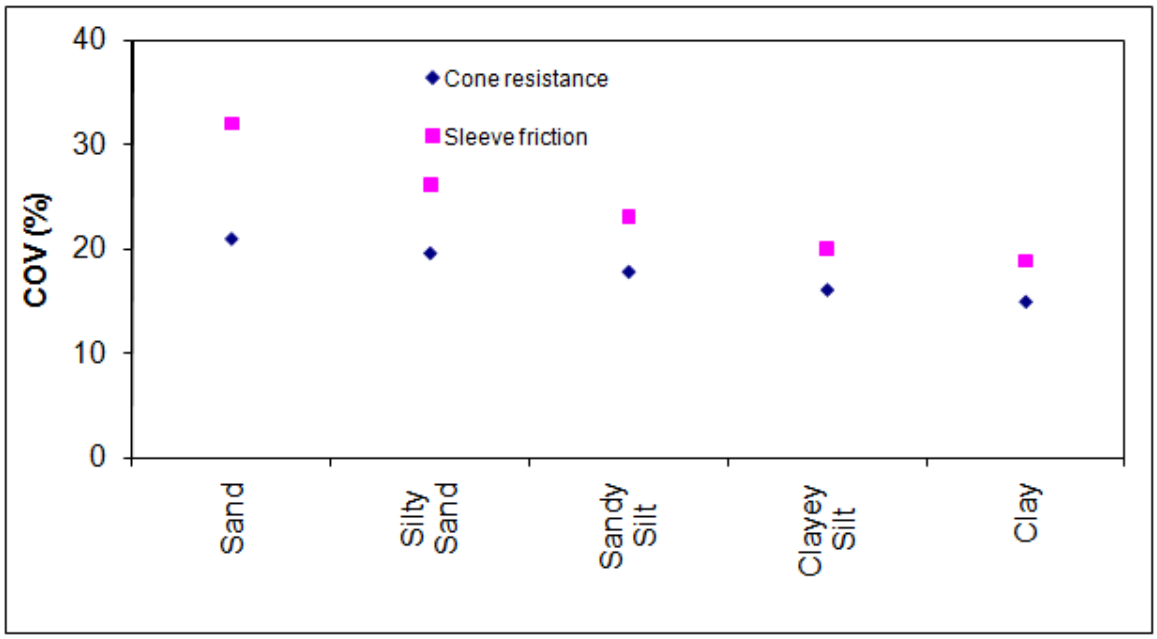

Figure 3.18 Average COV values of each soil layer for cone resistance and sleeve friction in the Piedmont Province

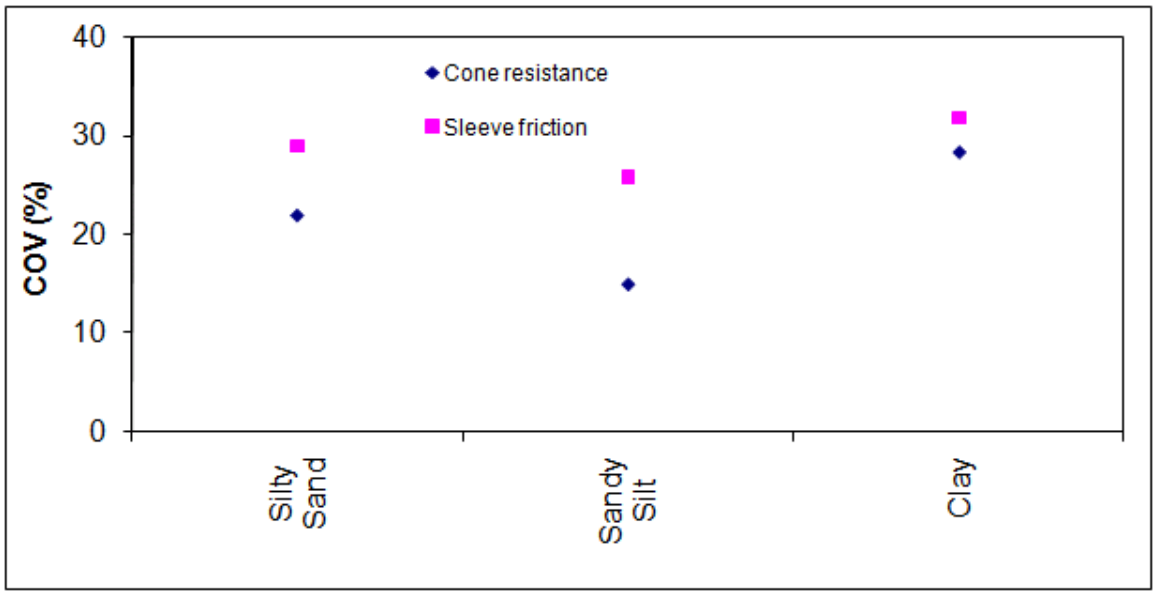

Figure 3.19 Average COV values of each soil layer for cone resistance and sleeve friction in the Coastal Plain Province

3.3.2. SPT

In the previous section, the values of COV of the CPT data obtained from the three zones based on the process of soil formation were estimated. In this section, the COVs of SPT data from the areas of the Memphis subregion (Upper Mississippi Embayment) and the Piedmont Province are estimated.

In the case of the Memphis subregion, all SPTs were performed with a sampling interval of 2 feet (around 61 cm). The Piedmont Province has *N* values with a sampling interval of 5 feet (around 152 cm). Tables 3.5–3.6 summarize the average values of the COV for *N* values of each soil type. Figure 3.20 illustrates the first quartile, the third quartile, median, maximum, and minimum values of COV of *N* values for coarse-grained and fine-grained soils of each area.

Table 3.5 Results of average values of COV of coarse- and fine-grained soil layers for SPT data in the Memphis subregion (Upper Mississippi Embayment)

Area	Soil Property	COV	Soil Type	
			Coarse-Grained Soil	Fine-Grained Soil
Upper Mississippi Embayment	No. of Samples		337	639
	N Value	Average (%)	29	34
		Standard Deviation (%)	16	17

Table 3.6 Results of average values of COV of coarse- and fine-grained soil layers for SPT data in the Piedmont Province

Area	Soil Property	COV	Soil Type	
			Coarse-Grained Soil	Fine-Grained Soil
Piedmont Province	No. of Samples		57	53
	N Value	Average (%)	23	20
		Standard Deviation (%)	9	8

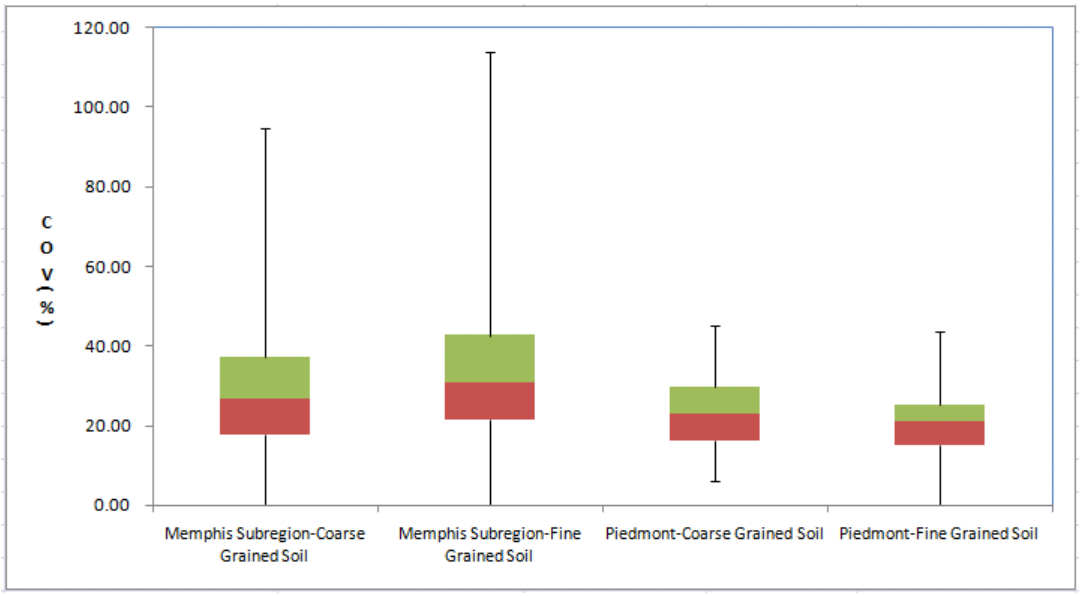

Figure 3.20 The first quartile, the third quartile, median, maximum, and minimum values of COV of coarse-grained and fine-grained soil layers for SPT data in each area

The two-sample *t* test was employed to interpret the results of data analysis in a statistical sense. For the null hypothesis, it was assumed that the mean values of COV of the two soil type layers are equal to each other. SP, SP-SM, SM, SM-SC, and SC type

soils were categorized as coarse-grained soils and ML, ML-CL, CL, CH type soils were categorized as fine-grained soils. A 10% level of significance for this hypothesis testing was applied to make a valid statistical conclusion. An emphasis was put on the statistical significance between granular soil type layers and fine soil type layers. As a result, the average COV values of *N* values between granular and fine soil layers in the Memphis subregion and the Piedmont Province presented statistically significant differences. In the Memphis subregion, the average COV value of *N* values of granular soil layers was lower than that of fine soil layers. In the Piedmont Province, the average COV value of *N* value of granular soil layers was greater than that of fine soil layers. From the above evidence, one can reach a conclusion consistent with the previous section: the Memphis subregion under the control of sedimentation has granular soil layers that tend to associate with lower levels of variation of soil property than do very fine soil layers; in the Piedmont Province, which is governed by a process of the chemical weathering of intact rock, granular soil layers tend to have soil properties with higher variation than do granular soil layers. Figure 3.21 exhibits the average values of COV of each soil layer for *N* values in these zones.

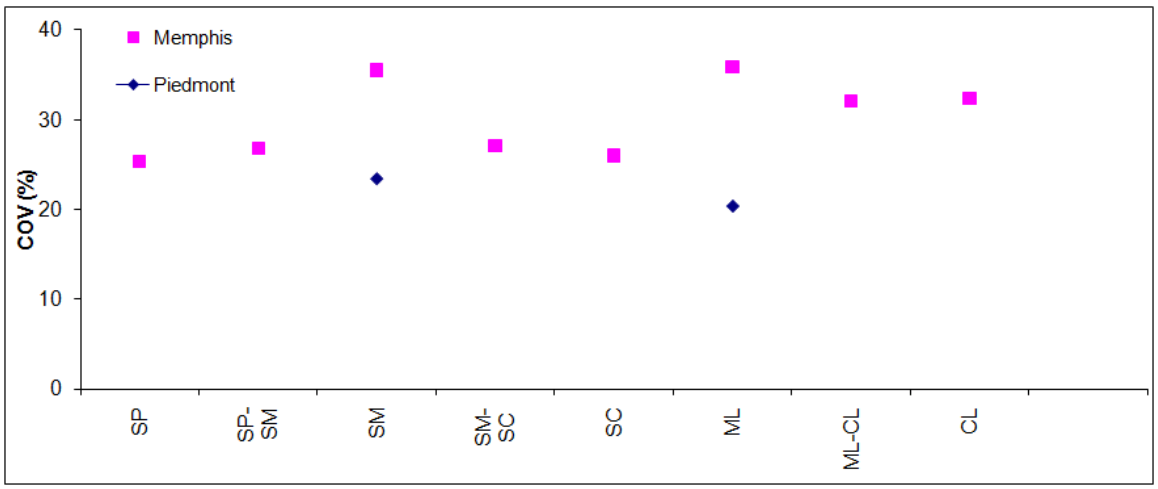

Figure 3.21 Average COV values of each soil layer for SPT data in each area

In this figure, one can see that average *N* values between granular soil type and fine soil type layers are in a common trend depending on the soil formation processes: in the Memphis subregion, the more granular a soil layer becomes (except for SM), the lower average COV value it has; in the Piedmont Province, the more granular a soil layer becomes, the higher average COV value it has. Taking into account the processes of soil formation, COV is an indicator for the degree of variation of soil property.

3.4. Correlation coefficient function in vertical direction

3.4.1. CPT

(1) Zero-correlation distance

The correlation coefficient function is obtained when the covariance function is divided by the variance of data. This decreases with increasing lag distance and has a maximum value of unity at zero lag distance; the lag distance is the relative distance between data points. This occurs because a soil property for closely separated data has, in general, greater affinity than for more widely separated data. That is, the closer the data points are, the stronger correlation of the soil property. The zero-correlation distance is the distance at which the spatial correlation coefficient function decays to zero. It is the distance within which the soil property shows relatively strong correlation from point to point. The effects of change in fluctuation on the statistical characteristics of soil properties using a simple sinusoidal sequence can be approximated. In brief, the value of the zero-correlation distance for a simple sinusoidal sequence with

at least 4 cycles tends to be approximately equal to a quarter value of its wavelength. More detailed factors that affect the statistical characteristics of soil properties will be discussed in Chapter 4. In this section, using CPT data from the three zones mentioned previously, based on the process of soil formation, zero-correlation distances of the data are estimated. Figures 3.22–3.24 provide examples to estimate zero-correlation distances for soil layers of CPT data.

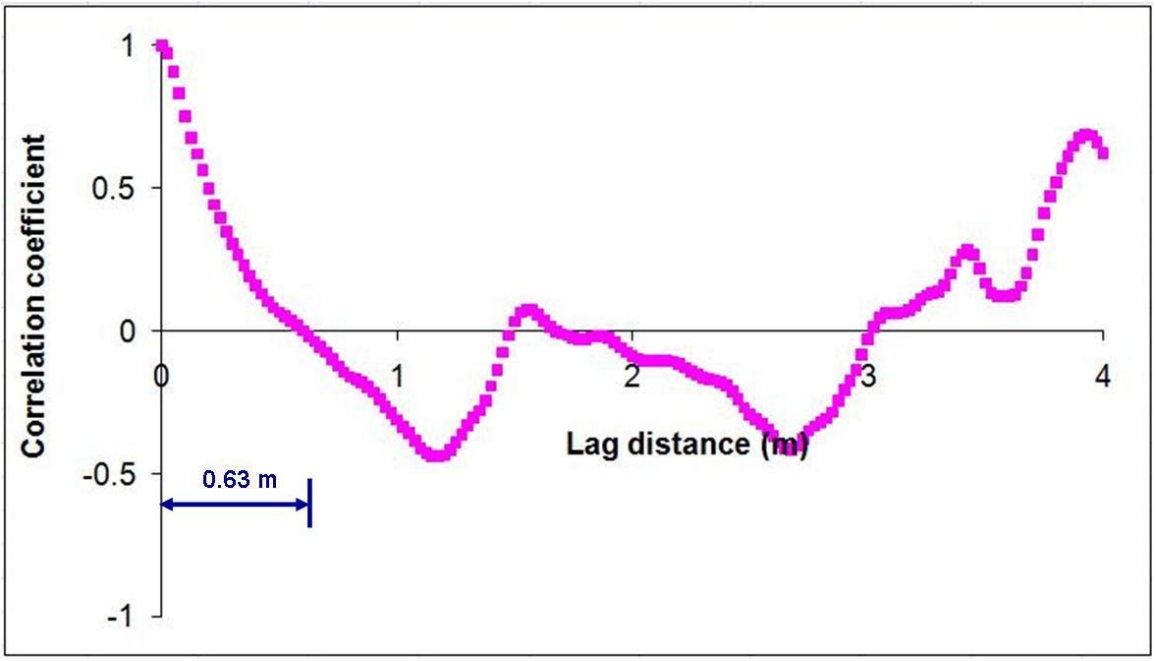

Figure 3.22 Estimation of zero-correlation distance for sand layer of CPT-90 data in Wyatt, MO

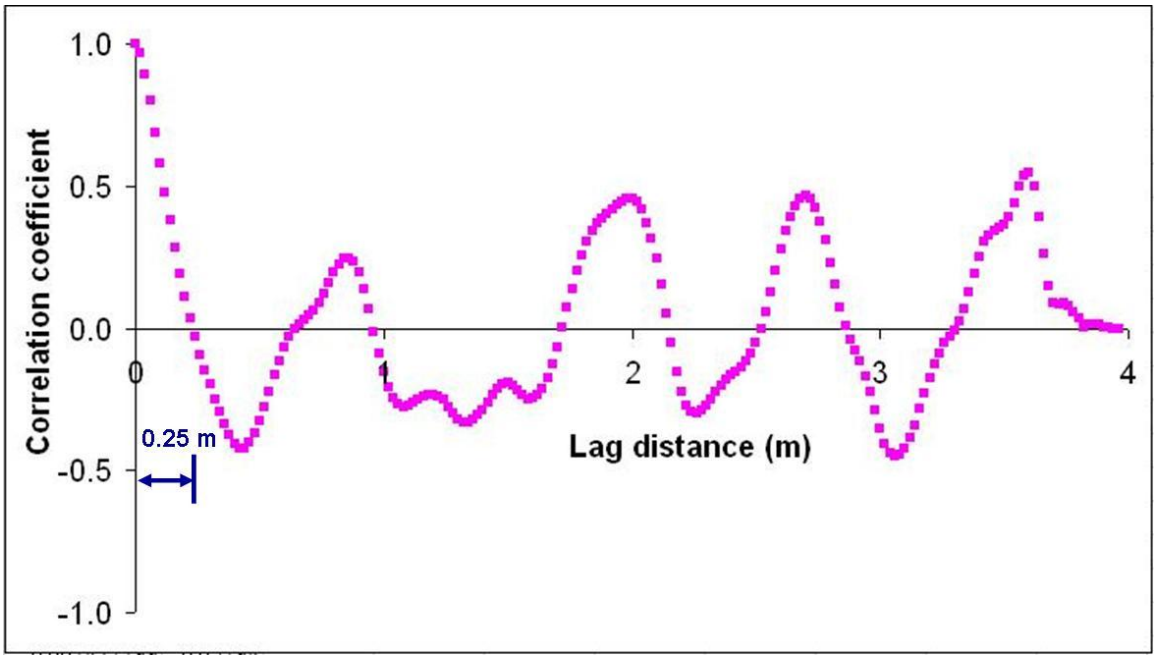

Figure 3.23 Estimation of zero-correlation distance for clay layer of CPT-62 data in Spring Villa, AL

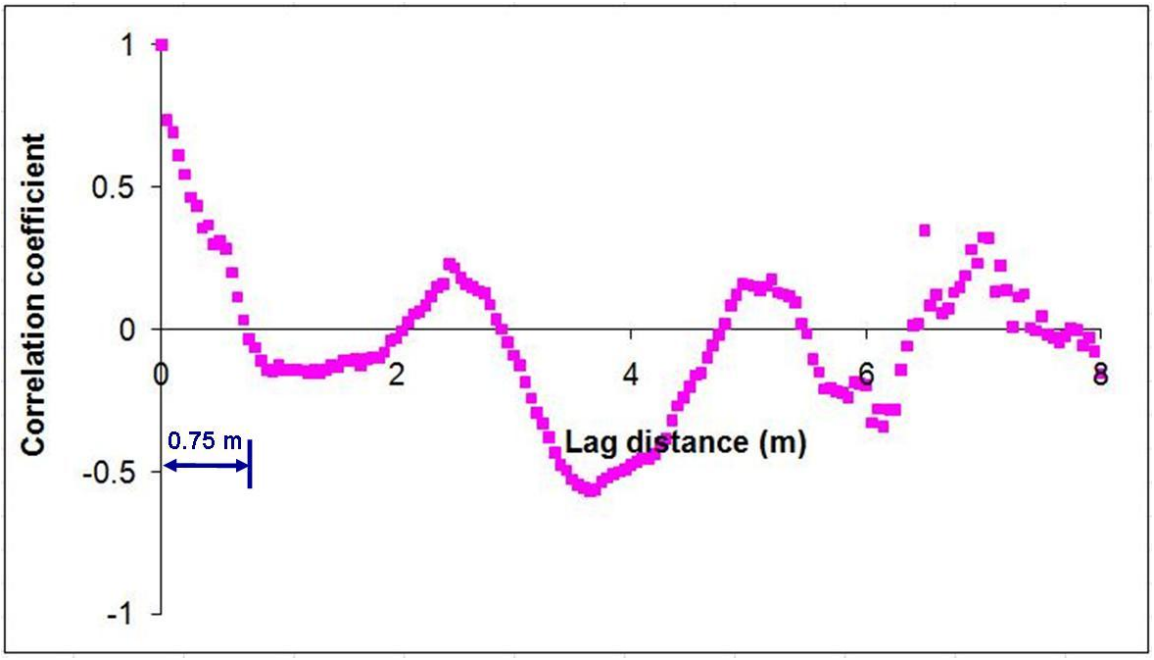

Figure 3.24 Estimation of zero-correlation distance for sandy silt layer of CPT-1 data in Charleston, SC

As mention in the previous section, sand and silty sand were defined as coarse-grained soils; sandy silt, clayey silt, and clay were defined as fine-grained soils. The results of zero-correlation distances of CPT data from these areas are summarized in Tables 3.7–3.9.

Table 3.7 Comparison of the zero-correlation distance of cone resistance and sleeve friction for each soil type in the Upper Mississippi Embayment

Area	Soil Property	Zero Correlation Distance	Soil Type	
			Coarse-Grained Soil	Fine-Grained Soil
Upper Mississippi Embayment	No. of Samples		77	38
	Cone Resistance	Average (m)	0.93	0.49
		Standard Deviation (m)	0.28	0.16
	Sleeve Friction	Average (m)	1.01	0.47
		Standard Deviation (m)	0.37	0.11

Table 3.8 Comparison of the zero-correlation distance of cone resistance and sleeve friction for each soil type in the Piedmont Province

Area	Soil Property	Zero Correlation Distance	Soil Type	
			Coarse-Grained Soil	Fine-Grained Soil
Piedmont Province	No. of Samples		23	88
	Cone Resistance	Average (m)	0.27	0.43
		Standard Deviation (m)	0.06	0.27
	Sleeve Friction	Average (m)	0.23	0.38
		Standard Deviation (m)	0.03	0.22

Table 3.9 Comparison of the zero-correlation distance of cone resistance and sleeve friction for each soil type in the Coastal Plain Province

Area	Soil Property	Zero Correlation Distance	Soil Type	
			Coarse-Grained Soil	Fine-Grained Soil
Coastal Plain Province	No. of Samples		13	22
	Cone Resistance	Average (m)	0.29	0.31
		Standard Deviation (m)	0.06	0.15
	Sleeve Friction	Average (m)	0.35	0.41
		Standard Deviation (m)	0.16	0.19

Figures 3.25–3.26 illustrate the first quartile, the third quartile, median, maximum, and minimum values of zero-correlation distances of coarse-grained and fine-grained soil layers for cone resistance and sleeve friction in the three zones.

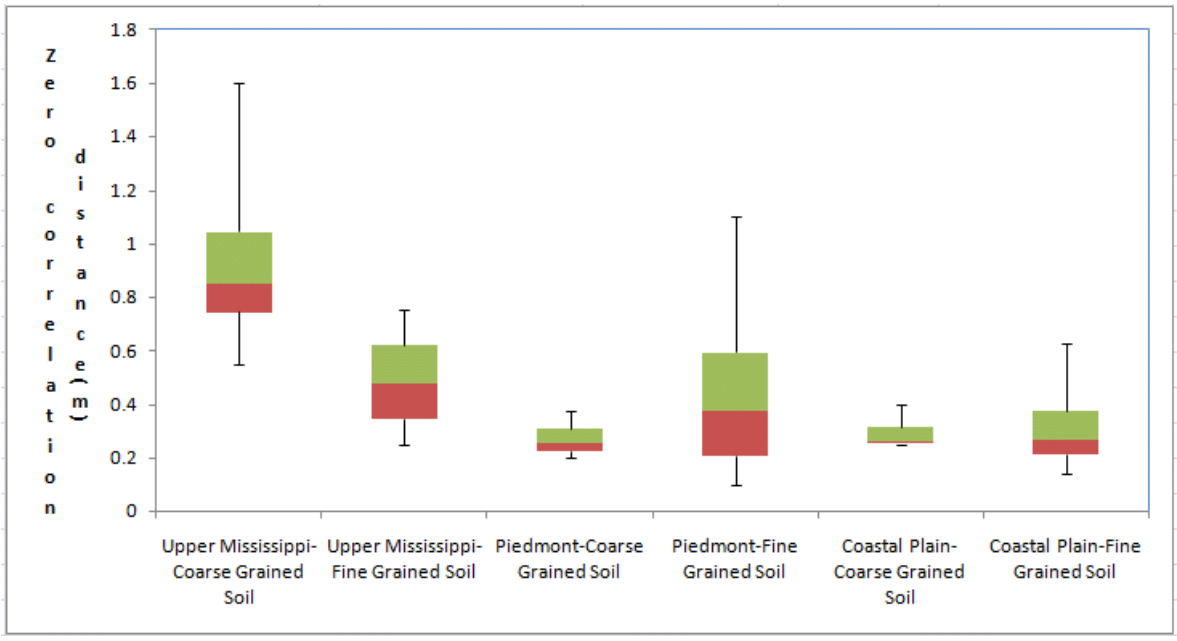

Figure 3.25 The first quartile, the third quartile, median, maximum, and minimum values of zero-correlation distances of each soil layer for cone resistance

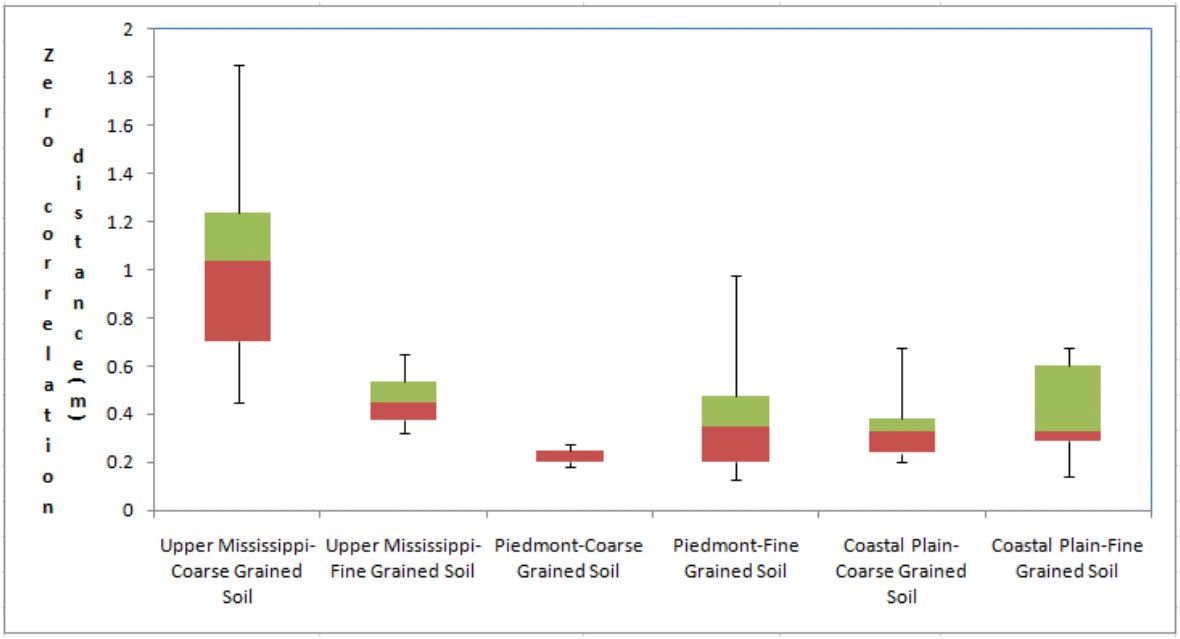

Figure 3.26 The first quartile, the third quartile, median, maximum, and minimum values of zero-correlation distances of each soil layer for sleeve friction

Hypothesis testing was employed to estimate the statistical differences between granular soil layer (i.e., sand and silty sand layers) and fine soil layer (i.e., sandy silt, clayey silt, and clay layers). A 10% level of significance for this hypothesis testing was applied to make a valid statistical conclusion. Table 3.10 shows the statistically meaningful soil types for the average zero-correlation distances of cone resistance and sleeve friction in each subregion.

Table 3.10 Statistically meaningful soil types for the average zero-correlation distances (ZCD) of cone resistance and sleeve friction in each subregion

	Cone Resistance	Sleeve Friction
Upper Mississippi Embayment	ZCD of Sand ≠ ZCD of Clayey Silt ZCD of Sand ≠ ZCD of Silty Clay ZCD of Sand ≠ ZCD of Clay ZCD of Silty Sand ≠ ZCD of Clayey Silt ZCD of Silty Sand ≠ ZCD of Silty Clay ZCD of Silty Sand ≠ ZCD of Clay where ≠ : statistically different from each other	ZCD of Sand ≠ ZCD of Clayey Silt ZCD of Sand ≠ ZCD of Silty Clay ZCD of Sand ≠ ZCD of Clay ZCD of Silty Sand ≠ ZCD of Clayey Silt ZCD of Silty Sand ≠ ZCD of Silty Clay ZCD of Silty Sand ≠ ZCD of Clay
Piedmont Province	ZCD of Sand ≠ ZCD of Clay ZCD of Silty Sand ≠ ZCD of Clay ZCD of Sandy Silt ≠ ZCD of Clay ZCD of Clayey Silt≠ ZCD of Clay	ZCD of Sand ≠ ZCD of Clay ZCD of Silty Sand ≠ ZCD of Clay ZCD of Sandy Silt ≠ ZCD of Clay ZCD of Clayey Silt≠ ZCD of Clay
Coastal Plain Province	None	None

The average values of zero-correlation distance of cone resistance and sleeve friction between granular and fine soil layers in the Upper Mississippi Embayment and the Piedmont Province presented statistically significant differences. In the Upper Mississippi Embayment, the average values of zero-correlation distance of cone resistance and sleeve friction of granular soil layer were greater than those of fine soil

layer. In the Piedmont Province, average values of zero-correlation distance of cone resistance and sleeve friction of granular soil layers were smaller than those of fine soil layers. In the Coastal Plain Province, due to the limit in the number of soil types, the average values of zero-correlation distance of cone resistance and sleeve friction between granular and fine soil layers did not show statistically meaningful results. Figures 3.27–3.29 illustrate the average zero-correlation distances of each soil layer for cone resistance and sleeve friction in the three zones.

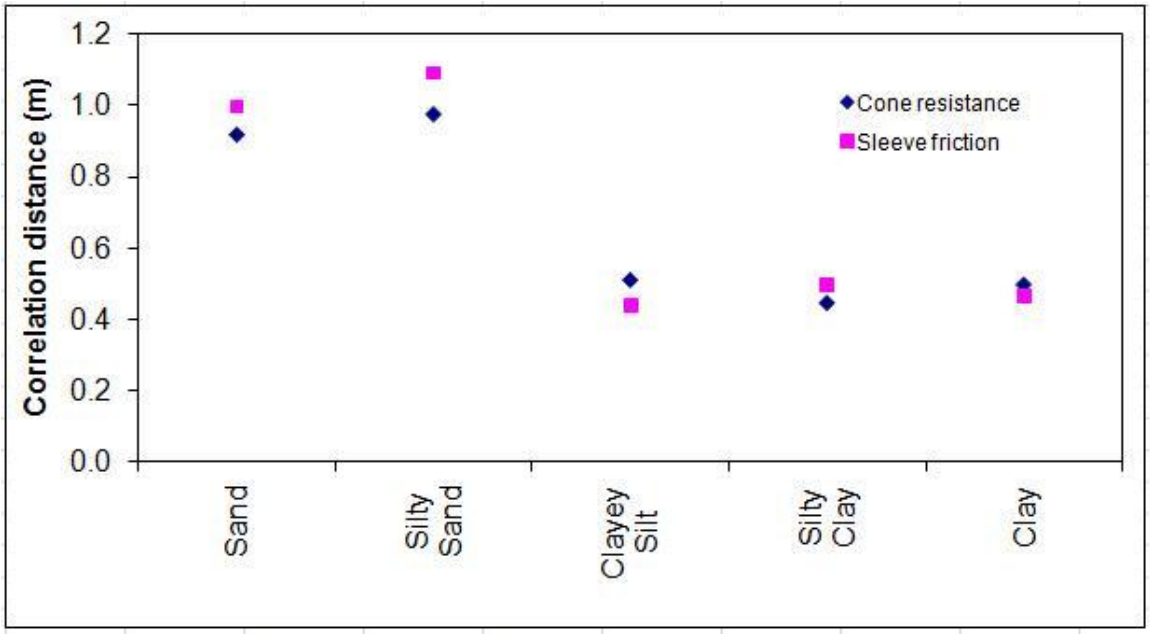

Figure 3.27 Average zero-correlation distances of each soil layer for cone resistance and sleeve friction in the Upper Mississippi Embayment

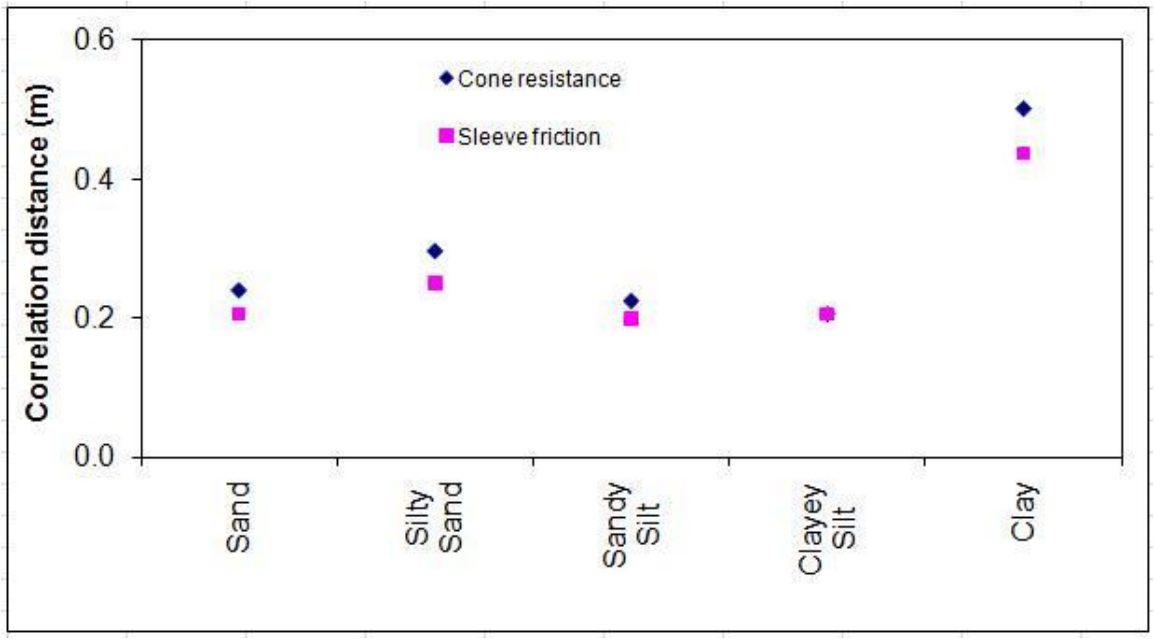

Figure 3.28 Average zero-correlation distances of each soil layer for cone resistance and sleeve friction in the Piedmont Province

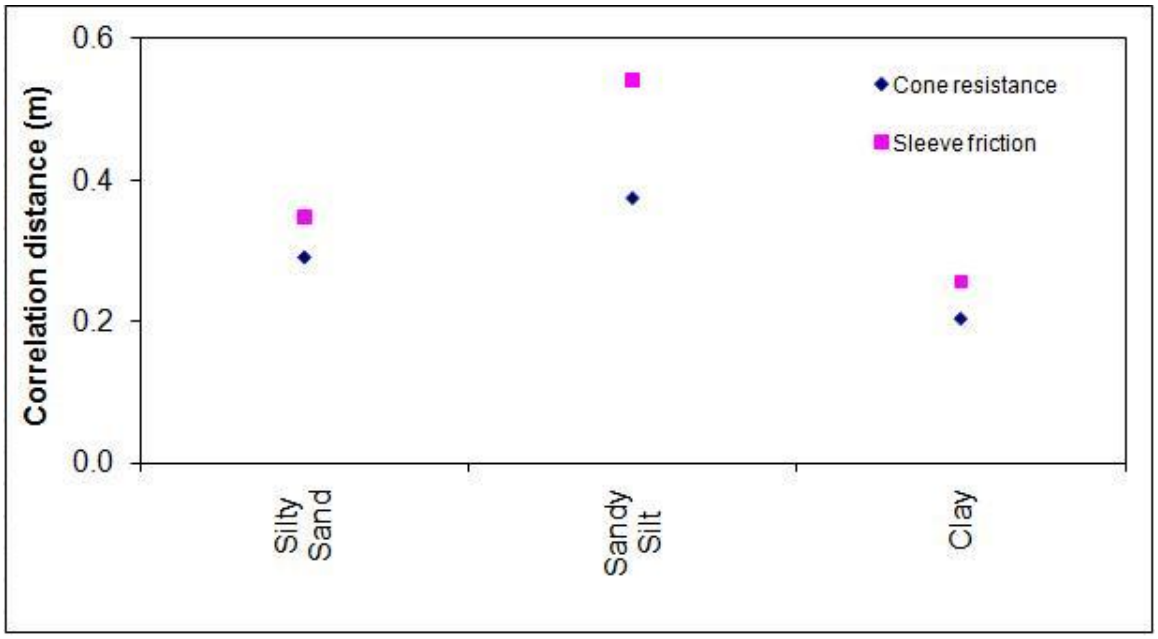

Figure 3.29 Average zero-correlation distances of each soil layer for cone resistance and sleeve friction in the Coastal Plain Province

In the Upper Mississippi Embayment and the Coastal Plain Province, the more granular a soil layer becomes, the higher the average of its zero-correlation distance. On the other hand, in the Piedmont Province, the more granular a soil layer becomes, the lower the average of its zero-correlation distance. Hence, soil formation process may be considered a major factor that affects correlation of soil properties. In the section 3.3.1, the level of variation of soil property for CPT data was studied. The Upper Mississippi Embayment has granular soil layers with a lower level of variation in soil properties when compared with the level of variation in soil properties for fine soil layers, and the Piedmont Province demonstrates that fine soil layers have soil properties with lower variation than do granular soil layers. It is observed that there is an apparent contrast between the level of variation and zero-correlation distance. The above evidence demonstrates that the zero-correlation distance is in inverse proportion to the coefficient of variation. That is, a soil layer with a small zero-correlation distance has a relatively highly fluctuating or a relatively highly variable soil profile, comparing the trend of COV with the trend of zero-correlation distance.

(2) Scale of fluctuation

In order to determine a model to best fit a correlation coefficient function of soil data, the coefficient of determination in least-squares regression was used. The single exponential model is most commonly used for correlation coefficient function due to a great deal of related research and mathematical feasibility (DeGroot, 1996). Thus, the estimation of the correlation coefficient function of soil property by the exponential model is introduced in this section.

The strength of correlation expressed by the exponential model using regression analysis is referred to as the scale of fluctuation. The scale of fluctuation is distinguished from zero-correlation distance using CPT data from the three zones under investigation: the Upper Mississippi Embayment, the Piedmont Province, and the Coastal Plain Province, which are separated on the basis of soil formation processes. The scales of fluctuation of soil type for the CPT data in these areas are estimated. Figures 3.30–3.32 show how to estimate the scales of fluctuation of several soil types for the CPT data. Regression analysis was employed to determine exponential models that best fit the correlation coefficient functions of each CPT data.

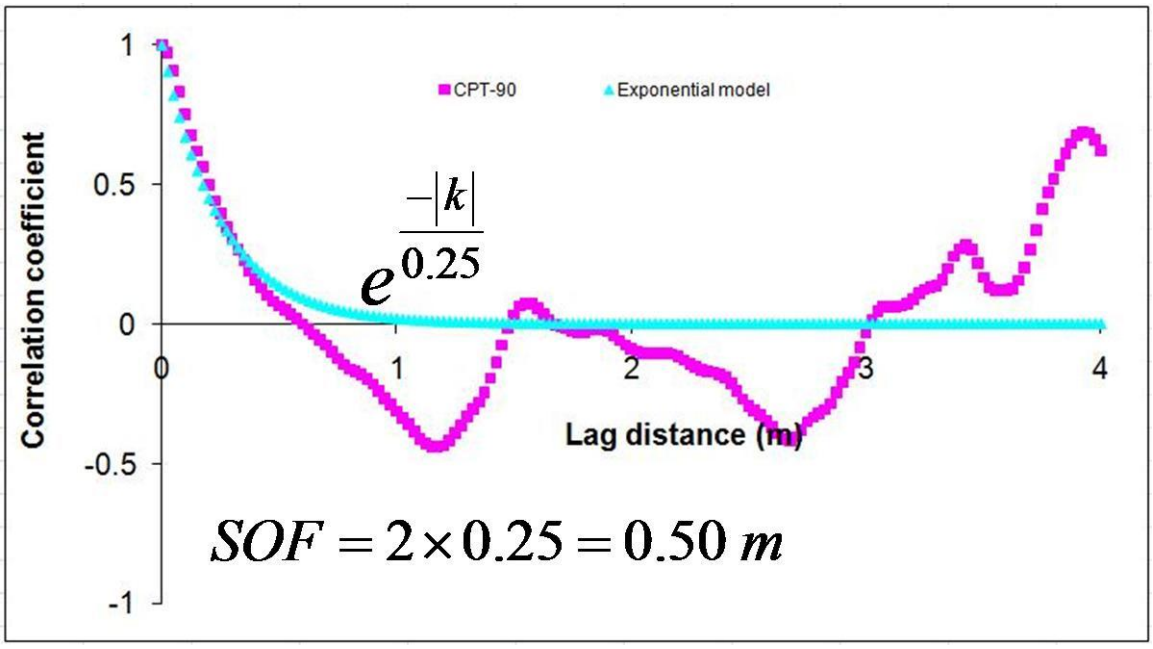

Figure 3.30 Estimation of scale of fluctuation (SOF) for sand layer of CPT-90 data in Wyatt, MO

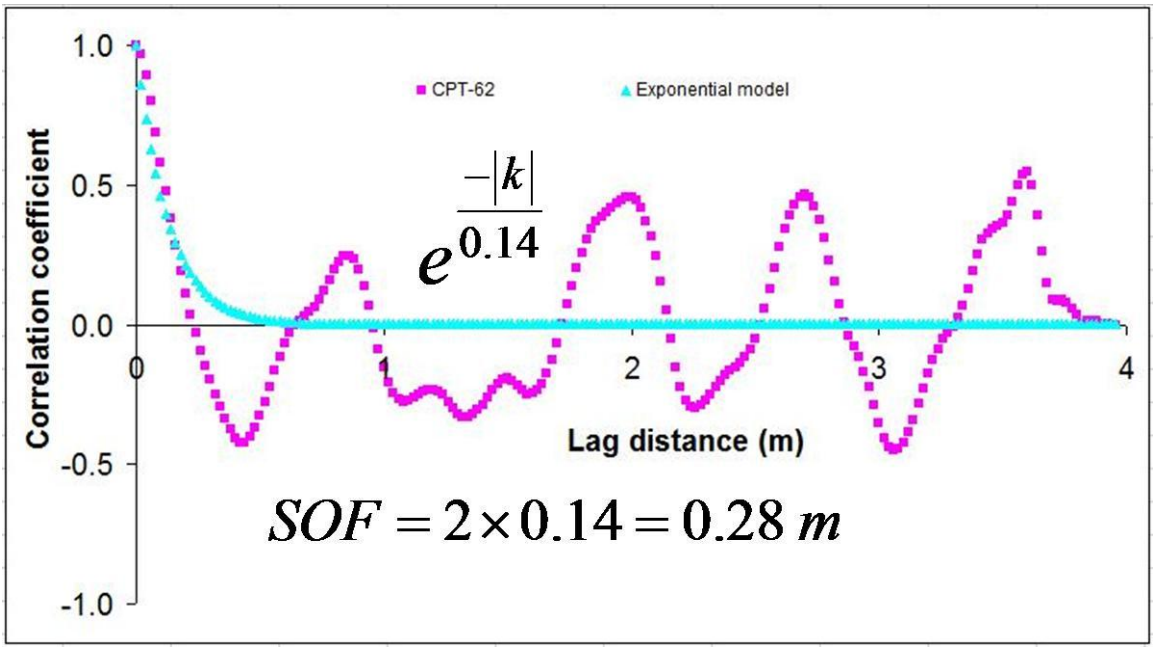

Figure 3.31 Estimation of scale of fluctuation for clay layer of CPT-62 data in Spring Villa, AL

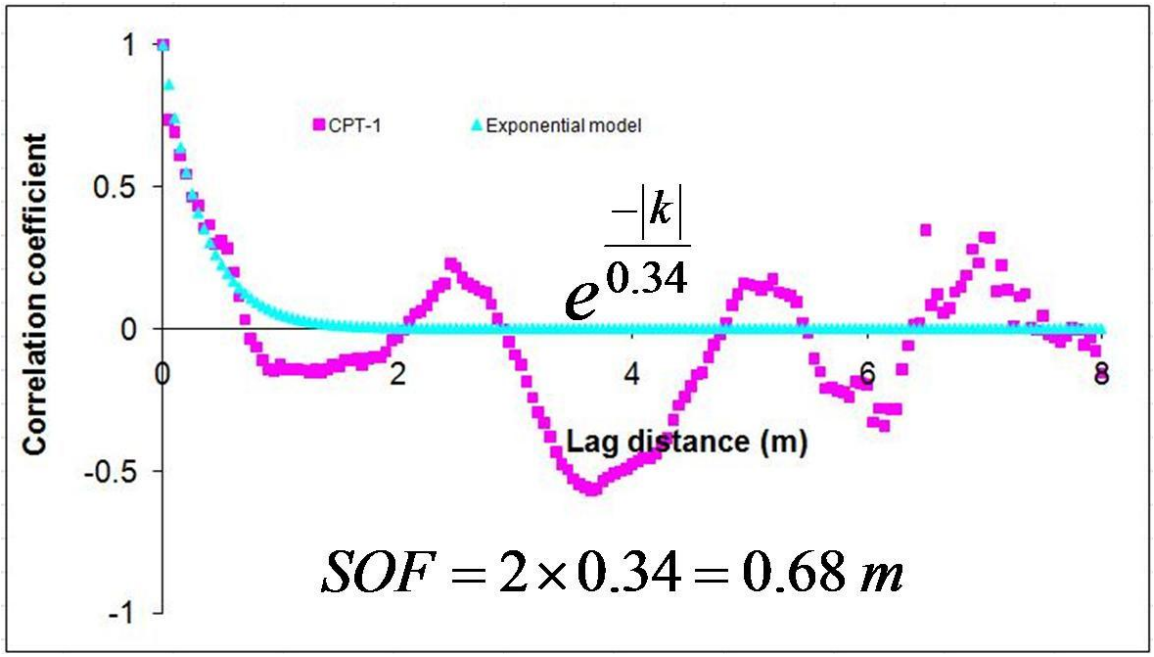

Figure 3.32 Estimation of scale of fluctuation for sandy silt layer of CPT-1 data in Charleston, SC

The results of scale of fluctuation of CPT data from these areas are summarized in Tables 3.11–3.13. Figures 3.33–3.34 illustrate the first quartile, the third quartile, median, maximum, and minimum values of scale of fluctuation of coarse-grained and fine-grained soil layers for cone resistance and sleeve friction in the three zones.

Table 3.11 Comparison of the scale of fluctuation of cone resistance and sleeve friction for each soil type in the Upper Mississippi Embayment

Area	Soil Property	Scale of fluctuation	Soil Type	
			Coarse-Grained Soil	Fine-Grained Soil
Upper Mississippi Embayment	No. of Samples		77	38
	Cone Resistance	Average (m)	0.60	0.22
		Standard Deviation (m)	0.29	0.10
	Sleeve Friction	Average (m)	0.56	0.24
		Standard Deviation (m)	0.27	0.12

Table 3.12 Comparison of the scale of fluctuation of cone resistance and sleeve friction for each soil type in the Piedmont Province

Area	Soil Property	Scale of fluctuation	Soil Type	
			Coarse-Grained Soil	Fine-Grained Soil
Piedmont Province	No. of Samples		23	88
	Cone Resistance	Average (m)	0.16	0.24
		Standard Deviation (m)	0.05	0.13
	Sleeve Friction	Average (m)	0.14	0.26
		Standard Deviation (m)	0.03	0.16

Table 3.13 Comparison of the scale of fluctuation of cone resistance and sleeve friction for each soil type in the Coastal Plain Province

Area	Soil Property	Scale of fluctuation	Soil Type	
			Coarse-Grained Soil	Fine-Grained Soil
Coastal Plain Province	No. of Samples		13	22
	Cone Resistance	Average (m)	0.18	0.17
		Standard Deviation (m)	0.05	0.08
	Sleeve Friction	Average (m)	0.17	0.19
		Standard Deviation (m)	0.03	0.09

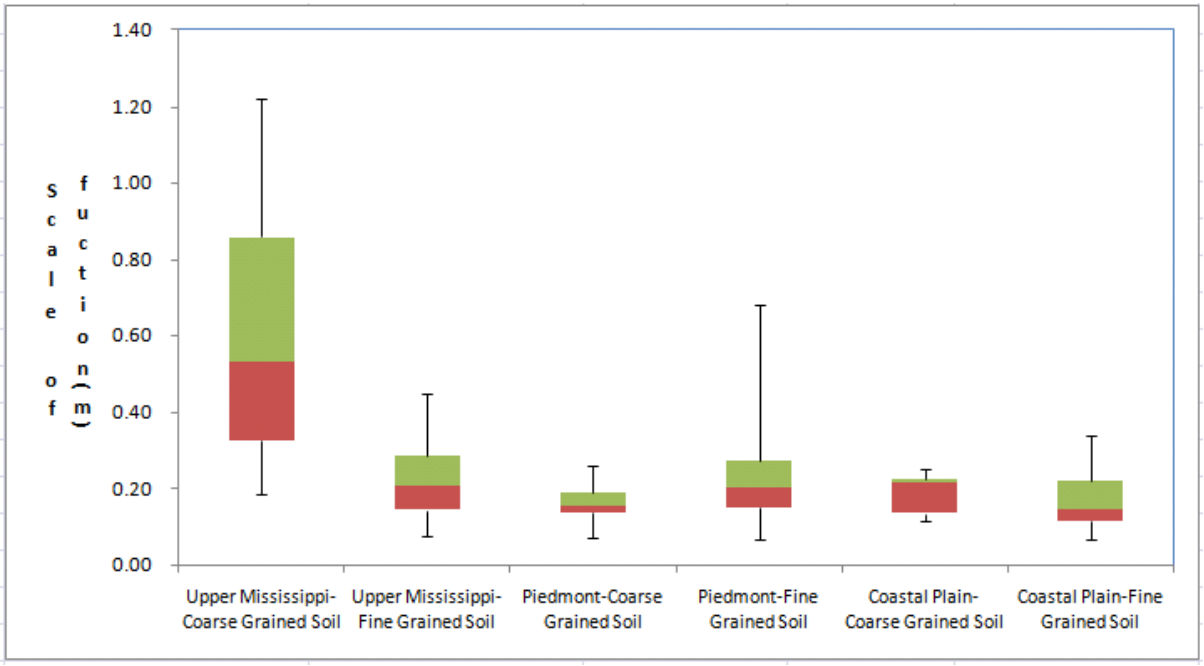

Figure 3.33 The first quartile, the third quartile, median, maximum, and minimum values of scales of fluctuation of each soil layer for cone resistance

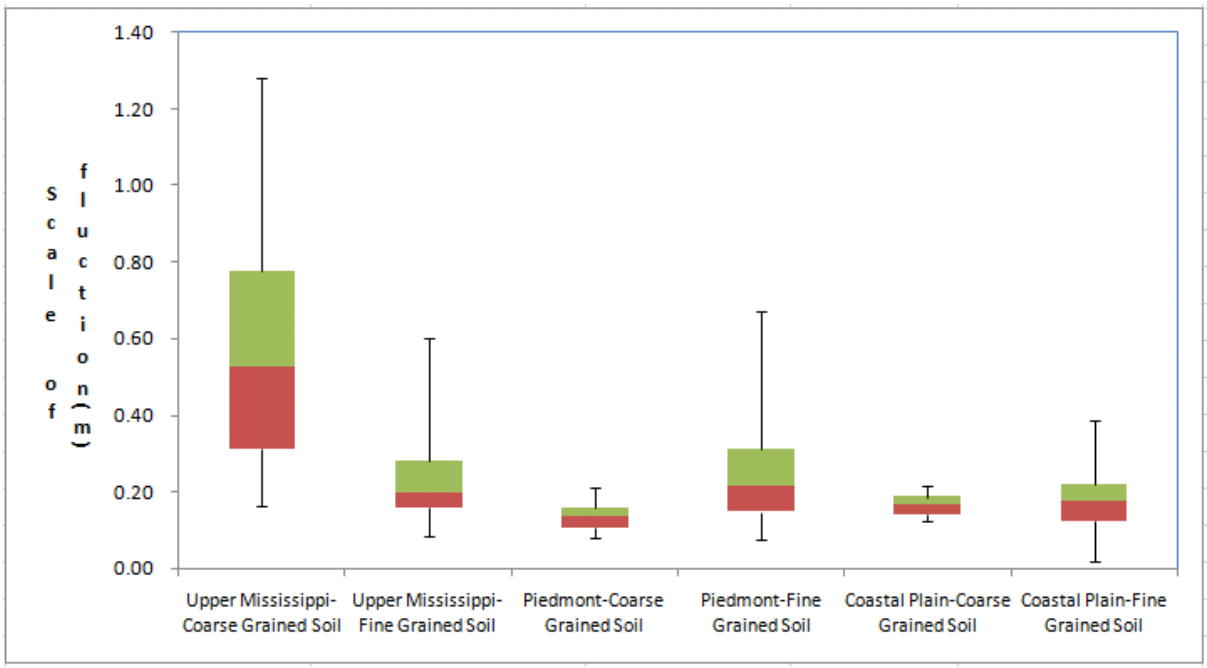

Figure 3.34 The first quartile, the third quartile, median, maximum, and minimum values of scales of fluctuation of each soil layer for sleeve friction

Hypothesis testing with 10% level of significance was employed to estimate the statistical differences between granular soil layers (i.e., sand and silty sand layers) and fine soil layers (i.e., sandy silt, clayey silt, and clay layers). Table 3.14 shows the statistically meaningful soil types for the average scales of fluctuation of cone resistance and sleeve friction in each subregion. The average values of scale of fluctuation of cone resistance and sleeve friction between granular and fine soil layers in the Upper Mississippi Embayment and the Piedmont Province presented statistically significant differences. In the Upper Mississippi Embayment, the average values of scale of fluctuation of cone resistance and sleeve friction of granular soil layers were greater than those of fine soil layers. In the Piedmont Province, the average values of scale of fluctuation of cone resistance and sleeve friction of granular soil layers were smaller than

those of fine soil layers. In the Coastal Plain Province, due to the limit in the data of various soil types, the average values of scale of fluctuation of cone resistance and sleeve friction between granular and fine soil layers did not show statistically meaningful results. Table 3.14 shows the statistically meaningful soil types for the average scales of fluctuation of cone resistance and sleeve friction in each subregion.

Table 3.14 Statistically meaningful soil types for the average scales of fluctuation (SOF) of cone resistance and sleeve friction in each subregion

	Cone Resistance	Sleeve Friction
Upper Mississippi Embayment	SOF of Sand ≠ SOF of Clayey Silt SOF of Sand ≠ SOF of Silty Clay SOF of Sand ≠ SOF of Clay SOF of Silty Sand ≠ SOF of Clayey Silt SOF of Silty Sand ≠ SOF of Silty Clay SOF of Silty Sand ≠ SOF of Clay where ≠ : statistically different from each other	SOF of Sand ≠ SOF of Clayey Silt SOF of Sand ≠ SOF of Silty Clay SOF of Sand ≠ SOF of Clay SOF of Silty Sand ≠ SOF of Clayey Silt SOF of Silty Sand ≠ SOF of Silty Clay SOF of Silty Sand ≠ SOF of Clay
Piedmont Province	SOF of Sand ≠ SOF of Clay SOF of Silty Sand ≠ SOF of Clay SOF of Sandy Silt ≠ SOF of Clay SOF of Clayey Silt≠ SOF of Clay	SOF of Sand ≠ SOF of Clay SOF of Silty Sand ≠ SOF of Clay SOF of Sandy Silt ≠ SOF of Clay SOF of Clayey Silt≠ SOF of Clay
Coastal Plain Province	None	None

Figures 3.35–3.37 illustrate the average values of scale of fluctuation of each soil layer for cone resistance and sleeve friction in the three zones. The results for scale of fluctuation of each soil type for CPT data have analogous features to the zero-correlation distances of each soil type for CPT data: the Upper Mississippi Embayment, the formation of which was dominated by sedimentation, has granular soil layers associated with larger values of scale of fluctuation than do fine soil layers; on the contrary, in the

case of the Piedmont Province, whose formation was essentially governed by a process of the chemical weathering of intact rock, fine soil layers have soil properties with larger values of zero scale of fluctuation than do granular soil layers. From the above evidence, it is concluded that soil formation process may be considered a major factor affecting correlation of soil properties.

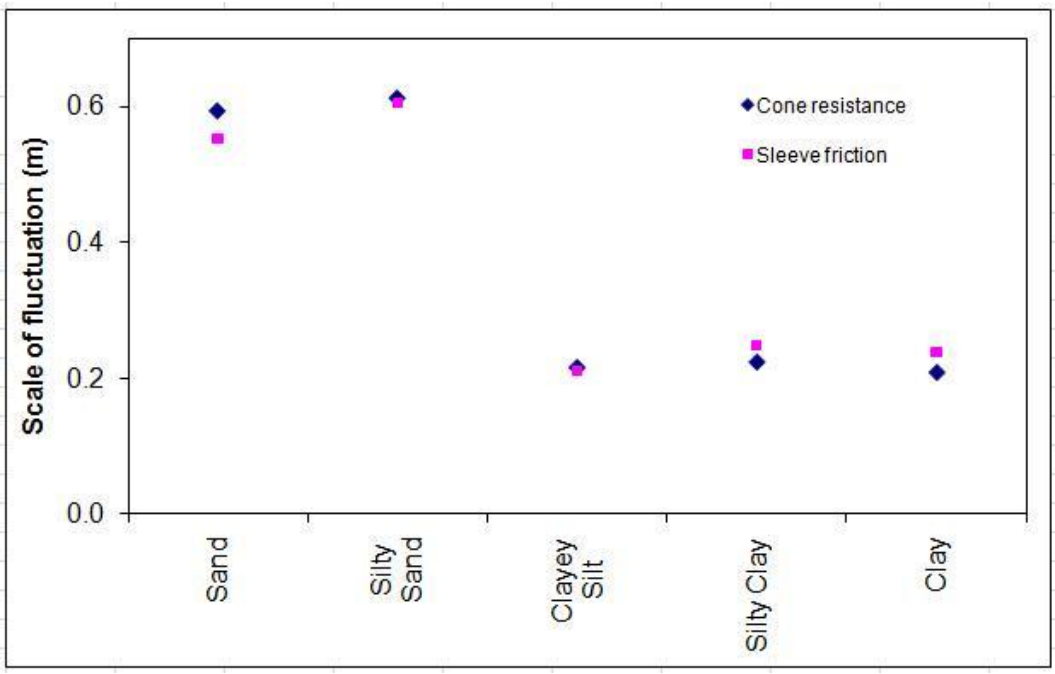

Figure 3.35 Average scales of fluctuation of each soil layer for cone resistance and sleeve friction in the Upper Mississippi Embayment

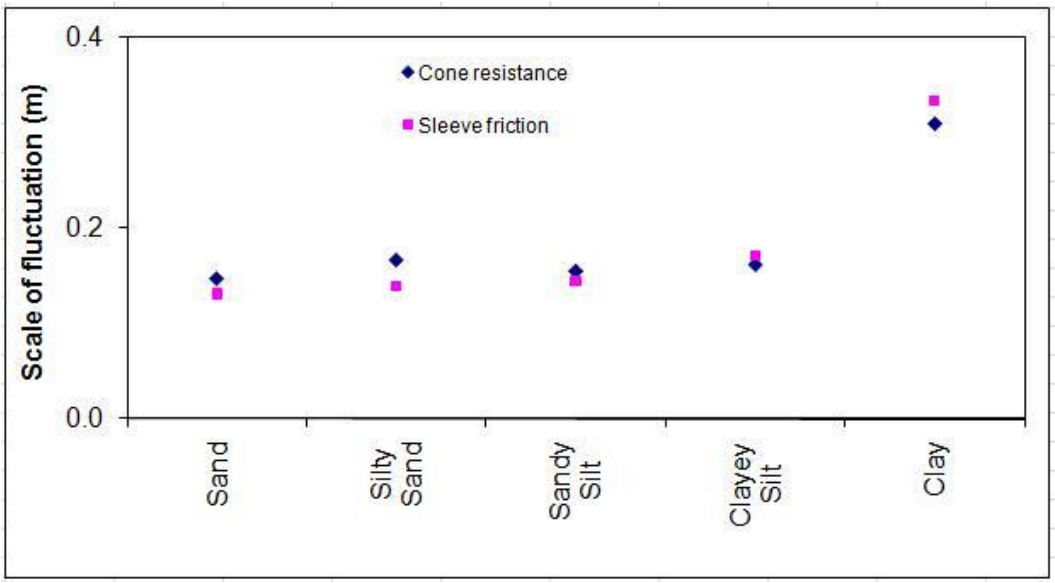

Figure 3.36 Average scales of fluctuation of each soil layer for cone resistance and sleeve friction in the Piedmont Province

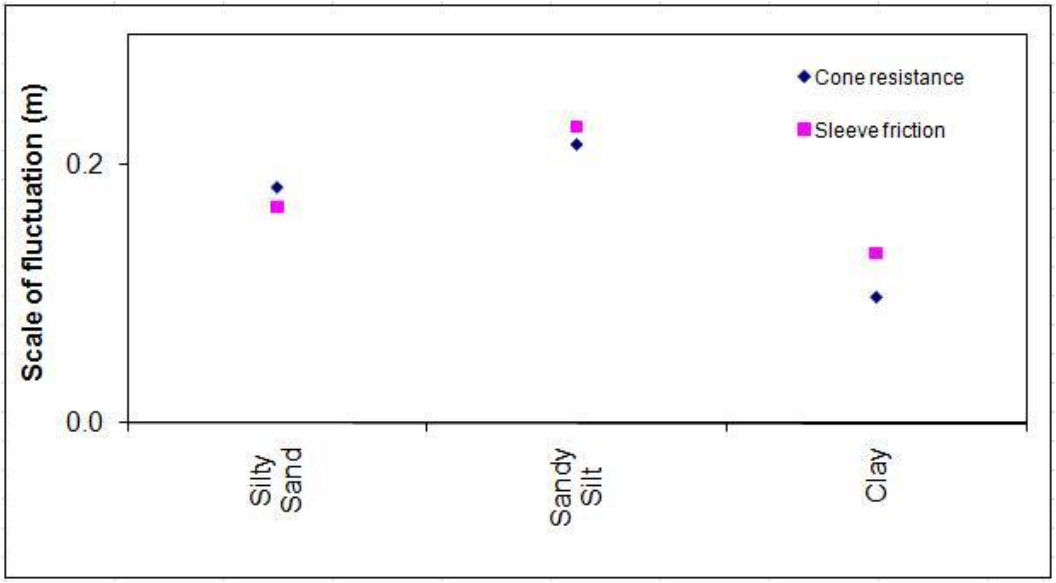

Figure 3.37 Average scales of fluctuation of each soil layer for cone resistance and sleeve friction in the Coastal Plain Province

3.4.2. SPT

(1) Zero-correlation distance

In the section 3.4.1, using CPT data from the three zones distinguished by different processes of soil formation, the zero-correlation distances of the data were estimated. In this section, zero-correlation distances of SPT data from such areas as the Memphis subregion (Upper Mississippi Embayment) and the Piedmont Province are estimated.

In the case of Memphis subregion, all SPTs were performed with a sampling interval of 2 feet (around 61 cm). The Piedmont Province has *N* values with a sampling interval of 5 feet (around 152 cm). Figures 3.38 –3.39 provide examples to estimate zero-correlation distances for soil layers of SPT data.

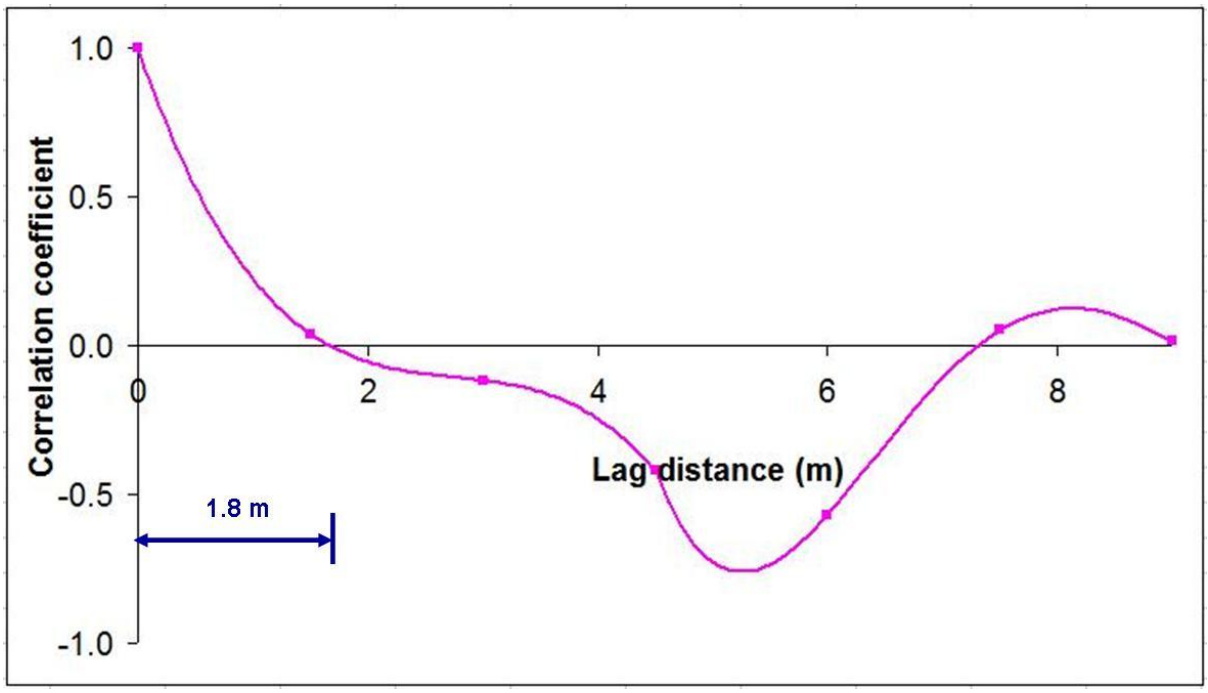

Figure 3.38 Estimation of zero-correlation distance for ML type soil layer of B-12 data in West Point, GA

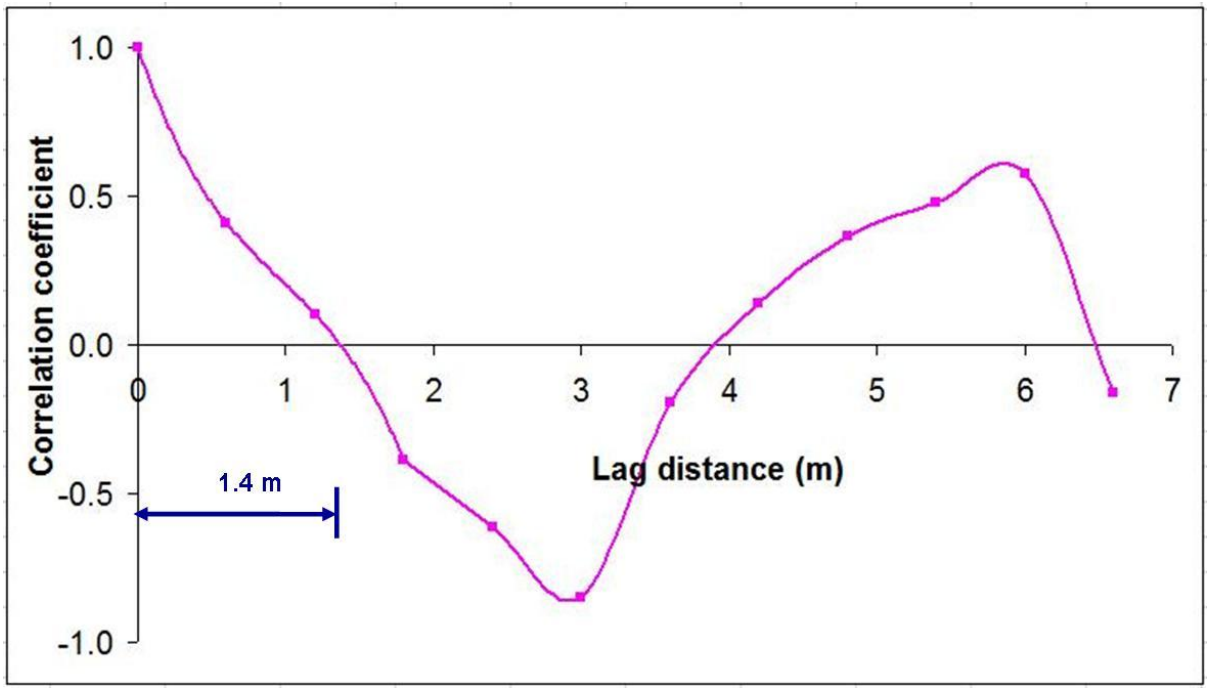

Figure 3.39 Estimation of zero-correlation distance for SM type soil layer of HB93013B35 data in Memphis, TN

The results of zero-correlation distance of SPT data from these areas are summarized in Tables 3.15–3.16. Figure 3.40 illustrates the first quartile, the third quartile, median, maximum, and minimum values of values of zero-correlation distance of coarse-grained and fine-grained soil layers for *N* values in the two zones. In the Piedmont Province, the zero-correlation distances of coarse-grained and fine-grained soil layers showed considerably narrow deviation levels.

Table 3.15 Comparison of the zero-correlation distance of N value for coarse-grained and fine-grained soils in the Memphis subregion (Upper Mississippi Embayment)

Area	Soil Property	Zero Correlation Distance	Soil Type	
			Coarse-Grained Soil	Fine-Grained Soil
Upper Mississippi Embayment	No. of Samples		337	639
	N Value	Average (m)	1.47	1.30
		Standard Deviation (m)	0.52	0.52

Table 3.16 Comparison of the zero-correlation distance of N value for coarse-grained and fine-grained soils in the Piedmont Province

Area	Soil Property	Zero Correlation Distance	Soil Type	
			Coarse-Grained Soil	Fine-Grained Soil
Piedmont Province	No. of Samples		57	53
	N Value	Average (m)	1.74	1.70
		Standard Deviation (m)	0.53	0.57

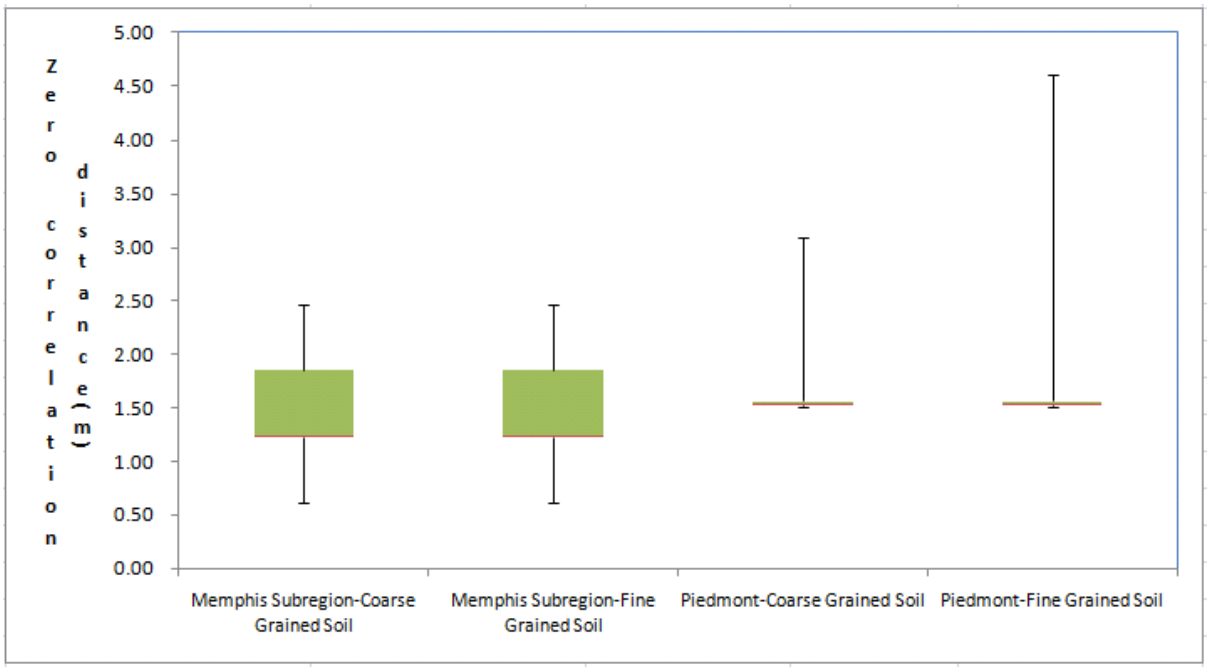

Figure 3.40 The first quartile, the third quartile, median, maximum, and minimum values of zero-correlation distances of coarse-grained and fine-grained soils for N value in each zone

Hypothesis testing with 10% level of significance was employed to estimate the statistical differences between granular soil layers (i.e., SP, SP-SM, SM, SM-SC, and SC type soil layers) and fine soil layers (i.e., ML, ML-CL, CL, and CH type soil layers). As a result, the average values of zero-correlation distance of *N* value between granular and fine soil layers in the Memphis subregion presented a statistically significant difference. The data sequence in geotechnical engineering has regular fluctuations (Jaksa, 1995; Jaksa et al., 1997). As discussed in Chapter 4, a representative fluctuation, or so-called equivalent wavelength, can be estimated from the lag distance corresponding to the second positive peak of the correlation coefficient function of a data sequence. The average value of zero-correlation distance of *N* values of granular soil layers was greater than that for fine soil layers. However, due to the limit in the number of soil types and the

sampling interval (5 feet) anticipated to be relatively greater than half an equivalent wavelength, the average values of zero-correlation distance of *N* value between granular and fine soil layers in the Piedmont Province did not show a statistically meaningful difference. Figure 3.41 illustrates the average zero-correlation distances of each soil layer for *N* values in these zones. These findings are in concert with the results of the zero-correlation distance obtained in CPT analysis. The evidence obtained from the Memphis subregion supports the fact that the process of soil formation has to some extent an impact on zero-correlation distance.

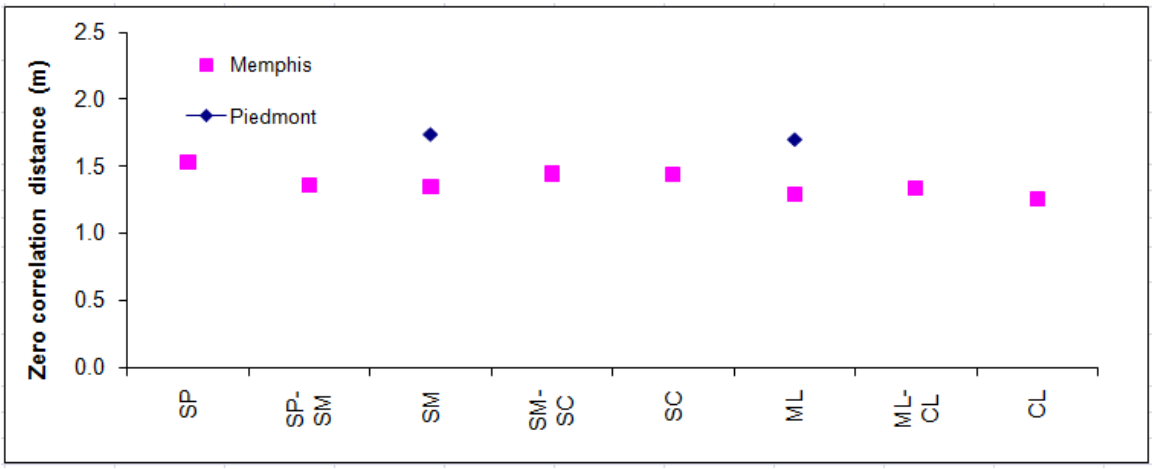

Figure 3.41 Average zero-correlation distances of each soil layer for N value in each zone

The effect of change in the sampling interval on the pattern of correlation structure will be discussed later. It was ascertained that the statistically acceptable sampling interval should be smaller than half an equivalent wavelength. A sampling interval larger than half an equivalent wavelength causes the correlation coefficient function to have a large zero-correlation distance in proportion to the scale of the sampling interval. This happens because samples with sampling intervals larger than half

an equivalent wavelength generate cyclic waves with lower frequency different from an original data sequence; that is, the sampled data do not show the same periodic replication with the original sequence.

Remarkably, all the zero-correlation distances estimated for SPT data are larger than those for CPT data. Taking the effect of sampling interval on correlation structures into consideration, most SPT data were probably undersampled. Possibly, the condition of allowable sampling interval could have been violated because soils with the same process of soil formation do not have accurate consequences of correlation structures, but do have a consistently similar trend of correlation structure such as zero-correlation distance regardless of the type of in situ test. The actual zero-correlation distances possibly are smaller than the values that result from SPT data. Therefore, when evaluating the correlation structures of soil property at a site of interest, it is always recommended to use more accurate data obtained from an in situ test such as CPT employing the smallest possible sample spacing.

(2) Scale of fluctuation

The single exponential model is most commonly used for correlation coefficient function due to a great deal of related research and mathematical feasibility (DeGroot, 1996). Thus, an estimation of the correlation coefficient function of soil properties by the single exponential model is also made use of in this section. Figures 3.42 – 3.43 show how to estimate the scales of fluctuation of several soil types for the SPT data. Regression analysis was employed to determine exponential models that best fit the correlation coefficient functions of each SPT data.

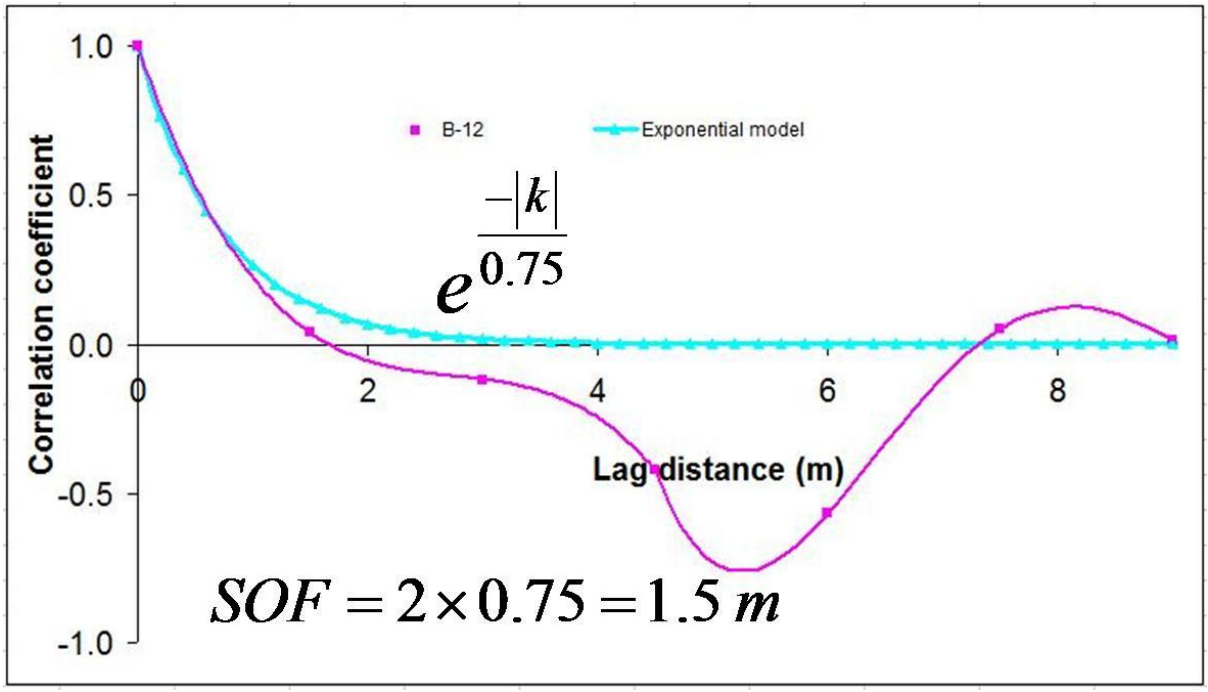

Figure 3.42 Estimation of scale of fluctuation for ML type soil layer of B-12 data in West Point, GA

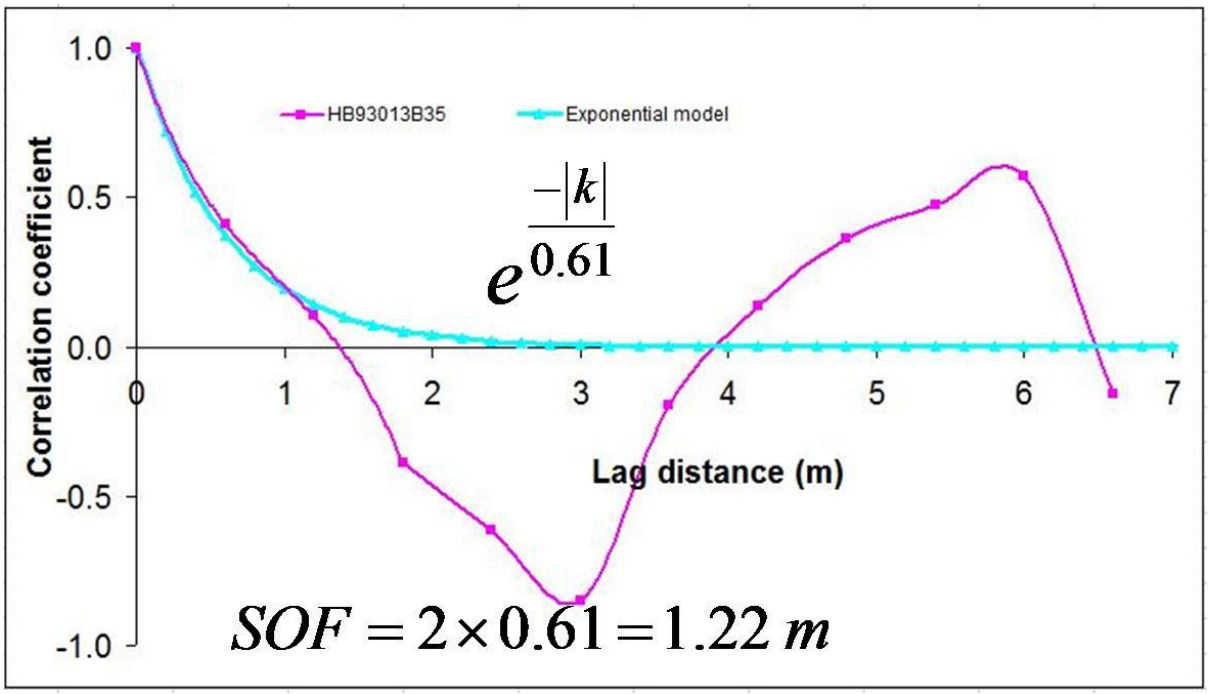

Figure 3.43 Estimation of scale of fluctuation for SM type soil layer of HB93013B35 data in Memphis, TN

The estimation of scales of fluctuation for SPT data from the two zones, the Memphis subregion (Upper Mississippi Embayment) and the Piedmont Province, is summarized in Tables 3.17–3.18, respectively.

Table 3.17 Comparison of the scale of fluctuation of N value for coarse-grained and fine-grained soils in the Memphis subregion (Upper Mississippi Embayment)

Area	Soil Property	Scale of Fluctuation	Soil Type	
			Coarse-Grained Soil	Fine-Grained Soil
Upper Mississippi Embayment	No. of Samples		337	639
	N Value	Average (m)	1.00	0.92
		Standard Deviation (m)	0.63	0.58

Table 3.18 Comparison of the scale of fluctuation of N value for coarse-grained and fine-grained soils in the Piedmont Province

Area	Soil Property	Scale of Fluctuation	Soil Type	
			Coarse-Grained Soil	Fine-Grained Soil
Piedmont Province	No. of Samples		57	53
	N Value	Average (m)	1.06	1.17
		Standard Deviation (m)	0.63	0.27

Figure 3.44 illustrates the first quartile, the third quartile, median, maximum, and minimum values of scales of fluctuation of coarse-grained and fine-grained soil layers for *N* values in the two zones.

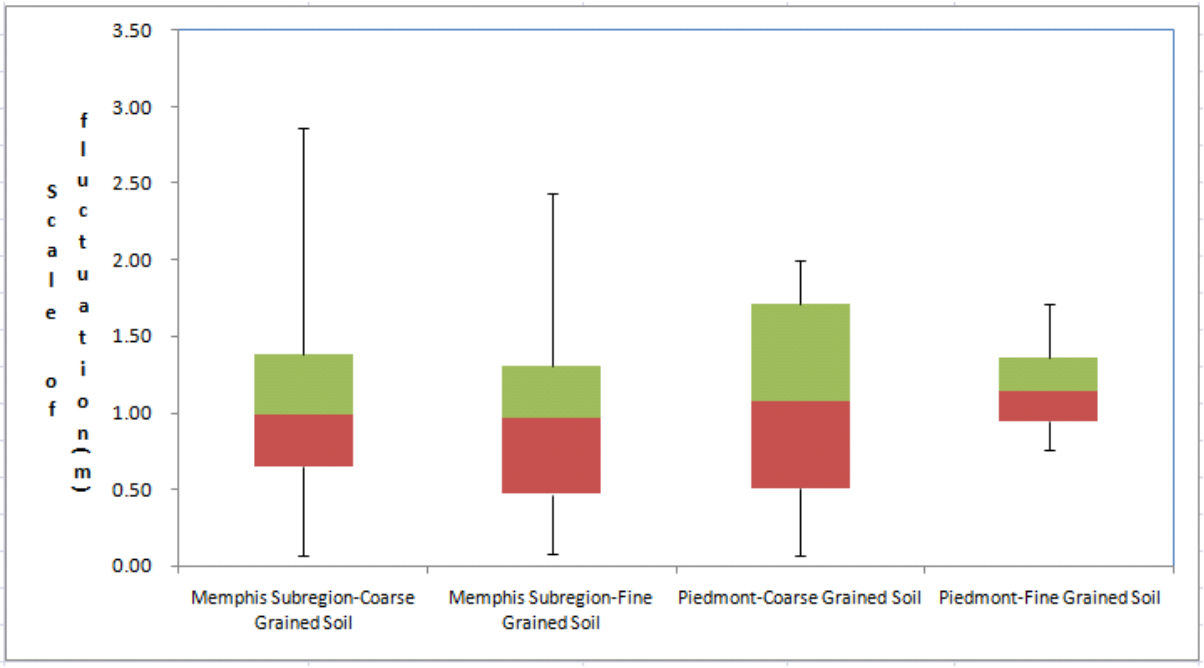

Figure 3.44 The first quartile, the third quartile, median, maximum, and minimum values of scale of fluctuation of coarse-grained and fine-grained soils for N value in each zone

When hypothesis testing with 10% level of significance was employed to estimate the statistical differences between granular soil layers and fine soil layers, the results of the hypothesis testing were the same as those of the zero-correlation distance: the average values of scale of fluctuation of *N* value between granular and fine soil layers in the Memphis subregion presented statistically significant differences; the average value of scale of fluctuation of *N* value of granular soil layers was greater than that of fine soil

layers; however, due to the limit in the number of soil types, and the sampling interval (5 feet) anticipated to be relatively greater than half a wavelength, the average values of scale of fluctuation of *N* value between granular and fine soil layers in the Piedmont Province did not show a statistically meaningful difference.

Figure 3.45 illustrates the average scales of fluctuation of each soil layer for *N* values in these zones. The estimation of the scale of fluctuation of each soil type for SPT data has analogous features to the zero-correlation distances of each soil type for CPT data. Although most SPT data were probably undersampled, they have consistently similar trends of correlation structures regardless of the type of in situ test. Therefore, the above evidences support the previous conclusion that when evaluating the correlation structures of soil property at a site of interest, it would always be recommended to use more accurate data obtained from in situ test employing the smallest possible sample spacing.

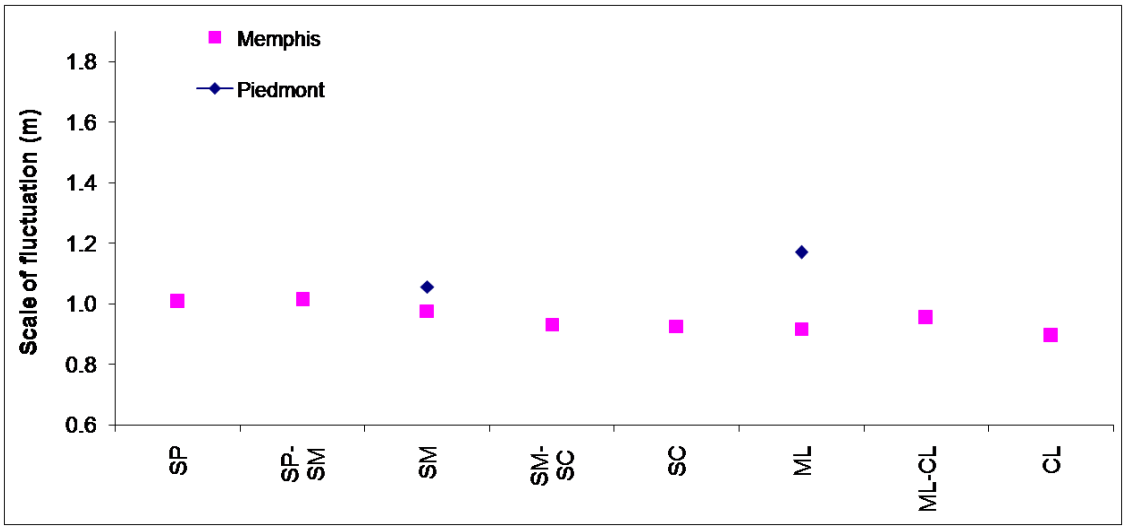

Figure 3.45 Average scales of fluctuation of each soil layer for N value in each area

3.5. Correlation structures with non-uniform lag (or relative) distance in the horizontal direction

In this section, correlation structures are estimated using five CPT data sets collected at Bridge A-1700, Caruthersville, Missouri. This site, which is near the Mississippi River, pertains to the Upper Mississippi Embayment; soils at the site are primarily governed by the process of sedimentation. The five CPT data sets were performed at approximately 78 to 138-foot intervals along the Bridge A-1700 as illustrated in Figure 3.46. Sand and clay layers were identified in common in the profile between approximately 16.5 and 28.0 m and between approximately 6.5 and 11.5 m, respectively, using the soil classification system suggested by Robertson et al. (1986). Commercial software, called CPeT-IT, which was developed by the *Geologismiki*, was used to estimate soil profile. Shoulder porewater pressure, u_2, was approximated using a net area ratio of 0.8 and hydrostatic water pressures estimated from ground water table shown in Table 3.19.

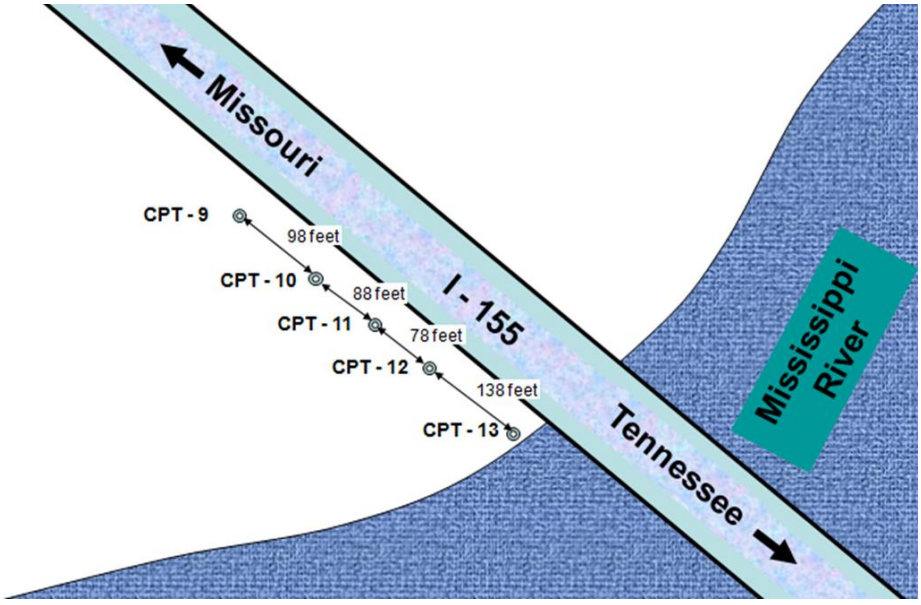

Figure 3.46 Overview of CPT sounding locations nearby the Bridge A – 1700

Table 3.19 Ground water table measured at each CPT boring location of Bridge A-1700, Caruthersville, Missouri (supplied by FMSM Engineers, Inc.)

	CPT-9	CPT-10	CPT-11	CPT-12	CPT-13
Ground Water Table	23.0 feet (7.01 m)	25.0 feet (7.62 m)	29.5 feet (8.99 m)	10.0 feet (3.05 m)	33.0 feet (10.06 m)

Figure 3.47 shows the results of a representative CPT performed at Bridge A-1700, Caruthersville, Missouri. The rest of the CPT boring profiles are attached in Appendix E.

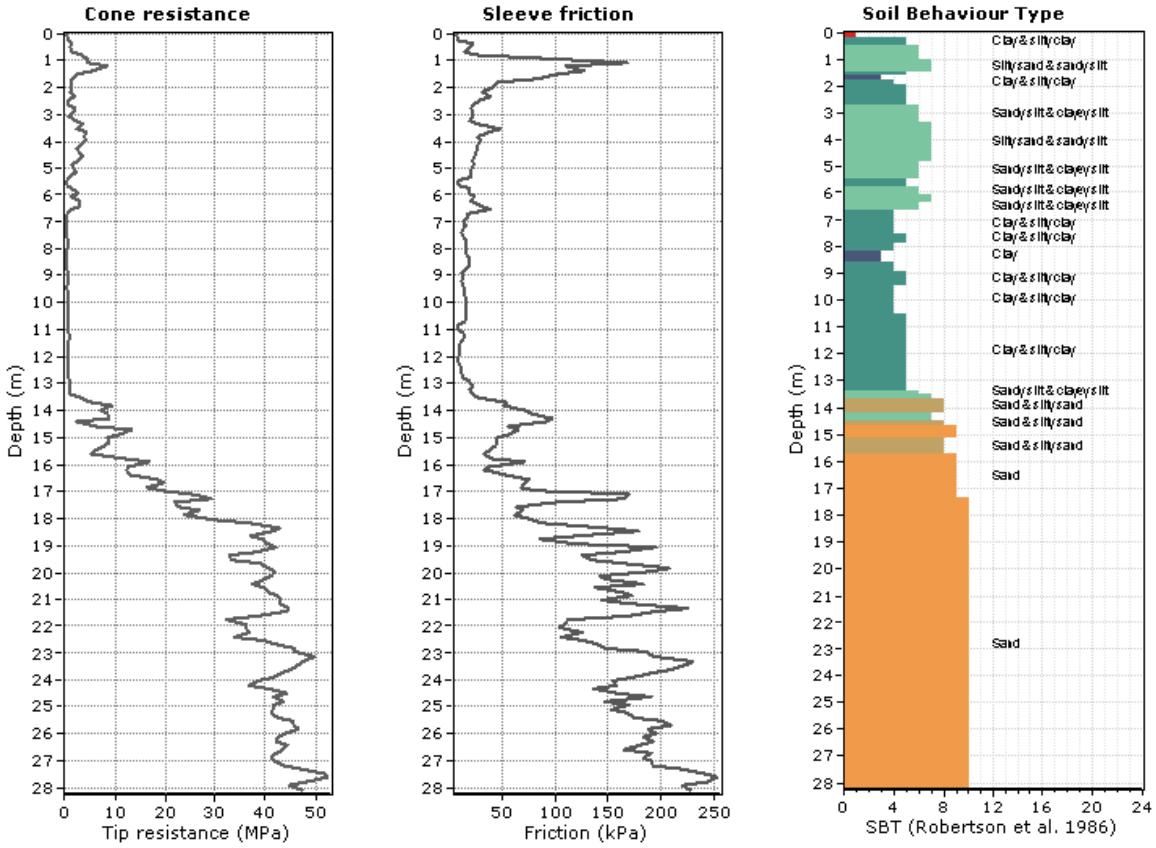

Figure 3.47 Result of CPT-12 at Bridge A-1700, Caruthersville, Missouri (supplied by FMSM Engineers, Inc.)

Table 3.20 summarizes the average values of COV of each soil layer in the horizontal direction for CPT data obtained from the site. The COV values of cone resistance and sleeve friction in horizontal direction estimated in the clayey soil layers are 21 percent and 24 percent, respectively, while for sandy soil layers, the COV values are 16 and 32 percent, respectively. The correlation coefficient function in the horizontal direction was estimated using the technique for non-uniform lag (relative) distances described Chapter 2. Figures 3.48–3.51 exhibit the correlation coefficient functions of sandy and clayey layers for CPT data obtained.

Table 3.20 Results of average values of COV of each soil layer in the horizontal direction for CPT data near the Mississippi River (Upper Mississippi Embayment)

Area	Soil Property	COV	Soil Type	
			Clay	Sand
Mississippi River	Cone Resistance	Average (%)	21	16
		Standard Deviation (%)	18	8
		No. of Samples	34	78
	Sleeve Friction	Average (%)	24	32
		Standard Deviation (%)	13	9
		No. of Samples	34	78

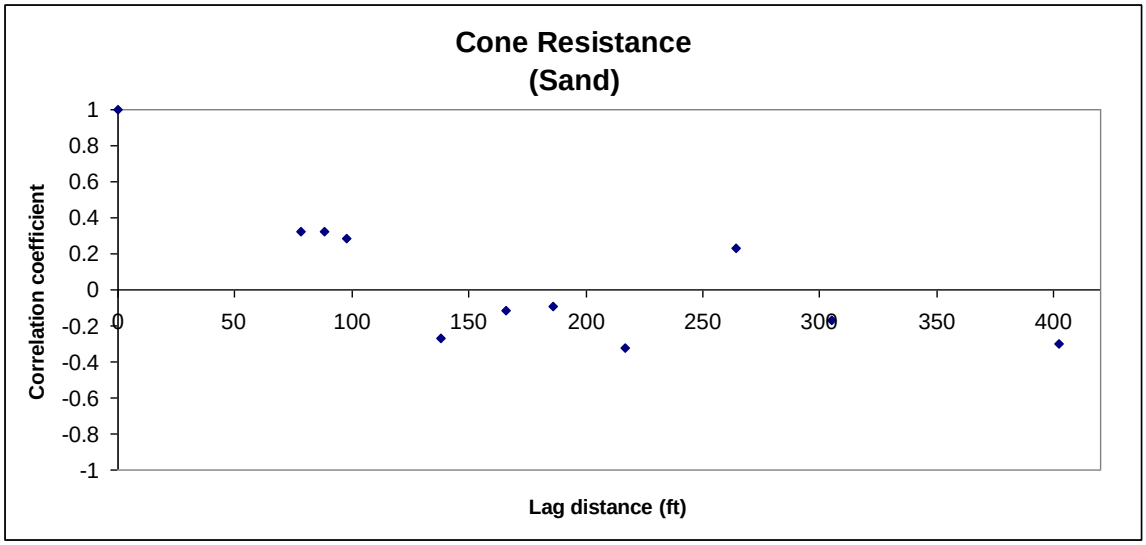

Figure 3.48 Correlation coefficient function of sand layers in the horizontal direction for cone resistance near the Mississippi River (Upper Mississippi Embayment)

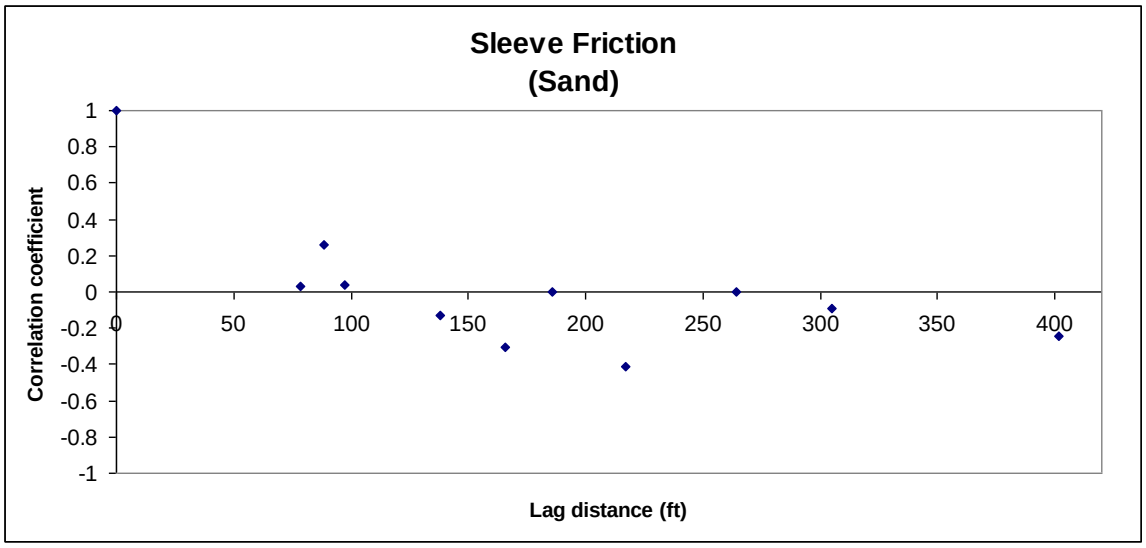

Figure 3.49 Correlation coefficient function of sand layers in the horizontal direction for sleeve friction near the Mississippi River (Upper Mississippi Embayment)

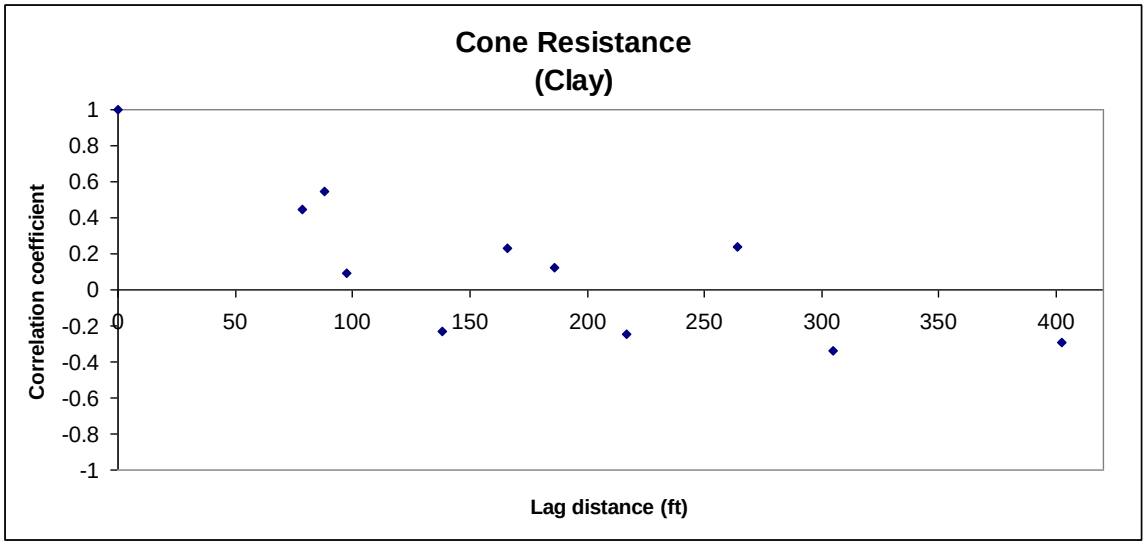

Figure 3.50 Correlation coefficient function of clay layers in the horizontal direction for cone resistance near the Mississippi River (Upper Mississippi Embayment)

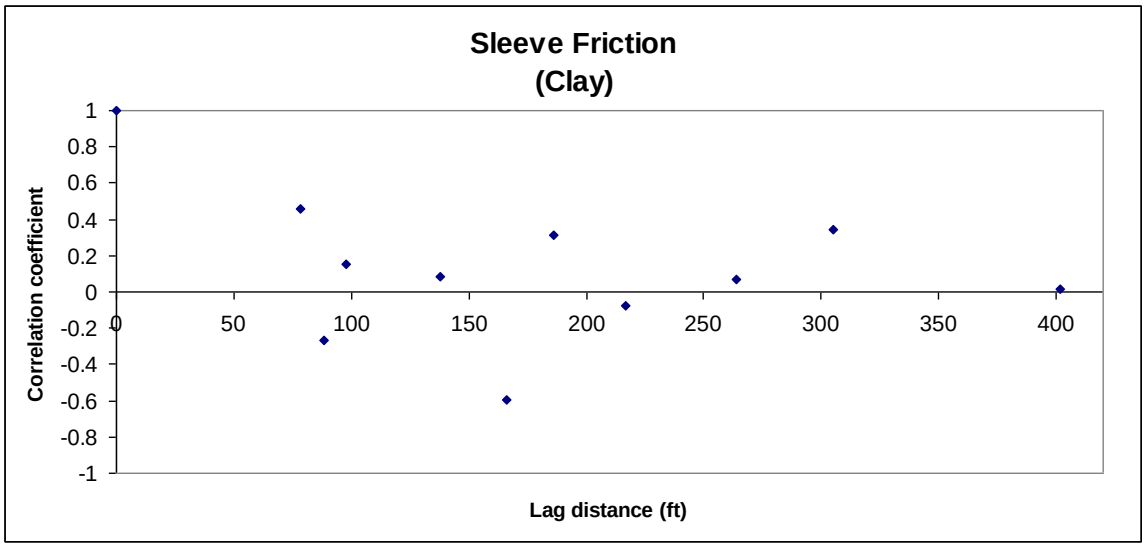

Figure 3.51 Correlation coefficient function of clay layers in the horizontal direction for sleeve friction near the Mississippi River (Upper Mississippi Embayment)

3.6. Conclusions

For the purposes of this study, the processes of soil formation in three disparate zones (the Upper Mississippi Embayment, the Atlantic Coastal Plain Province, and the Piedmont Province) in the Eastern United States were examined. In order to estimate the statistics of spatial variability based on the results of common in-situ soil tests, these sites were considered. It was demonstrated through hypothesis testing using the two-sample *t* test that the average COV values of the sleeve friction between clay and silty sand layers in the Upper Mississippi Embayment, the average COV values of the cone resistance between clay and sandy silt layers in the Coastal Plain Province, and the average COV values of the cone resistance between sand and clayey silt layers, sand and clay layers, and clay and silty sand layers and the average COV values of the sleeve friction between sand and clay layers and between clay and silty sand layers in the Piedmont Province presented statistically meaningful results. It also was verified that the COV value of the *N* values of the CL type soil layer in the Memphis subregion was statistically significant with the COV values of *N* value of some soil type layers (i.e., the SP, SP-SM, SC, and ML type soil layers) and the COV value of *N* value of the SP type soil layers in the Memphis subregion was statistically significant with the COV values of the SM, ML, ML-CL, CL, and CH type soil layers. Although not all the soil properties of each soil type layer were statistically significant, it is statistically valid that soil type layers in each area are categorized into two soil layers such as granular soil layer and fine soil layer for estimates of COV values. From the above evidence, one can establish general trends of COV with soil composition and soil formation process: in the Memphis subregion, the

more granular a soil layer becomes, the lower its average COV value; in the Piedmont Province, the more granular a soil layer becomes, the higher its average COV value.

The Upper Mississippi Embayment and the Coastal Plain Province have granular soil layers with higher levels of correlation of soil properties than do fine soil layers. In the Piedmont Province, fine soil layers have soil properties with larger values of zero-correlation distance than that of granular soil layers. In general, comparison of the trend of COV values for individual soil types with the trend of zero-correlation distance for individual soil types shows that a soil layer with a low level of correlation is likely to have a highly variable soil profile, while a soil layer with a high level of correlation is likely to have a weakly fluctuating or a weakly variable soil profile.

Taking the effect of sampling interval on correlation structures such as zero-correlation distance and scale of fluctuation into consideration, to avoid the loss of important data information, it is important to obtain data in the field using a proper sampling interval. Comparing the consequences of correlation structures for SPT data with those for CPT data, it is evident that it would always be better to use data obtained from an in situ test such as CPT wherein the smallest sample spacing possible is used to estimate the correlation structures of soil property.

In summary, the processes of soil formation and soil configuration are factors that play important roles in estimating and understanding correlation structures for a specific area.

The estimates of the statistical structures of soil properties obtained from the above three areas can approximate the statistical characteristics of soil property at a potential site in these or similar areas. The estimates of statistical structures of soil

properties achieved in this chapter offer valuable information for simulating random fields of soil properties at undersampled or unsampled locations in these areas or similar areas. The estimates of the statistical structures of soil properties obtained in this chapter can be a guideline for geotechnical engineers involved in these or similar areas to make sound engineering judgments for geotechnical design and analysis. Obviously, while these three regions may not be sufficient to provide a comprehensive database, they provide a diversity of physical and statistical characteristics of soil properties due to widely dissimilar soil formation processes.

CHAPTER 4

ESTIMATION OF MAXIMUM STATISTICALLY ALLOWABLE SAMPLING INTERVAL BASED ON THE CORRELATION STRUCTURES OF SOIL PROPERTIES

4.1. Introduction

The statistical characterization of soil properties consists of deterministic and stochastic computational structures. The uncertainties associated with estimating soil properties may translate into inaccuracies in the estimation of the statistical features of soil properties using data collected in the field. However, regardless of this important point, geotechnical engineers have traditionally been more interested in the practical aspects needed to reduce the cost of projects by means of the reduction in superfluous data obtained from a given site investigation program; that is, superfluous data allow geotechnical engineers to calculate more precisely the soil property in the design of geotechnical facilities, but at an additional cost. However, when less site investigation than required is performed, the results may be significantly corrupted. According to the research carried out by Jaksa et al. (1997) on the effect of the sampling interval on covariance function and correlation coefficient function with regard to soil properties in the vertical and the horizontal directions, it is evident that the sampling interval of data in both directions greatly affects the statistical quantities. Therefore, it is imperative to

simultaneously satisfy both requirements—cost containment and sufficient data collection.

When the sampling interval is smaller than half the period of an original data sequence, a series of data samples replicates its period without loss of its property. This effect is called aliasing (Santamarina and Fratta, 1998). In this chapter, the concept of aliasing is applied to the estimation of the maximum statistically allowable sampling interval from data obtained in three zones: the Upper Mississippi Embayment, the Atlantic Coastal Plain Province, and the Piedmont Province. This method may suggest a useful way to enhance the identification of soil profiles as well as to reduce the collection of unnecessary data, thereby increasing the site investigation capabilities of in situ tests.

Prior to moving on to the study of spatial variability in the practice of geotechnical engineering, it is necessary to first understand the characteristics of the statistical structures discussed above using simple sinusoidal waves that can be considered as ideal patterns for residuals of soil properties.

4.2. Effect of change in period of sinusoidal wave

4.2.1. Coefficient of variation (COV)

Table 4.1 exhibits the values of the coefficient of variation with changing periods for a variety of sinusoids that have integer cycle(s) within the range of x between 0 and 2π and have the mean of one; the random numbers are uniformly distributed between 0 and 2 over the range of x between 0 and 2π and have the mean of one. It is significant that the variation in the period of a sinusoidal wave does not affect the value of COV since

the value of COV corresponds not to the degree of periodicity, but to the degree of relative deviation.

Table 4.1 Values of coefficient of variation with change of wavelength for each wave type with the mean value of one

Wave type of residuals	**sin x +1**	**sin 2x +1**	**sin 4x +1**	**sin 10x +1**	**random + 1**
COV (%)	70.4	70.4	70.4	70.4	57

4.2.2. Correlation coefficient

Simple sinusoidal waves can be considered as ideal patterns for residuals of soil properties. In order to facilitate the understanding of patterns of correlation coefficients based on the periods of waves, the correlation coefficients of a variety of sinusoidal waveforms are estimated first. Figure 4.1 illustrates that an individual sinusoidal waveform, when generated within the same range and variance, i.e., 2π and a constant value, respectively, results in a peculiar shape using the correlation coefficient on the basis of scale of fluctuation. Again, the correlation coefficient in this case is computed as a function of angle. In Figure 4.1, each of the waveforms with apparent periodicity (except for those with random numbers of a non-periodical sequence) shows a correlation coefficient function that decreases and increases periodically with lag distance, finally converging on zero value because the correlation coefficient functions for the amplitudes of sinusoids only within the range of between 0 and 2π were estimated.

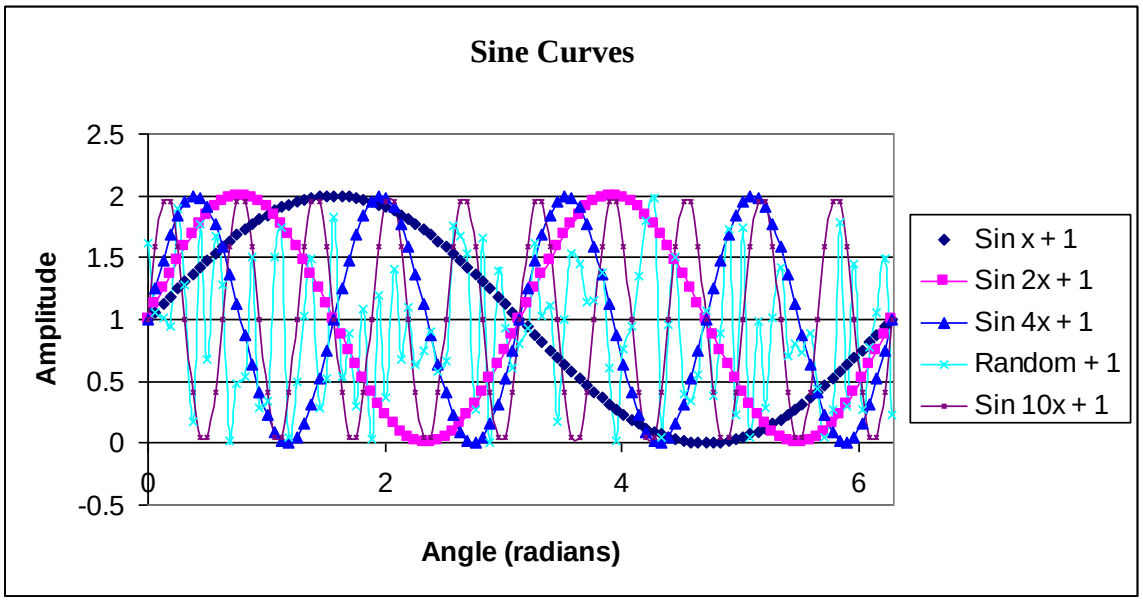

(a)

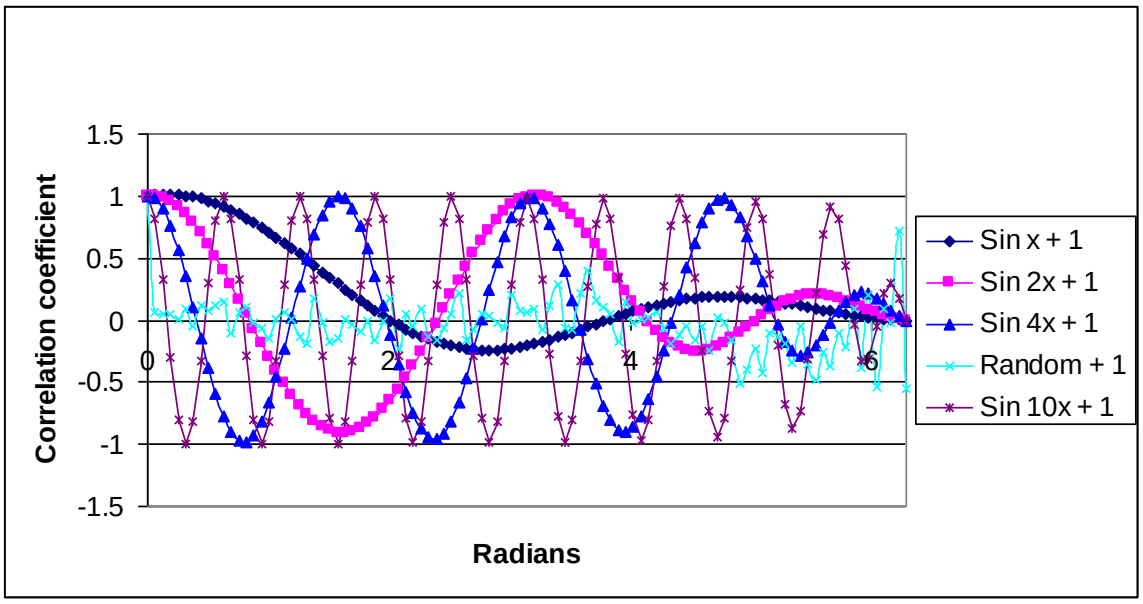

(b)

Figure 4.1 (a) Patterns of sinusoidal waves for analysis of correlation structures; (b) results of correlation coefficient of each sinusoidal wave

As shown in Figure 4.2, when a data sequence has a theoretically ideal periodicity like a sinusoidal wave pattern in appearance, the lag distance, *k*, corresponding to the

second positive peak is equal to the wavelength, W_L, of a sinusoidal form except for a sinusoid with a cycle because a sinusoid with a cycle does not show an apparent second positive peak. That is,

$$\boldsymbol{W_L} \;=\; \boldsymbol{k}_{\text{second positive peak}} \qquad (4.2.1)$$

In other words, an interval between positive/negative peaks is equal to the wavelength of a sinusoidal form except for sinusoid with a cycle. The wavelength of a sinusoidal form with at least 4 cycles, i.e., (x) over the range of x between 0 and 2π, is equal to four times the zero-correlation distance of data sequence, ζ_{corr} :

$W_L = 4 \times \zeta_{\text{corr}}$ for sinusoids with at least 4 cycles (4.2.2)

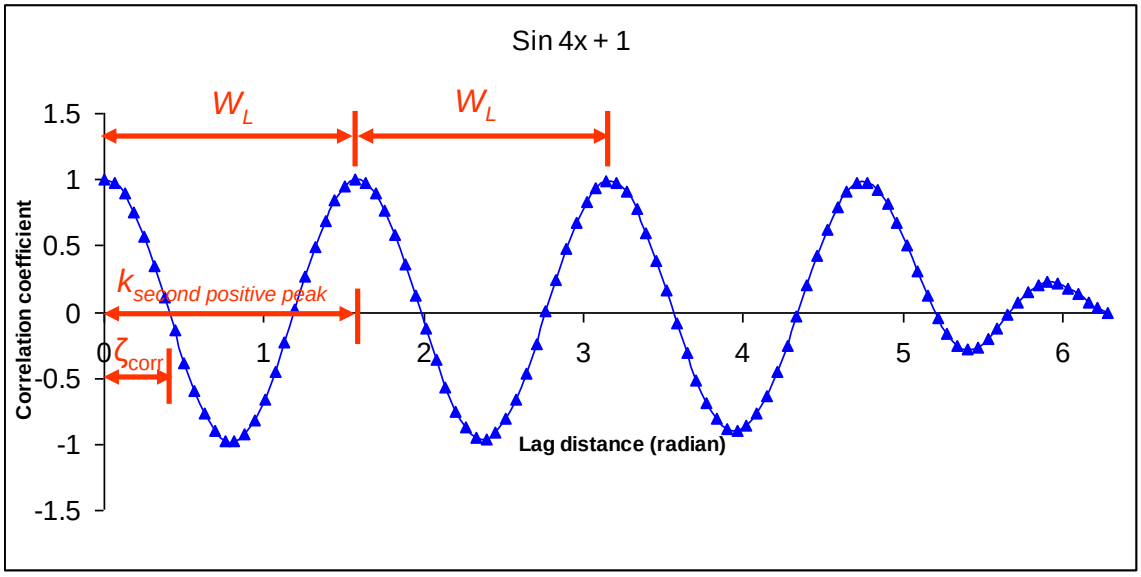

Figure 4.2 Concept of wavelength of correlation coefficient function of a sinusoid (*sin 4x + 1*)

Correlation coefficient functions of sinusoids with a few cycles fluctuate a few times and finally converge on the lag distance, which is equal to the total length of a data sequence. The number of repetitions decreases as the relative length of the period within a range of analysis increases. For example, the waveform of (sin $4x$) + 1 has a larger number of repetitions as compared to the waveform of (sin x) + 1 as a result of the smaller wavelength of sin $4x$ + 1 within the same range. It is noteworthy that the waveform of sin x + 1, which has the longest fluctuation among the estimated waves, has a larger correlation distance than any other sinusoidal waveform; the longer wavelength a data set has, the greater correlation distance it has. A sequence of uncorrelated random numbers seems to decay very quickly to a near-zero autocorrelation value, even at a short lag distance: this result strongly supports a theory that uncorrelated random values have a correlation function that equals 1.0 at zero lag and exactly 0.0 at all other lags. Therefore, it is reasonable to assume that a waveform with a larger scale of fluctuation mentioned in Chapter 2 holds a stronger correlation.

4.3. Effects of the change in sampling intervals of sinusoidal waves

4.3.1. Coefficient of variation (COV)

Sampling in digital signal processing is the process of representing and reconstructing a continuous signal by a series of discrete samples. In Section 4.5, it is shown that when residuals of soil properties in geotechnical engineering are strictly stationary, the residuals can be represented as a fluctuation or so-called equivalent wavelength. In this section, the effects of change in sampling interval on correlation

structures are estimated using a simple sinusoid. Table 4.2 shows the values of the coefficient of variation with change in sampling interval; it is assumed that the values of means for each waveform are constant. Obviously, the degree of variation COV is not sensitive to the change of sampling interval because the standard deviation for each waveform is nearly constant.

Table 4.2 Values of coefficient of variation with change of sampling interval, assuming constant average values

Sampling interval	1/25 wave length	1/10 wave length	1/8 wave length	1/4 wave length	1/3 wave length	3/5 wave length	3/4 wave length
COV (%)	70.4	69.8	69.6	68.6	67.9	68.3	68.7

4.3.2. Correlation coefficient

With regard to sampling, the primary concern is just how fast a given continuous sequence must be sampled without loss of its property. When the sampling interval is larger than half the period, a series of data samples does not have the same periodic replication as an original sequence. This effect is referred to as aliasing (Santamarina and Fratta, 1998).

As noted earlier, the sampling interval must be small enough to avoid the corruption of the original sequence. However, it would be very impractical to make the sampling interval too small because then there would be too many data measurements to be processed. In general, a rapidly varying waveform must be sampled at a small sampling interval, whereas a slowly varying waveform may be sampled at a larger sampling interval.

This section describes how to determine a proper sampling interval for the accurate representation of an original sequence by applying a variety of sampling intervals to a simple sinusoidal waveform that is considered as an ideal pattern for residuals of soil properties. In Figure 4.3, the correlation coefficient functions are drawn with different sampling intervals.

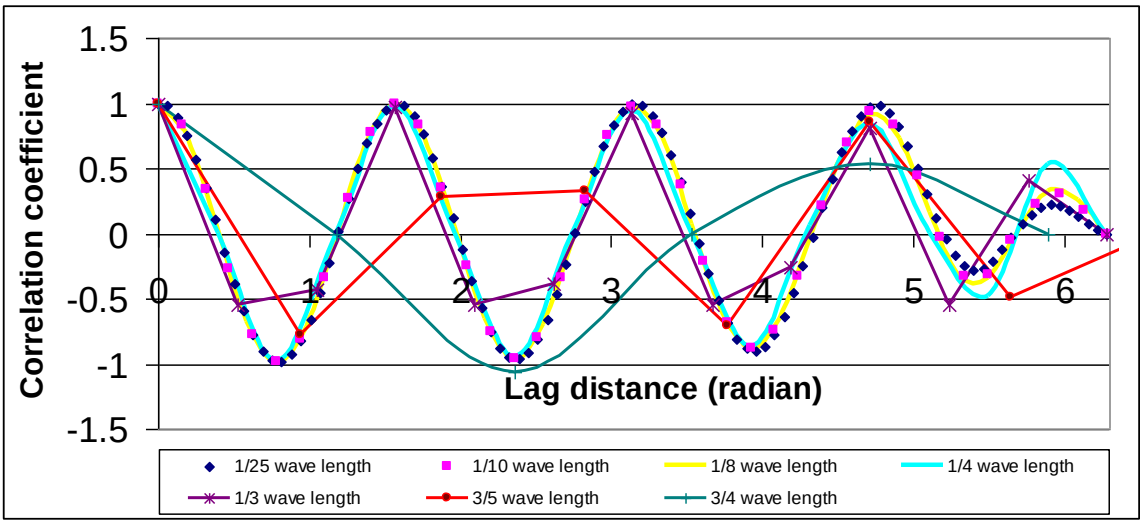

Figure 4.3 Results of correlation coefficient with change in sampling interval

Simple inspection of these features leads to the conclusion that the maximum acceptable sampling interval is half the wavelength because at least it incorporates the basic up-and-down aspect of a sinusoidal waveform. However, when sampling occurs at the zero crossings instead of at the peaks of the sinusoidal waveform, the representation of a sinusoid by two samples per wavelength is hardly adequate. Hence, it is suggested that the maximum acceptable sampling interval should be smaller than half the wavelength to avoid samplings at the zero crossings. The correlation coefficient functions with such

sampling intervals as $^{3}/_{5}$ and ¾ of the wavelengths larger than half the wavelength have correlation distances in proportion to sampling intervals. Samples with sampling intervals larger than half the wavelength form cyclic waves with a lower frequency than an original data sequence; the sampled data do not show the same periodic replication as the original sequence.

4.4. Effect of change in input duration of sinusoidal waves

4.4.1. Coefficient of variation (COV)

In order to carry out the estimation of general correlation structures of spatial variability in soil properties, it is necessary to understand the variation in patterns of correlation structures with variation in duration of input sequence. Table 4.3 shows the values of the coefficient of variation (COV) of a sinusoidal waveform, i.e., (sin 4x) + 1, based on the variation in input duration. The function sin 4x + 1 with 135° duration, which is not a harmonic of the minimum frequency of sin 4x + 1, shows a relatively small value of COV. However, when the non-harmonic input duration increases over a few cycles such as sin 4x + 1 with 315° duration, the effect of the lack of full cycles on COV can be reduced. When COV values of soil properties are estimated, the fluctuations of the soil properties may not be harmonic. When a soil property fluctuates over a few times, the estimates of COV value of the soil property may not be affected by the non-harmonic fluctuation of the soil property.

Table 4.3 Values of coefficient of variation with change of input duration, assuming constant average values

Wave range (degree)	(Sin 4x)+1 of 360 °	(Sin 4x)+1 of 315 °	(Sin 4x)+1 of 180 °	(Sin 4x)+1 of 135 °
COV (%)	70.4	69.9	70	66.4

4.4.2. Correlation coefficient

In addition to Section 4.4.1 on the patterns of COV with variation in input duration of a sinusoidal waveform, in this section, the change in patterns of correlation coefficients based on the variation in input duration of a sinusoidal wave is estimated. As illustrated in Figure 4.4, the correlation coefficient is computed as a function of angle. The correlation coefficients result from a sinusoidal waveform with the same scale of fluctuation and a variety of input durations. Although variation in input duration other than duration of one and half cycles (135°) is employed, values of correlation distance for each correlation coefficient are hardly changed. However, in order to accurately express the correlation coefficient of a continuous sequence, it is recommended that a series of samples should be an input sequence of at least a few cycles. In geotechnical engineering, sampling intervals can be determined from correlation coefficients that are estimated through field data obtained from a preliminary site investigation performed on a site of interest or through field data from previous site investigations performed near the site of interest.

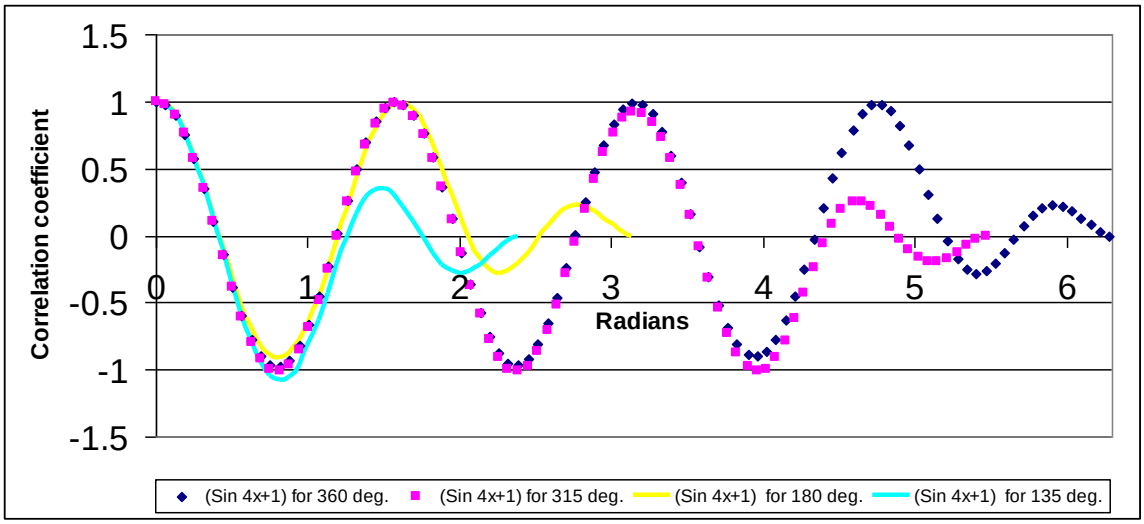

Figure 4.4 Results of correlation coefficient with change in input duration

4.5. Estimation of equivalent wavelength

Jaksa and Kaggwa (1992) have studied on the establishment of trends and relationships of various geotechnical parameters (i.e., water content and dry density) in soil layers. As a result, they found that although there exists no consistent trend for either water content or dry density in each soil layer, the two geotechnical parameters fluctuate considerably with depth. In addition, as a precursor to the development by Marr et al. (2004) of a practical method for predicting volumetric strains caused by moisture changes in highly plastic, expansive soils, they realized that the water content of the soil varies with different total stress levels. In the study by McCord et al. (1991) on the macroscopic state-dependent anisotropy in unsaturated media, it was shown that the variation in water content can cause a texturally homogeneous porous medium profile to behave anisotropically under transient unsaturated conditions. Geotechnical basic parameters

such as water content, specific gravity, and dry density fluctuate even in a spatially homogeneous soil layer.

The variation in material composition and physicochemical properties such as authigenesis, consolidation, and cementation during the process of soil formation would result in fluctuations in geotechnical parameters such as water content, specific gravity, and dry density on a small scale in a soil layer which is spatially homogeneous. Furthermore, the fluctuations in geotechnical parameters significantly affect small-scale spatial variability of soil properties, which are obtained from field tests, in a spatially homogeneous soil layer.

From the definition of strict stationarity discussed in Chapter 2, when a data sequence is said to be strictly stationary, the data sequence has regular fluctuations (Jaksa, 1995; Jaksa et al., 1997). In practice, field data in geotechnical engineering can be represented as a fluctuation. That is, a representative fluctuation, or so-called equivalent wavelength, can be estimated from the lag distance corresponding to the second positive peak of the correlation coefficient function of a data sequence as mentioned in Section 4.2.

When data points in a data sequence with stationarity have correlated relationships with the other data points, an equivalent wavelength for the data sequence can be estimated from the correlation coefficient between data points, as is the case of simple sinusoidal waves presented in the earlier sections. A wavelength of a soil property may be determined directly from raw data. On the whole, the method for determining wavelengths from raw data sequences is relatively more difficult and less accurate than the method for obtaining wavelengths through correlation coefficient functions. Once an

equivalent wavelength of soil property is examined, a sampling interval for in situ tests and laboratory tests is determined to properly estimate the characteristics of the soil properties, thereby bringing about an economical and time-saving site investigation without the loss of important soil information. In addition, it can be a useful tool for simulating soil properties when less site investigation is performed than required.

Studies on the equivalent wavelength have been already carried out with simple and ideal sinusoidal waveforms in Sections 4.1–4.4. It was shown that the lag distance at the second positive peak of correlation coefficient function is equal to the wavelength of a sinusoidal form. It is of great importance to apply the above relation to geotechnical practice. The CPT boring profiles collected at Bridge A-1700, Caruthersville, Missouri are attached in Appendix E. Figures 4.5–4.8 illustrate the correlation coefficient function for the sandy soil layer (between approximately 16.5 and 28.0 m) of each CPT sounding at the Bridge A1700.

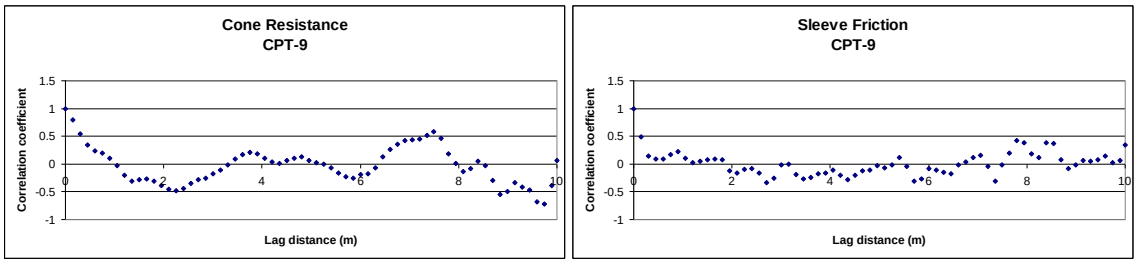

(a) (b)

Figure 4.5 Correlation coefficient functions for (a) cone resistance and (b) sleeve friction at sandy soil layer of CPT – 9 of the Bridge A1700

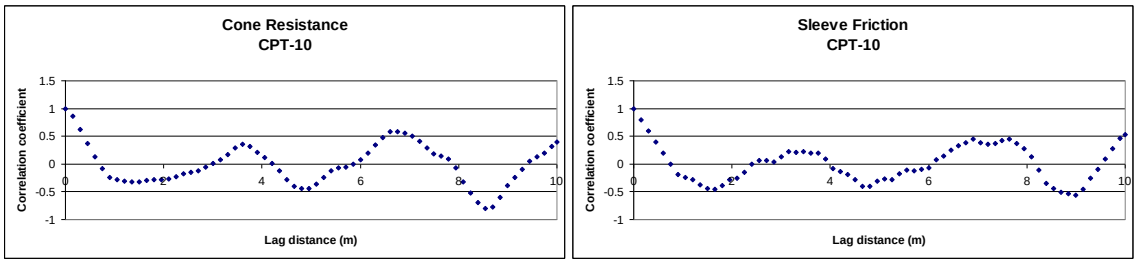

(a) (b)

Figure 4.6 (a) Correlation coefficient functions for (a) cone resistance and (b) sleeve friction at sandy soil layer of CPT – 10 of the Bridge A1700

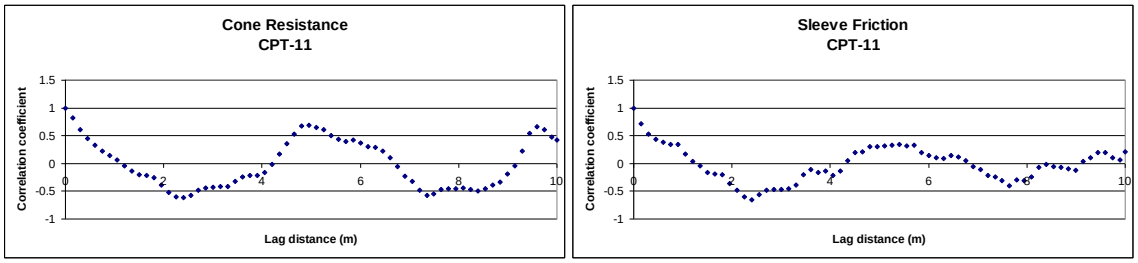

(a) (b)

Figure 4.7 (a) Correlation coefficient functions for (a) cone resistance and (b) sleeve friction at sandy soil layer of CPT – 11 of the Bridge A1700

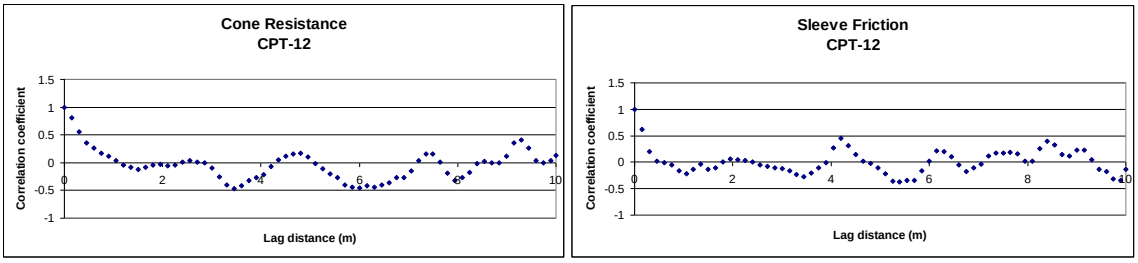

(a) (b)

Figure 4.8 (a) Correlation coefficient functions for (a) cone resistance and (b) sleeve friction at sandy soil layer of CPT – 12 of the Bridge A1700

The equivalent wavelengths of sandy soil layers for cone resistance and sleeve friction were estimated in Table 4.4 by means of the correlation coefficient function. Moreover, in order to observably determine a wavelength of a soil property, it is necessary to study how statistical structures of geotechnical real data change with the variation in sampling interval. For this purpose, the original CPT data at the Bridge A1700 (Upper Mississippi Embayment) were reconstituted according to different sampling intervals (0.15, 0.3, 0.6, 0.9, 1.2, and 2.4 m). It was observed in the earlier sections that the level of variation, COV, of a simple sinusoidal waveform is not sensitive to changes in sampling interval.

Table 4.4 Equivalent wavelength of sandy soil layers estimated in the vertical direction by the correlation coefficient function for CPT data at the Bridge A1700 (Upper Mississippi Embayment) (unit: m)

Soil Property	Method	Sounding Number			
		CPT - 9	CPT - 10	CPT - 11	CPT - 12
Cone Resistance	Correlation Coefficient	3.8	3.4	4.8	2.7
Sleeve Friction	Correlation Coefficient	2.9	3.4	5.0	2.1

Table 4.5 shows the values of COV for sand layers with a variety of sampling intervals for CPT data reconstituted from original CPT data at the Bridge A1700 according to different sampling intervals. In Table 4.5, the average values of COV of CPT data reconstituted with a variety of sampling intervals in sand layers are nearly constant. This evidence supports the conclusion that the variation of a soil property is

insensitive to changes in sampling interval as seen in the analysis of a simple sinusoidal waveform. Thus, the use of COV values is not recommended for the estimation of the effect of sampling intervals on the statistical structures of soil properties.

Table 4.5 Estimated COVs of sand layers with change in sampling interval for CPT data at the Bridge A1700 (Upper Mississippi Embayment)

Soil Property	COV	Sampling Interval					
		0.15m	0.3m	0.6m	0.9m	1.2m	2.4m
Cone Resistance	Average (%)	21	21	22	21	21	24
	Standard Deviation (%)	3	2	4	4	2	4
	No. of Samples	4	4	4	4	4	4
Sleeve Friction	Average (%)	33	32	33	31	33	29
	Standard Deviation (%)	5	5	6	6	3	5
	No. of Samples	4	4	4	4	4	4

Figures 4.9–4.12 illustrate the correlation coefficient functions of data sets reconstituted using a variety of sampling intervals from cone resistance and sleeve friction at the Bridge A1700 (Upper Mississippi Embayment).

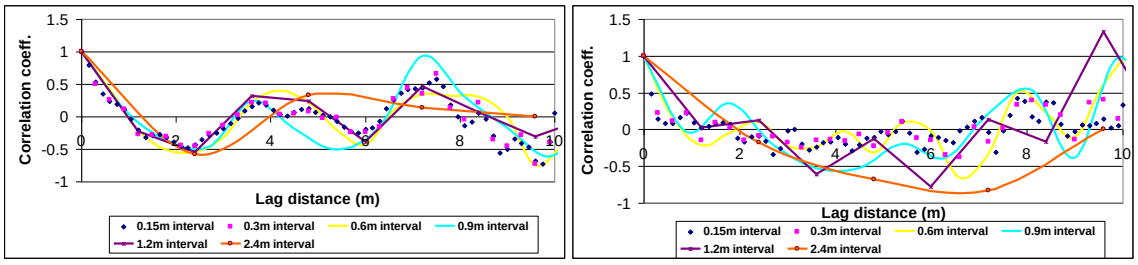

(a) (b)

Figure 4.9 Correlation coefficient functions with change in sampling interval for (a) cone resistance and (b) sleeve friction at CPT – 9 of the Bridge A1700

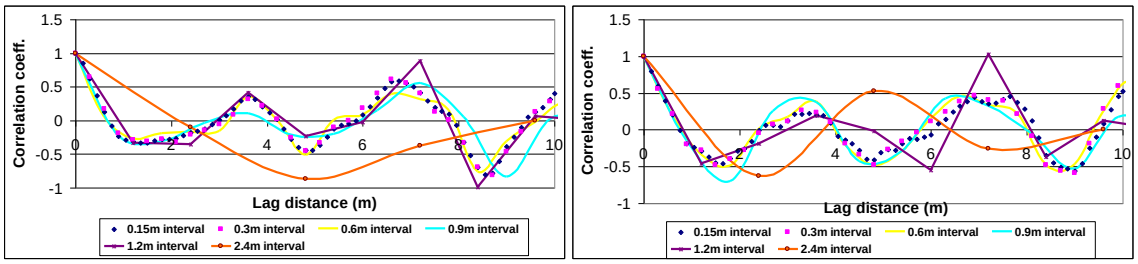

(a) (b)

Figure 4.10 Correlation coefficient functions with change in sampling interval for (a) cone resistance and (b) sleeve friction at CPT – 10 of the Bridge A1700

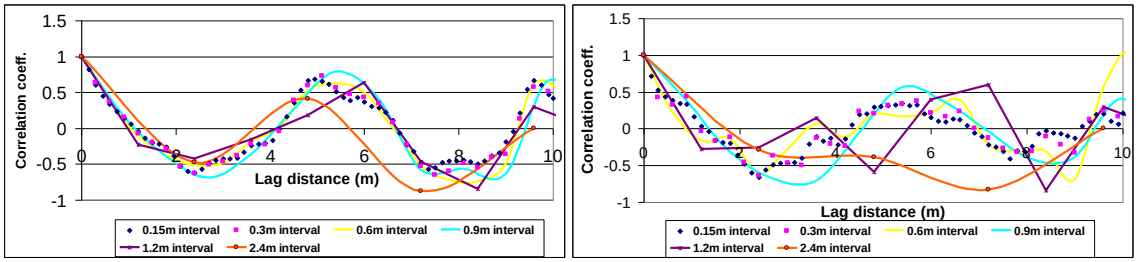

(a) (b)

Figure 4.11 Correlation coefficient functions with change in sampling interval for (a) cone resistance and (b) sleeve friction at CPT – 11 of the Bridge A1700

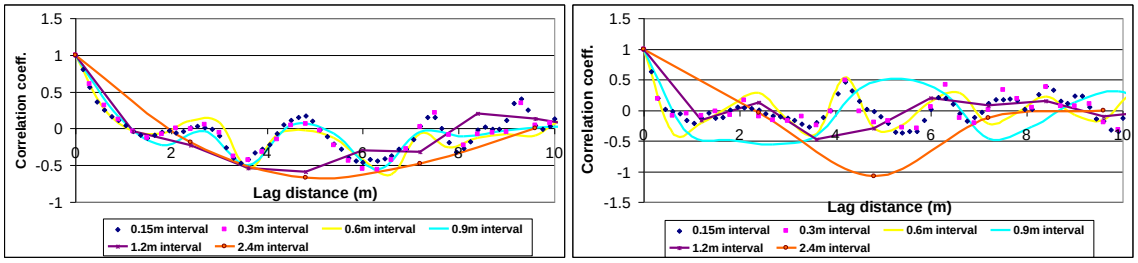

(a) (b)

Figure 4.12 Correlation coefficient functions with change in sampling interval for (a) cone resistance and (b) sleeve friction at CPT – 12 of the Bridge A1700

When a sampling interval is greater than half of the estimated equivalent wavelength, the correlation coefficient functions of the following CPT data sets have significantly increased zero-correlation distances, while those correlation coefficient functions with sampling intervals of less than half the wavelength have almost constant

zero-correlation distances: cone resistance and sleeve friction at CPT-9; cone resistance and sleeve friction at CPT-10; cone resistance and sleeve friction at CPT-12. The correlation coefficient function of cone resistance at CPT-11 has a constant zero-correlation distance regardless of sampling interval because all sampling intervals are less than half of its equivalent wavelength. Although its sampling interval of sleeve friction at CPT-11 is 2.4 m, which is less than half of the estimated equivalent wavelength, its correlation coefficient function did not keep a constant zero-correlation distance, but the zero-correlation distance increased.

Taking zero-correlation distance as an indicator of the wavelength level of fluctuation of a data set into consideration, the aliasing concept is effective for explaining these cases except for sleeve friction at CPT-11, because the maximum statistically allowable sampling interval without the loss of periodic information is half a wavelength. Just as the above phenomenon seen in correlation coefficient functions held true for the analyses of simple sinusoidal waveforms, so the equivalent wavelengths of sand layers in the vertical direction summarized in Table 4.4 reasonably satisfied the above features in correlation coefficient functions except for sleeve friction at CPT-11. From the above, it is shown that an equivalent wavelength of a soil property can be derived from the lag distance at the second positive peak of correlation coefficient function or an interval between positive/negative peaks of correlation coefficient function.

Overall, in random field simulations, a simple model to separate the scatter data of soil properties in geotechnical engineering to two elements was used: a deterministic element called the trend and a stochastic element known as the residuals. From the statistical estimates of soil properties available to date, it was observed that most soil

properties with stationarity in geotechnical engineering can be represented as their own equivalent wavelengths obtained from the correlation coefficient function.

Therefore, the residuals in the above simple model can be expressed in more detail as a combination of an equivalent periodicity and a random element as shown in Figure 4.13.

That is, the spatial variability of a soil property, v_x, at a location x in geotechnical engineering can be modeled as

$$[v] = [t] + [\zeta] + [\xi] \qquad (4.5.1)$$

where t is a trend element of v at location x, ζ is an equivalent periodicity of v around the trend at location x, and ξ is a random element of v around the trend at location x.

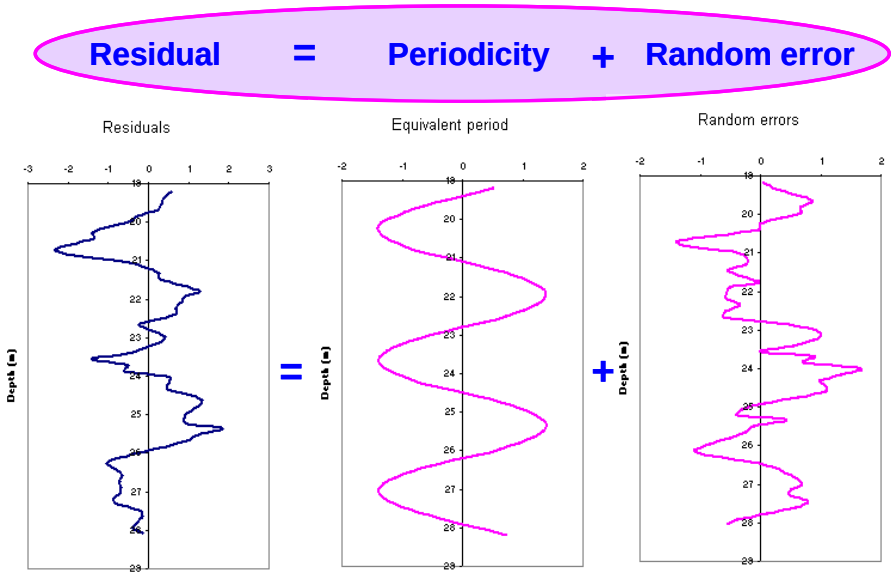

Figure 4.13 Concept of residuals consisting with equivalent periodicity and random error

4.6. Application of the concept of aliasing to soil properties for the maximum statistically allowable sampling interval

4.6.1. Definition of the maximum statistically allowable sampling interval by the concept of aliasing

In geotechnical engineering, the primary concern is just how fast and efficiently a given continuous soil profile must be sampled without incurring the loss of soil information. Surplus data collection results in extra cost when calculating more exact soil properties for the design of geotechnical facilities. In addition, cases where the performance of site investigation is less than required may even result in significant corruption of the original soil properties, i.e., significant loss of the statistical characteristics of the original soil properties. It follows that it is very important to find a balance between the two: cost and data quantity. As already mentioned, when the sampling interval is not chosen to be smaller than half the minimum period, a series of sampled data points does not have the same periodic replication as the original sequence. This effect is referred to as aliasing. To avoid this undesirable outcome, it is required that

$$\max \Delta < \frac{\min w_L}{2} \tag{4.6.1}$$

where Δ is the sampling interval and w_L is the estimated wavelength of a soil profile.

Therefore, as identified in Section 4.3, in order to replicate the periodicity of an original soil property without losing vital information, the maximum statistically allowable sampling intervals should satisfy the above inequality, at the least.

4.6.2. Maximum statistically allowable sampling interval in the vertical direction by the concept of aliasing

The aliasing concept, frequently used in the field of digital signal processing, is applied to the estimation of the maximum statistically allowable sampling interval as an alternative. In order to determine the maximum statistically allowable sampling intervals by the concept of aliasing, it is necessary to estimate the wavelengths of soil properties in advance. In Tables 4.6–4.8, the wavelengths of each soil type in the vertical direction for CPT data in the Upper Mississippi Embayment, the Piedmont Province, and the Coastal Plain Province are estimated by the lag distance at the second positive peak of correlation coefficient function or an interval between positive/negative peaks of correlation coefficient function.

Table 4.6 Estimated wavelength of each soil type in the vertical direction for CPT data in the Upper Mississippi Embayment

Area	Soil Property	Wavelength	Soil Type				
			Sand	Silty Sand	Clayey Silt	Silty Clay	Clay
Upper Mississippi Embayment	Cone Resistance	Average (m)	2.8	3.4	1.3	1.5	1.3
		Standard Deviation (m)	1.6	2.3	0.8	0.8	0.6
		No. of Samples	29	11	9	9	20
	Sleeve Friction	Average (m)	3.0	3.3	1.4	2.0	1.4
		Standard Deviation (%)	1.5	2.1	0.8	0.8	0.7
		No. of Samples	27	11	9	9	20

Table 4.7 Estimated wavelength of each soil type in the vertical direction for CPT data in the Piedmont Province

Area	Soil Property	Wavelength	Soil Type				
			Sand	Silty Sand	Sandy Silt	Clayey Silt	Clay
Piedmont Province	Cone Resistance	Average (m)	0.7	1.0	0.8	0.8	2.5
		Standard Deviation (m)	0.3	0.4	0.4	0.6	2.3
		No. of Samples	9	13	11	11	32
	Sleeve Friction	Average (m)	0.7	0.8	0.7	0.7	2.5
		Standard Deviation (%)	0.3	0.3	0.3	0.2	2.2
		No. of Samples	9	13	11	11	32

Table 4.8 Estimated wavelength of each soil type in the vertical direction for CPT data in the Coastal Plain Province

Area	Soil Property	Wavelength	Soil Type		
			Silty Sand	Sandy Silt	Clay
Coastal Plain	Cone Resistance	Average (m)	1.3	1.5	0.7
		Standard Deviation (m)	0.7	0.7	0.6
		No. of Samples	12	11	9
	Sleeve Friction	Average (m)	1.4	1.7	0.9
		Standard Deviation (%)	1.0	0.7	0.7
		No. of Samples	12	10	9

The smallest value among subtraction values of the standard deviations from the average equivalent wavelengths of each soil type in individual areas was chosen as a critical wavelength for each area. When the critical wavelength is selected, the maximum statistically allowable sampling interval to avoid the loss of original periodic information of most soil types in the area can be estimated using Eq. 4.6.1. For example, the

maximum statistically allowable sampling interval in the Upper Mississippi Embayment is estimated by subtracting the standard deviation from the average wavelength of cone resistance of the clayey silt layer: the maximum statistically allowable sampling interval = (1.3 − 0.8)/2 = 0.25 m. The maximum statistically allowable sampling interval in the Piedmont Province estimated from the subtraction of the standard deviation from the average wavelengths of cone resistance of the clayey silt layer or the clay layer is equal to 0.1 m. The maximum statistically allowable sampling interval in the Coastal Plain Province estimated from the subtraction of the standard deviation from the average wavelength of cone resistance of the clay layer is equal to 0.05 m.

Correlation coefficients of soil properties can be easily estimated through field data obtained from a preliminary site investigation performed on a site of interest or through field data from previous site investigations performed near the site of interest. Therefore, in order to measure soil data without the loss of correlation information in the vertical direction, a systematically and statistically meaningful allowable sampling (measurement) interval at a specific site needs to be estimated by using the concept of aliasing.

4.6.3. Maximum statistically allowable sampling interval (boring/sounding spacing) in the horizontal direction by the concept of aliasing

The concept of aliasing is used to determine the maximum statistically allowable sampling interval in the horizontal direction in this section. Correlation coefficient functions of soil properties of each soil layer in the horizontal direction should be

determined prior to the estimation of the maximum statistically allowable sampling interval.

A wavelength of a soil property may be determined directly from raw data. On the whole, the method of determining wavelengths from raw data sequences is relatively more difficult and less accurate than the method of obtaining wavelengths through correlation coefficient functions. As mentioned in Section 4.2, a wavelength of a soil property is equal to the lag distance at the second positive peak of correlation coefficient function. The ensuing wavelengths of soil properties are applied to Eq. 4.6.1 to determine the maximum statistically allowable sampling intervals in the horizontal direction. Table 4.9 summarizes the maximum statistically allowable sampling intervals of each soil layer with the aliasing concept in the horizontal direction for CPT data at the Bridge A1700 (Upper Mississippi Embayment).

Table 4.9 Estimated maximum statistically allowable sampling interval of each soil layer by applying the aliasing concept in the horizontal direction for CPT data at the Bridge A1700 (Upper Mississippi Embayment)

Test Type	Soil Type	Property	Maximum Statistically Allowable Sampling Interval (m)
CPT	**Clay**	**Cone resistance**	13.5
		Sleeve friction	14
CPT	**Sand**	**Cone resistance**	13
		Sleeve friction	14.5

As mentioned in Section 4.5, the analysis of soil properties yields a trend, an equivalent wavelength, and random errors. Most site investigation programs have the spatial locations of borings with an irregular pattern, rather than a systematic pattern, and a limited number of borings. The limited number of borings performed at a specific site is

usually sufficient to estimate the correlation structures of each spatially homogeneous soil layer. In order to perform a systematically and statistically meaningful site investigation program without the loss of correlation information of each spatially homogeneous soil layer, however, a maximum statistically allowable sampling interval obtained by using the concept of aliasing is estimated to determine the minimum statistically required number of borings/soundings at a specific site.

4.7. Minimum statistically required sampling number in the horizontal direction

In this section, a new mathematical method is suggested for deriving the boring/sounding number for a site investigation at a specific site. In order to measure field data without the loss of original periodic information of each soil type in the horizontal direction at an area, the smallest value among equivalent wavelengths of each soil type at the area should be chosen for a critical wavelength for the area. Field data obtained from a preliminary site investigation performed on a site of interest or from site investigations previously performed near the site can be used to approximate correlation coefficients of soil properties at the site of interest.

When the critical wavelength is selected, the maximum statistically allowable sampling interval to avoid the loss of original periodic information of most soil types at the area can be estimated using Eq. 4.6.1. Given a maximum statistically allowable sampling interval for a site, the allowable influential zone of the maximum statistically allowable sampling interval is easily considered as a circle, as shown in Figure 4.14. The

radius, r_{inf}, of the influence circle is equal to half the sampling interval, Δ, in the horizontal direction as

$$r_{\text{inf}} = \frac{\Delta}{2}. \qquad (4.7.1)$$

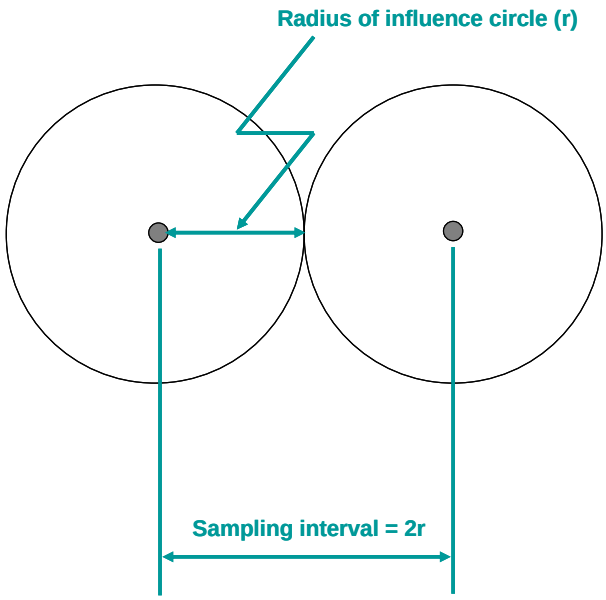

Figure 4.14 Concept of an influence circle of a sounding with half the sampling interval

Given a site of $m \times n$ dimensions as illustrated in Figure 4.15, the minimum statistically required number of soundings N_{sounding} is the total number of influence circles in a given site area as follows:

$$N_{\text{sounding}} \geq \text{Total number of influence circles in a given site area}. \qquad (4.7.2)$$

As an exercise, assuming that a site investigation is performed at a building site (100 m × 100 m dimensions) near the Bridge A1700, Missouri, the critical sampling interval for this site is 13 m according to Table 4.9. The minimum statistically required number of borings needed at the site to consider only sandy and clayey soil layers is

equal to the total number of influence circles for a given site area as. While maintaining original periodic information at the site, the minimum statistically required number of borings needed to perform the site investigation is 49.

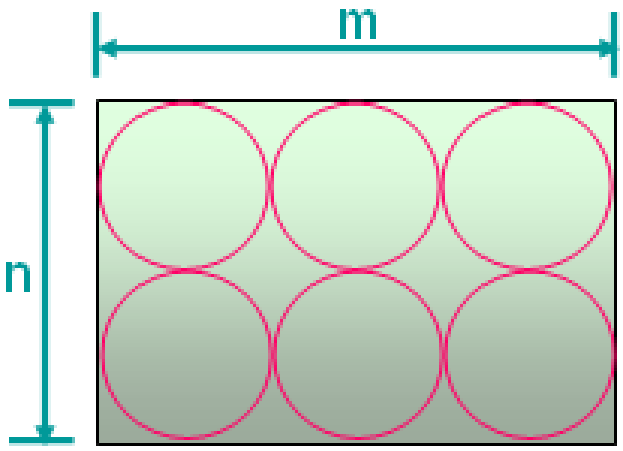

Figure 4.15 Arrangement of samplings at a site with a size of $n \times m$

Several authors (Sowers and Sowers, 1970; Das, 1997; Bowles, 1996; Henry, 1986; NAVFAC DM-7.1, 1982) have proposed a minimum of 15-meter boring spacing for rigid frame structures. Using this formula, the minimum number of borings is estimated to be 49.

The U.S. Army Corps of Engineers (2001) recommended that one perform one boring per 230 square meters for a building area. Based on this boring spacing formula, the minimum number of borings is estimated to be 44.

Compared with the minimum number of borings estimated by the existing formulae mentioned above, the minimum statistically required number of borings estimated by the proposed method is reasonable. Due to the limited extent of the data set, it is necessary to estimate the number of borings by use of the proposed method and the

existing formulae in order to strongly support that the minimum statistically required number of borings estimated by the proposed method is effective. However, it is meaningful to note that while the proposed method considers statistical structures of soil properties at a site of interest for estimating the number of borings, the existing formulae indiscriminately estimates the number of borings regardless of the statistical structures of soil properties at a site of interest.

4.8. Conclusions

In this chapter, the aliasing concept was employed to estimate the maximum statistically allowable sampling interval of data obtained from three zones: the Upper Mississippi Embayment, the Atlantic Coastal Plain Province, and the Piedmont Province. The aliasing concept is a function of wavelength: it was suggested to use this concept to derive wavelengths.

From the statistical estimates of soil properties, the spatial variability of a soil property in geotechnical engineering can be represented by a modified model composed of three elements: the trend, an equivalent wavelength and a random element.

The Upper Mississippi Embayment area and the Coastal Plain Province, whose soil formation processes are mainly governed by sedimentation, have a relatively higher maximum statistically allowable sampling interval in granular soil layers than fine soil layers. On the other hand, in the case of the Piedmont Province, which is governed by a process of the chemical weathering of intact rock, clayey soil layers have larger maximum statistically allowable sampling intervals than do granular soil layers.

Although a site investigation is not performed at a site, the statistical characteristics of soil properties at the site can be approximated by the estimates of the statistical characteristics of soil properties obtained from the same or similar soil formation process areas. Once a proper sampling interval for a specific site is determined, a method may be derived for ascertaining the minimum statistically required number of soundings/borings needed to perform a proper site investigation. It is noticeable that while the proposed method considers statistical structures of soil properties at a site of interest for estimating the number of borings, existing spacing formulae indiscriminately estimate the number of borings regardless of the statistical structures of soil properties at a site of interest.

In a typical site investigation, a few SPT borings are performed, and in some cases are supplemented by a few cone penetration tests. When every point at a given site could be tested, soil properties could be accurately estimated. However, this is not feasible, neither practically and economically. At this point, the proposed method may play a useful role in improving the identification of soil profiles as well as reducing the collection of unnecessary data without the loss of important soil information, thereby increasing the functionality of in situ tests in site investigation. However, it is necessary to estimate the number of borings by use of the proposed method and the existing formulae in order to strongly support that the minimum statistically required number of borings estimated by the proposed method is effective.

CHAPTER 5

EFFECTS OF DYNAMIC LOADING ON STATISTICAL STRUCTURES OF SOIL PROPERTIES

5.1. Introduction

It has long been known that soil parameters such as the strength or stiffness of saturated granular soils may be changed when subjected to natural or man-made dynamic loadings such as earthquakes and blastings (Casagrande, 1965; Seed and Lee, 1966). These loadings cause excess pore water pressure, which may result in liquefaction. Furthermore, existing granular soil structures are broken and rearranged by the dynamic loadings. It is anticipated that the correlation structures of soil property in an area of interest that includes granular soil layer(s) may be influenced by liquefaction that could be caused by past seismic activity. In this connection, it is of particular interest to understand how changes in the structure of soils are reflected in the statistical descriptors. Before moving on to a discussion of the effect of blasting on soil structure, however, it is necessary to understand how the mechanism of blasting densifies a soil mass by rearranging existing soil particles.

A blasting generates multiple types of sources such as impact and gas. The impact source lasts in soils only for a few milliseconds. However, a gas source lasts for a relatively long time, in general, ranging from several weeks to several years. The gas forms a considerable part of the energy caused by blasting (Konya and Water, 1990). The

gas generated from blasting has a strong expansive energy within a confining condition. The energy leads the gas to resonate in soils to reach an equilibrium condition. Most of the energy of the gas does not escape out of the confining condition of soils, so that the gas resonates in saturated soils. The gas is first compressed and then expands two to four times in the saturated soils before reaching an equilibrium condition (Charlie et al., 1980). Then, how can a soil mass be densified after blasting? Densification of saturated cohesionless soils takes place (Konya and Water, 1990; Studer and Kok, 1980; Narin van Court and Mitchell, 1994) due to

- radial compressive pressure destroying the existing soil structure;
- volumetric strains in soil mass generating excess pore water pressures; the excess pore water pressures cause soil liquefaction and the existing soil structures are rearranged;
- shear stress, caused by wave reflection between boundaries and gas resonance, resulting in excess pore water pressure and soil liquefaction, thereby leading to the densification of cohesionless soils.

Furthermore, soil densification continuously increases for several years after blasting (Konya and Water, 1990). This is called the time effect of soil densification. The excess pore water pressure dissipates in minutes or several days depending on the drainage condition of soils (Dowding and Hryciw, 1986). The excess pore water pressure is not considered due to the short duration. The time effect is mostly attributed to the dissolved gas, which does not escape out of the confining condition of soils.

The effects of blasting depend on soil type, relative density of soil, saturation degree, and site condition at the time of blasting (Narin van Court and Mitchell, 1994). In

order to effectively densify soils, the soil should have low in situ relative density and soils should be fully saturated. Energy generated by blasting is readily damped in the dry condition. The gas resonance, as mentioned earlier, lasts for a relatively longer time in saturated soils than in dry soils, thereby causing volumetric strains in the soil mass. Soil effectively densified by the blasting technique should have high permeability, namely granular soils. In order to densify soils, an increase in the effective stress should occur. In general, the existing soil particle structures are destroyed and can be rearranged into a denser configuration by the dissipation of gas. The high proportion of fine soils such as clay and silt in the soil mixture affects the level of soil densification. Clay and silt disturb the dissipation of gas and lower the permeability of soils.

5.2. Description of sites

5.2.1. Embayment Seismic Excitation Experiment project area

The Embayment Seismic Excitation Experiment project was carried out to estimate strong ground motions in the Mississippi Embayment area using a blasting technique to generate surface waves (Liao, 2005). For this purpose, blasting was employed at two test sites: Marked Tree, Arkansas, and Mooring, Tennessee, as shown in Figure 5.1.

Figure 5.1 Locations of test sites (Liao, 2005)

Cone penetration tests (CPTs) were carried out at these sites by Dr. Mayne's team at Georgia Tech in three intervals: prior to (boring B-1); and a few days (boring B-2) and about 230 days (boring B-3) after blasting. These field tests were necessary in order to obtain information about the subsurface stratigraphy and to explore the spatial variability of soil properties for evaluation of changes in the statistical properties of CPTs after blasting. The subsurface soils at these sites generally consist of sands with weak layers of fine-grained soils (silts and clays). Figures 5.2 and 5.3 illustrate the profiles of CPTs

related to blasting events at the Marked Tree site, AR, and Mooring site, TN, respectively.

Emphasis is placed on estimating the effect of blasting on the statistical characteristics of soil properties in a sand type layer (ranging from 8.0 to 18.38 m) at the Marked Tree site, AK, and in a sand type layer (ranging from 13.58 to 22.82 m) at the Mooring site, TN.

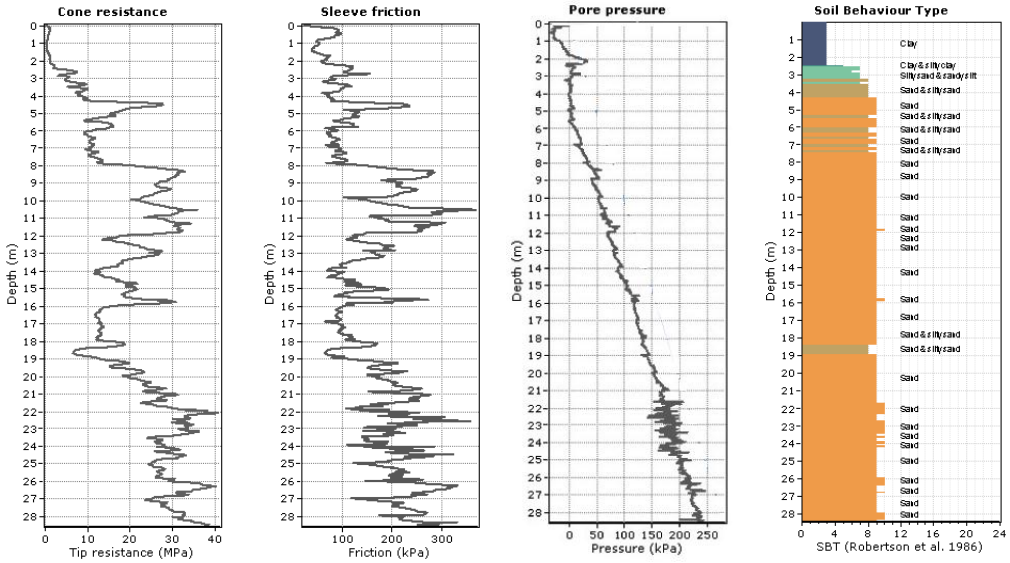

(a)

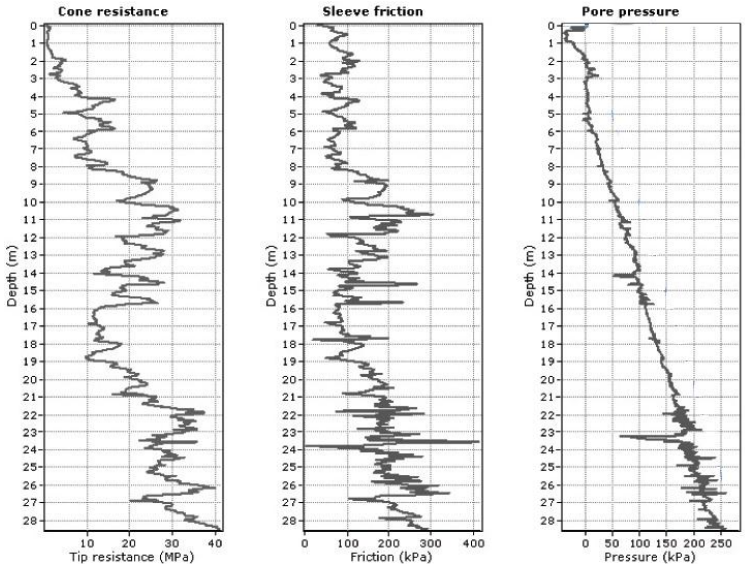

(b)

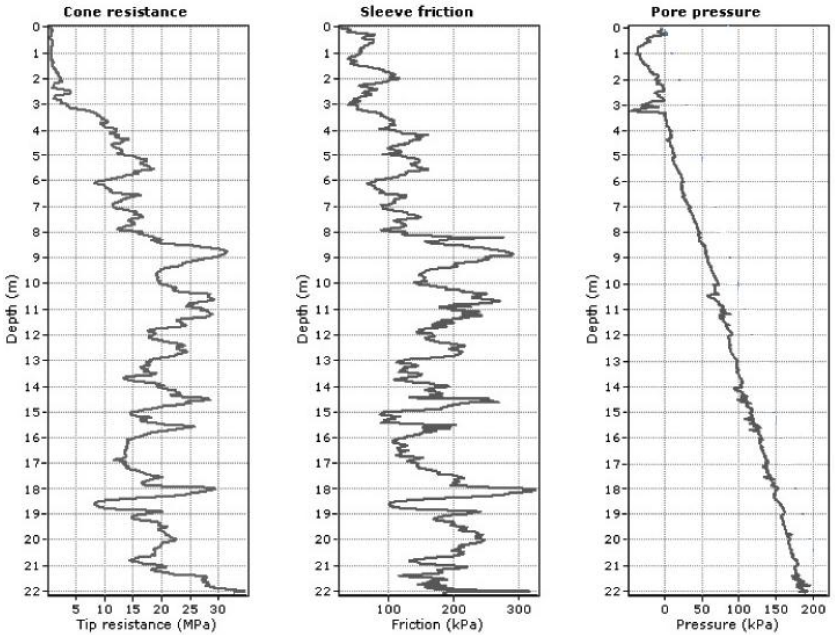

(c)

Figure 5.2 Results of cone penetration tests of (a) boring B-1 (pre-blasting) with a soil profile, (b) boring B-2 (a few days after blasting), and (c) boring B-3 (about 230 days after blasting) at Marked Tree, AR
(reference: http://geosystems.ce.gatech.edu/Faculty/Mayne/Research/index.html)

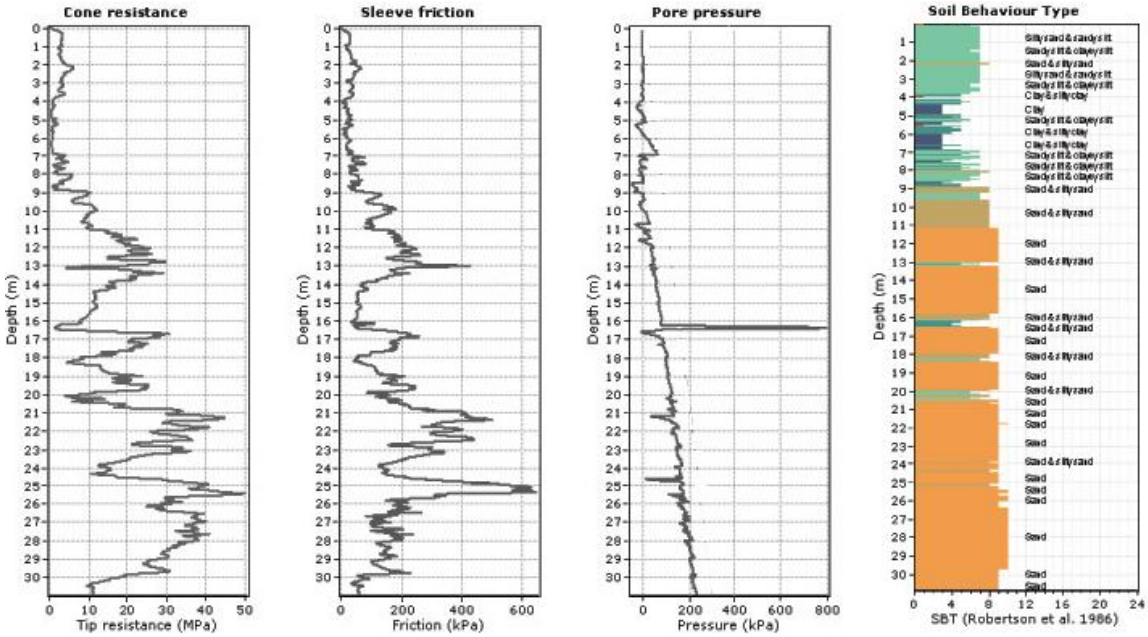

(a)

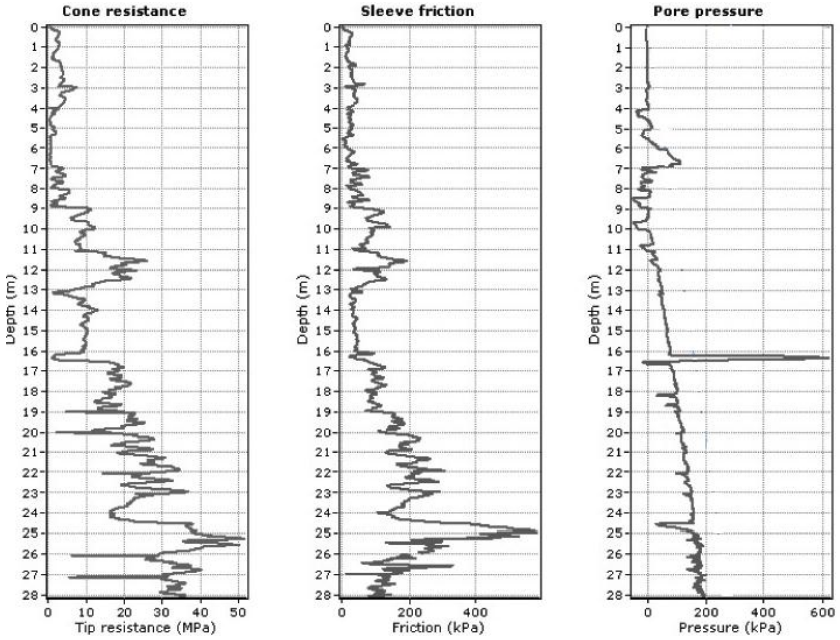

(b)

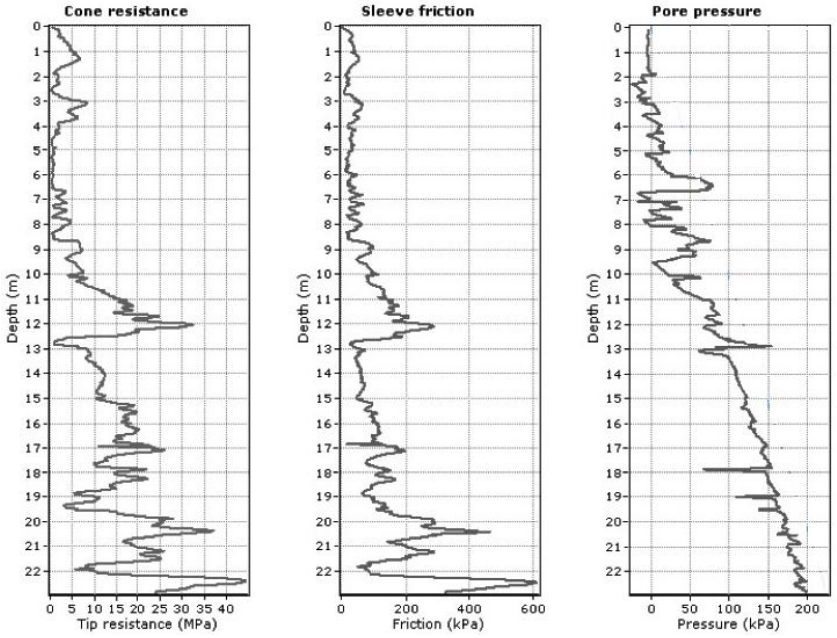

(c)

Figure 5.3 Results of cone penetration tests of (a) boring B-1 (pre-blasting) with a soil profile, (b) boring B-2 (a few days after blasting), and (c) boring B-3 (about 230 days after blasting) at Mooring, TN
(reference: http://geosystems.ce.gatech.edu/Faculty/Mayne/Research/index.html)

5.2.2. Jebba Hydroelectric project area

The Jebba hydroelectric project near Jebba, Nigeria involves the construction of a rockfill dam on the Niger River alluvium (Solymar, 1984). Figure 5.4 presents the location of the Jebba hydroelectric project. The alluvium consists of fine- to coarse-grained quartzitic sands with a trace of gravel to the depth of about 70 m. Most of the alluvium soils range from 0.075 to 4 mm in size and the uniformity coefficient of the alluvium soils ranges from 1.52 to 8.83. According to the Unified Soil Classification System (USCS), the alluvium soils are classified as clean sands (SW – SP). The loose in-place sands did not satisfy the in situ density criteria for foundation design. Thus, blasting and vibrocompaction methods were employed to make the in-place sands dense enough to meet the in situ density criteria.

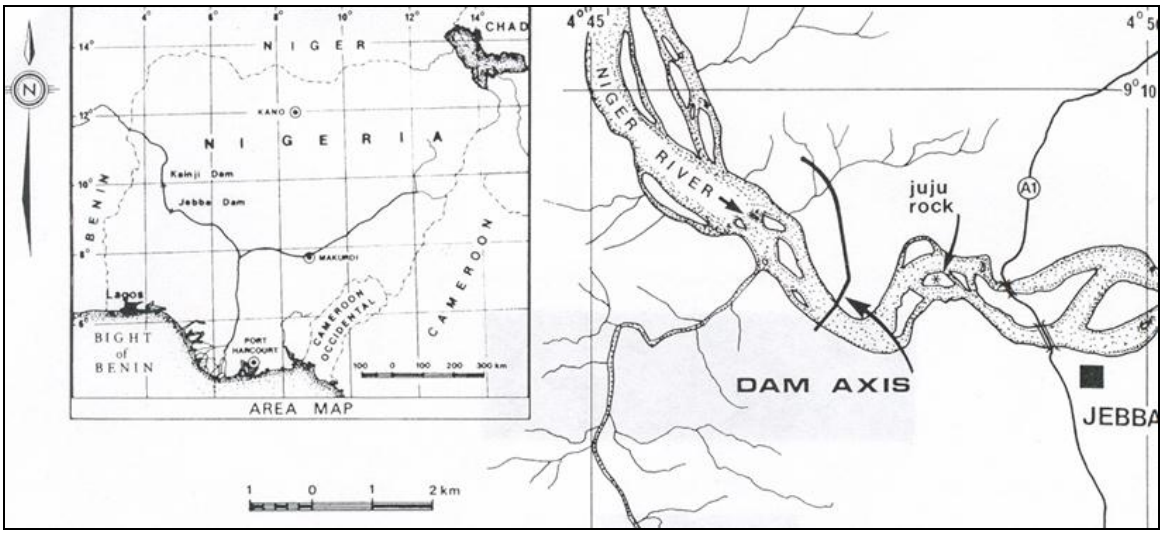

Figure 5.4 Location of the Jebba hydroelectric project (Solymar, 1984)

Test blastings such as Tests 3 and 17 were executed to determine whether suitable compaction of dredged fill materials would result from blasting. Based on the in situ data obtained from the above test blastings, blasting and vibrocompaction methods were applied to the main dam left bank as shown in Figure 5.5. The left bank of the main dam was divided into five zones based on the in situ density criteria for foundation design. Blasting techniques were employed to densify loose alluvium soils in all the zones. Cone resistance obtained from boring locations (such as Holes 117, 119, and 138 in Zone 1) were used to analyze changes in the statistical features of soil properties induced by blasting. Cone resistance obtained from Hole 141 was used to analyze the effect of the vibrocompaction method on the statistical structure of soil properties. This site is described in more detail in the paper written by Solymar (1984).

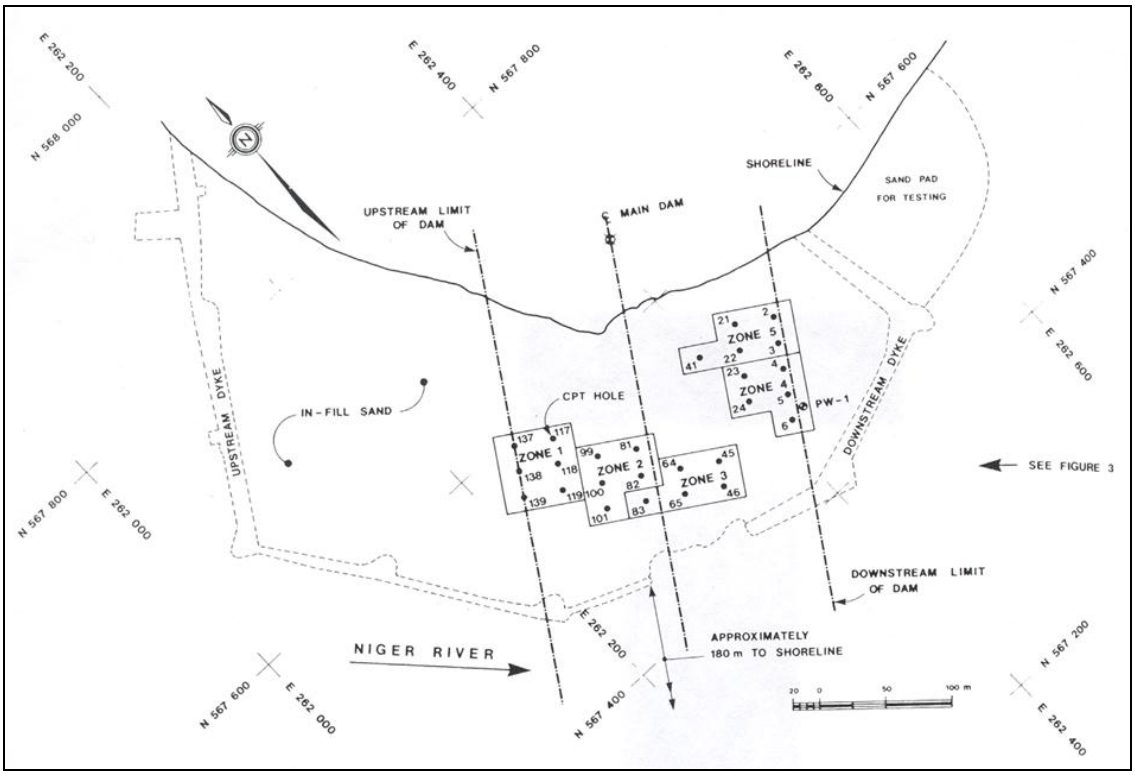

Figure 5.5 Five zones in the main dam left bank (Solymar, 1984)

5.3. Changes in strength

5.3.1. Embayment Seismic Excitation Experiment project area

Tables 5.1–5.2 show the average values of cone resistance and sleeve friction in a sand layer before and after blasting at this area as well as the range of charges. Explosives were charged between 24.4 and 48.8 m in depth at each test boring at Marked Tree, AR, and Mooring, TN. Cone resistance of CPTs is in general used as an indicator of soil strength. These tables show changes in average cone resistance for each sand layer resulting from blasting. Explosives of 1,180 kg per blasting were used at Marked Tree, AR, and explosives of 2,268 kg were set up for two test holes at Mooring, TN. Contact forces within soil particles were in equilibrium before blasting. The blastings destroyed the equilibrium of forces within soil particles as well as existing soil particle structures. Blasting instantly resulted in a reduction in the average values of cone resistance and sleeve friction in a sand layer. That is, blasting resulted in the decrease in soil strength during a short period after blasting. However, a rebound in soil strength occurred with time after blasting, although the differences in average values of cone resistance measured between a few days after blasting and 230 days after blasting are statistically significant. It is postulated that macro-scale time (i.e., several years) is needed to recover a steady state of forces within soils. This is referred to as a time effect. In reality, comparing cone resistance values measured a few days after blasting with those measured 230 days after blasting, the average values of cone resistance and sleeve friction in a sand layer increased with time after blasting. This is attributed to dissolved gas, since gas dissolved in pore water between soil particles usually leads to the densification of coarse

grained soils for several years after blasting (Konya and Water, 1990; Dowding and Hryciw, 1986).

Table 5.1 Average values of cone resistance and sleeve friction between 8.0 and 18.38 m at Marked Tree, AR

Type	B-1	Blasting	B-2	B-3
Date	10/28/2002	10/29/2002	11/1/2002	6/14/2003
Range of charges (m)	---	24.4 ~ 48.8	---	---
Average q_t (MPa)	21.3	---	20.2	20.6
Average f_s (kPa)	164	---	135	179

Table 5.2 Average values of cone resistance and sleeve friction between 13.58 and 22.82 m at Mooring, TN

Type	B-1	Blasting	B-2	B-3
Date	10/28/2002	10/29/2002	10/31/2002	6/14/2003
Range of charges (m)	---	24.4 ~ 48.8	---	---
Average q_t (MPa)	18.5	---	17.1	17.6
Average f_s (kPa)	171	---	118	156

5.3.2. Jebba Hydroelectric project area

5.3.2.1. Changes in strength after blasting

Figures 5.6–5.11 illustrate the profiles of cone resistance obtained from the site of the Jebba hydroelectric project, Nigeria. Tables 5.1–5.6 show the average values for cone resistance in sand fill layers before and after blasting at the site as well as the range of charges. Explosives of 13 to 30 kg were used per blasting. Each boring hole was surrounded by several charged holes filled up with explosives of 8.3 to 10.0 kg. As a result of blasting, it seems that a strong impact wave caused stresses to be distributed in

the soil and generated excess pore water pressures, thus decreasing the overall strength of the soil, although immediate surface settlements were observed. Comparing with cone resistances measured a short time after blasting, cone resistances obtained from the same locations several months after blasting show an increase of soil strength. As mentioned in Section 5.3.1, the dissipation of gas dissolved in the pore water between soil particles generated by blasting brings about an increase in effective stress. The increase in effective stress lasts until the dissolved gas fully escapes out of the pore water so that the gradual increase in soil strength continuously occurs for several months to years after blasting. Furthermore, compared with the results of a single explosion that used a higher amount of explosive charge in the Embayment Seismic Excitation Experiment project area, several subsequent explosions with several small charged holes cumulatively improved the soil strength over the short term.

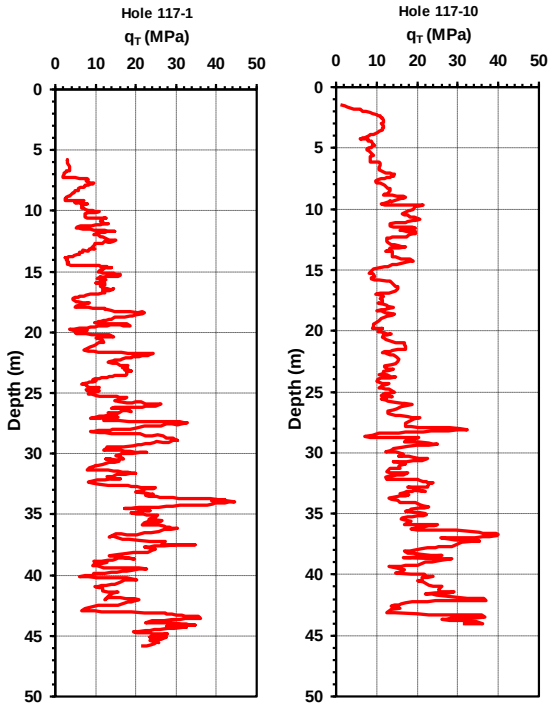

Figure 5.6 Profiles of cone resistances of before-and-after blasting at Hole 117 (Solymar, 1984)

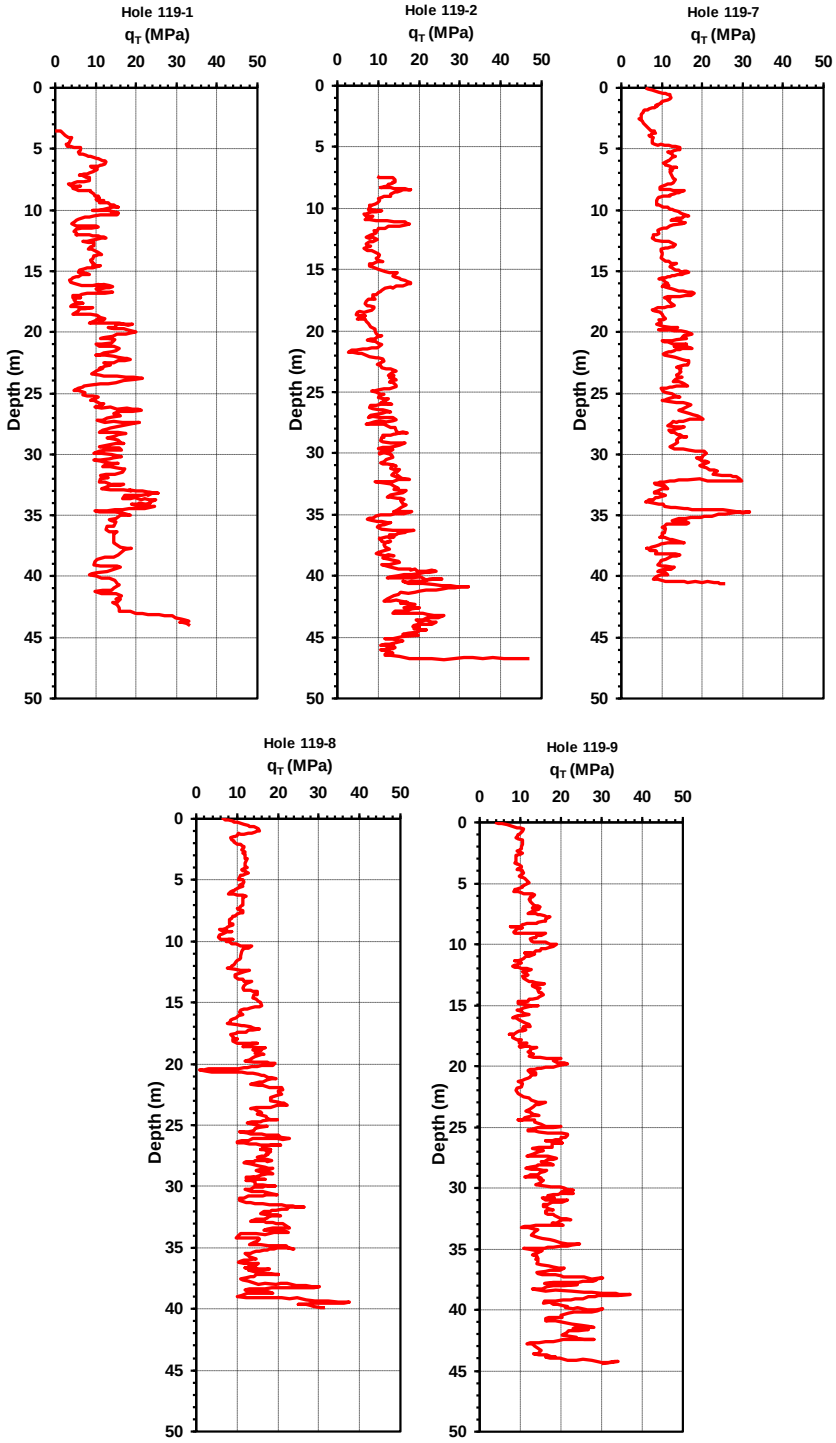

Figure 5.7 Profiles of cone resistances of before-and-after blasting at Hole 119 (Solymar, 1984)

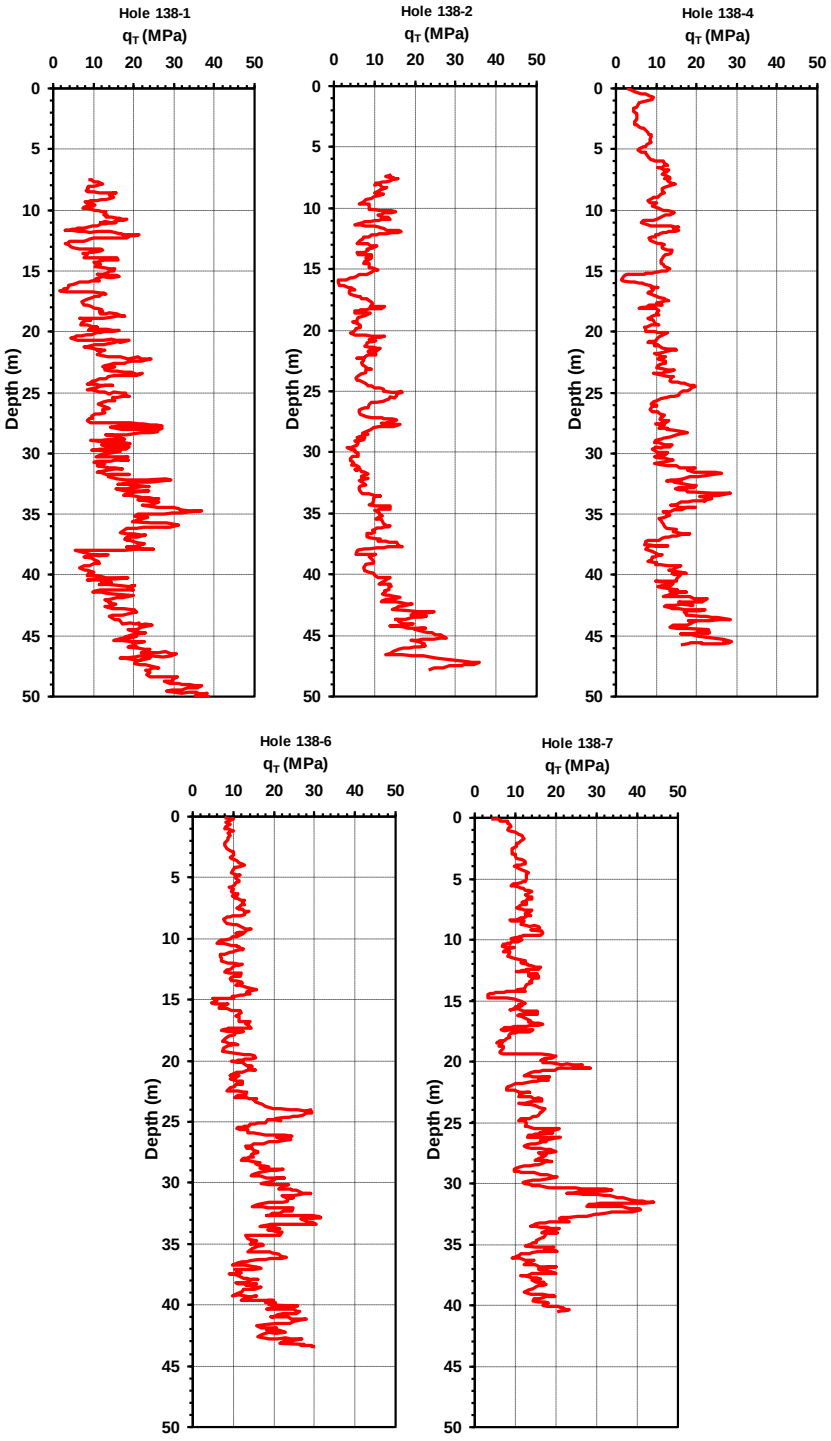

Figure 5.8 Profiles of cone resistances of before-and-after blasting at Hole 138 (Solymar, 1984)

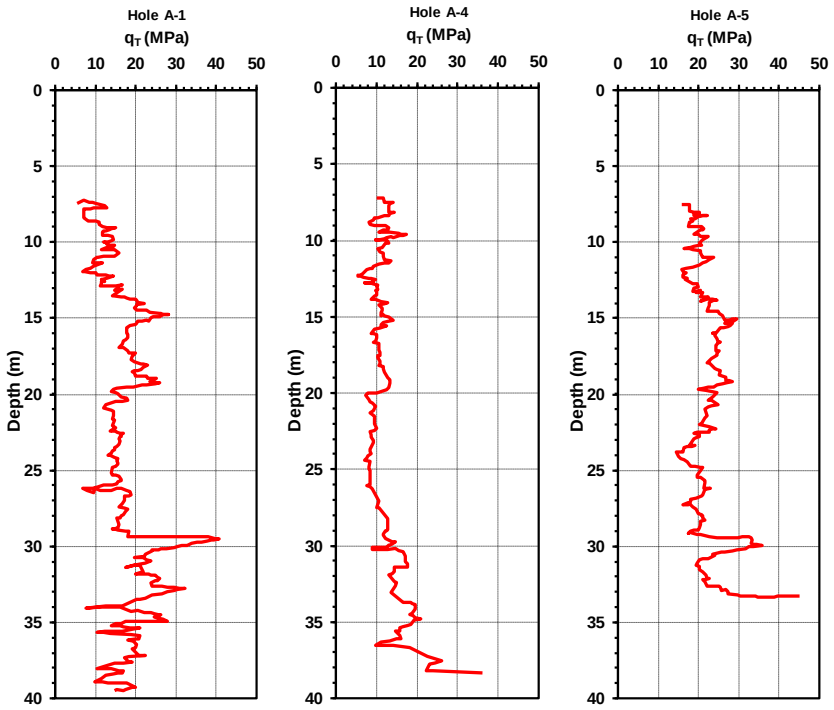

Figure 5.9 Profiles of cone resistances of before-and-after blasting at Hole A, Test 3 (Solymar, 1984)

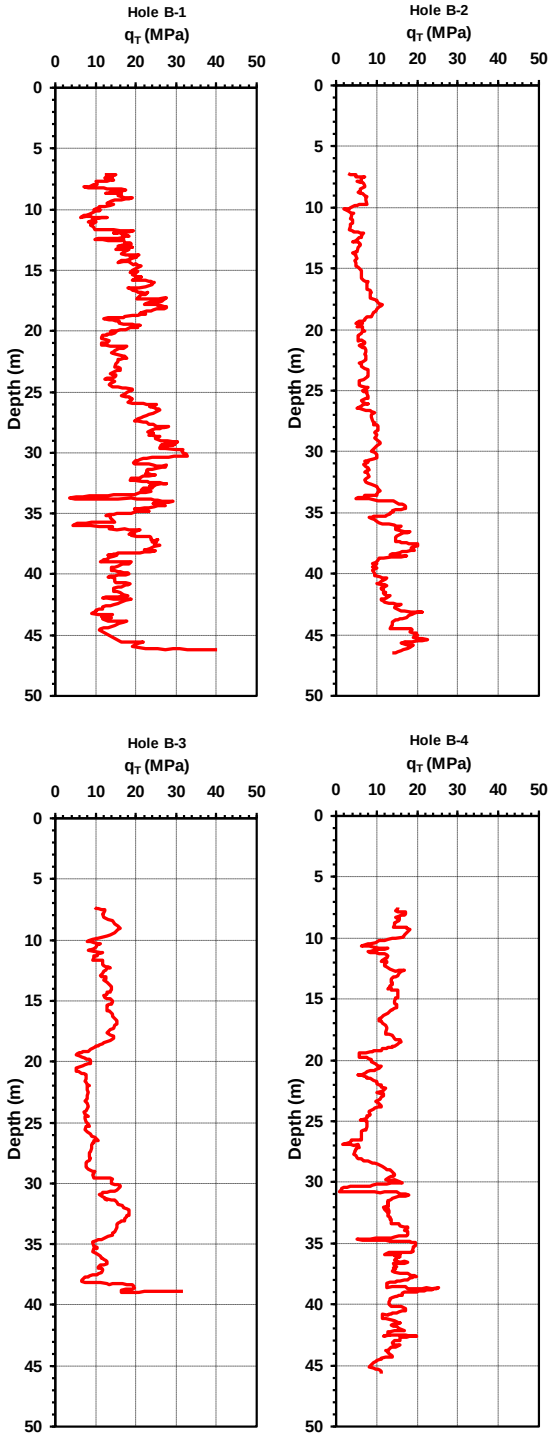

Figure 5.10 Profiles of cone resistances of before-and-after at Hole A, Test 3 (Solymar, 1984)

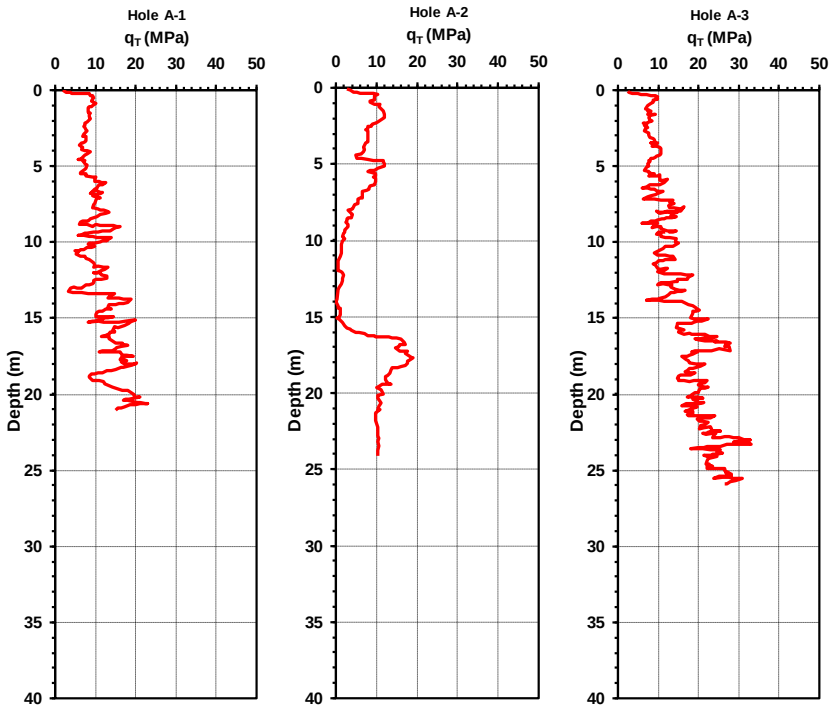

Figure 5.11 Profiles of cone resistances of before-and-after at Hole A, Test 17 (Solymar, 1984)

Table 5.3 Average values of cone resistance between 30 and 44 m at Hole 117

Type	Hole 117-1	First Blasting	Second Blasting	Third Blasting	Hole 117-10
Date	1/24 /1980	5/12 /1980	5/22 /1980	6/19 /1980	11/21 /1980
Range of charges (m)	---	38 ~ 45	38 ~ 45	31 ~ 35, 40 ~ 45	---
Average q_t (MPa)	18.9	---	---	---	21.5

Table 5.4 Average values of cone resistance between 30and 40 m at Hole 119

Type	Hole 119-1	First Blasting	Second Blasting	Hole 119-2	Third Blasting	Hole 119-7	Hole 119-8	Hole 119-9
Date	3/23 /1980	5/12 /1980	5/22 /1980	5/24 /1980	6/19 /1980	7/18 /1980	8/14 /1980	11/12 /1980
Range of charges (m)	---	34 ~ 44	34 ~ 44	---	31 ~ 35, 39 ~ 44	---	---	---
Average q_t (MPa)	15.0	---	---	13.4	---	14.1	17.0	18.5

Table 5.5 Average values of cone resistance between 30 and 40 m at Hole 138

Type	Hole 138-1	First Blasting	Hole 138-2	Second Blasting	Third Blasting	Hole 138-4	Hole 138-6	Hole 138-7
Date	3/7 /1980	5/12 /1980	5/14 /1980	5/22 /1980	6/19 /1980	7/19 /1980	8/14 /1980	11/29 /1980
Range of charges (m)	---	36 ~ 43	---	36 ~ 43	30 ~ 34, 38 ~ 43	---	---	---
Average q_t (MPa)	17.7	---	8.8	---	---	14.2	18.2	19.7

Table 5.6 Average values of cone resistance between 7.5 and 32 m at Hole A, Test 3

Type	Hole A-1, Test 3	First Blasting	Second Blasting	Third Blasting	Hole A-4, Test 3	Hole A-5, Test 3
Date	10/30 /1979	11/5 /1979	11/7 /1979	11/10 /1979	11/12 /1979	2/19 /1980
Range of charges (m)	---	34 ~ 37	35 ~ 37	36 ~ 37	---	---
Average q_t (MPa)	16.6	---	---	---	10.9	21.6

Table 5.7 Average values of cone resistance between 7.7 and 37 m at Hole B, Test 3

Type	Hole B-1, Test 3	First Blasting	Hole B-2, Test 3	Second Blasting	Hole B-3, Test 3	Third Blasting	Hole B-4, Test 3
Date	10/30 /1979	11/5 /1979	11/5 /1979	11/7 /1979	11/7 /1979	11/10 /1979	11/11 /1979
Range of charges (m)	---	34 ~ 37	---	35 ~ 37	---	36 ~ 37	---
Average q_t (MPa)	18.6	---	8.12	---	11.2	---	12

Table 5.8 Average values of cone resistance between 5.0 and 19.0 m at Hole A, Test 17

Type	Hole A-1, Test 17	Blasting	Hole A-2, Test 17	Hole A-3, Test 17
Date	12/20 /1979	12/21 /1979	12/29 /1979	3/25 /1980
Range of charges (m)	---	15 ~ 19	---	---
Average q_t (MPa)	11.3	---	5.79	14.1

5.3.2.2. Changes in strength after vibrocompaction

Figure 5.12 shows the profiles of cone resistance obtained from Hole 141 mainly densified by the vibrocompaction method, which is a soil improvement method to densify loose sandy soils by a water-jetting vibrator. As a result, as shown in Table 5.9, cone resistance measured eleven days after applying the vibrocompaction method has a lower average value than the average value of cone resistance measured before vibrocompaction. This is attributed to the steady-state soil structures being disturbed and rearranged by the vibrocompaction method. Additional cone resistance was measured at Hole 141 about one month after vibration. Compared with cone resistance measured eleven days after vibration, the soil strength was significantly improved by the vibrocompaction method. The existing soil particle structures are destroyed and can be rearranged into a denser configuration by the liquefaction caused by vibration. Compared with the improvement period of soil strength after blasting, the improvement period of soil strength after vibrocompaction is shorter, as the gas dissolved in pore water between soil particles generated by blasting takes a relatively long time to dissipate. The dissolved gas in pore water between soil particles can be considered an important factor in terms of a time effect on soil strength, which is increased by blasting.

Table 5.9 Average values of cone resistance between 8.0 and 20.0 m at Hole 141

Type	Hole 141	Vibration	Hole 141-G1	Hole 141-G2
Date	2/29/1980	6/8/1980	6/19/1980	7/4/1980
Average q_t (MPa)	16.1	---	15.4	22.7

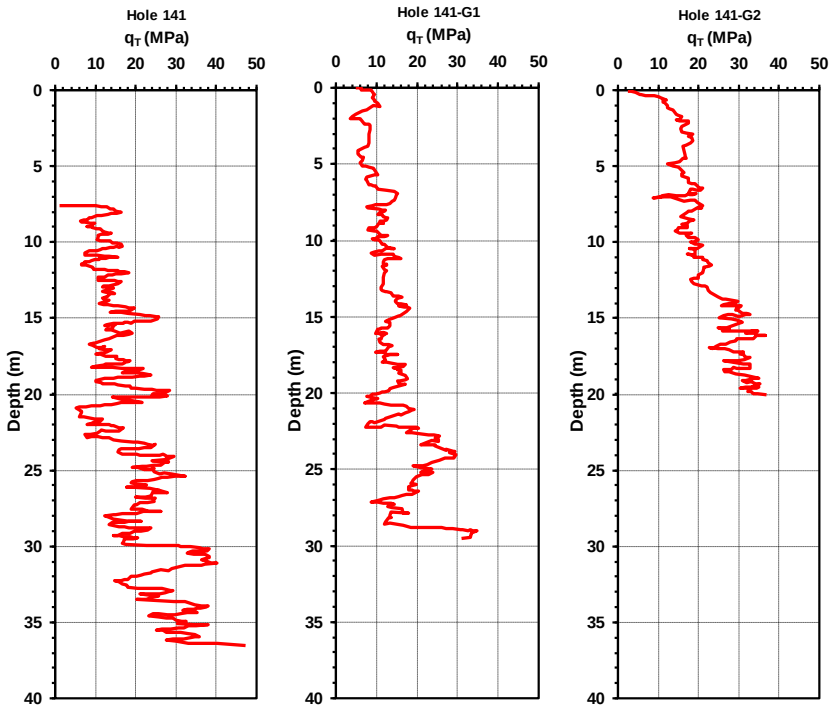

Figure 5.12 Profiles of cone resistances of before-and-after vibrocompaction at Hole 141 (Solymar, 1984)

5.4. Changes in the coefficient of variation (COV)

5.4.1. Embayment Seismic Excitation Experiment project area

Tables 5.10 and 5.11 show the average values of COV for cone resistance and sleeve friction in sand layers before and after blasting at Marked Tree, AR, and Mooring, TN, respectively. The COV values for cone resistance and sleeve friction measured a short time after blasting at Marked Tree, AR, decreased over the long term. However, the COV values for cone resistance and sleeve friction measured a short time after blasting at Mooring, TN, increased over the long term. Comparing the COV values of cone resistance and sleeve friction measured at both sites prior to blasting with those measured about 8 months after blasting, the COV values (except for sleeve friction of B-3 at

Mooring) for cone resistance and sleeve friction measured at both sites decreased over the long term. From the above evidence, it is concluded that the gas confined between soil particles after blasting leads to rearranging soil structures until the gas is dissipated, thereby gradually reducing the variation level of original soil property.

Table 5.10 Coefficient of variation of cone resistance and sleeve friction between 8.0 and 18.38 m at Marked Tree, AR

Type		B-1	Blasting	B-2	B-3
Date		10/28 /2002	10/29 /2002	10/31 /2002	6/14 /2003
Range of charges (m)		---	24.4 ~ 48.8	---	---
COV (%)	q_t	31.5	---	28.2	23.2
	f_s	40.6	---	38.0	27.7

Table 5.11 Coefficient of variation of cone resistance and sleeve friction between 13.58 and 22.82 m at Mooring, TN

Type		B-1	Blasting	B-2	B-3
Date		10/28 /2002	10/29 /2002	11/1 /2002	6/14 /2003
Range of charges (m)		---	24.4 ~ 48.8	---	---
COV (%)	q_t	53.2	---	42.8	44.9
	f_s	68.3	---	59.3	74.7

5.4.2. Jebba Hydroelectric project area

5.4.2.1. Changes in the coefficient of variation after blasting

Tables 5.12–5.17 show the results of COV for cone resistance before and after blasting at the site of the Jebba hydroelectric project, Nigeria. The COV values at Hole A

and Hole B of Test 3 and Hole A of Test 17 were estimated through a wide range of explosives to investigate the influence of blasting on soil properties.

Compared with the cone resistances measured prior to blasting, the following cases of cone resistance measured after blasting(s) show a decrease in the COV value: between 30 and 44 m at Hole 117; between 30 and 40 m at Hole 138; between 7.5 and 32.0 m at Hole A - Test 3; and between 5.0 and 19.0 m at Hole A - Test 17. On the other hand, the following cases of cone resistance finally measured after blasting(s) show a small increase in the COV value: between 30 and 40 m at Hole 119 and between 7.7 and 37 m at Hole B - Test 3.

Combining these analysis results with those of CPT data obtained from the Marked Tree, AR, and Mooring, TN, in the previous section, 7 of total 10 soil properties finally measured after blasting(s) show a decrease in the COV value. This evidence supports the conclusion that the gas confined between soil particles after blasting leads to rearranging soil structures until the gas is dissipated, thereby gradually reducing the variation level of original soil property. That is, blasting decreases the deviation level of soil properties to some extent.

Table 5.12 Coefficient of variation of cone resistance between 30 and 44 m at Hole 117

Type	Hole 117-1	First Blasting	Second Blasting	Third Blasting	Hole 117-10
Date	1/24/1980	5/12/1980	5/22/1980	6/19/1980	11/21/1980
COV(%)	41.6	---	---	---	31.3

Table 5.13 Coefficient of variation of cone resistance between 30 and 40 m at Hole 119

Type	Hole 119-1	First Blasting	Second Blasting	Hole 119-2	Third Blasting	Hole 119-7	Hole 119-8	Hole 119-9
Date	3/23 /1980	5/12 /1980	5/22 /1980	5/24 /1980	6/19 /1980	7/18 /1980	8/14 /1980	11/12 /1980
COV(%)	23.4	---	---	19.7	---	44.2	31.5	25.3

Table 5.14 Coefficient of variation of cone resistance between 30 and 40 m at Hole 138

Type	Hole 138-1	First Blasting	Hole 138-2	Second Blasting	Third Blasting	Hole 138-4	Hole 138-6	Hole 138-7
Date	3/7 /1980	5/12 /1980	5/14 /1980	5/22 /1980	6/19 /1980	7/19 /1980	8/14 /1980	11/29 /1980
COV(%)	36.6	---	30.9	---	---	31.1	29.6	41.9

Table 5.15 Coefficient of variation of cone resistance between 7.5 and 32 m at Hole A, Test 3

Type	Hole A-1, Test 3	First Blasting	Second Blasting	Third Blasting	Hole A-4, Test 3	Hole A-5, Test 3
Date	10/30 /1979	11/5 /1979	11/7 /1979	11/10 /1979	11/12 /1979	2/19 /1980
COV(%)	32	---	---	---	21.7	16.5

Table 5.16 Coefficient of variation of cone resistance between 7.7 and 37 m at Hole B, Test 3

Type	Hole B-1, Test 3	First Blasting	Hole B-2, Test 3	Second Blasting	Hole B-3, Test 3	Third Blasting	Hole B-4, Test 3
Date	10/30 /1979	11/5 /1979	11/5 /1979	11/7 /1979	11/7 /1979	11/10 /1979	11/11 /1979
COV(%)	30.1	---	40.8	---	27.3	---	33.2

Table 5.17 Coefficient of variation of cone resistance between 5.0 and 19.0 m at Hole A, Test 17

Type	Hole A-1, Test 17	Blasting	Hole A-2, Test 17	Hole A-3, Test 17
Date	12/20 /1979	12/21 /1979	12/29 /1979	3/25 /1980
COV(%)	31.0	---	98.8	33.7

5.4.2.2. Changes in the coefficient of variation after vibrocompaction

Table 5.18 shows the results of COV for cone resistance before and after vibrocompaction at the site of the Jebba hydroelectric project, Nigeria. The vibrocompaction method decreased the amplitude of the variation of soil properties in the sand layer. Although the COV value decreased over the long term due to the effects of vibration, it would be desirable to estimate an apparent change in the relative deviation of soil properties caused by vibration using more data sets.

Considering the analysis results of the changes in the COV value of soil properties after blasting, however, it is concluded that dynamic loadings such as vibration and blasting decrease to some extent the deviation level of soil properties.

Table 5.18 Coefficient of variation of cone resistance between 8 and 20 m at Hole 141

Type	Hole 141	Vibration	Hole 141-G1	Hole 141-G2
Date	2/29/1980	6/8/1980	6/19/1980	7/4/1980
COV(%)	32.5	---	17.0	23.4

5.5. Changes in the correlation coefficient

5.5.1. Embayment Seismic Excitation Experiment project area

The correlation coefficients of CPT data from the same range of sand layers at Marked Tree, AR, and Mooring, TN, were analyzed in order to obtain the effect of blasting on the correlation coefficient function. The results of the correlation coefficient functions for cone resistance and sleeve friction, respectively, at Marked Tree, AR, are drawn in Figures 5.13 and 5.14. In comparison to the correlation coefficient function of CPT data at Marked Tree, AR, before blasting, the CPT data measured 2 days after blasting presented increases in zero-correlation distances of both cone resistance and sleeve friction, and the CPT data measured about 8 months after blasting presented a small decrease in zero-correlation distance of cone resistance and an increase in zero-correlation distance of sleeve friction.

Zero-correlation distances of cone resistance and sleeve friction at Mooring, TN, significantly decreased after blasting as shown in Figures 5.15 and 5.16. Compared with the zero-correlation distances of cone resistance and sleeve friction at the Mooring site measured 3 days after blasting, the zero-correlation distances of cone resistance and sleeve friction obtained from the same location about 8 months after blasting showed a gradual increase. These features may be related to a time effect of soil densification after blasting that is mentioned in Section 5.1. However, it is necessary to analyze a variety of blasting data sets in order to explain these features.

Comparing the zero-correlation distances of soil properties measured prior to blasting with those measured about 8 months after blasting, 3 of 4 cases showed a decrease in zero-correlation distance. This means that the equivalent wavelength of soil

properties overall decreased after blasting. In other words, to some extent blasting made original soil structures more randomized, that is to say, less correlated.

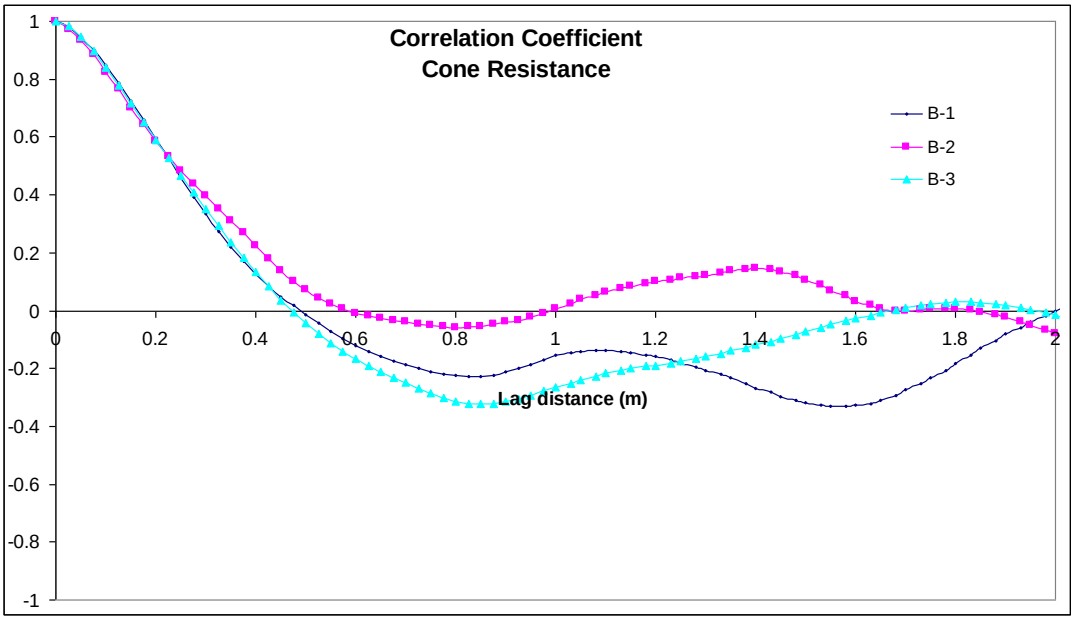

Figure 5.13 Results of correlation coefficients of cone resistance between 8.0 and 18.38 m at boring B-1 (pre-blasting), boring B-2 (a few days after blasting), and boring B-3 (230 days after blasting) at Marked Tree, AR

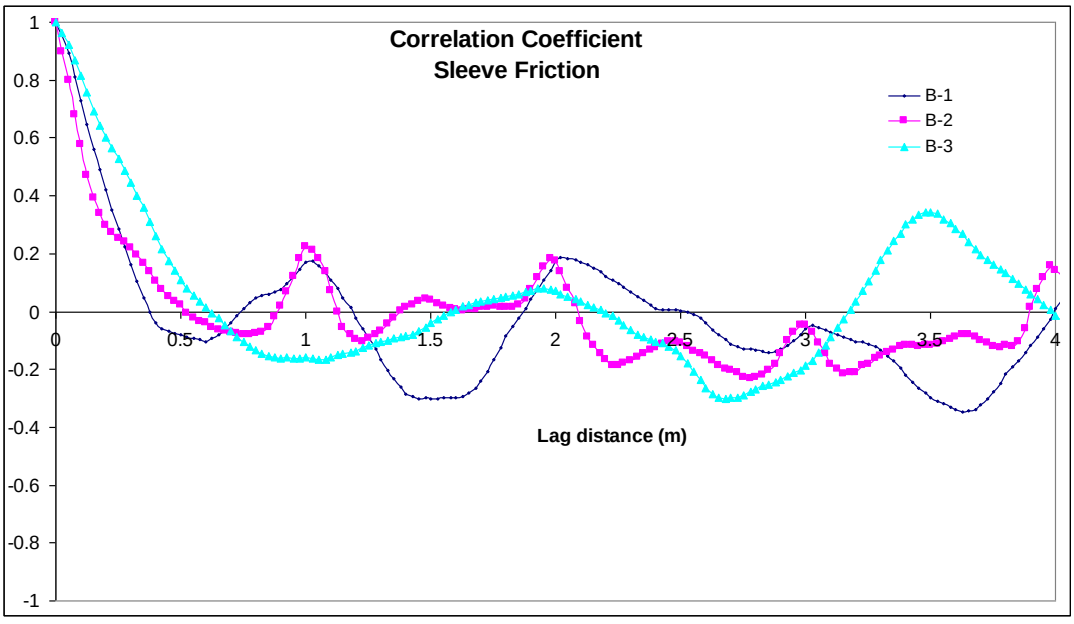

Figure 5.14 Results of correlation coefficients of sleeve friction between 8.0 and 18.38 m at boring B-1 (pre-blasting), boring B-2 (a few days after blasting), and boring B-3 (230 days after blasting) at Marked Tree, AR

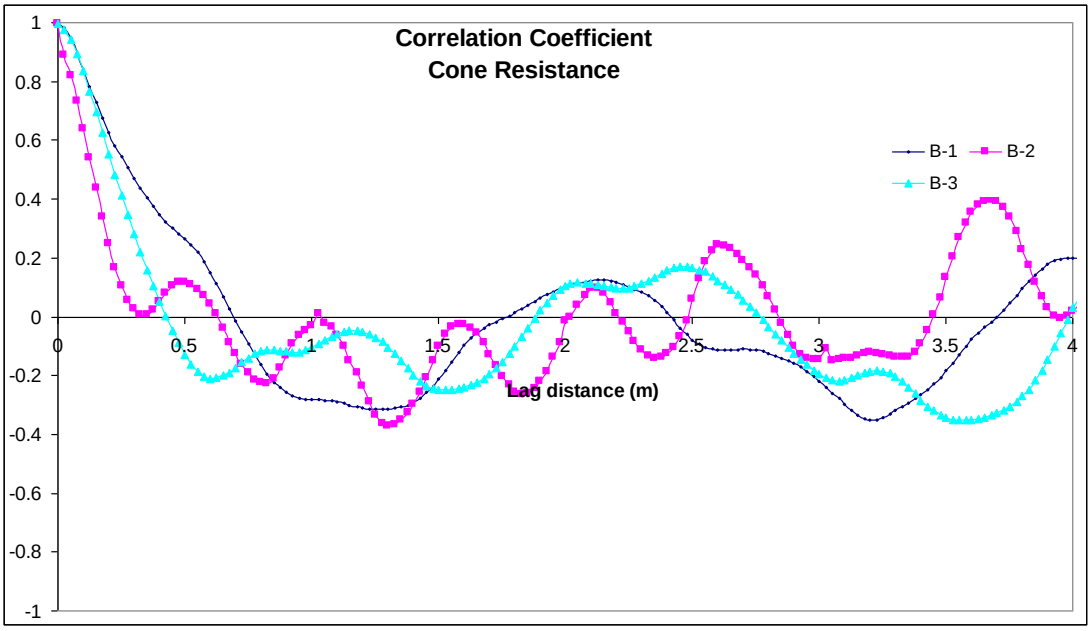

Figure 5.15 Results of correlation coefficients of cone resistance between 13.58 and 22.82 m at boring B-1 (pre-blasting), boring B-2 (a few days after blasting), and boring B-3 (230 days after blasting) at Mooring, TN

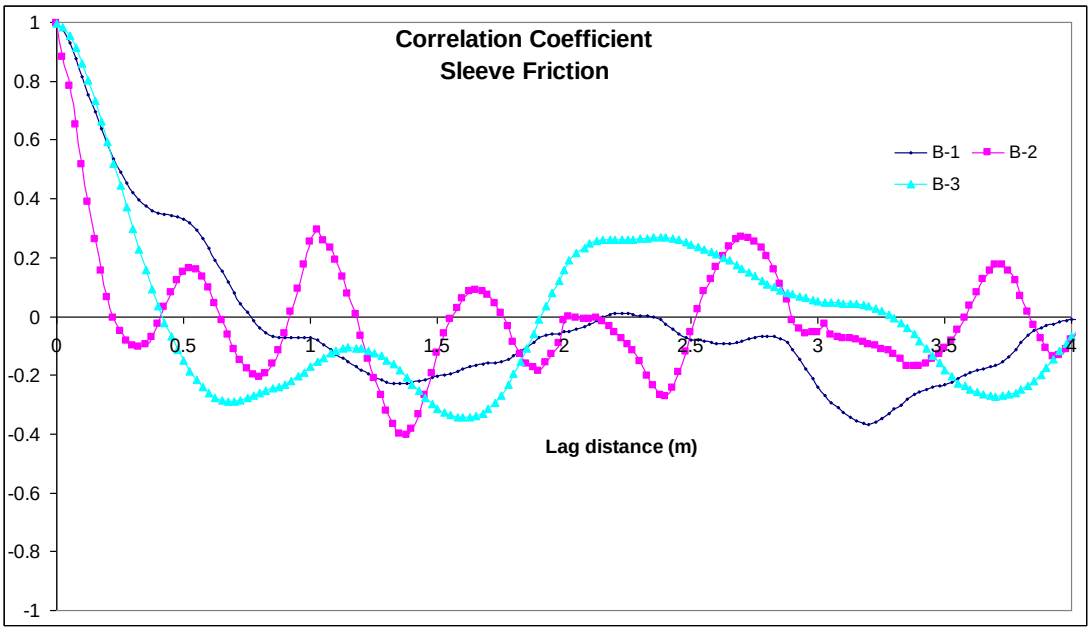

Figure 5.16 Results of correlation coefficients of sleeve friction between 13.58 and 22.82 m at boring B-1 (pre-blasting), boring B-2 (a few days after blasting), and boring B-3 (230 days after blasting) at Mooring, TN

5.5.2. Jebba Hydroelectric project area

5.5.2.1. Changes in the correlation coefficient function after blasting

Figures 5.17–5.22 illustrate the results of correlation coefficients for the cone resistances obtained from the Jebba hydroelectric development site, Nigeria. Compared with the zero correlation distances of cone resistance measured prior to blasting, the zero correlation distances of cone resistance finally measured after blasting at Hole 117, Hole 119, Hole 138, and Hole A - Test 3 decreased and those at Hole B - Test 3 and Hole A - Test 17 increased.

Combining these analysis results with the results obtained from the Marked Tree, AR, and Mooring, TN, in the previous section, 7 of total 10 soil properties finally measured after blasting(s) showed a decrease in zero correlation distance. Obviously, although these estimates may not be sufficient to verify the effect of blasting on the zero correlation distance of soil properties, the results show that to some extent blasting decreases the correlation level of soil properties; in general, blasting makes the original soil structures more randomized.

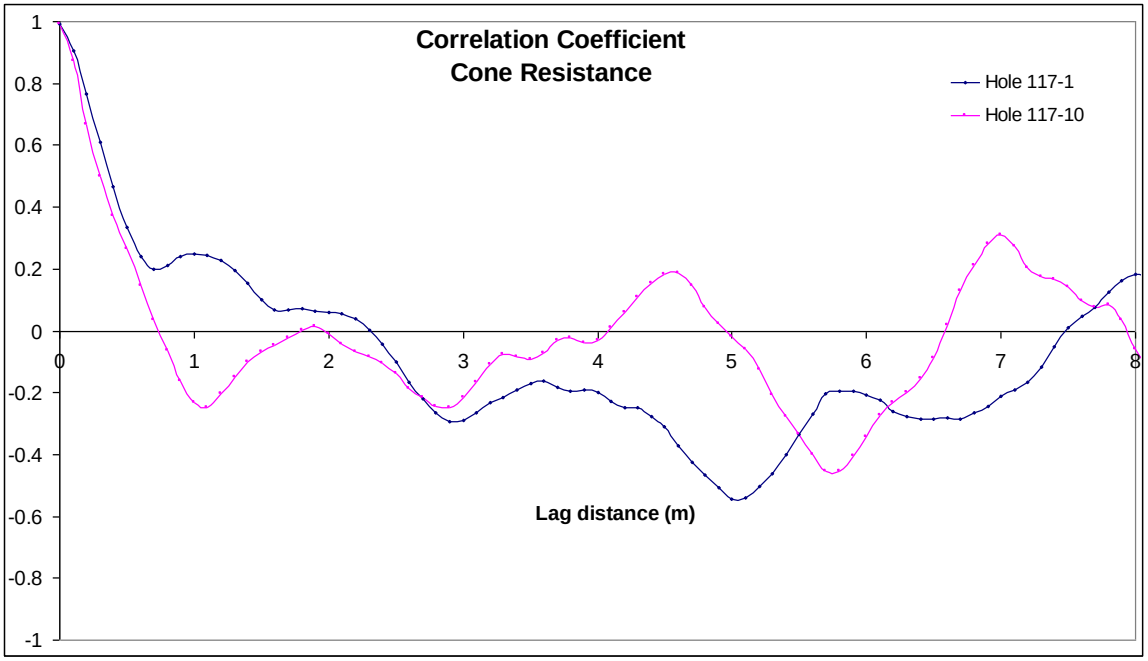

Figure 5.17 Result of correlation coefficients before and after blasting between 30 and 44 m at Hole 117

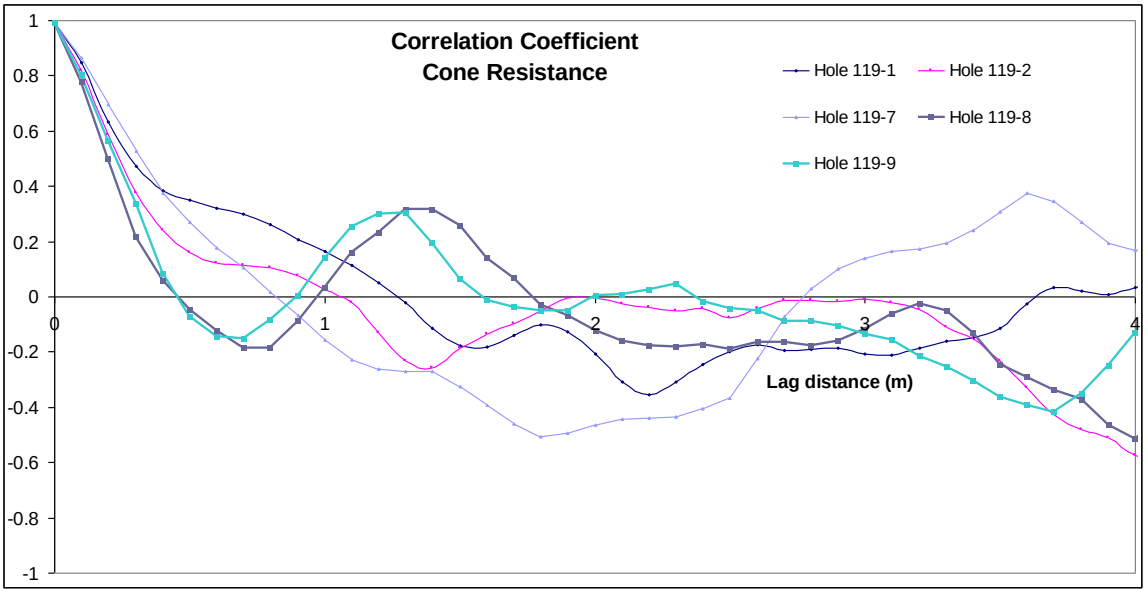

Figure 5.18 Result of correlation coefficients before and after blasting between 30 and 40 m at Hole 119

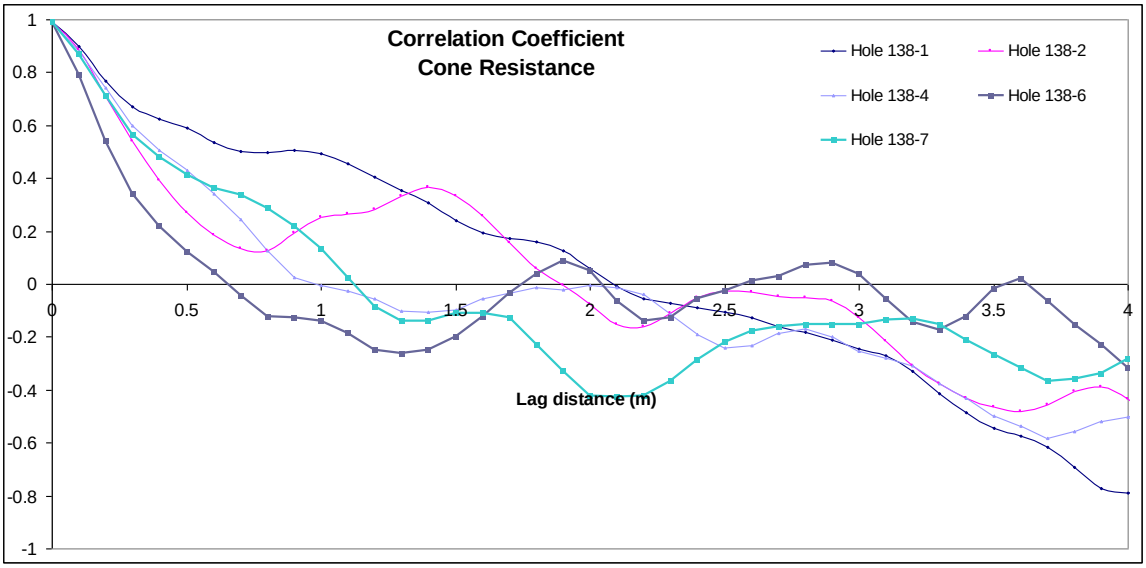

Figure 5.19 Result of correlation coefficients before and after blasting between 30 and 40 m at Hole 138

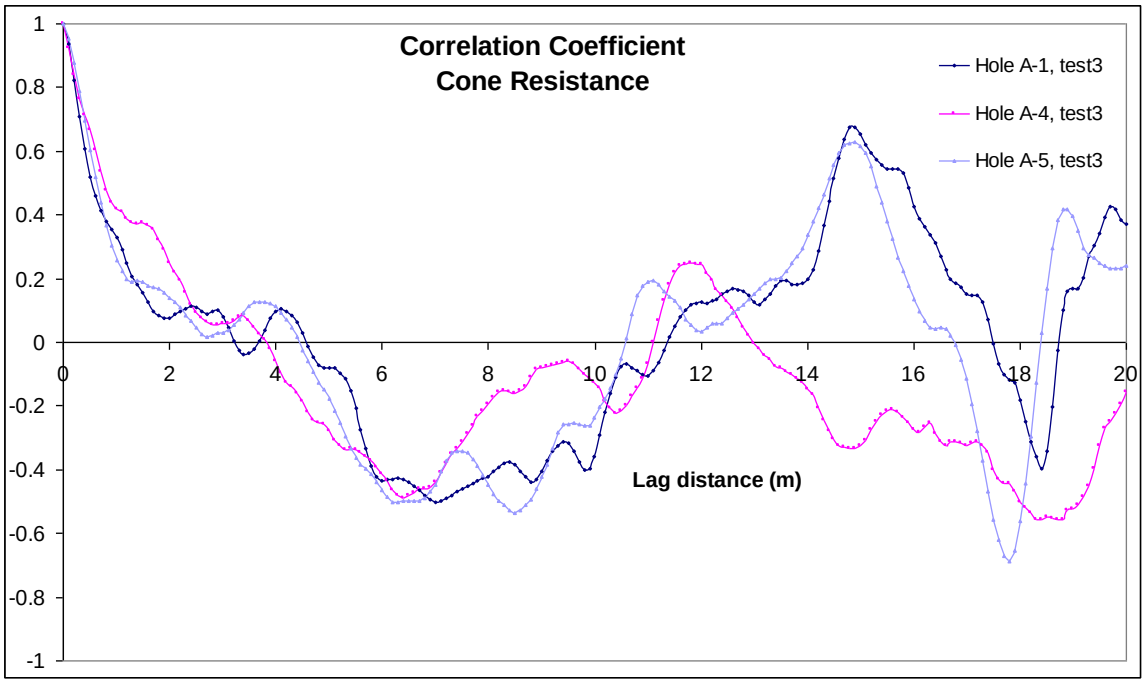

Figure 5.20 Result of correlation coefficients before and after blasting between 7.5 and 32 m at Hole A, Test 3

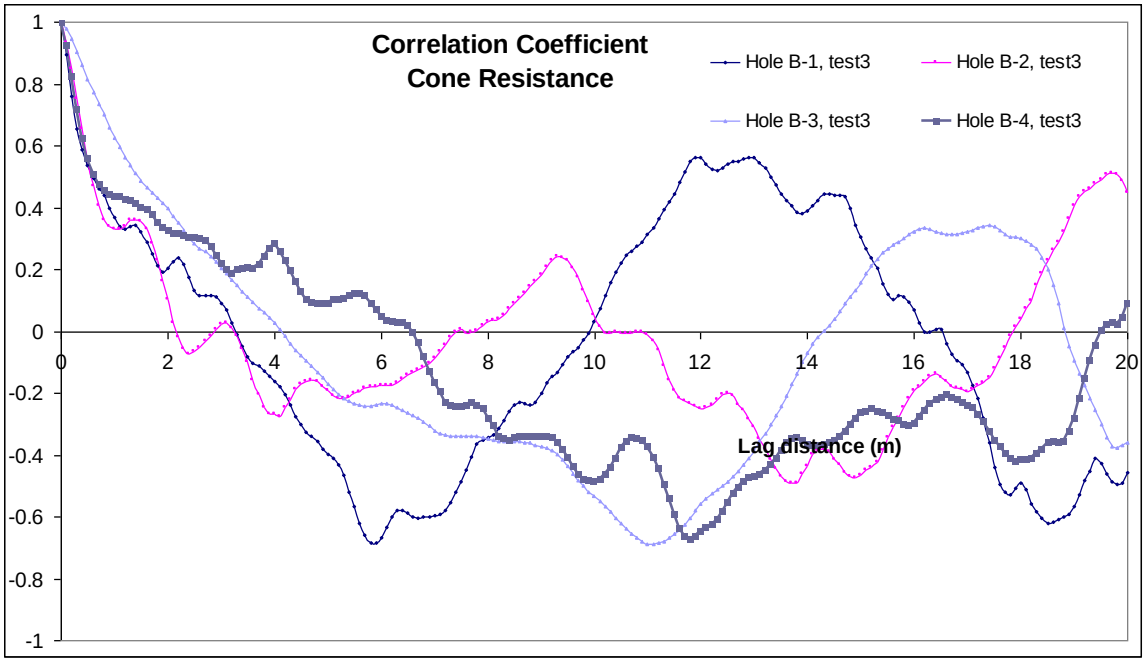

Figure 5.21 Result of correlation coefficients before and after blasting between 7.7 and 37 m at Hole B, Test 3

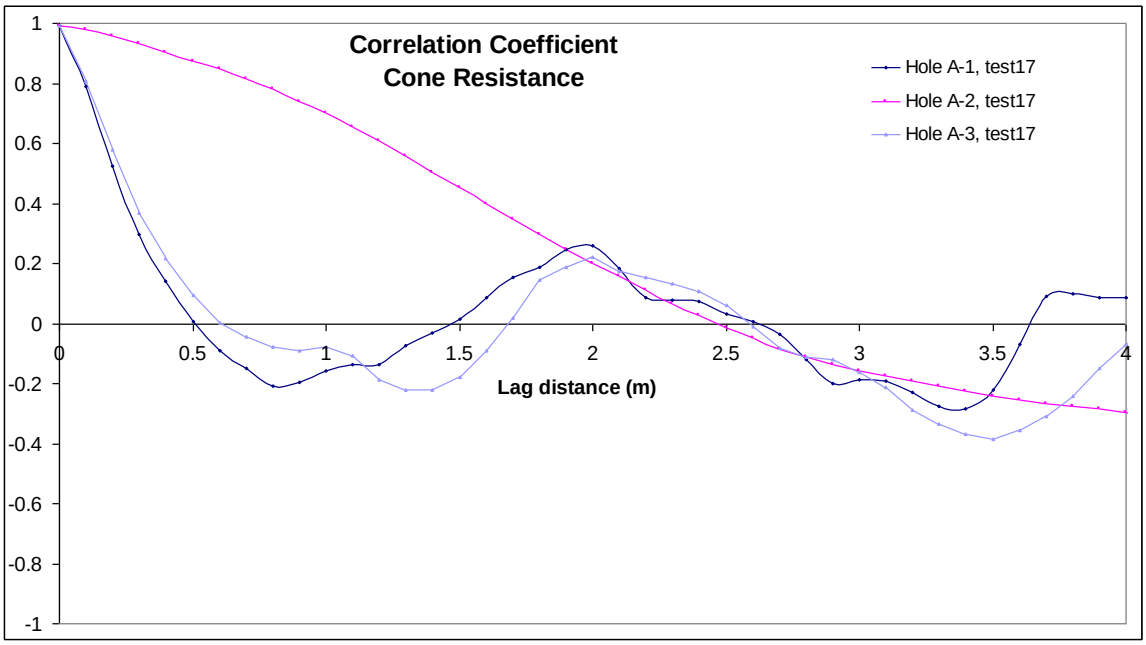

Figure 5.22 Result of correlation coefficients before and after blasting between 5.0 and 19.0 m at Hole A, Test 17

5.5.2.2. Changes in the correlation coefficient function after vibrocompaction

Figure 5.23 shows correlation coefficients for the cone resistances mainly densified by vibrocompaction. Compared with the correlation coefficient function before vibrocompaction, the correlation coefficient function after vibrocompaction showed a slightly higher degree of correlation. The zero-correlation distance of cone resistance measured at Hole 141 significantly increased a short time after vibration as shown in Figure 5.23. The zero-correlation distance gradually decreased over time after vibration. However, the result may not be statistically significant due to the limited number of data sets; it would be desirable to estimate the apparent changes in the correlation of soil properties caused by vibration using a larger quantity of data.

Considering the analysis results of the change in the zero-correlation distance of soil properties after blasting, however, it is reasonable to conclude that dynamic loadings such as vibration and blasting decrease the correlation level of soil properties to some extent.

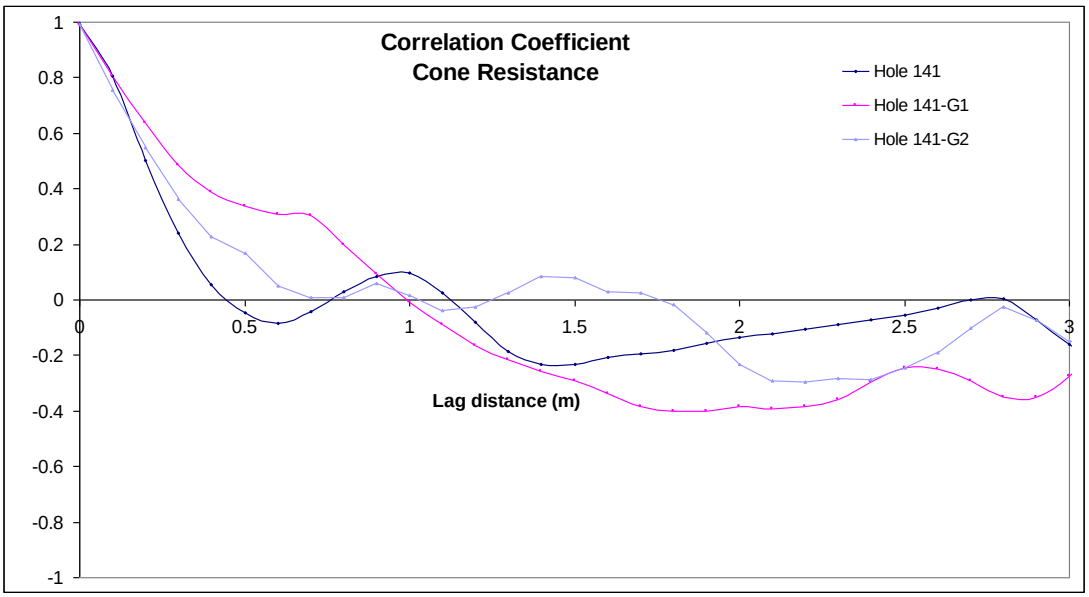

Figure 5.23 Result of correlation coefficients before and after vibrocompaction between 8 and 20 m at Hole 141

5.6. Conclusions

As mentioned earlier, the strengths, coefficients of variation (COV), and correlation coefficients of CPT data within the same range of sand layers at each boring location at the Jebba hydroelectric project site in Nigeria and at the Embayment Seismic Excitation Experiment project area were analyzed in order to obtain the effect of dynamic loadings such as blasting and vibration on correlation structures.

The average values of cone resistance after blasting and vibrocompaction increased when compared with those of cone resistance measured a short time (i.e., several months) after blasting and vibrocompaction.

Compared with the results of a single explosion that used a higher amount of explosive charge in the Embayment Seismic Excitation Experiment project area, several subsequent explosions with several small charged holes cumulatively improved the soil strength over the short term.

The analysis results of the changes in the COV value and the zero-correlation distance of soil properties after blasting and vibration at the Jebba hydroelectric project site in Nigeria and at the Embayment Seismic Excitation Experiment project area support the conclusion that dynamic loadings such as vibration and blasting decrease the deviation and correlation levels of soil properties to some extent. That is, dynamic loadings make overall original soil structures more randomized.

Soil structures that have been long formed by such processes as authigenesis, consolidation, and cementation reach a steady state regarding forces within soils. However, in general terms, it does not seem rash to suggest that dynamic loadings such as blastings and earthquakes cause the steady-state soil structures to disrupt and

rearrange. From the above, consideration should be made of the effects that dynamic loadings have on estimates of statistical characteristics of field data. Furthermore, the history of seismic activities at an area of interest that includes granular soil layer(s) should be an important consideration when estimating its correlation structures because correlation structures are not invariable, but may be influenced by liquefaction that could be caused by past seismic activities.

CHAPTER 6

SIMULATION OF RANDOM FIELDS IN GEOTECHNICAL ENGINEERING

6.1. Introduction

Statistical approaches are usually used to quantify the spatial variability in soil properties. The deterministic approach as the traditional method of soil-property analysis did not treat the uncertainties in soil properties in a rigorous manner. Baecher (1986) pointed out that the estimates of soil properties without uncertainties in geotechnical engineering may be prone to be conservative in geotechnical practice due to unsubstantiated confidence caused by its oversimplification of soil property analysis. As a result, valuable information on soil properties for systematically treating the sources of uncertainty in soil property measurements may not be sufficiently provided for performing reliability analysis in geotechnical practice, thereby giving rise to poorly qualified confidence in geotechnical practice.

This realization has provoked several researchers to develop alternatives to the traditional deterministic approach. One of the alternatives is simulation. Simulation allows engineers to understand behaviors of a system under a variety of circumstances that would be too risky or expensive to practice in reality. Simulation, in general, is a technique used to reduce cost and risk of damage to expensive systems, which inexperienced operators may often cause. On the other hand, simulation generally uses

mathematical models to represent behaviors of the system, so it may have a limit in terms of characterizing system behaviors in the real world. Furthermore, the results of simulation may be varied with input parameters in use. However, well-modeled simulation has the potential to help engineers to apply their knowledge and experience acquired in the real world to behaviors of a system in the real world.

In order to enhance the performance in geotechnical practice as well as supplement the traditional deterministic approach, Matheron (1963) introduced the "kriging" method as a stochastic interpolation. Nadim (1988) illustrated the spatial variation of cone resistances under a foundation in three dimensions, using the kriging method. His 3-D plots enabled designers to perform more detailed reliability analysis in geotechnical practice. Davis (1987) showed a simple technique for performing a conditional simulation using the lower-upper triangular decomposition of the covariance matrix. Although the simulation technique is simple and fast, the total running time of the simulation technique may increase during the process of decomposing the covariance matrix of a large amount of data. Yamazaki and Shinozuka (1988) developed a simulation technique to generate random fields with non-Gaussian distributions. They used a mapping technique to transform Gaussian homogeneous processes into non-Gaussian processes. The mapping technique is a spectrum-based method, which is based on a spectral density. More recently, Fenton (1999) presented an estimation procedure and a case study to model cone penetration test (CPT) data using a random field model. He used the fractal model, of which the main parameters are independent of the domain size, instead of a finite-scale model, whose scale should be adjusted to the domain size.

This chapter presents a supplement to an effort to develop alternatives to the deterministic approach by demonstrating how to generate accurate multi-dimensional simulations of soil properties that are consistent with the observed or proposed correlation structures in both the vertical and the horizontal domains of soil properties. The representative simulation techniques of random fields and how they relate to the representation of soil properties are discussed in Section 6.3. A proposed simulation method and how it differs from the representative simulation techniques of random fields are discussed in Section 6.4. Moreover, conclusions are presented with a brief review of the capabilities and limits of the proposed technique.

6.2. Motivation

In a typical site investigation, a limited number of borings or soundings are drilled. In some cases, the soundings are supplemented by a few data sets from cone penetration tests. However, it is not practical and economical that comprehensive site investigation should be performed at every point of a site. The traditional approach in geotechnical engineering is to interpolate between known data by use of trends estimated by some simple regression analyses. This approach disregards the correlation between data, and assumes that soil properties between data points are independent of each other. The statistical estimates of soil properties with the traditional approach may be inaccurate if correlation effects are unaccounted for. This realization has motivated many engineers and researchers to explore alternatives where unknown soil properties are simulated using the statistical structures of known soil properties. These efforts have generated a variety

of simulation techniques. The simulation techniques can be broadly divided into covariance-based methods and spectrum-based methods. The covariance-based simulation methods to generate random fields are the decomposition method, conditional simulation, and the simple or ordinary kriging method. The most popular spectral approaches for the generation of random fields are probably the turning bands method and the direct fast Fourier transform method. Most simulation techniques (except for interpolation methods such as conditional simulation and the simple or ordinary kriging method) simulate random fields by use of random number generators with a specific distribution model.

When a multi-dimensional simulation is performed based on the statistical structures of measured data, the simulation techniques that use random number generators in simulation bring about "random" results: that is, these techniques appear to somewhat satisfy required statistical aspects such as standard deviation and correlation distance. However, they are limited in their ability to simulate soil properties that have high correlation levels with sampled soil properties. This is attributed to the random number generators used, which just randomly distribute data based on a specific distribution model.

For the reasons discussed above, the effectiveness of the existing simulation techniques used in multi-dimensional simulations has been brought into question. This issue played a role in developing a new simulation technique that ameliorates the weak points of the existing simulation techniques. Thus, in this section, the theoretical basis for a new simulation technique in multi-dimensional random fields is introduced. The simulation technique for generating more correlated replicates is developed on the basis

of the correlation between normalized CPT data sets of each boring location in the space domain.

6.3. Representative simulations of random fields

6.3.1. Fast Fourier transform (Fenton, 1994; Kottegoda and Kassim, 1991)

The fast Fourier transform method is a technique to temporally and spatially simulate a homogeneous and continuous random field. A random field, $Z(x)$, can be expressed to a discrete Fourier transform as

$$Z(x_j) = \sum_{k=-M}^{M} \left[a_k \cdot \cos(\omega_k \cdot x) + b_k \cdot \sin(\omega_k \cdot x) \right] \qquad (6.3.1)$$

where the subscript ***j*** is a point number of ***n*** discrete numbers of x, $\omega_k = k\pi / M$, and coefficients a_k and b_k are independent, identically distributed zero-mean random variables. Since the process of the random field is real and the variances of coefficients a_k and b_k can be written by means of a one-sided spectral density function, the random field, $Z(x)$, can be rearranged as

$$\begin{aligned} Z(x_j) &= \sum_{k=1}^{M} \left[a_k \cdot \cos(\omega_k \cdot x) + b_k \cdot \sin(\omega_k \cdot x) \right] \\ &= \sum_{k=1}^{M} (a_k - i \cdot b_k) \cdot \exp(i \cdot 2\pi (k-1)(j-1)/M) \end{aligned} \qquad (6.3.2)$$

If $Z(x_j)$ is real, then

$$a_k = \frac{1}{M}\sum_{j=1}^{M} Z(x_j)\cdot\cos(2\pi(k-1)(j-1)/M) = a_{M-k} \tag{6.3.3}$$

and

$$b_k = \frac{1}{M}\sum_{j=1}^{M} Z(x_j)\cdot\sin(2\pi(k-1)(j-1)/M) = -b_{M-k} \tag{6.3.4}$$

This technique enables one to easily simulate anisotropic (non-square) random fields. However, one must pay careful attention in order to avoid considerable errors when defining the size and discretization of the spatial field.

6.3.2. Decomposition matrix method (Davis, 1987)

When the matrix K_m is a symmetric and positively covariant matrix, it is possible to decompose the matrix K_m into a lower triangular matrix, L_m, and an upper triangular matrix, U_m, i.e., $\boldsymbol{K}_m = \boldsymbol{L}_m \cdot \boldsymbol{U}_m$. The covariance matrix is obtained from the exponential decaying covariance function with a uniform distance between data values. The symmetric decomposition establishes that the upper triangular matrix, U_m, is the transpose of the lower triangular matrix, L_m, i.e., $L_m' = U_m$. When a unit vector, V, of

Gaussian random numbers with an independent mean zero and unit variance is applied to the lower triangular matrix, a random field, Z, can be simulated as

$$Z = L_m \cdot V \tag{6.3.5}$$

6.3.3. Turning bands method (Fenton, 1994; Matheron, 1973; Mantoglu and Wilson, 1981)

The tuning bands method (TBM) is a simulation technique to generate random fields from random values simulated along each of lines, which have zero mean and a covariance function. The random values along each of N lines with index i = 1, 2, 3, . . . , N are generated by other existing simulation techniques such as the fast Fourier transform (FFT) algorithm and decomposition matrix method by use of zero mean and a given covariance function. Then, one should estimate random values, $Z_i(m_k)$, at the coordinate m_k of each line where each coordinate x_k in random fields is orthogonally projected onto each of L lines. Using relevant random values, $Z_i(m_k)$, of each line, a value, $Z(x_k)$, of random fields at a coordinate x_k is estimated as

$$\boldsymbol{Z(x_k) = \frac{1}{\sqrt{N}} \sum_{i=1}^{N} Z_i(m_k)} \tag{6.3.6}$$

The TBM brings about accurate and fast random fields, in particular, in multi-dimensional processes in spite of the inefficiency of using a large number of lines (Fenton, 1994). However, this technique depends on other simulation techniques such as

FFT algorithm and decomposition matrix methods to generate random values along each of the lines.

6.3.4. Ordinary kriging method (Matheron, 1963; Baecher and Christian, 2003)

The kriging method is a simulation method to estimate data values at unsampled points in one- or multi-dimensional processes through the variogram model, γ, to describe the dissimilarity of a data sequence with relative distance, estimated from a set of sample data. Ordinary kriging is the most popular and simple type of the kriging. A data value $\tilde{Z}(x_0)$ at an unsampled point x_0 is estimated by

$$\tilde{Z}(x_0) = \sum_{i=1}^{N} \lambda_i \cdot Z(x_i) \tag{6.3.7}$$

where the subscript i is the index of sampled points, $x_1, x_2, \ldots, x_N$, λ are the weights of data values, and Z are data values at sampled points. The vector of weights $(\lambda_1, \lambda_2, \ldots, \lambda_N)$ is expressed in matrix form as

$$V = A^{-1} \cdot B \tag{6.3.8}$$

where

$$A=\begin{bmatrix} \gamma(x_1, x_1) & \gamma(x_1, x_2) & \cdots & \gamma(x_1, x_N) & 1 \\ \gamma(x_2, x_1) & \gamma(x_2, x_2) & \cdots & \gamma(x_2, x_N) & 1 \\ \vdots & \vdots & \cdots & \vdots & \vdots \\ \gamma(x_N, x_1) & \gamma(x_N, x_2) & \cdots & \gamma(x_N, x_N) & 1 \\ 1 & 1 & \cdots & 1 & 0 \end{bmatrix} \tag{6.3.9}$$

and

$$B=\begin{bmatrix} \gamma(x_1, x_0) \\ \gamma(x_2, x_0) \\ \vdots \\ \gamma(x_N, x_0) \\ 1 \end{bmatrix} \tag{6.3.10}$$

6.4. Basic algorithm

For two random variables $X(i)$ and $Y(i)$, the correlation coefficient functions, $\rho_{XY}(k)$, can be expressed as (Box and Jenkins, 1970)

$$\rho_{XY}(k) = \frac{\mathrm{Cov}[X(i), Y(i+k)]}{\sigma_X . \sigma_Y} = \frac{E[\{X(i) - \bar{U}_X\} \cdot \{Y(i+k) - \bar{U}_Y\}]}{\sigma_X . \sigma_Y} \tag{6.4.1}$$

where i is a data index, $\bar{U}_X$ and $\bar{U}_Y$ are the average values of $X(i)$ and $Y(i)$, which are the same for all the points in homogeneous fields, and σ_X and σ_Y are the standard deviations of $X(i)$ and $Y(i)$, respectively. When a data set of soil property is divided into N sections, $X_1(i)$, $X_2(i)$, . . . , $X_N(i)$ are measured data sets of N sections of a soil property and $T_1(i)$,

$T_2(i), \ldots, T_N(i)$ can represent target data sets of N sections to simulate a soil property at a specific lag distance, L, using the horizontal correlation coefficient functions for each section estimated by all known data of soil property measured at a specific site. The difference between the dependent variable, $\rho_{XY}(k)$, and the right-hand side of Eq. 6.4.1 calculated by both a target data set in a section and a measured data set in a section should theoretically be zero. The most important step is to estimate target data sets of N sections to minimize the sum of N absolute values of the difference between the dependent variable and the right-hand side of Eq. 6.4.1. When the correlation between the target data set in each section and the measured data set in each section is estimated using Eq. 6.4.1, in reverse, it is theoretically reasonable that data sets of N sections, which best satisfy the following condition, may be considered a desirable target data sequence:

$$\text{Minimize}\left\{\sum_{m=1}^{N}\left(\text{abs}\left|\frac{E[\{X_m(i)-\bar{U}_{X_m}\}\cdot\{T_m(i)-\bar{U}_{T_m}\}]}{\sigma_{X_m}\cdot\sigma_{T_m}}-\rho_{L_m}\right|\right)\right\} \qquad (6.4.2)$$

where ρ_{Lm} is a horizontal correlation coefficient function of measured data in a section m at a lag distance L. The above theoretical analysis provides a basis for the multi-dimensional simulation of soil properties considering x-, y-, and z-directions in geotechnical engineering. This simulation can be applied for the simulation of soil properties at undersampled sites where at least one boring or sounding is performed, given that the statistical characteristics of soil properties at the undersampled sites can be approximated by the estimates of the statistical characteristics of soil properties obtained from the same or similar soil formation process areas. As described in Figure 6.1, the following steps for the generation of a sequence of soil properties are suggested:

Step 1. Perform regression analyses on all the raw data sequences measured at a site to model a representative trend: It is a step to split soil properties into deterministic and stochastic components. Regression analyses are applied to all the measured raw data to estimate a representative trend that best fits all the raw data measured at a site.

Step 2. Remove the representative trend from each measured data sequence and normalize each detrended data sequence with the standard deviation of each detrended data sequence: This process is a dimensionless method designed to eliminate the effects of using different soil characteristics for analysis. Non-stationary data need to be transformed into stationary data. The first step in the standardization of soil properties is to remove the trend from the original data. The second is to normalize the detrended data by the standard deviation of each detrended data sequence to attain zero-mean, unit-variance, and homogeneous fields.

Step 3. Check the stationarity of each normalized data sequence: Each normalized data sequence in the previous step is tested for stationarity: stationarity is a necessary precondition for analyzing the spatial variability of soil properties in geotechnical engineering. In this step, the reverse arrangement test introduced by Bendat and Piersol (1986) is employed for the assessment of stationarity.

Step 4. Divide the length of soil property into various sections with a uniform length: The reason that a range of soil property is split into various sections with a uniform length is that the simulated target data in the individual section must be calculated accurately using a horizontal correlation coefficient function of normalized data in

each section and the running time used to calculate target data in the individual section needs to be reduced.

Step 5. Estimate the horizontal correlation coefficient functions using all normalized detrended data sets in the individual section: The horizontal correlation coefficient functions can be estimated based on the length of an individual section prior to simulating a set of target data in the individual section. In particular, it is imperative to regard the negative values of the correlation coefficient function. Thus it is important to use a more flexible correlation coefficient function, with an exponential sinusoidal type like the cosine exponential correlation coefficient function introduced in Chapter 2.

Step 6. Obtain a set of target data in an individual section to satisfy Eq. 6.4.2: Each datum value of target data in an individual section ranges from −1 to +1. The resultant target data sequence is estimated through an automatic process to change each datum value of target data in an individual section between −1 and +1 to best satisfy Eq. 6.4.2. For example, for each section with four target data, −1.0s are input for four temporary datum values of target data in a section and the value of the Eq. 6.4.2 is calculated from the four −1.0s. Then, the first temporary datum value of target data is increased incrementally by 0.01 up to +1.0. Every increment in the values of the Eq. 6.4.2 should be calculated by use of the combination of four temporary datum values. The second, the third and the last temporary datum values of target data should take the same steps with the first one. Finally, the combination of four temporary datum values by which the value

of the Eq. 6.4.2 is calculated as the closest to zero should be chosen for target data in a section.

Step 7. Adjust the standard deviation of the estimated whole target data sequence to unity: Each datum value of the estimated whole target data is divided by the standard deviation of the estimated whole target data. This step is taken to convert the deviation of the estimated whole target data to a desirable deviation.

Step 8. Apply a representative standard deviation of detrended raw data sequences to the unity-variance target data resulting from Step 7: A representative standard deviation can be estimated from all known detrended raw data. The representative standard deviation is applied to the unity-variance target data resulting from Step 7.

Step 9. Combine the trend of the raw data with the above resultant data: This is a step to combine a deterministic component (the trend) with a stochastic component (detrended residual data obtained in simulation).

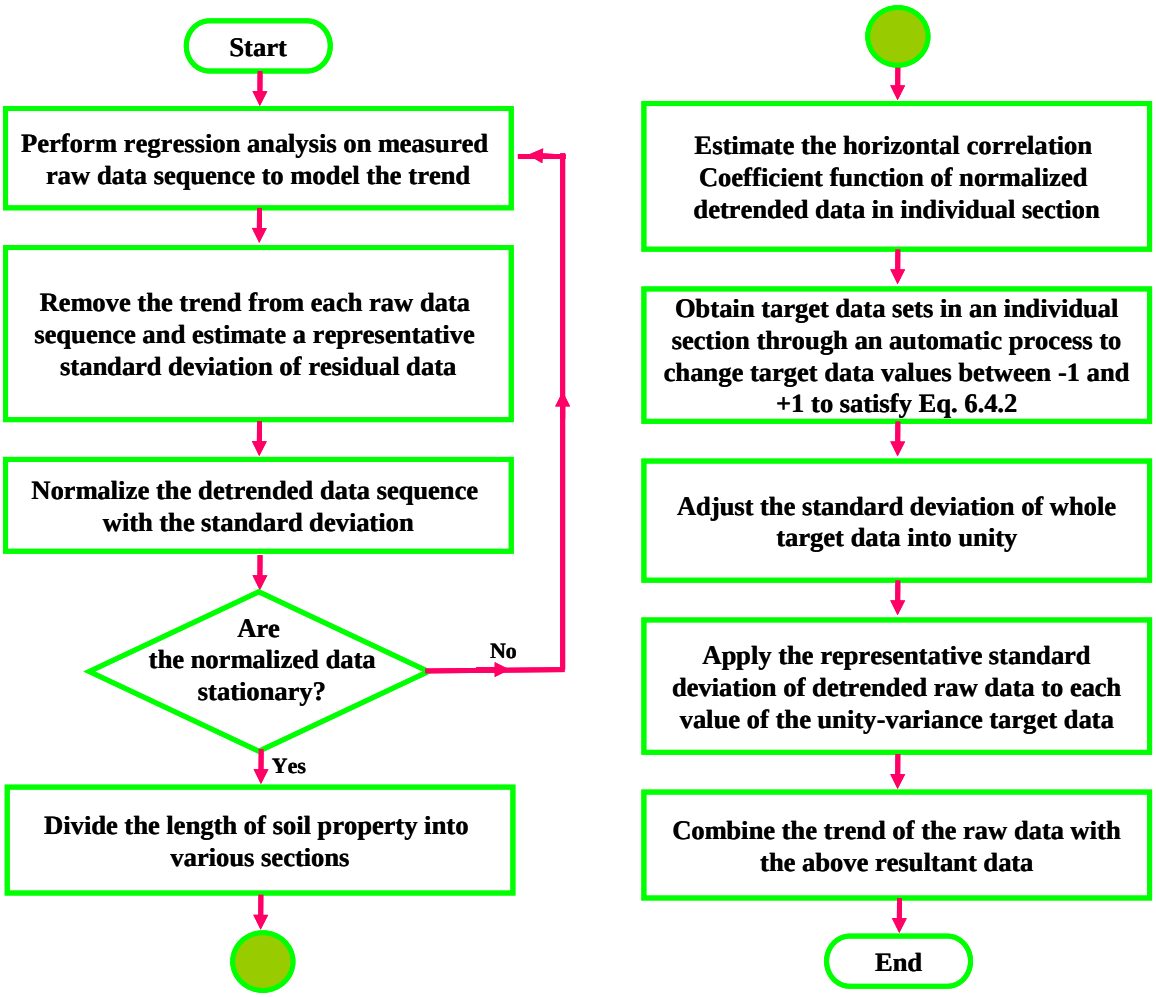

Figure 6.1 Flow chart of the proposed simulation technique

6.5. Application of a proposed simulation technique

The proposed simulation technique was used to interpolate between the data of cone penetration tests obtained at Bridge A – 1700 of I – 155. Selected CPTs were performed at 24-to-41-meter intervals along Bridge A – 1700. The depth of penetration was 30 meters. Prominent sand layers were identified in common in the profile between approximately 16 and 28 m using the soil classification system discussed in Chapter 2. The thickness of the sand layer analyzed is on average 11.5 meters. The boring locations

performed at the Bridge A – 1700 of I – 155 were already presented in Chapter 3. In this example application, the cone profiles of sand layers at CPT-9, CPT-10, CPT-11, and CPT-13 were used to predict the cone profile of sand layer at CPT-12. Thus, a comparison was drawn between the predicted profile and the real cone resistance profile obtained.

The individual sleeve friction profiles of sand layers for CPT-9 and CPT-10 are illustrated in Figure 6.2 and those for CPT-11 and CPT-13 in Figure 6.3. Prior to the estimation of the correlation coefficient functions, the profile of sleeve friction at each hole was detrended as illustrated in Figure 6.4. Then, the detrended profile was normalized for stationarity. The stationarity of normalized data was confirmed using the reverse arrangement test introduced by Bendat and Piersol (1986). The profiles of sleeve friction at CPT-9, CPT-10, CPT-11, and CPT-13 were used to simulate the profile of sleeve friction at CPT-12. The data in the vertical direction were divided into twenty sections so that the spacing of data points for a section is equal to 60 cm since the measurement interval of the CPT in the vertical direction represents 15 cm. A small spacing of data points for a section is effective to alleviate load and computing time to generate unknown data points with the corresponding correlation coefficient functions. However, the estimated correlation coefficient functions may be possibly affected by outliers, which give rise to corrupted simulation results. Selection for an appropriate number of data points for a section may be important from both aspects of simulation accuracy and cost efficiency.

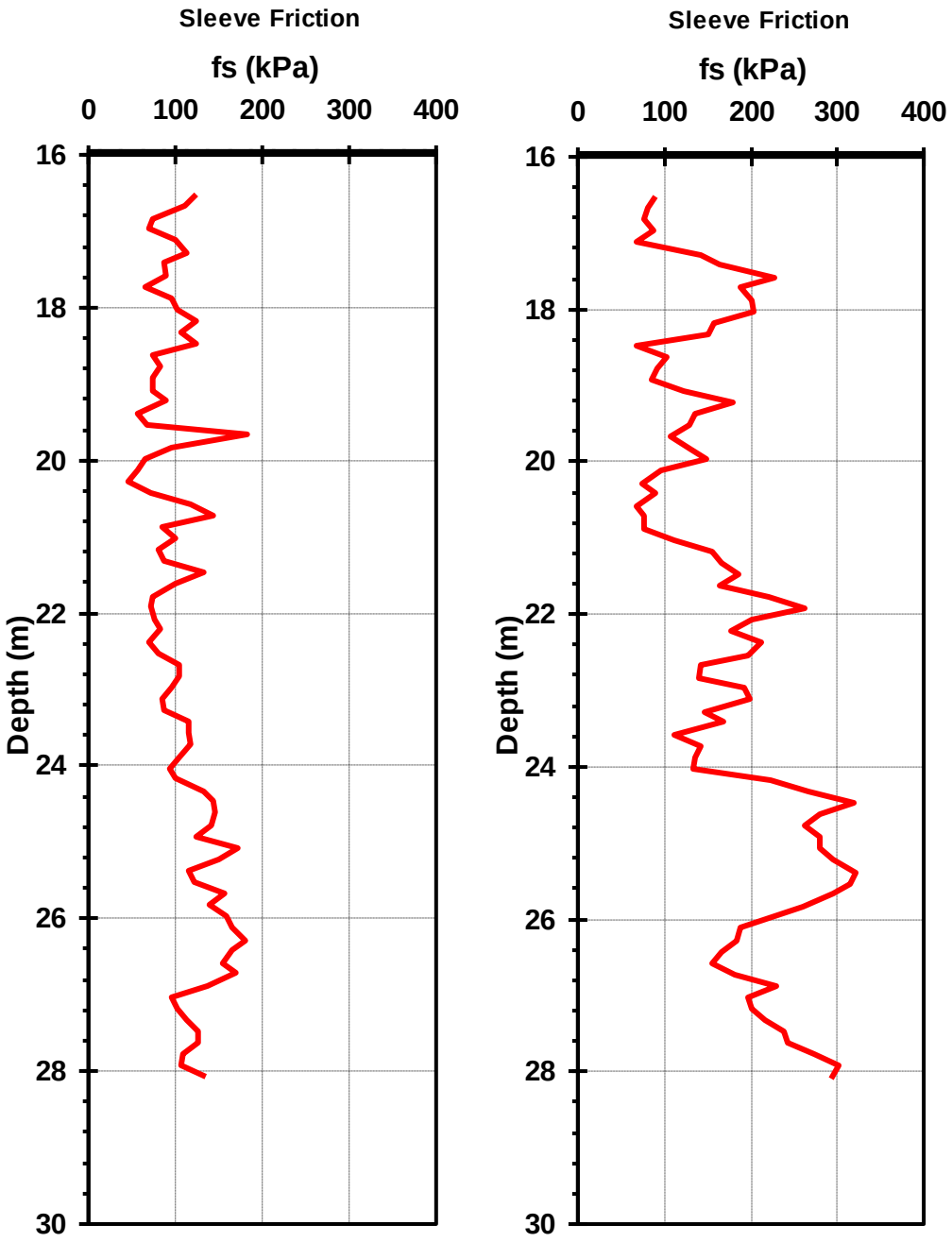

(a) (b)

Figure 6.2 Sleeve friction profiles at (a) CPT-9 and (b) CPT-10 in the sand layer of the Bridge A-1700

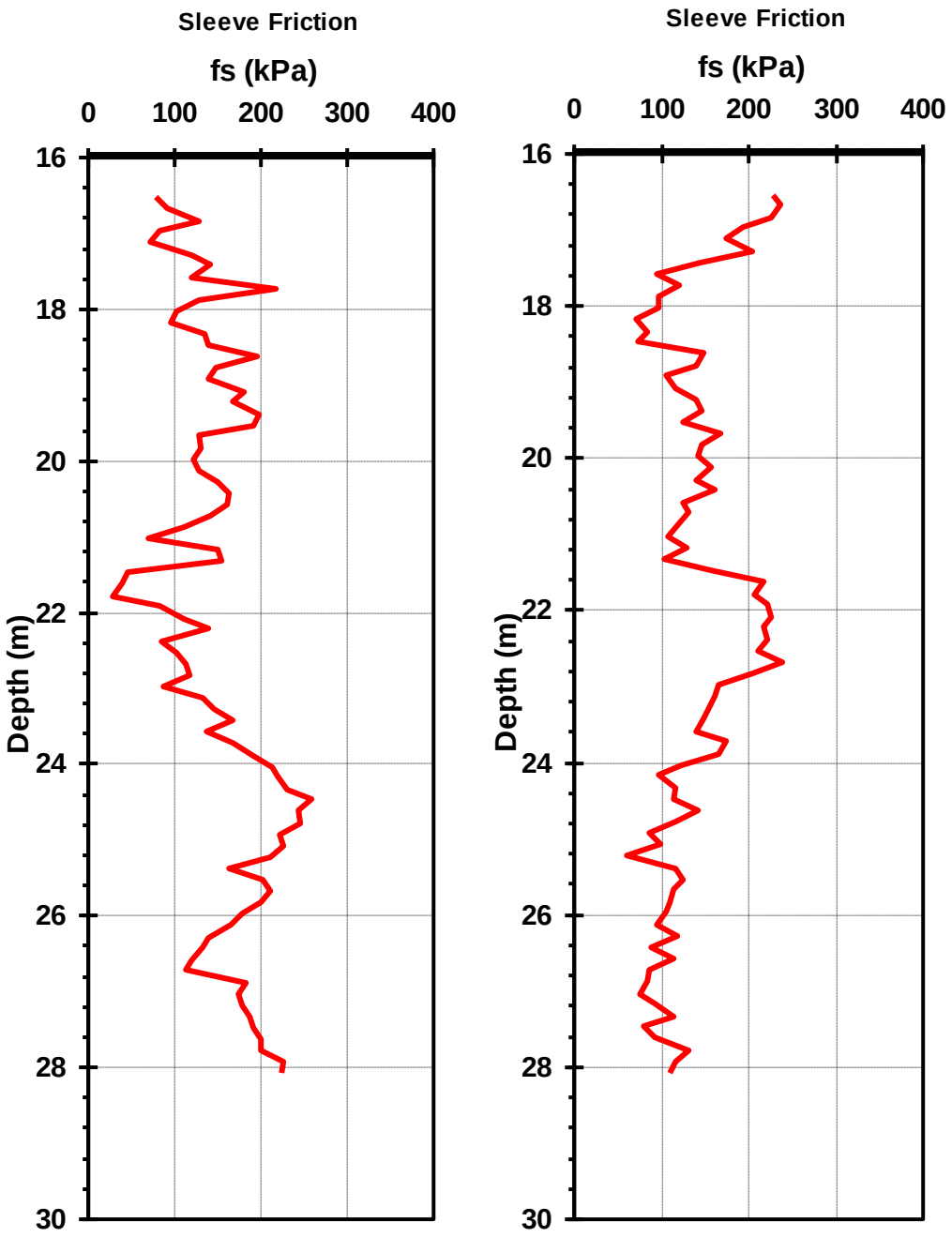

(a) (b)

Figure 6.3 Sleeve friction profiles at (a) CPT-11 and (b) CPT-13 in the sand layer of the Bridge A-1700

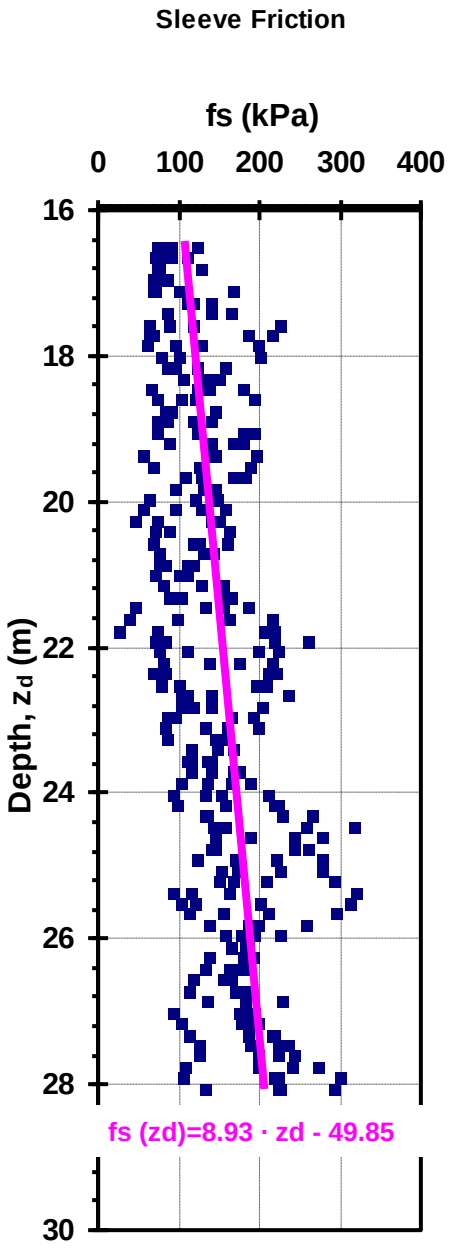

Figure 6.4 Application of a linear regression model to all sleeve friction profiles except for CPT-12 in the sand layer of the Bridge A-1700

It is common in geotechnical engineering to obtain negative values for the correlation coefficient function. Since the correlation coefficient functions at this site exhibited both negative and positive values, it is necessary to consider the negative values as well as the positive ones. The cosine exponential correlation coefficient function introduced in Chapter 2 could represent the above correlation feature better than any other correlation coefficient function. The cosine exponential correlation coefficient function is expressed as

$$\rho(r) = e^{-r/k_1} \cdot \cos(r/k_2) \qquad (6.5.1)$$

Figures 6.5 to 6.9 show horizontal correlation coefficient functions estimated using the sleeve friction within each individual section with 60 cm in length at CPT-9, CPT-10, CPT-11, and CPT-13. In order to determine a model to best fit a correlation coefficient function, least-squares regression was used. The horizontal equivalent wavelengths of each section range from 18 m to 53 m. The average equivalent wavelength is approximately 27 m. This result is consistent with the average equivalent wavelength value investigated in Chapter 4.

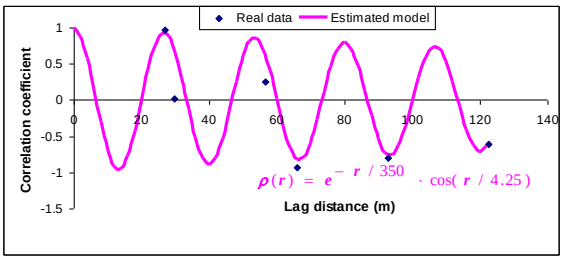

(a)

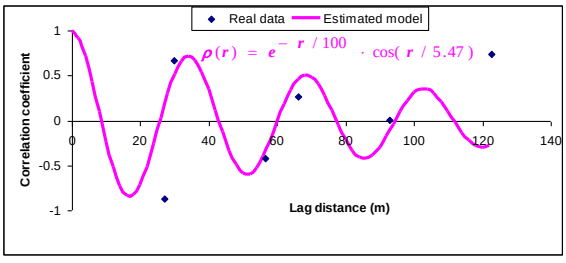

(b)

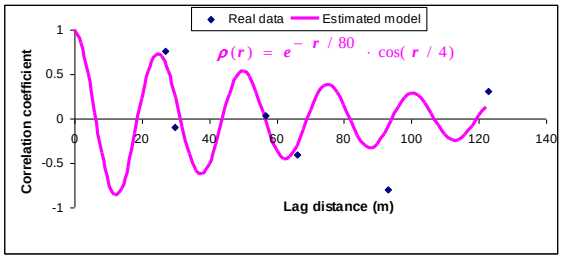

(c)

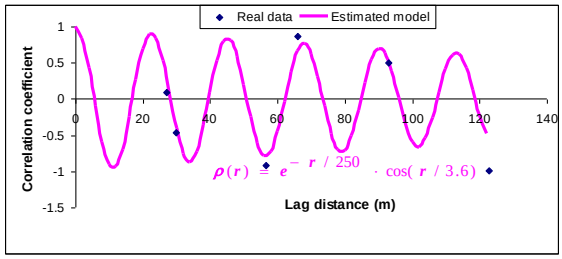

(d)

Figure 6.5 Horizontal correlation coefficient functions (a) between 16.53 m and 16.98 m; (b) between 16.98 m and 17.58 m; (c) between 17.58 m and 18.18 m; (d) between 18.18 m and 18.78 m

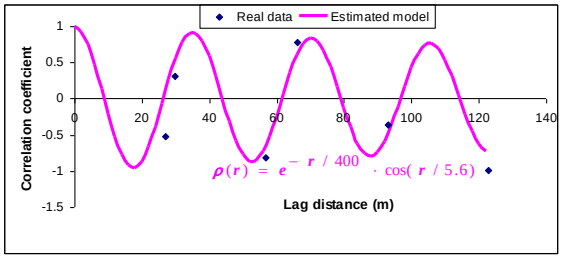

(a)

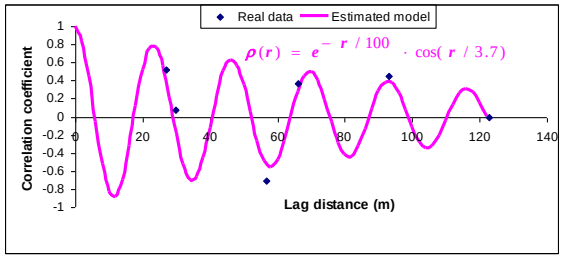

(b)

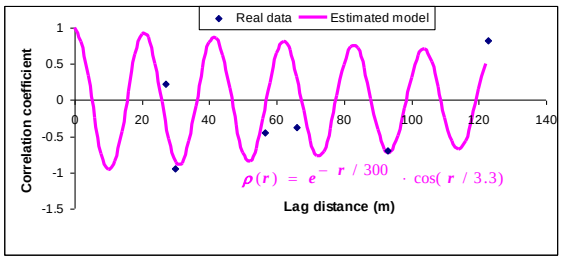

(c)

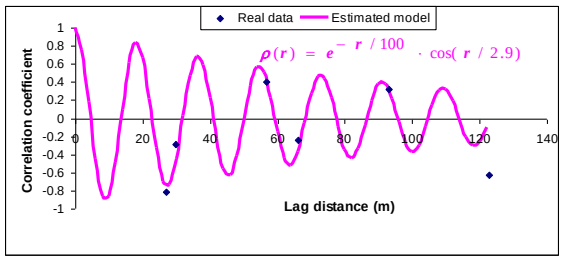

(d)

Figure 6.6 Horizontal correlation coefficient functions (a) between 18.78 m and 19.38 m; (b) between 19.38 m and 19.98 m; (c) between 19.98 m and 20.58 m; (d) between 20.58 m and 21.18 m

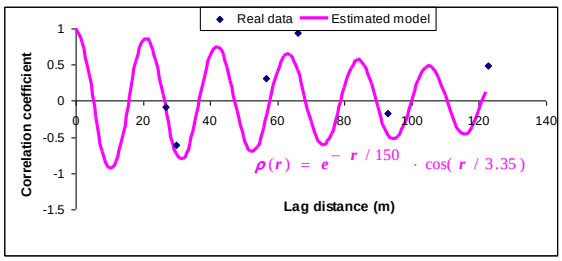

(a)

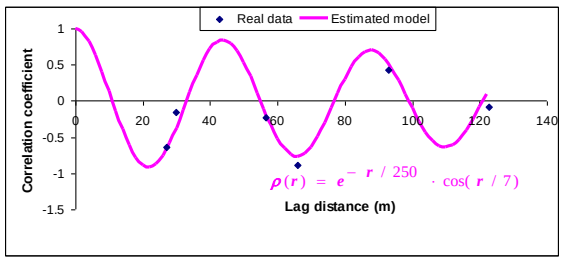

(b)

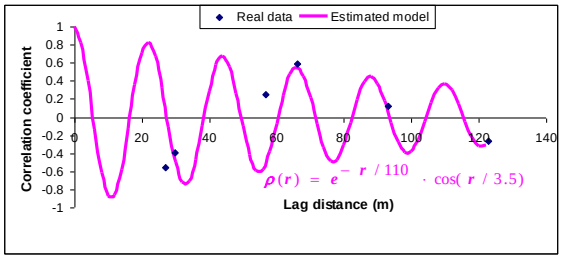

(c)

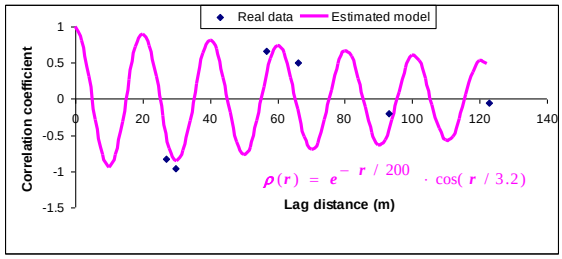

(d)

Figure 6.7 Horizontal correlation coefficient functions (a) between 21.18 m and 21.78 m; (b) between 21.78 m and 22.38 m; (c) between 22.38 m and 22.98 m; (d) between 22.98 m and 23.58 m

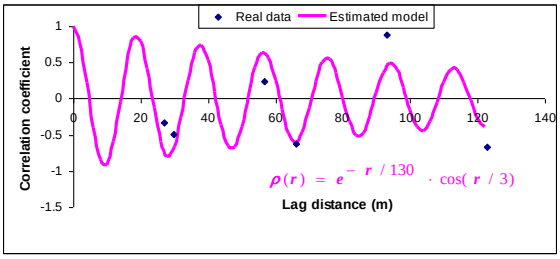

(a)

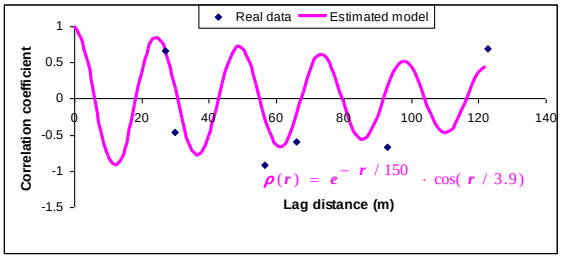

(b)

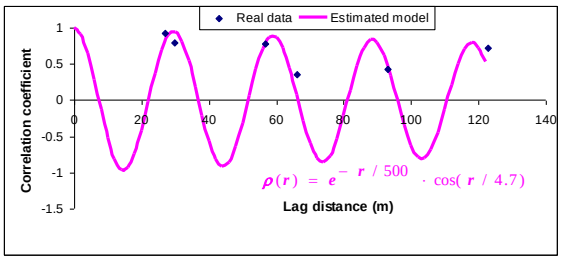

(c)

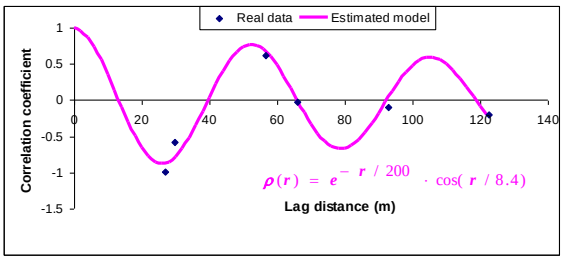

(d)

Figure 6.8 Horizontal correlation coefficient functions (a) between 23.58 m and 24.18 m; (b) between 24.18 m and 24.78 m; (c) between 24.78 m and 25.38 m; (d) between 25.38 m and 25.98 m

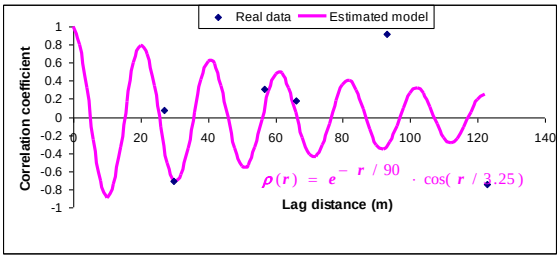

(a)

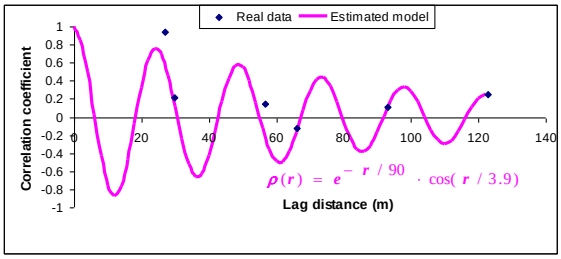

(b)

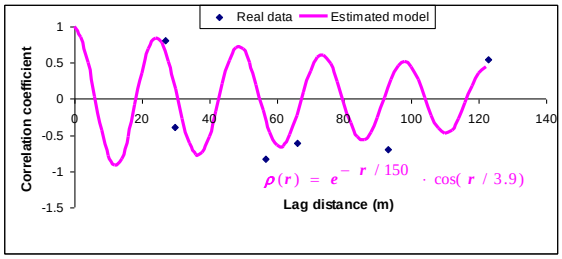

(c)

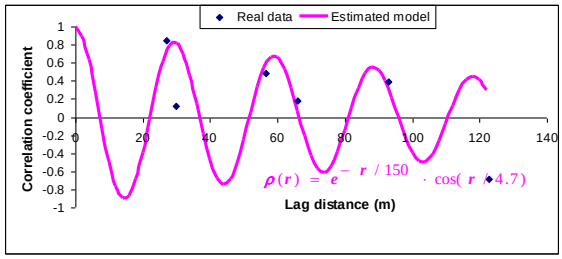

(d)

Figure 6.9 Horizontal correlation coefficient functions (a) between 25.98 m and 26.58 m; (b) between 26.58 m and 27.18 m; (c) between 27.18 m and 27.78 m; (d) between 27.78 m and 28.08 m

The fit to the individual correlation coefficient function for a section of data was found to be extremely good especially at the closer lags. In the development of the correlation coefficient function for each section of data, all the available data except for the data of sleeve friction at CPT-12 were used. With the correlation coefficient function for each section of data, the profile of sleeve friction at CPT-12 was simulated through an automatic process to estimate each datum value of target data between −1 and +1 with an increment of 0.01 in each individual section to best minimize Eq. 6.4.2. The whole simulated profile of the sand layer at CPT-12 is given in Figure 6.10 together with the real measured profile. Figures 6.11 and 6.13 show the profiles of sleeve friction simulated by the Cholesky method, the fast Fourier transform (FFT) method, and the ordinary kriging method, respectively, together with the profile of real sleeve friction at CPT-12 of the site of the Bridge A – 1700. The simulation would exhibit even better results if the data of CPTs were more correlated.

Both the autocorrelation coefficient function and the correlation coefficient function were employed to estimate the accuracy of the simulation. In order to determine if the profiles simulated by the above four methods replicate the correlation feature of the

real data set, the autocorrelation coefficient function was used. Figures 6.14 to 6.17 compare the autocorrelation coefficient functions of sleeve friction simulated by the proposed method, the Cholesky method, the FFT method, and the ordinary kriging method, respectively, with the autocorrelation coefficient function of real sleeve friction at CPT-12 of the site of the Bridge A – 1700. The profiles of sleeve friction simulated by the four methods showed somewhat greater correlation distances in comparison to the correlation distance of real sleeve friction.

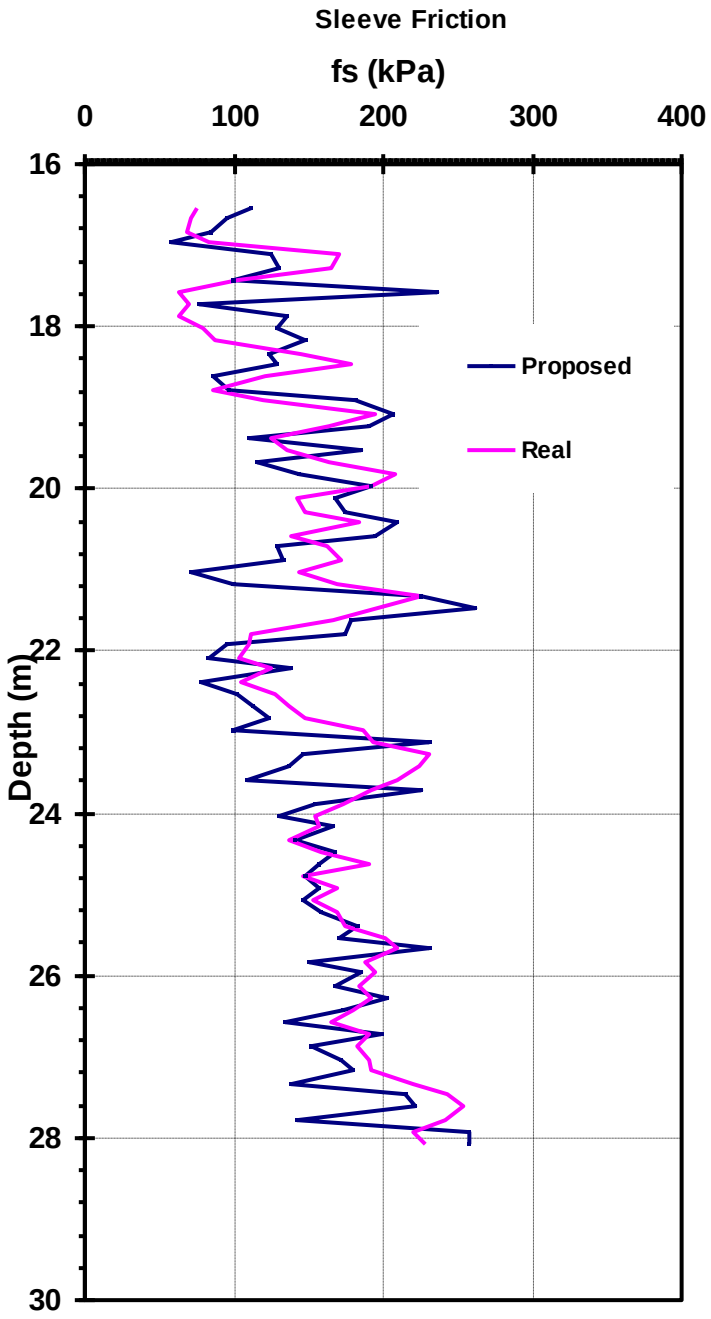

Figure 6.10 Comparison of the profile of the sleeve friction simulated by the proposed method with the profile of real sleeve friction at CPT-12 of the site of the Bridge A - 1700

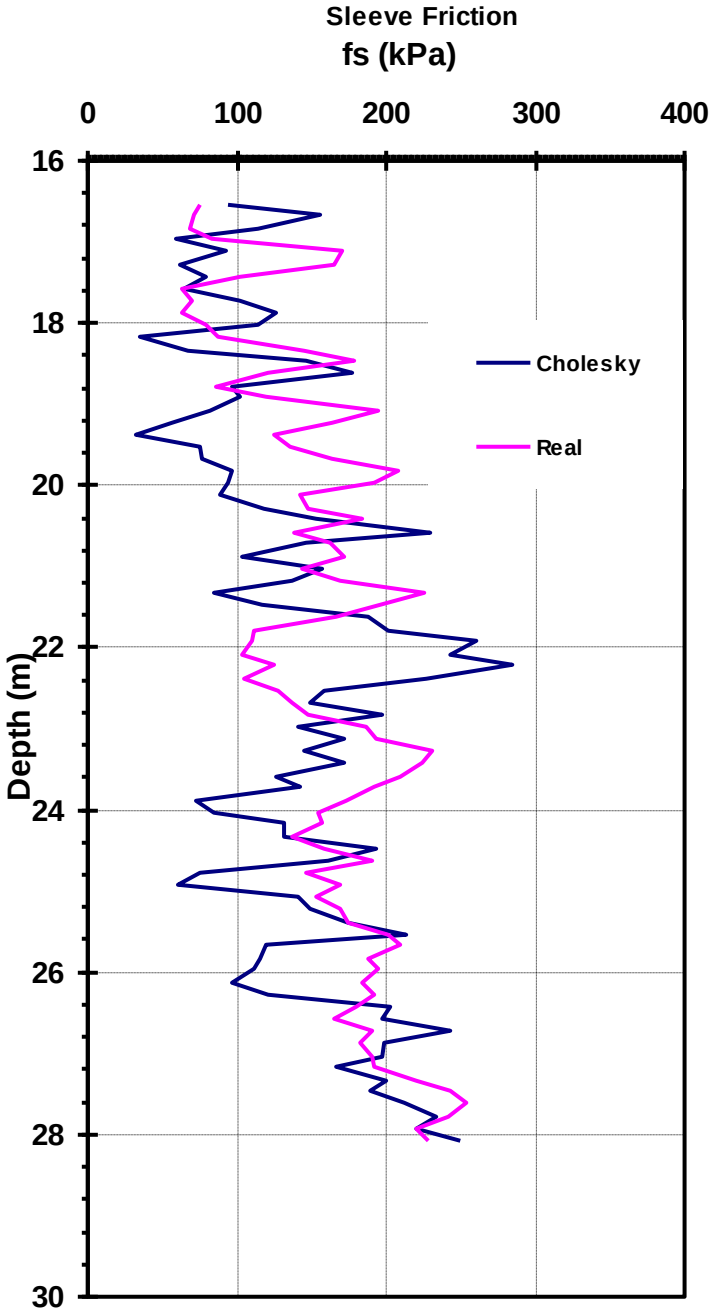

Figure 6.11 Comparison of the profile of the sleeve friction simulated by the Cholesky method with the profile of real sleeve friction at CPT-12 of the site of the Bridge A - 1700

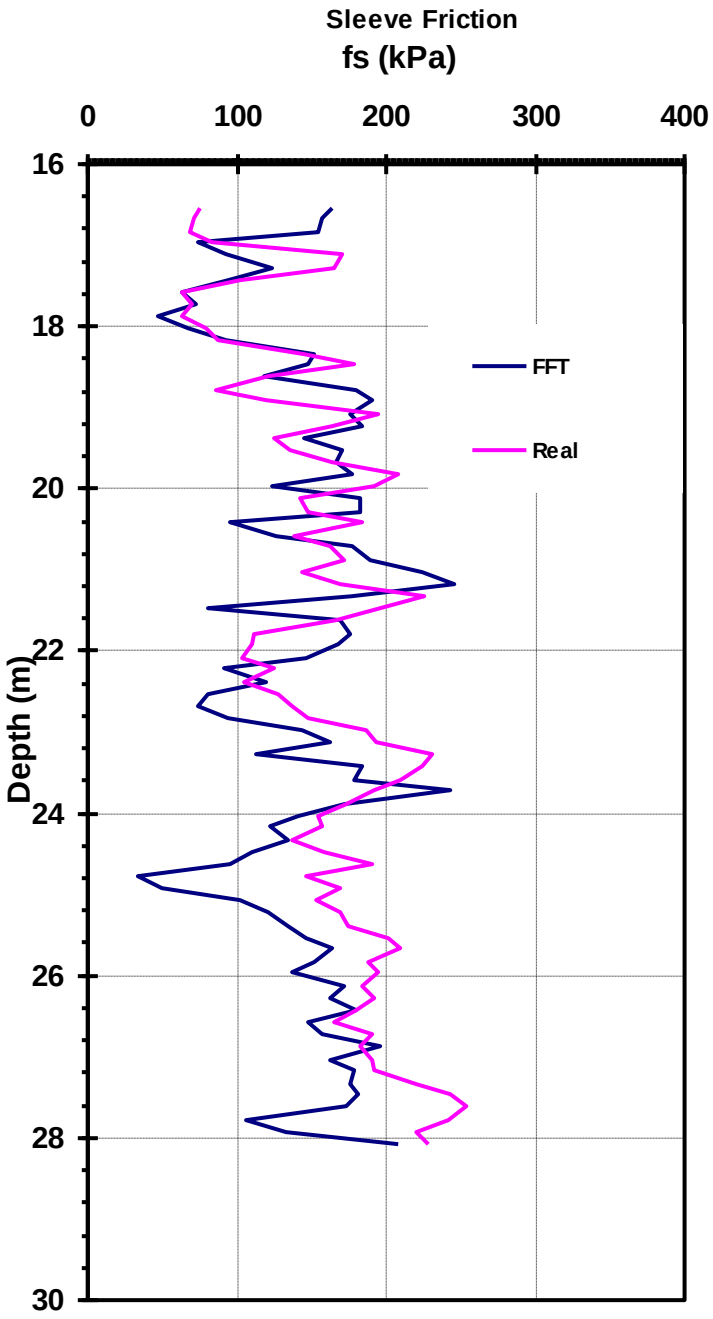

Figure 6.12 Comparison of the profile of the sleeve friction simulated by the fast Fourier transform (FFT) method with the profile of real sleeve friction at CPT-12 of the site of the Bridge A - 1700

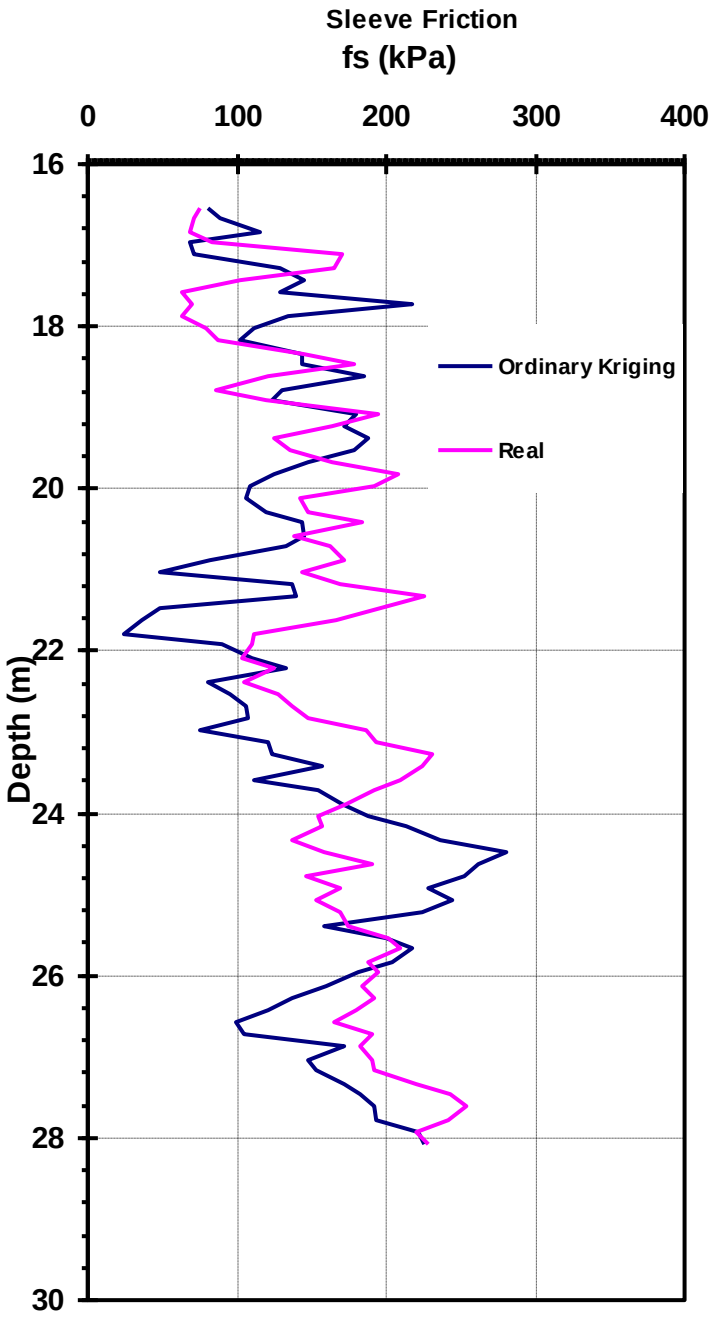

Figure 6.13 Comparison of the profile of the sleeve friction simulated by the ordinary kriging method with the profile of real sleeve friction at CPT-12 of the site of the Bridge A - 1700

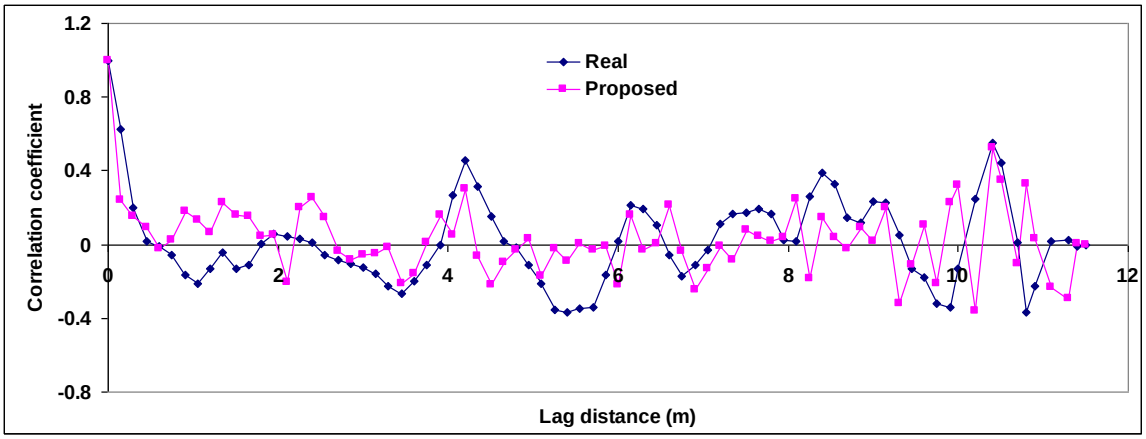

Figure 6.14 Comparison of the autocorrelation coefficient function of the sleeve friction simulated by the proposed method with the autocorrelation coefficient function of real sleeve friction at CPT-12 of the site of Bridge A - 1700

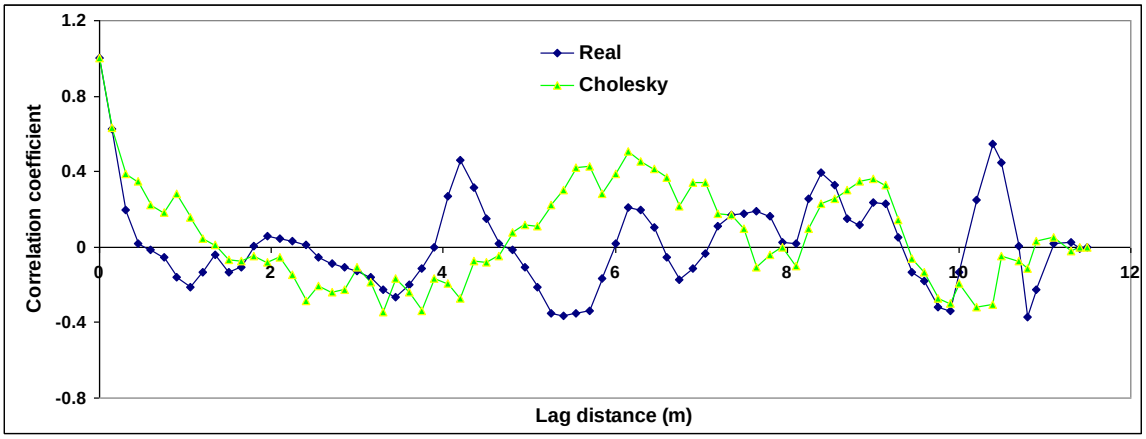

Figure 6.15 Comparison of the autocorrelation coefficient function of the sleeve friction simulated by the Cholesky method with the autocorrelation coefficient function of real sleeve friction at CPT-12 of the site of Bridge A - 1700

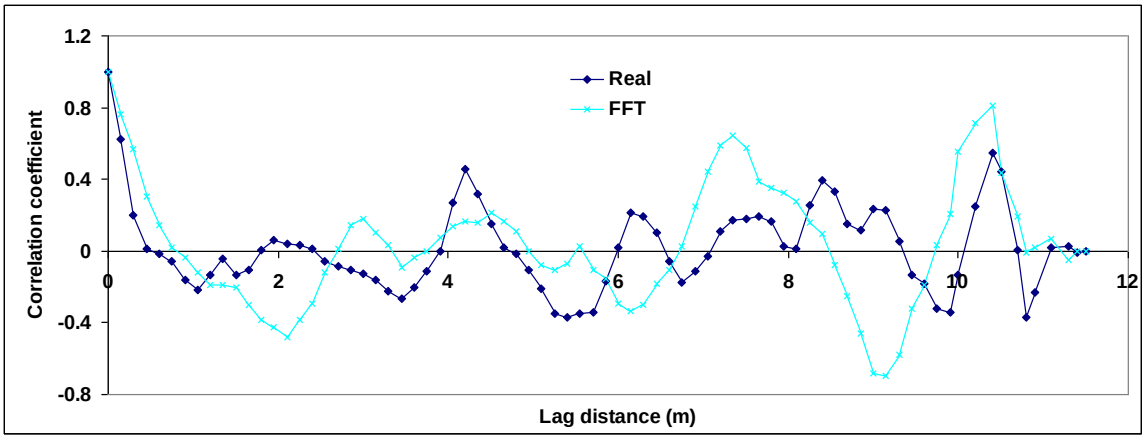

Figure 6.16 Comparison of the autocorrelation coefficient function of the sleeve friction simulated by the fast Fourier transform (FFT) method with the autocorrelation coefficient function of real sleeve friction at CPT-12 of the site of Bridge A - 1700

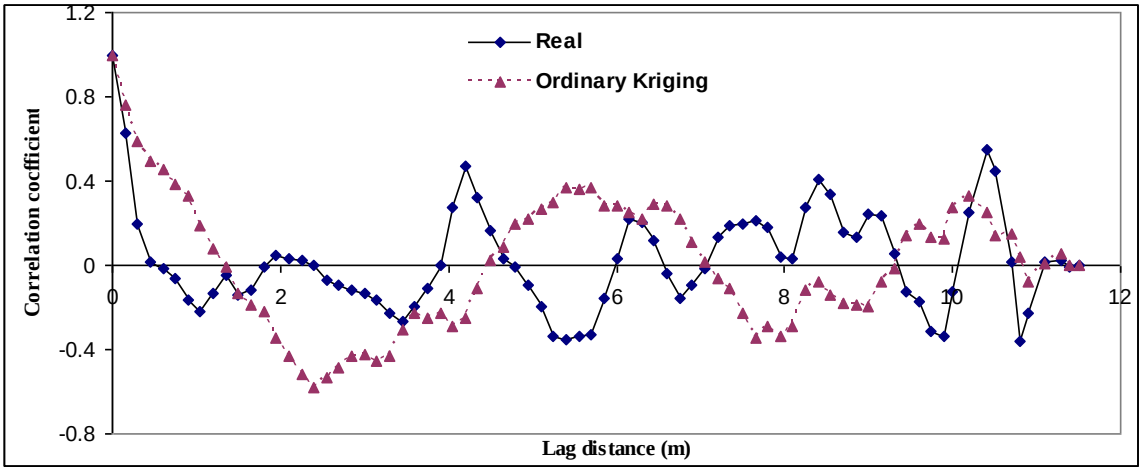

Figure 6.17 Comparison of the autocorrelation coefficient function of the sleeve friction simulated by the ordinary kriging method with the autocorrelation coefficient function of real sleeve friction at CPT-12 of the site of Bridge A - 1700

In order to determine how much the profiles simulated by the above four methods are correlated with the real data, the correlation coefficient function is used to estimate the correlation between two data sequences. Thus, Table 6.1 presents the standard

deviation and correlation of sleeve friction simulated by the proposed method together with those of sleeve friction simulated by the Cholesky method, the FFT method, and the ordinary kriging method.

Table 6.1 Comparison of the standard deviation and the correlation in terms of the profile of sleeve friction at CPT-12 of the site of the Bridge A – 1700

Standard deviation (kPa)					**Correlation**			
CPT-12 data	**Proposed method**	**Cholesky method**	**FFT**	**OK**	**Proposed method**	**Cholesky method**	**FFT**	**OK**
47.18	47.54	58.49	63.54	54.61	0.40	-0.19	-0.09	-0.02

Note: FFT=Fast Fourier Transform; OK=Ordinary Kriging

The fairly high variations of the profiles of sleeve friction simulated by the above four methods are caused by the use of a relatively small amount of measured data, which is a common case in the site investigation of geotechnical engineering. This is mainly attributed to the use of a representative trend and a representative standard deviation value instead of the use of the real trend and the real standard deviation value of the CPT-12 data. Although a common variation, which is estimated from the data at CPT-9, CPT-10, CPT-11, and CPT-13, was applied to the simulations of the proposed method, the Cholesky method, the FFT method, and the ordinary kriging method, the simulation using the proposed method has a standard deviation closer to that of the CPT-12 data than the simulations using the Cholesky method, the FFT method, and the ordinary kriging method. The correlation between the simulation of the proposed method and real data of CPT-12 is a positive value as well as a greater absolute value than the correlation

between the other methods and real data of CPT-12. That is, it is evident that the profile of sleeve friction simulated by the proposed method is more correlated with the real data than the other methods.

The simulation of cone resistance at CPT-12 was executed using the profiles of cone resistance at CPT-9, CPT-10, CPT-11, and CPT-13. The simulation of cone resistance at CPT-12 followed the procedure performed for the simulation of sleeve friction at CPT-12. Figures 6.18 to 6.21 illustrate the profiles of cone resistance simulated by the proposed method, the Cholesky method, the FFT method, and the ordinary kriging method together with that of real cone resistance at CPT-12 of the site of the Bridge A – 1700.

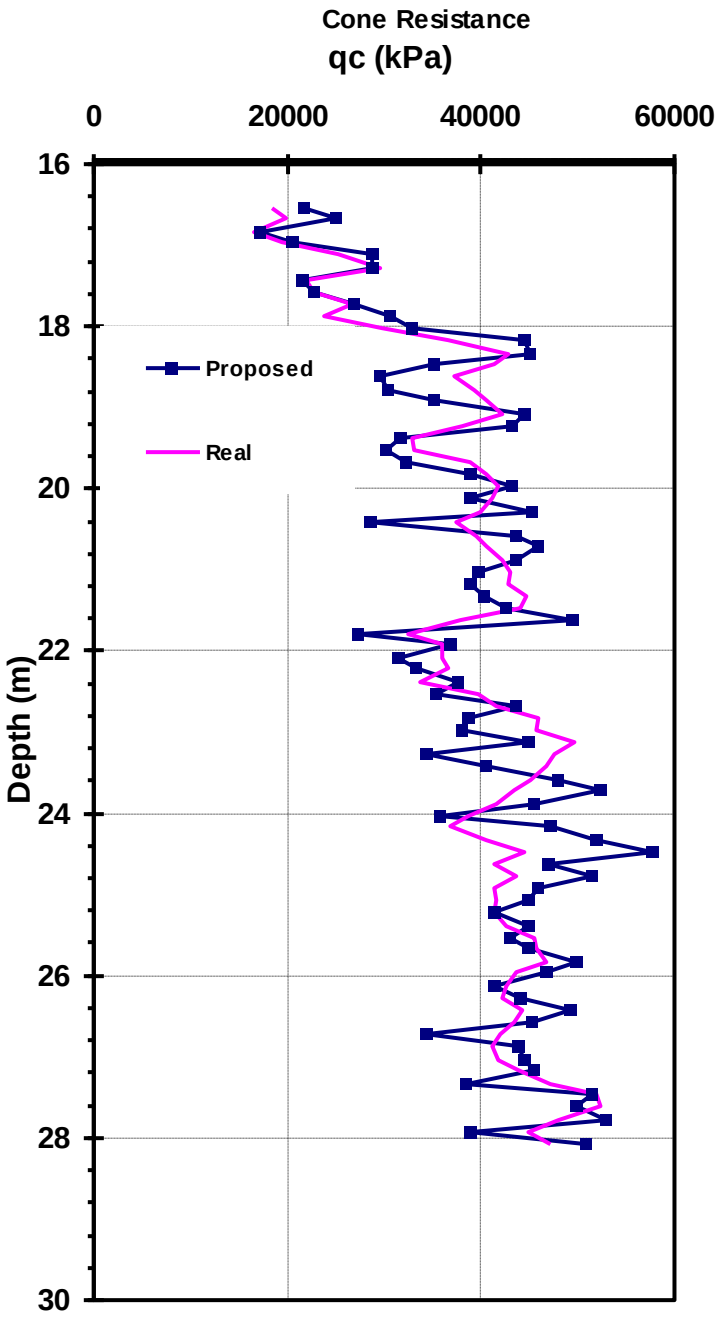

Figure 6.18 Comparison of the profile of the cone resistance simulated by the proposed method with the profile of real cone resistance at CPT-12 of the site of the Bridge A - 1700

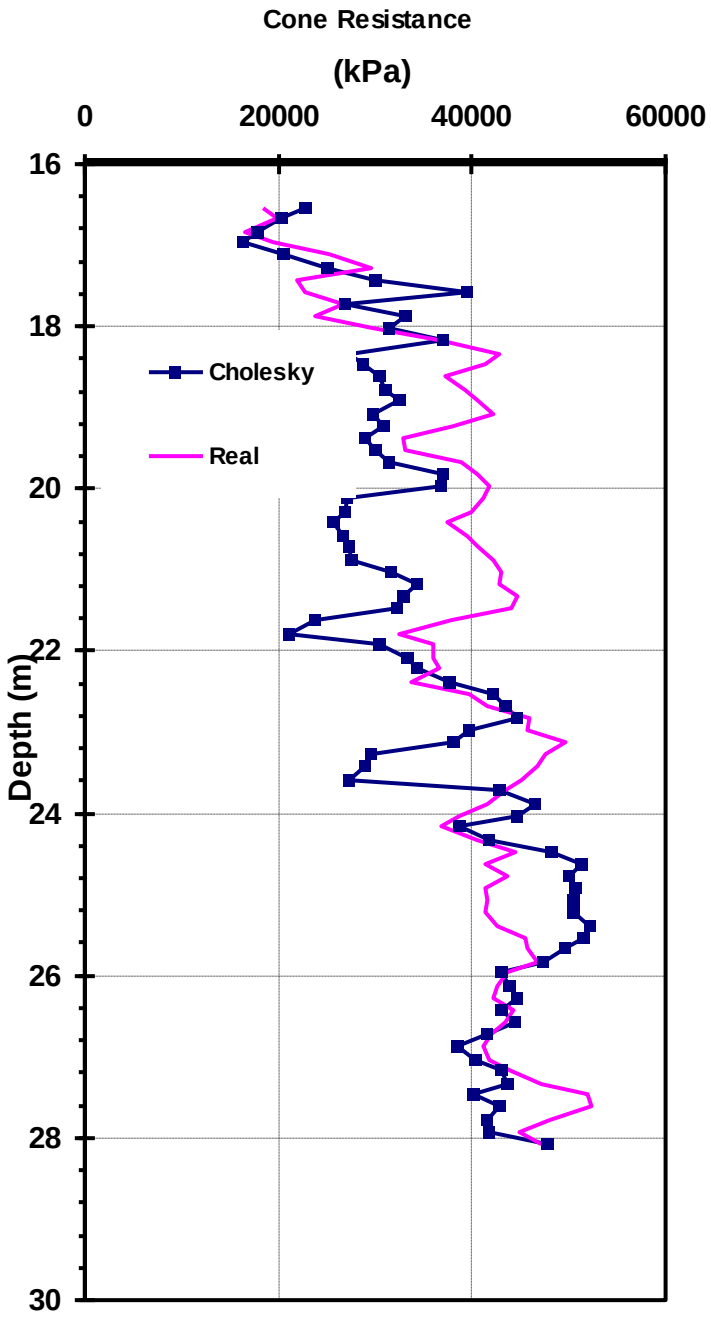

Figure 6.19 Comparison of the profile of the cone resistance simulated by the Cholesky method with the profile of real cone resistance at CPT-12 of the site of the Bridge A - 1700

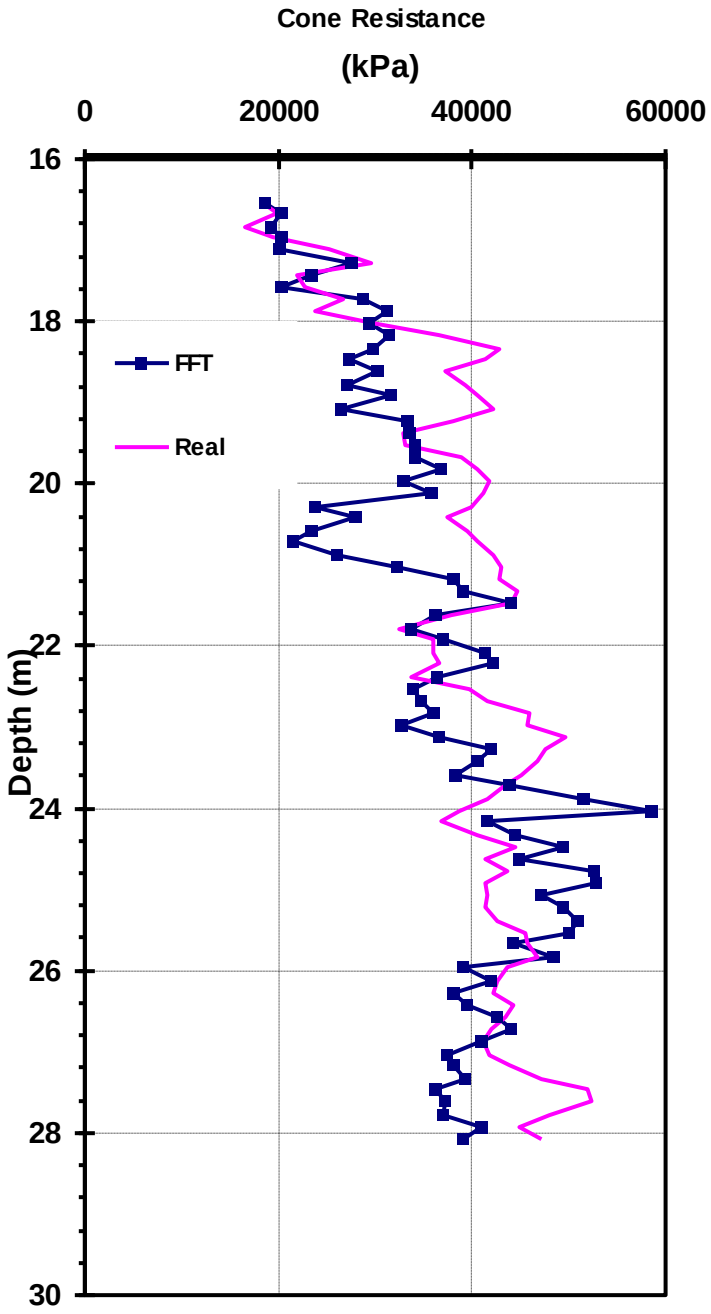

Figure 6.20 Comparison of the profile of the cone resistance simulated by the fast Fourier transform (FFT) method with the profile of real cone resistance at CPT-12 of the site of the Bridge A – 1700

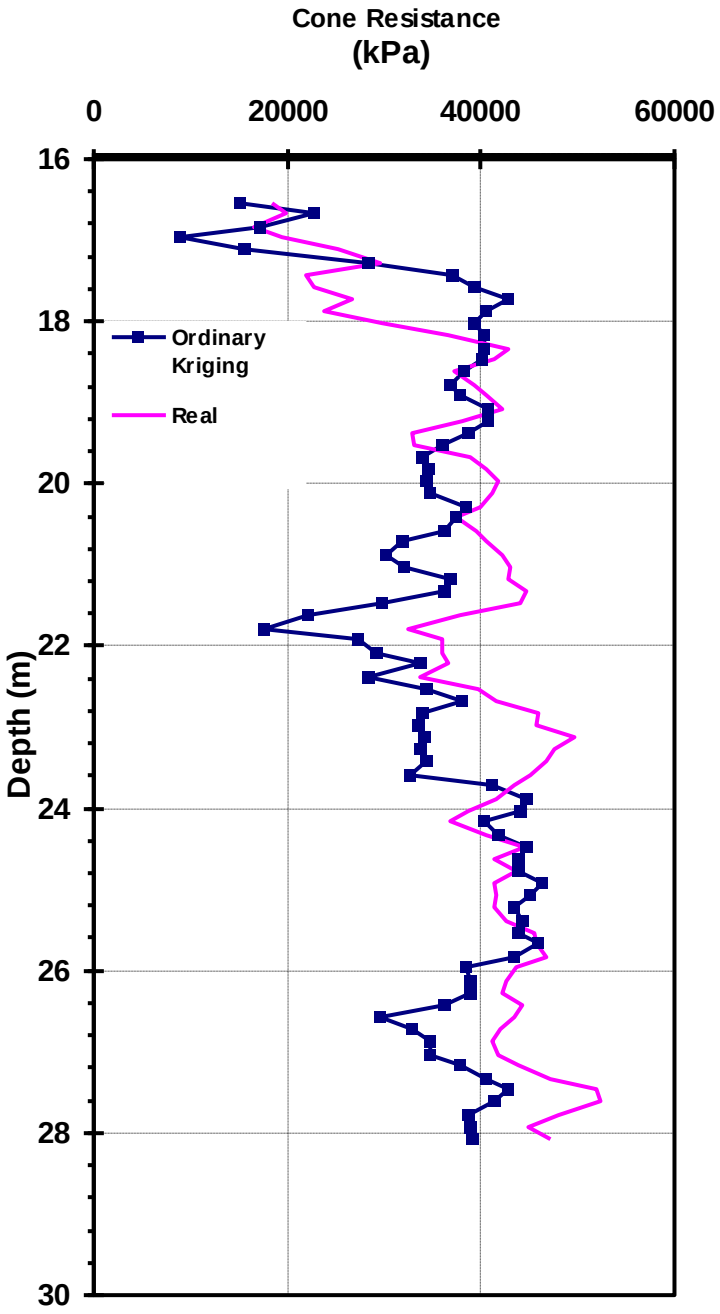

Figure 6.21 Comparison of the profile of the cone resistance simulated by the ordinary kriging method with the profile of real cone resistance at CPT-12 of the site of the Bridge A – 1700

Figures 6.22 to 6.25 present comparisons of the autocorrelation coefficient functions of cone resistance simulated by the proposed method, the Cholesky method, the FFT method, and the ordinary kriging method with the autocorrelation coefficient function of real cone resistance at CPT-12 of the site of the Bridge A – 1700. The autocorrelation coefficient functions of cone resistance simulated by four methods are analogous to that of real cone resistance at CPT-12 as a whole. Although the profiles of cone resistance simulated by the Cholesky method and the FFT method have a variety of features of the autocorrelation coefficient functions in every simulation trial due to the use of random number generators, even the correlation coefficient functions of the Cholesky method and the FFT method shown in Figures 6.20 and 6.21 are analogous to that of real cone resistance.

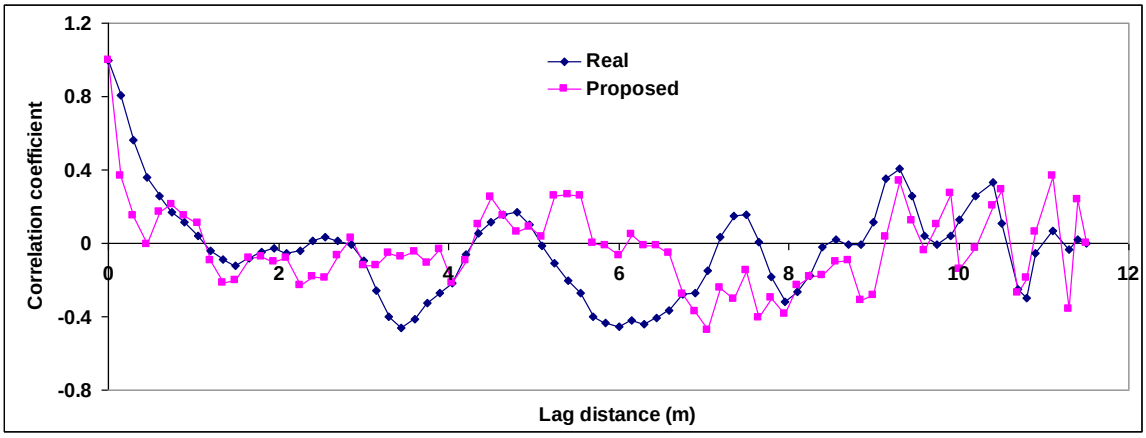

Figure 6.22 Comparison of the autocorrelation coefficient function of the cone resistance simulated by the proposed method with the autocorrelation coefficient function of real cone resistance at CPT-12 of the site of the Bridge A – 1700

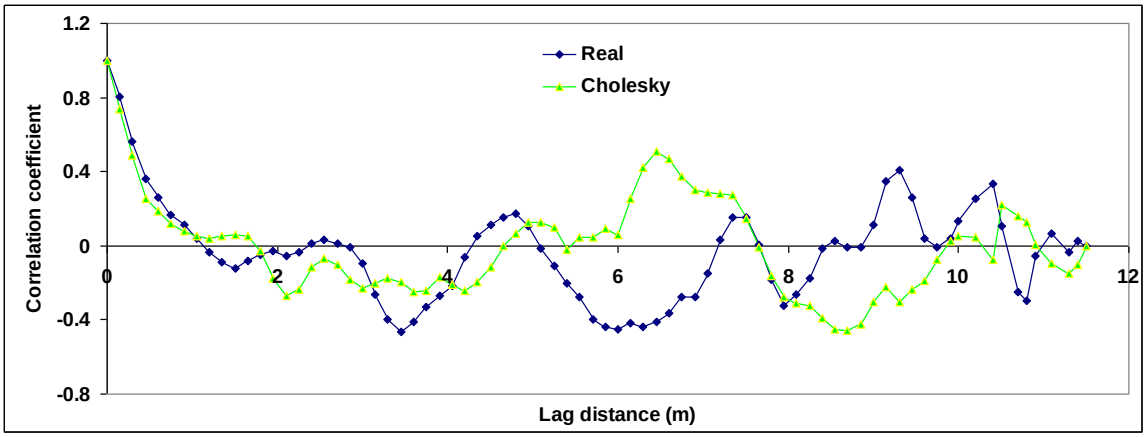

Figure 6.23 Comparison of the autocorrelation coefficient function of the cone resistance simulated by the Cholesky method with the autocorrelation coefficient function of real cone resistance at CPT-12 of the site of the Bridge A – 1700

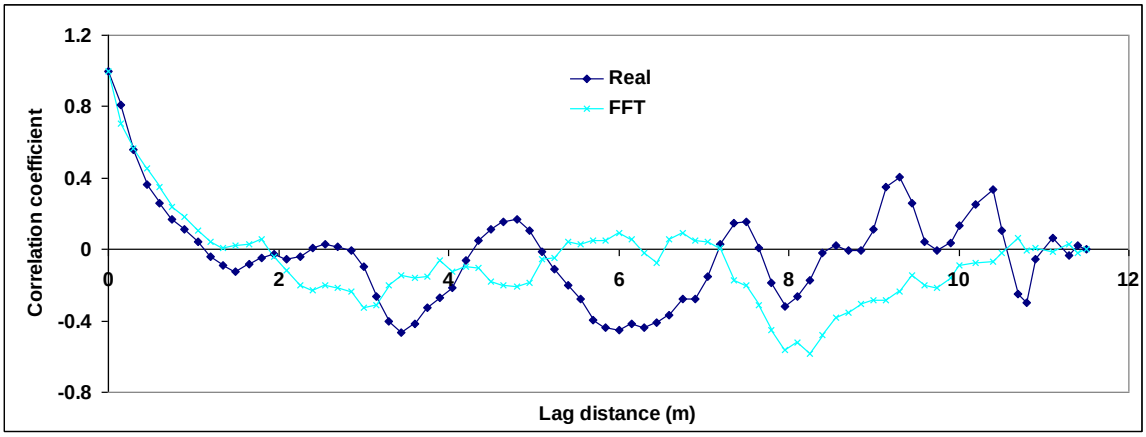

Figure 6.24 Comparison of the autocorrelation coefficient function of the cone resistance simulated by the fast Fourier transform (FFT) method with the autocorrelation coefficient function of real cone resistance at CPT-12 of the site of the Bridge A - 1700

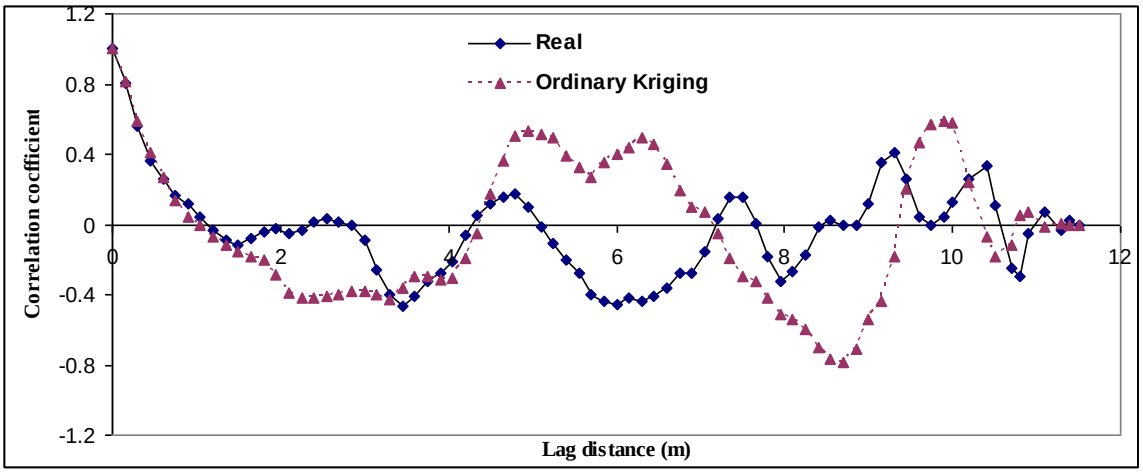

Figure 6.25 Comparison of the autocorrelation coefficient function of the cone resistance simulated by the ordinary kriging method with the autocorrelation coefficient function of real cone resistance at CPT-12 of the site of the Bridge A - 1700

In Table 6.2, the standard deviation and the correlation of the cone resistance simulated by the proposed method are compared with those of the cone resistance simulated by the Cholesky method, the FFT method, and ordinary kriging.

Table 6.2 Comparison of the standard deviation and the correlation in terms of the profile of cone resistance at CPT-12 of the site of the Bridge A – 1700

Standard deviation (kPa)					**Correlation**			
CPT-12 data	**Proposed method**	**Cholesky method**	**FFT**	**OK**	**Proposed method**	**Cholesky method**	**FFT**	**OK**
7797.73	8751.09	9109.40	8963.57	7572.01	0.59	0.04	0.12	0.35

Note: FFT=Fast Fourier Transform; OK=Ordinary Kriging

The profile of cone resistance generated by the proposed method has a standard deviation closer to that of the real data than the profiles generated by the Cholesky method and the FFT method; the profile of cone resistance generated by the ordinary kriging method shows the nearest standard deviation to that of the real data. When multi-

dimensional simulation is performed based on the statistical structures in the vertical domain of measured data, the Cholesky method and the FFT method bring about "random" results: that is, the simulated soil properties do not have high correlation levels with the real soil properties. This occurs because the random number generators randomly generate data based on a specific distribution model. Thus, statistical characteristics both in the vertical domain and the horizontal domain need to be considered to perform a multi-dimensional simulation.

The correlation between the cone resistance created by the proposed method and real cone resistance at CPT-12 is a positive value. In addition, this has a greater absolute value than correlations between cone resistances generated by the other methods and real data at CPT-12.

From the above evidence, it is evident that the profile simulated by the proposed method replicates many of statistical features of the real data.

As an additional test, cone resistance and sleeve friction at CPT-11 were simulated using statistical methods such as the mean, standard deviation, and autocorrelation coefficient functions obtained from cone resistances and sleeve frictions at boring locations CPT-9, CPT-10, CPT-12, and CPT-13.

Figures 6.26 to 6.29 show the profiles of the sleeve friction simulated by the proposed method, the Cholesky method, the FFT method, and the ordinary kriging method respectively, together with that of the real sleeve friction at CPT-11 of the site of Bridge A – 1700. Figures 6.34 to 6.37 illustrate the profiles of the cone resistance simulated by the proposed method, the Cholesky method, the FFT method, and the ordinary kriging method together, respectively, with that of the real cone resistance at

CPT-11 of the site of Bridge A – 1700. Figures 6.30 to 6.33 and Figures 6.38 to 6.41 present comparisons of the autocorrelation coefficient functions of sleeve friction and cone resistance simulated by the proposed method, the Cholesky method, the FFT method, and the ordinary kriging method, respectively, with those of real sleeve friction and the real cone resistance at CPT-11 of the site of Bridge A – 1700.

All the autocorrelation coefficient functions of sleeve friction simulated by the four methods for CPT-11 showed short correlation distances in comparison to that of real sleeve friction at CPT-11. However, the cone resistance simulated by the proposed method for CPT-11 showed a more accurate correlation distance than those simulated by any other methods; the cone resistances simulated by the Cholesky method and the FFT method showed greater correlation distances than real cone resistance at CPT-11; the cone resistance simulated by the ordinary kriging method showed a smaller correlation distance than real cone resistance at CPT-11.

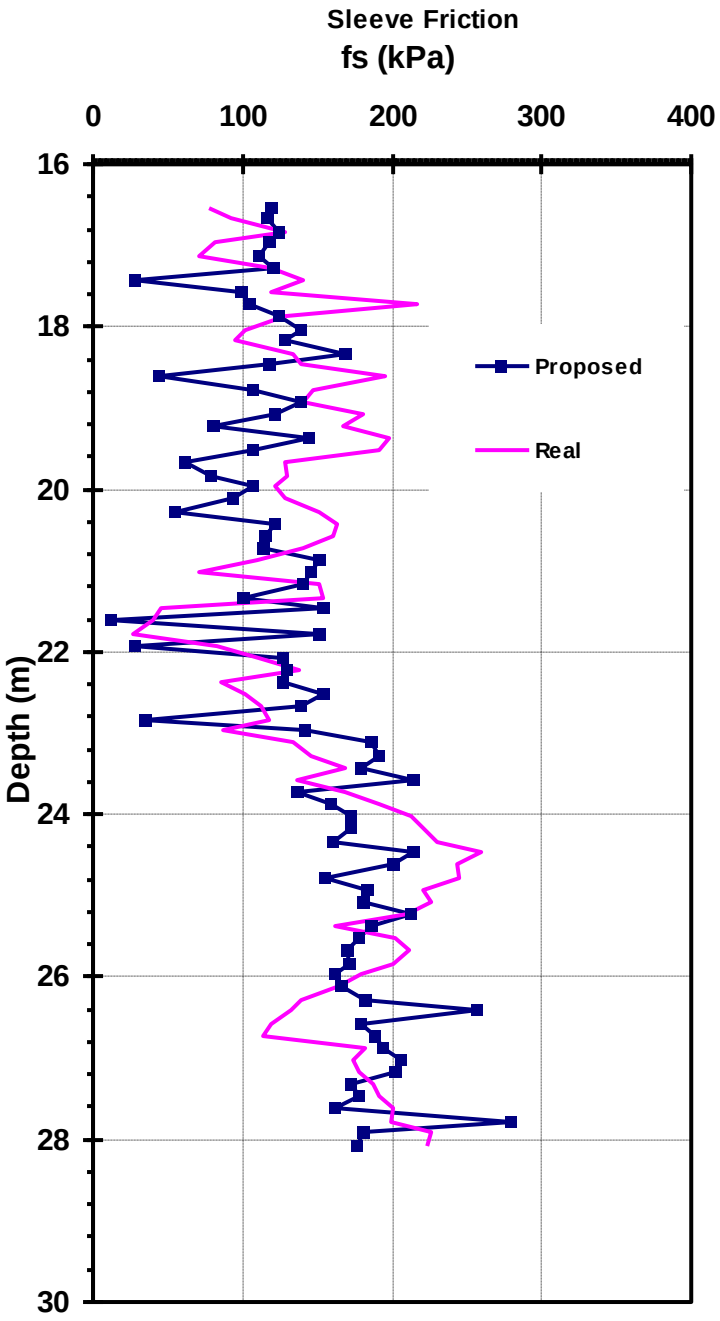

Figure 6.26 Comparison of the profile of the sleeve friction simulated by the proposed method with the profile of real sleeve friction at CPT-11 of the site of the Bridge A - 1700

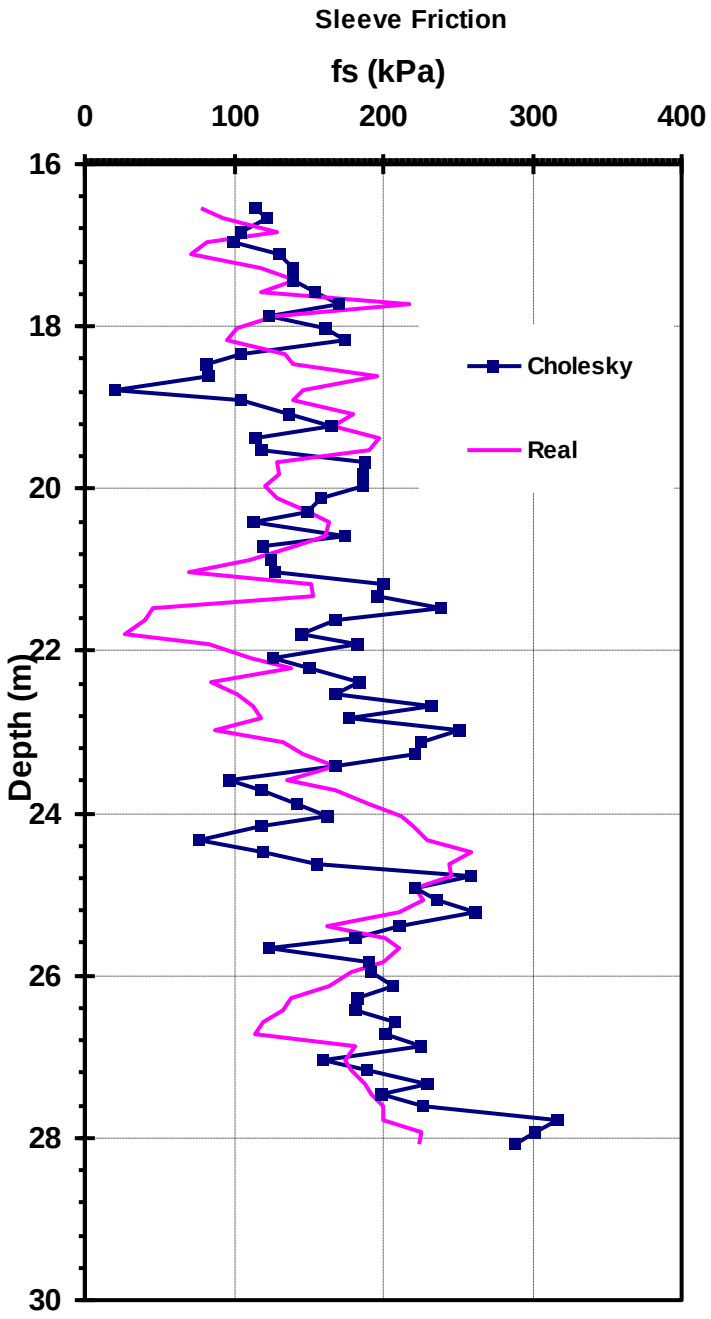

Figure 6.27 Comparison of the profile of the sleeve friction simulated by the Cholesky method with the profile of real sleeve friction at CPT-11 of the site of the Bridge A - 1700

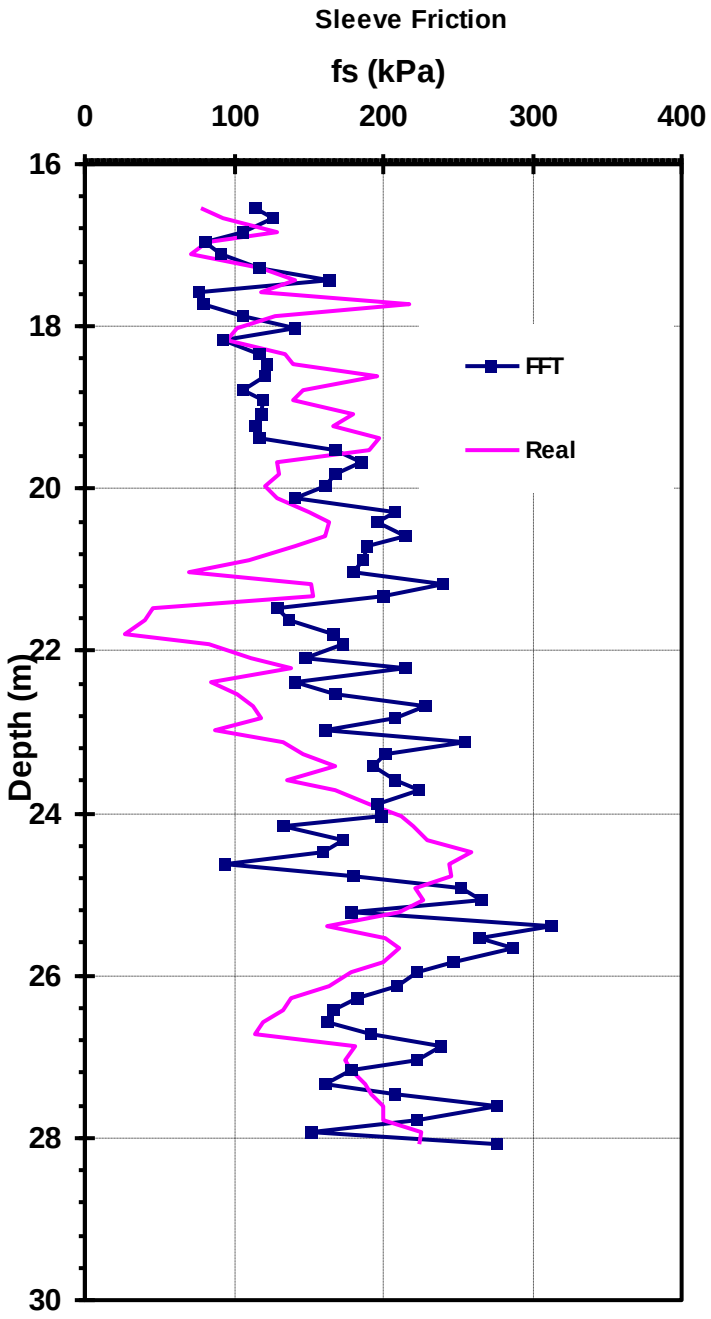

Figure 6.28 Comparison of the profile of the sleeve friction simulated by the fast Fourier transform (FFT) method with the profile of real sleeve friction at CPT-11 of the site of the Bridge A - 1700

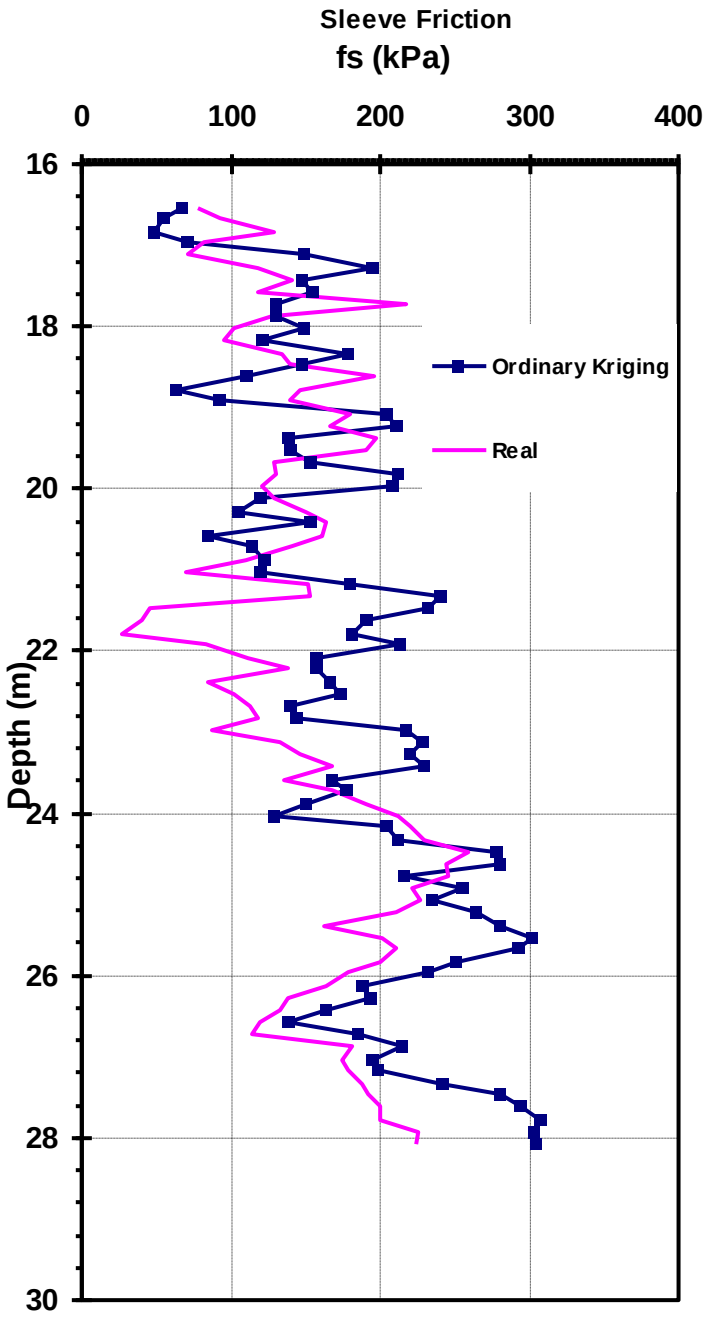

Figure 6.29 Comparison of the profile of the sleeve friction simulated by the ordinary kriging method with the profile of real sleeve friction at CPT-11 of the site of the Bridge A - 1700

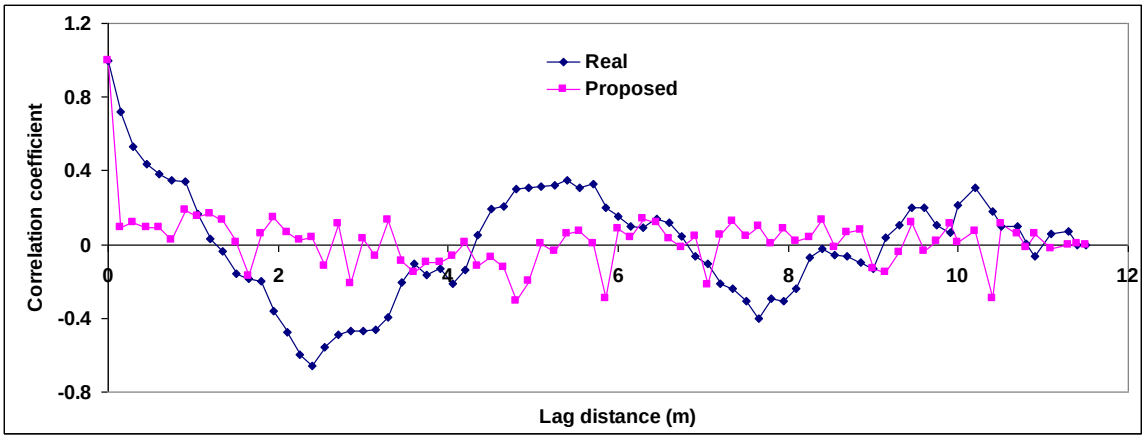

Figure 6.30 Comparison of the autocorrelation coefficient function of the sleeve friction simulated by the proposed method with the autocorrelation coefficient function of real sleeve friction at CPT-11 of the site of the Bridge A – 1700

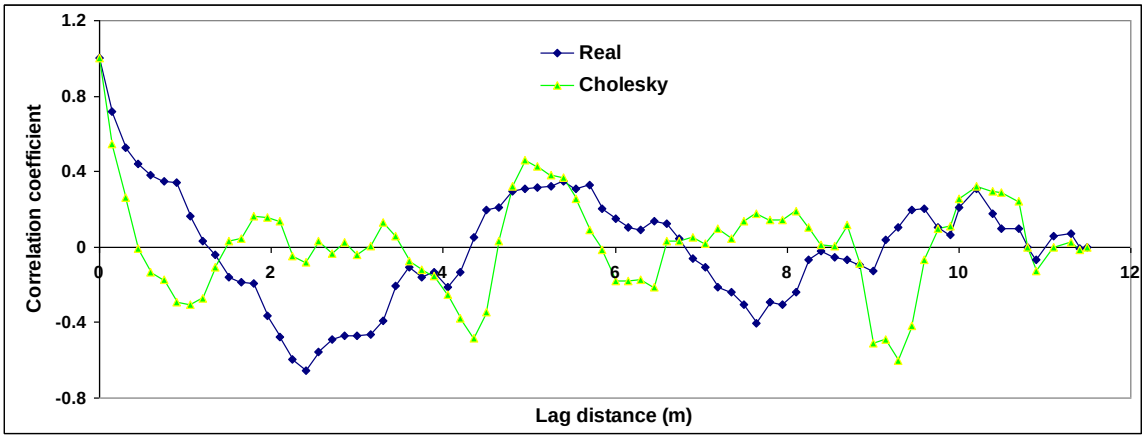

Figure 6.31 Comparison of the autocorrelation coefficient function of the sleeve friction simulated by the Cholesky method with the autocorrelation coefficient function of real sleeve friction at CPT-11 of the site of the Bridge A - 1700

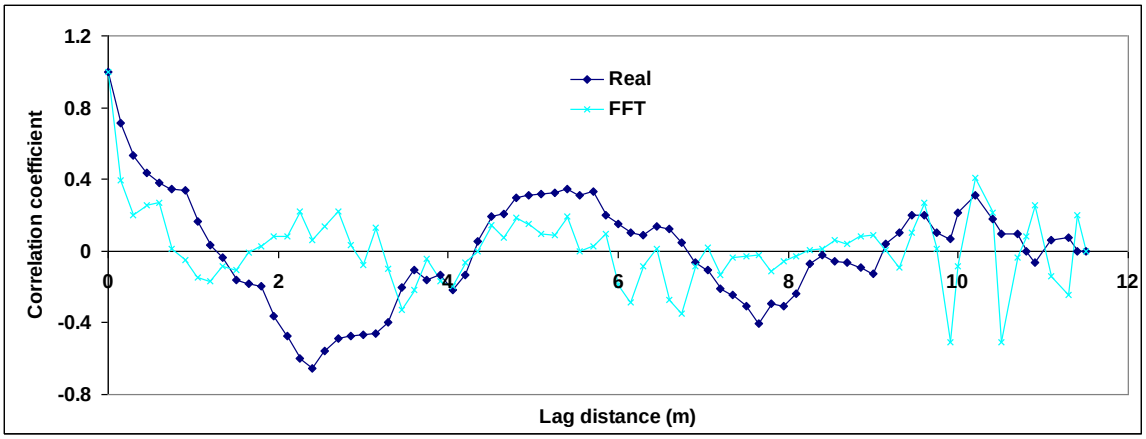

Figure 6.32 Comparison of the autocorrelation coefficient function of the sleeve friction simulated by the fast Fourier transform (FFT) method with the autocorrelation coefficient function of real sleeve friction at CPT-11 of the site of the Bridge A - 1700

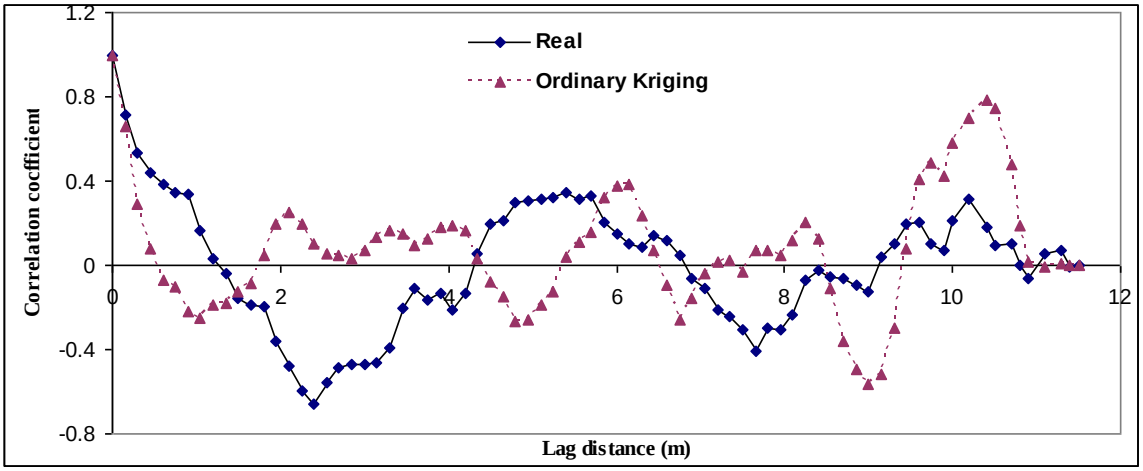

Figure 6.33 Comparison of the autocorrelation coefficient function of the sleeve friction simulated by the ordinary kriging method with the autocorrelation coefficient function of real sleeve friction at CPT-11 of the site of the Bridge A - 1700

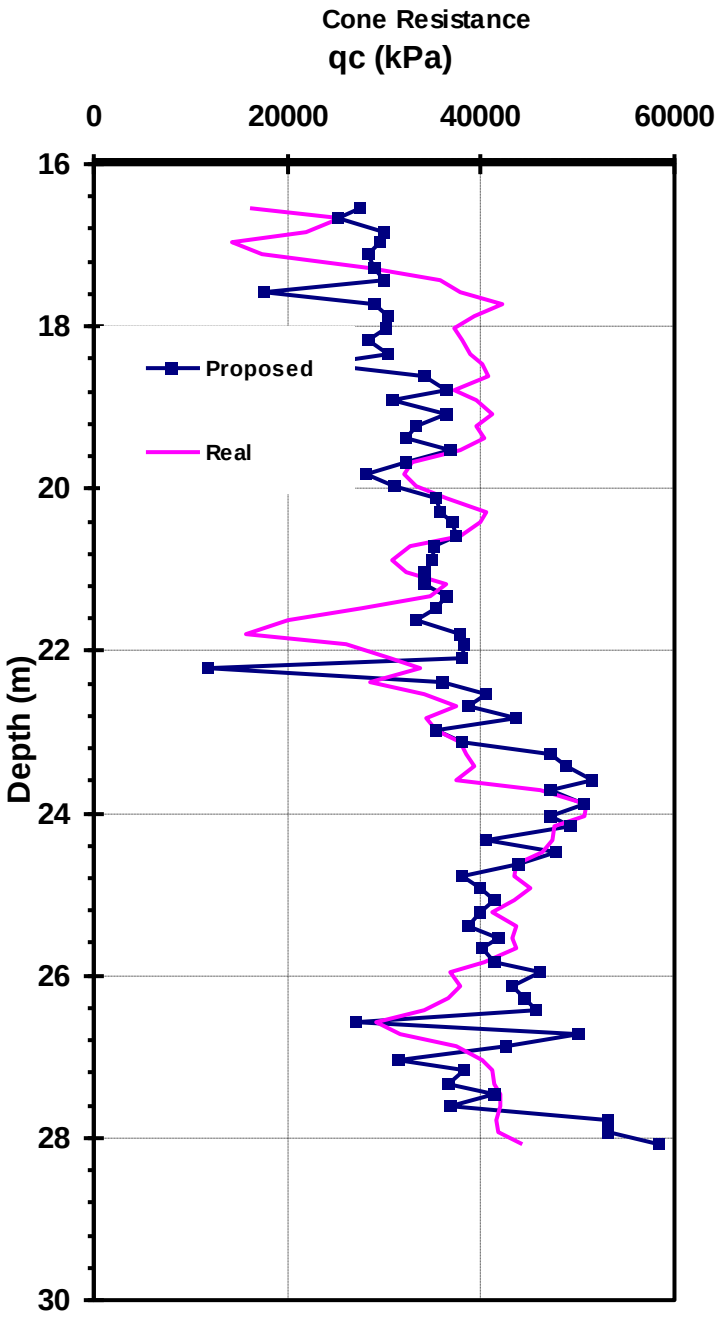

Figure 6.34 Comparison of the profile of the cone resistance simulated by the proposed method with the profile of real cone resistance at CPT-11 of the site of the Bridge A - 1700

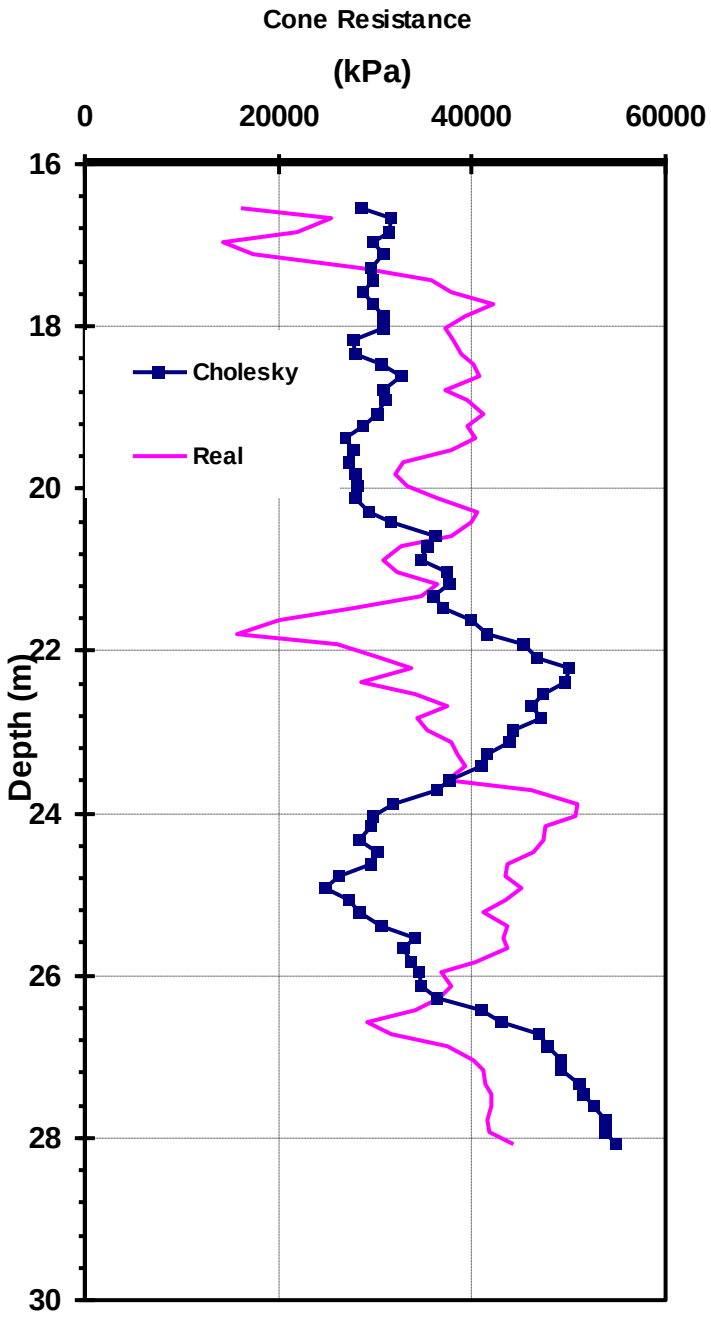

Figure 6.35 Comparison of the profile of the cone resistance simulated by the Cholesky method with the profile of real cone resistance at CPT-11 of the site of the Bridge A – 1700

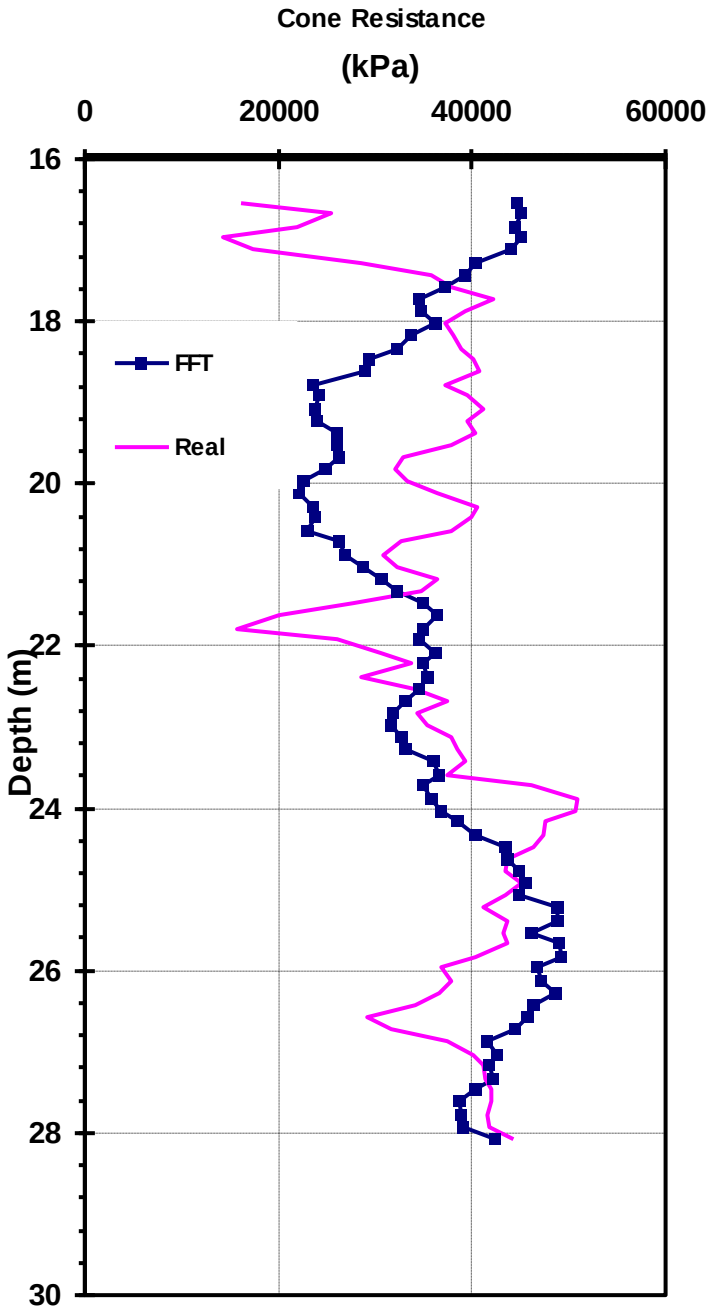

Figure 6.36 Comparison of the profile of the cone resistance simulated by the fast Fourier transform (FFT) method with the profile of real cone resistance at CPT-11 of the site of the Bridge A - 1700

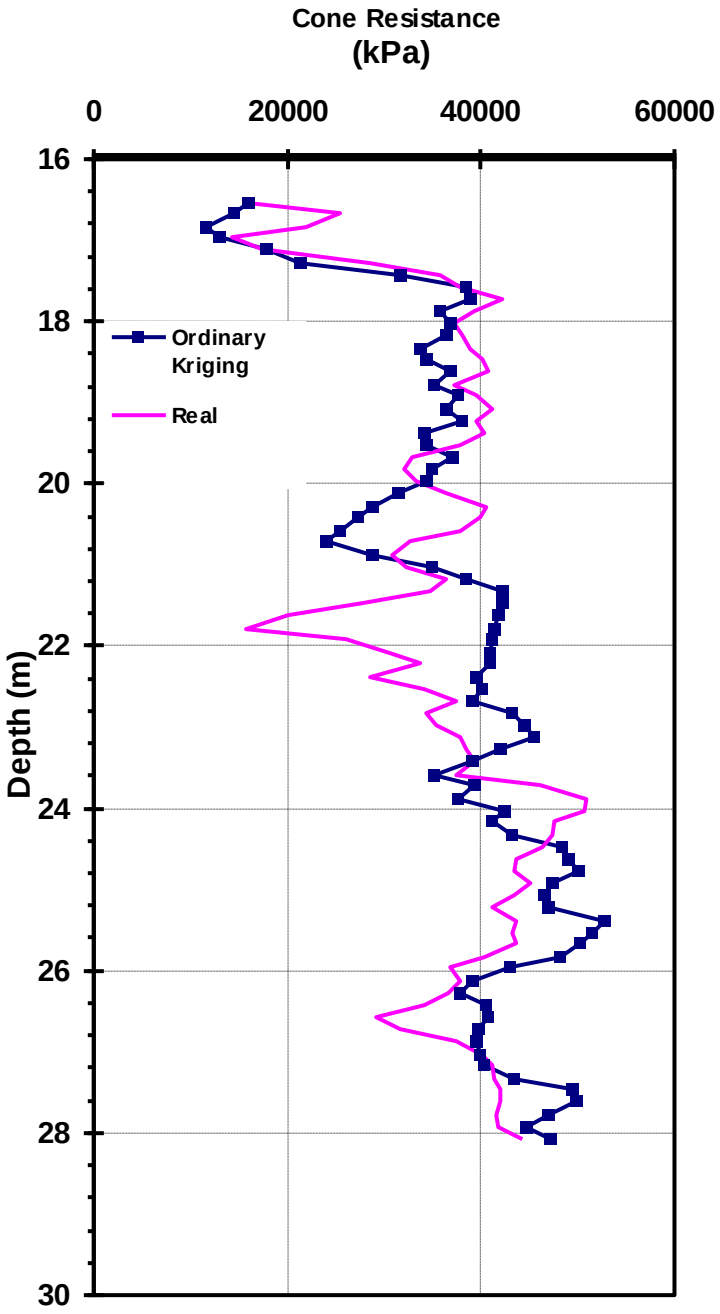

Figure 6.37 Comparison of the profile of the cone resistance simulated by the ordinary kriging method with the profile of real cone resistance at CPT-11 of the site of the Bridge A - 1700

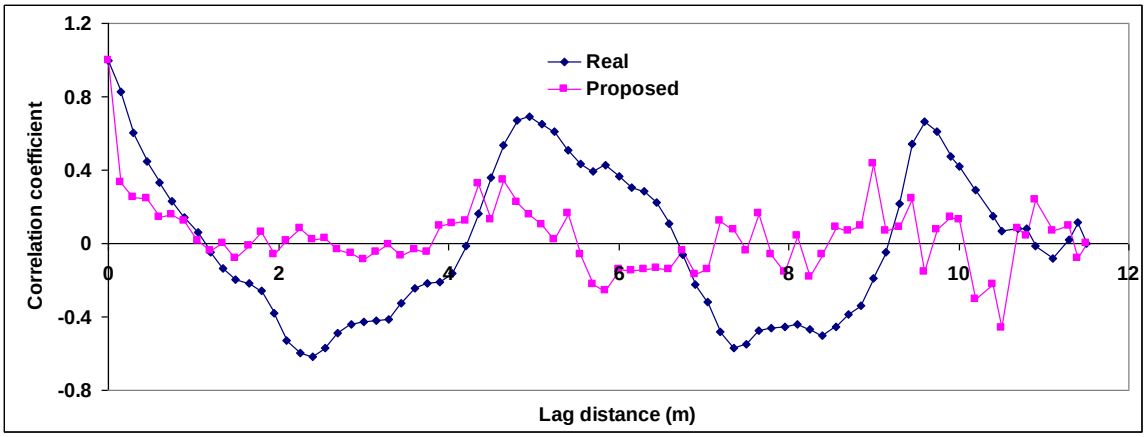

Figure 6.38 Comparison of the autocorrelation coefficient function of the cone resistance simulated by the proposed method with the autocorrelation coefficient function of real cone resistance at CPT-11 of the site of the Bridge A – 1700

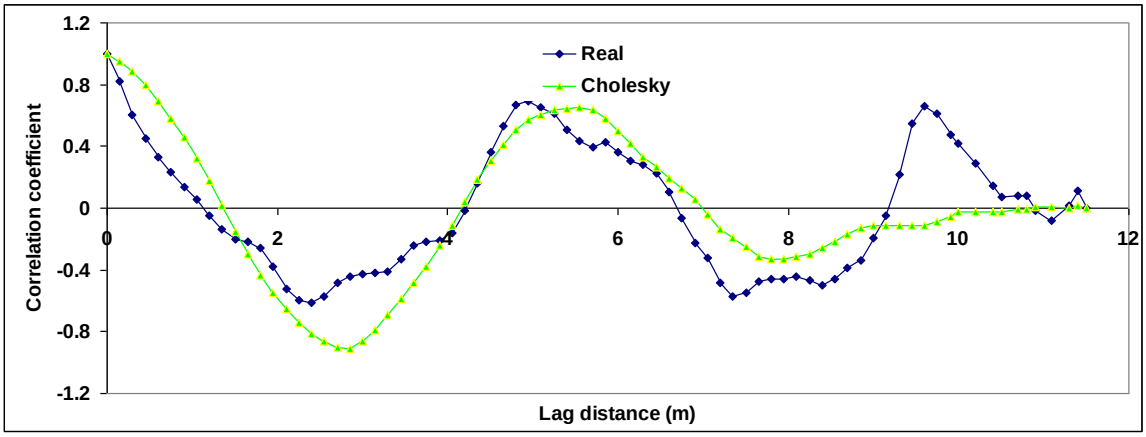

Figure 6.39 Comparison of the autocorrelation coefficient function of the cone resistance simulated by the Cholesky method with the autocorrelation coefficient function of real cone resistance at CPT-11 of the site of the Bridge A – 1700

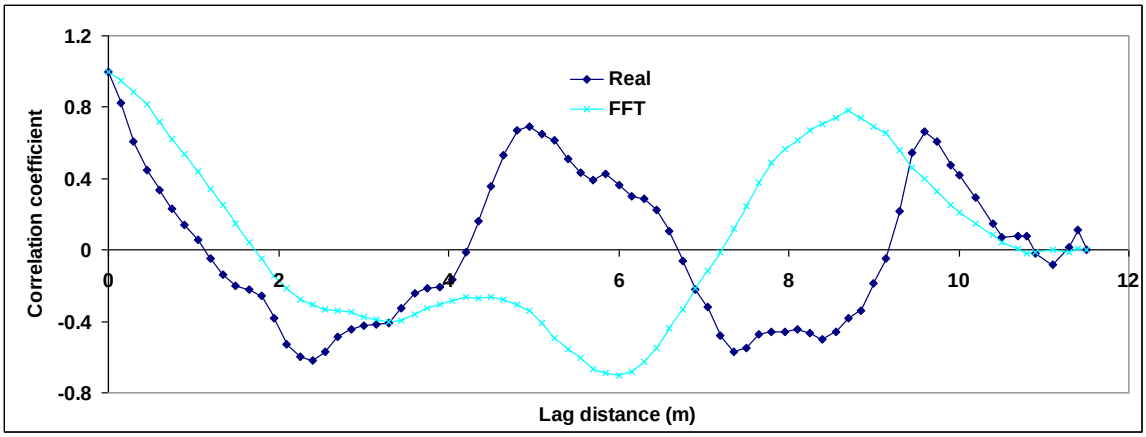

Figure 6.40 Comparison of the autocorrelation coefficient function of the cone resistance simulated by the fast Fourier transform (FFT) method with the autocorrelation coefficient function of real cone resistance at CPT-11 of the site of the Bridge A – 1700

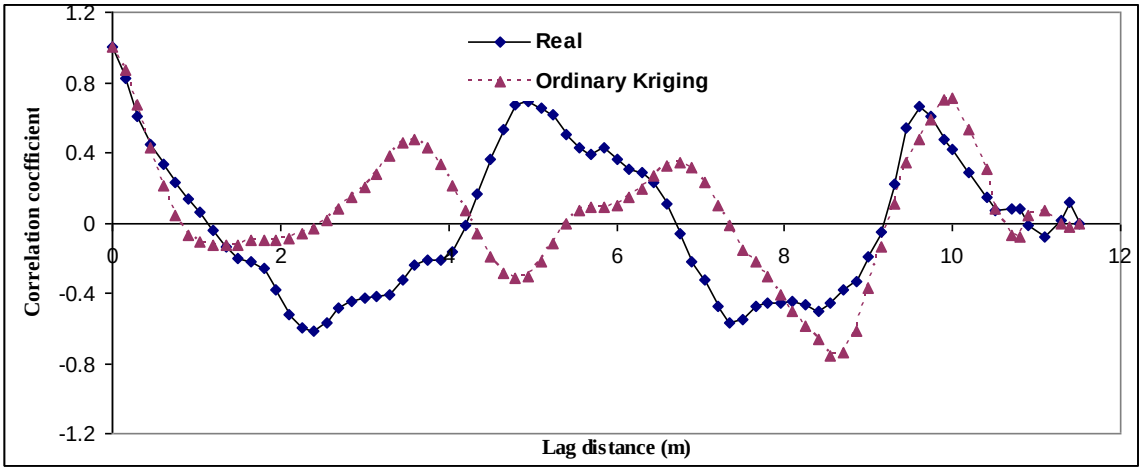

Figure 6.41 Comparison of the autocorrelation coefficient function of the cone resistance simulated by the ordinary kriging method with the autocorrelation coefficient function of real cone resistance at CPT-11 of the site of the Bridge A – 1700

In Tables 6.3 and 6.4, the standard deviations and the correlations of the sleeve friction and the cone resistance at boring CPT-11 simulated by the proposed method are compared with those of the sleeve friction and the cone resistance simulated by the Cholesky method and FFT method for boring CPT-11.

Table 6.3 Comparison of the standard deviation and the correlation in terms of the profile of sleeve friction at CPT-11 of the site of the Bridge A – 1700

Standard deviation (kPa)					**Correlation**			
CPT-11 data	**Proposed method**	**Cholesky method**	**FFT**	**OK**	**Proposed method**	**Cholesky method**	**FFT**	**OK**
51.50	60.89	54.68	54.10	64.39	0.21	-0.16	0.01	0.18
Note: FFT=Fast Fourier Transform; OK=Ordinary Kriging								

Table 6.4 Comparison of the standard deviation and the correlation in terms of the profile of cone resistance at CPT-11 of the site of the Bridge A – 1700

Standard deviation (kPa)					**Correlation**			
CPT-11 data	**Proposed method**	**Cholesky method**	**FFT**	**OK**	**Proposed method**	**Cholesky method**	**FFT**	**OK**
7682.75	8191.90	8385.64	7879.79	8842.94	0.19	-0.45	-0.30	0.40

Note: FFT=Fast Fourier Transform; OK=Ordinary Kriging

The FFT method generated the profiles of the CPT data at CPT-11, which have the most analogous deviations to the CPT data at CPT-11; the proposed method generated the profile of sleeve friction with a more analogous deviation to the real data than the ordinary kriging method and generated the profile of cone resistance with a more

analogous deviation to the real data than the Cholesky method and the ordinary kriging method. However, the Cholesky method did not generate more correlated profiles with real CPT data than the others. The correlation between the sleeve friction created by the proposed method and the real sleeve friction at CPT-11 showed larger positive values than the others. Although the correlation between the cone resistance created by the ordinary kriging method and the real cone resistance at CPT-11 showed the largest positive value, the correlation between the cone resistance created by the proposed method and the real cone resistance at CPT-11 showed larger positive values than those of the Cholesky method and FFT method. From the above evidence, it is concluded that profiles simulated by the proposed method have high correlation levels with the real data sets.

6.6. Conclusions

This chapter presented a simple technique to generate more accurate and more correlated multi-dimensional simulations of soil properties that are consistent with the observed or proposed correlation structures of soil properties. The proposed simulation method can estimate soil properties unknown at a specific location using the relative distances of soil data sets and the statistical structures of soil properties that have already been known through site investigation. Both the autocorrelation coefficient function and the correlation function were employed to estimate the accuracy of simulation generated by the proposed method compared with simulations created by the existing common simulation methods such as the FFT method, the Cholesky decomposition matrix method,

and the ordinary kriging method. Correlations between cone resistances and sleeve frictions created by the proposed method and real data were positive values. In addition, these had generally greater absolute values than correlations between cone resistances and sleeve frictions generated by the other methods and real data. This evidence shows that the profile simulated by the proposed method better replicates a great deal of statistical features of the real data.

The applications of the proposed technique have shown the need for the consideration of correlations where reasonable estimates are desirable. As a result, when correlation between data is disregarded, assuming that soil properties between data points are independent of each other, the estimates could be unreliable in the presence of correlation between geotechnical data because the estimates perform oversimplified analyses of soil properties and may not provide geotechnical designers with sufficient correlation information necessary to perform reliability analysis in geotechnical practice. It is common in geotechnical engineering to obtain negative values for the correlation coefficient function. Furthermore, it is necessary to consider both the positive and negative values of correlation coefficient functions. The cosine exponential correlation coefficient function was chosen to represent positive and negative values of the correlation coefficient function for a multi-dimensional simulation generated by the proposed method.

On the other hand, one of the shortcomings in this simulation procedure is that it is significantly dependent on the accuracy of the estimation of correlation between data: it is important to obtain more accurate soil properties of a site in order to improve the accuracy of simulation generated by this technique. The running time of the algorithm of

the proposed method increases as the data number of individual sections increases. The other drawback of this technique is that it is more applicable to large geotechnical projects with a considerable database. Taking into consideration, however, the results of correlation, the proposed method improves the accuracy in simulation.

In general terms, the proposed method to perform a simulation provides a convenient and logical way for dealing with the two types of different correlations that are present in the vertical and the horizontal directions in the soil properties of geotechnical engineering. The proposed simulation technique considering horizontal and vertical correlations allows the designer to simulate profiles of soil properties at any points based on limited data.

CHAPTER 7

SIMULATION OF GEOTECHNICAL SITE INVESTIGATION IN EDUCATION

7.1. Introduction

Traditional educational approaches often follow the Cartesian view of mind-matter dualism (Barab et al., 2001), which suggests that learning occurs prior to practice or vice-versa. That is, the learning of basic concepts is independent from the situational context and its application in practice. The expectation is that learners will later match up the concepts with specific situations and phenomena in practice. However, AbouRizk and Sawhney (1994) indicated that traditional teaching methods are incapable of providing students with all the skills necessary to solve real-world problems or to apply theoretical concepts to practice. Brown et al. (1989) recognized that although students can recall information learned via the dualistic methods on a test, they are often unable to apply the same concepts in practice. Thus, as indicated by Barab et al. (2001), separating the learner from the learning context can lead students' knowledge to become inactive and unserviceable due to the elimination of the natural complexity of content, the oversimplification of relations, and the absence of authentic problem solving and inquiry.

Teachers frequently use case studies and site visits as a means for students to acquire practical knowledge to overcome the limitations of dualistic educational approaches. However, Pennell et al. (1997) found that the necessary simplifications of

case studies may lead students to misapprehend that there are easy-to-find and universally correct results rather than viewing the results in the context of the case studies. Furthermore, visits by large groups to remote sites to observe site investigation techniques may not be welcome, involve risk, and may be impracticable (Echeverry, 1996).

Many of these issues apply to the learning of site investigation and characterization skills in geotechnical engineering education. The goals of site investigation and characterization are to determine soil types and engineering properties at a site of interest through in-situ and laboratory tests to facilitate subsequent geotechnical designs. Geotechnical engineers must make decisions regarding the number and depth of soil borings and/or soundings, the number and type of in-situ tests, and the number and type of laboratory tests subject to time and budget constraints. Experience and judgment are required to obtain the best possible information on soil types and properties for the least amount of time and cost.

Most traditional introductory geotechnical courses at the undergraduate level are focused on describing how individual laboratory and in-situ tests are used to measure or infer soil properties. However, students are usually not given the opportunity to exercise judgment and gain experience by planning and conducting a comprehensive site investigation program. Instead, existing geotechnical data and reports acquired from consulting companies are often provided for the students to use in homework and/or project assignments. However, this approach does not require students to exercise their own judgment in planning a site investigation.

7.2. Learning and training in simulation

The limitations of the dualistic approach to learning have motivated several researchers to explore alternatives where learners are more directly involved in the learning context. These efforts have led to the development of simulation environments. Simulation provides students with valuable hands-on experience in circumstances that would be too difficult or risky to practice in reality. Bourne and Brodersen (1995) stated several advantages for using simulations in engineering education:

- Simulations allow students to "use" equipment that is not available or too expensive to risk damage by inexperienced users.
- Students who have learned via simulations are able to apply principles more quickly once they enter practice, thus decreasing costs.
- On-line help and guidance incorporated in simulations can reduce the need for human guidance.

They believed that simulations could be used to create a common connection between classroom instruction and project-based learning experiences. Rezaei and Katz (1998) observed that simulations place the emphasis on student-oriented exploration, eliminating time-consuming processes related to data collection. Fu (2003) noted that computer-generated simulation techniques can save time and effort for both teachers and learners and that it can be applied to a broad range of learning levels from fundamental to advanced. He also argued that the use of computer simulations in university teaching help students establish a good connection with their future work in industry. Hall et al. (1998) studied the effects of simulation on cognitive processes and found that there was no statistical difference in knowledge retention between students using fully immersive,

three-dimensional educational applications and students using two-dimensional educational applications: two-dimensional simulation improved student's performance as much as 3-D simulation when the simulation environment was properly designed. Their study demonstrates that student performance does not depend on the complexity (i.e., 2-D vs. 3-D) of the simulation so long as it closely approximates the actual environment. Similarly, Hamel and Ryan-Jones (1997) observed that learning via simulation is as effective as real-world experience when the simulation environment is properly designed. Furthermore, Winkler et al. (2005) showed that significant increases in students' average scores in a course were achieved when computer simulations were used in the course. They also suggested that the use of simulations coupled with challenging homework assignments might improve performance in subsequent realistic situations.

On the contrary, Dowling (1997) pointed out the limitations of simulation:

- Simulations generally use mathematical models to represent phenomena rather than real data and thus may not represent real-world phenomena accurately.
- Users usually believe that simulations accurately describe dynamic processes and take users' actions into account.
- Cognitively, the computer leads users to how and what to think and learn.
- Developers' personal motives and value judgments are reflected in the generalization of behavior and the inclusion of certain elements in simulation.

According to Morineau et al. (1997), learners in a simulation environment initially experience a slower learning in comparison with learners in a real world environment. However, they discovered that the negative effect decreases over time as the learners gradually became accustomed to the simulation environment. Arduino et al.

(1997) noted that simulations should be used as a complement rather than a substitute for traditional educational approaches.

From these studies it may be concluded that well-designed simulation environments have the potential to help students to apply knowledge acquired via traditional educational approaches to real-world situations and practice.

7.3. Review of existing simulation models in teaching environments

In recent years, there have been a number of new and innovative approaches in engineering educational simulation techniques as summarized in Table 1. Simulation environments have also been developed for use in geotechnical engineering education. Davey-Wilson (1991) developed simulations of direct shear and consolidation tests including a tutorial mode based on artificial intelligence techniques, concluding that the tutorial mode was effective in reducing the required number of instructors. Penumadu et al. (1997) created Geo-Sim, an application for teaching soil behavior and the effects of individual soil parameters. Given a set of input parameters, Geo-Sim simulates the results of a triaxial test on cohesionless soil under drained and undrained conditions using soil models based on trained artificial neural networks for different soil types and stress paths. Glasgow University developed computer-assisted learning packages for geotechnical engineering. One is a computer simulation of the triaxial test called LabSim to help students understand soil behavior and train them in triaxial test procedures. The other is also a simulation for triaxial tests, Triaxial Cell, designed to allow students to view the test setup from different angles and control drainage and loading conditions. Similarly,

Arduino et al. (1997) developed a virtual geotechnical laboratory application based on a simple hyperbolic constitutive model to allow users to observe the test apparatus from any location or angle and adjust cell pressure or axial load increments.

Table 7.1 Educational simulations in teaching environment

Field	Name	Description	Reference
Geology	Virtual Earthquake	The simulation helps students explore the techniques to locate an earthquake's epicenter and determine its Richter magnitude	Novak (1999)
Geology	Virtual Dating	The simulation models the theory and techniques for radiometric dating of rocks and minerals.	Novak (1999)
Geology	Virtual Geology Laboratory	The application developed using HyperCard authoring software incorporates both still photographs and video to help learners to more accurately identify rock and mineral types, employing a tutoring module to provide advice and guidance.	Andris (1996)
Engineering	SESAM	Students manage a team of employees to complete a project on schedule, within budget, and at or above the required level of quality.	Drappa and Ludewig (2000)
Aerospace engineering	Virtual Aerospace Engineering Laboratory	The application developed using MacroMedia Authorware incorporates video and other graphical simulations.	Henning and Higuchi (1995)
Software engineering	Open Software Solutions	The application utilizes extensive graphics to provide students with interactive software engineering environment that the user needs to complete the project tasks.	Sharp and Hall (2000)
Software engineering		An educational simulation in a software project management training course stressing the management skill of the project leader as a significant factor necessary for the project to succeed.	Collofello (2000)
Software engineering	SimSE	The simulation was designed to teach students the process of software engineering.	Navarro and van der Hoek (2004)
Civil engineering		Applies communication and information technology in teaching civil engineering using computer imagery and visualization.	Bouchlaghem et al. (2000)
Civil engineering		The simulation uses Geographic Information Systems (GIS) to allow students to experiment with water quality management alternatives and observe their large-scale effects.	Camara et al. (2001)
Structural engineering		The application focuses on a deeper understanding of the structure with the assumption that there is no one correct answer to an engineering problem.	Webster and Archer (2001)
Construction	Interactive Visualizer	An object-oriented virtual reality platform	Op den Bosch and Baker (1994)
Construction	Virtual construction laboratory	The application simulates construction activities for students to experiment with different options and observe the system response.	Hadipriono (1996)
Construction	CYCLONE	The web-based application allows users to study and analyze construction processes using computer-based simulation systems.	Halpin et al. (2003)
Construction		The application incorporates the conceptual framework and implementation of a general-purpose situational simulation environment for construction education.	Rojas and Mukherjee (2005)

Wyatt and Macari (1999) presented the Soil-MIST (Model Instruction and Simulated Testing) program developed using the modified Cam-Clay constitutive model for the purpose of teaching theoretical concepts related to constitutive modeling. Users define the soil to be tested and control the loading and drainage conditions. Budhu (2000) introduced a geotechnical courseware package including triaxial, simple shear, direct shear, and consolidation tests on a compact disc that accompanies his textbook. The package focuses on the theoretical background, test procedures, and practical examples of each test. Sharma and Hardcastle (2001) developed Geotechnical Laboratory, which includes experiment modeling and simulation, an interactive tutorial and quiz, a handout, reference materials and Internet links for further study for common soil tests. Masala and Biggar (2003) developed a computer-based module for the permeability test in geotechnical engineering. They concluded that students who used the simulation better understood the test procedure, were better prepared for the physical experiment, and were better able to process the data afterwards. Hashash et al. (2002) developed VizCoRe, an interactive visualization learning and development software tool based on finite element and finite difference methods for material constitutive models to mathematically describe the stress-strain-strength behavior of engineering materials such as metals, plastics, concrete, and soils. Recently, El Shamy (2007) presented a laboratory simulation based on the discrete element method to enable students to understand the mechanism of tests by means of conducting basic laboratory tests.

These previous efforts to use simulation to enhance geotechnical engineering education have focused on basic soil behavior and laboratory testing. Although these are important components of geotechnical site characterization, site investigations via soil

borings and in-situ tests such as the Standard Penetration Test (SPT), Cone Penetration Test (CPT), and geophysical methods are playing an increasingly important role in geotechnical engineering (Mayne, 1995). As such, it is believed that it is important to develop a site investigation simulation program that includes these types of tests and provides students with an opportunity to plan and conduct a comprehensive site investigation.

7.4. Development of a simulation environment for geotechnical site investigation

7.4.1. Model architecture

A simulation environment for geotechnical site investigation that includes a variety of in-situ and laboratory tests was developed to allow students to plan and perform their own site investigation programs. A geotechnical site investigation simulation program was developed to help students connect basic principles of soil mechanics and concepts of geotechnical site investigation with their use in practice as well as to complement the traditional educational approaches of site investigation. Spatial variability in soil properties is modeled via the Cholesky decomposition method for correlated random fields and a Kriging method for interpolation in order to yield realistic geotechnical data. It is expected that via the simulation, students will be able to gain experience and judgment in an essential component of geotechnical engineering practice. The simulation environment is being coded in C++ and is compatible with Microsoft operating systems. The proposed site investigation simulation program consists mainly of four modules: (1) Instructor Input Module; (2) Student Input Module; (3) Test Simulation

Module; and (4) Evaluation Module. The algorithm for the proposed site investigation simulation program is illustrated in Figure 7.1. The function of each module is described below.

Previous chapters have demonstrated the important role of spatial variability of soil properties in improving the capabilities of site investigation in geotechnical engineering. In order to overcome a limitation of existing correlation equations in terms of generating correlated soil properties of in-situ tests in site investigation simulations, it is necessary to employ such random field theories as Kriging and the Cholesky decomposition method. Statistical structures obtained from a variety of in-situ tests in geotechnical engineering are used as data of an input file. Some authors (Das, 1997; Bowles, 1996; Henry, 1986; NAVFAC DM-7.1, 1982) suggested that at least one boring at each corner of a proposed multi-story building plan should be performed. The simulation program estimates boring numbers for each corner performed by student based on the criterion suggested by the above authors. Furthermore, U.S. Army Corps of Engineers (2001) recommended one boring per 230 square meters of ground floor for rigid frame structures. Using the boring spacing formula, a target boring number per unit area for a building area at a specific site is calculated to estimate student's site investigation performance.

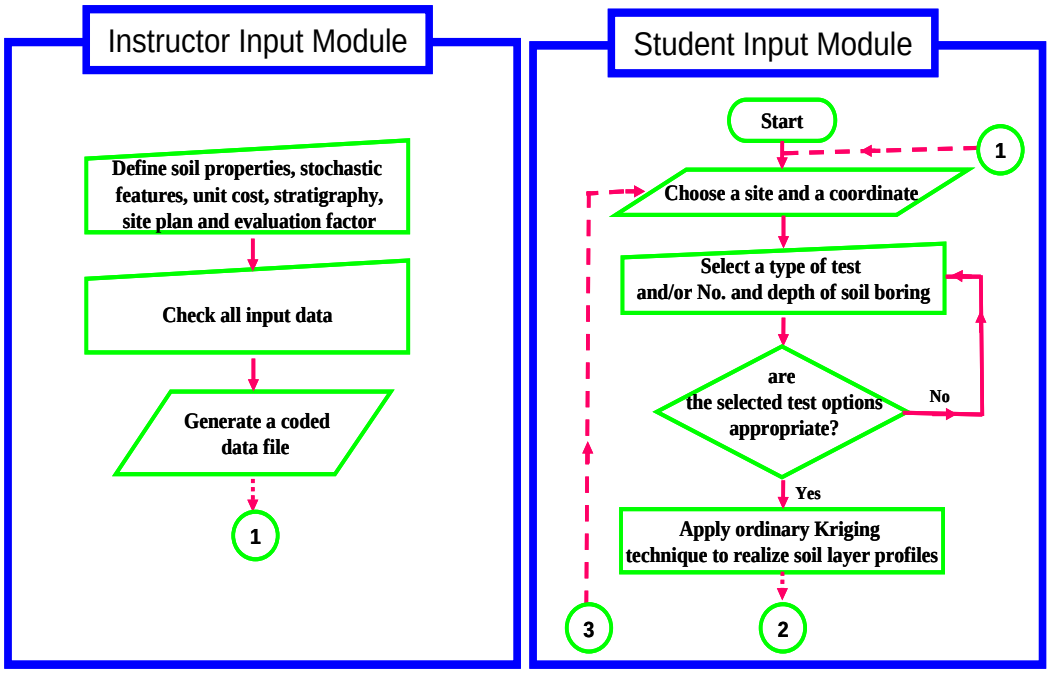

Figure 7.1 Algorithm of the proposed site investigation program: (a) Student Input Module; (b) Test Simulation Module; (c) Instructor Input Module; (d) Evaluation Module

7.4.2. Instructor Input Module

The Instructor Input Module allows instructors to define the site conditions and generate a data file to be used in the site investigation simulation. The module consists of six subordinate elements: soil properties; correlation information; surface topography; unit costs; building footprint; and evaluation factors. The instructors enter site information for a given site into the instructor input module. This information includes site location, structure type, plan dimension, and condition proposed for a given site. The Instructor Input Module then uses this information to assign site investigations to students. In the soil properties element, the instructor can define the stratigraphy of the site for which the investigation will be performed including the geometry of the individual soil layers, groundwater conditions, and basic soil properties. The essential soil properties are composed of void ratio, degree of saturation, liquid limit, plastic limit, grain size information (corresponding to 50% and 10% passing by weight), specific gravity, and overconsolidation ratio for simulation of in-situ tests and laboratory tests as illustrated in Figure 7.2.

Figure 7.2 Soil property subordinate tab

In the correlation distances element, the instructor can characterize the spatial correlation properties of the soils within a given soil layer as shown in Figure 7.3. The exponential correlation coefficient function was employed to generate correlated random fields. Standard deviation input values are used to generate the standard deviations of random fields defined by instructors. These statistical inputs are used to represent the spatial variability of soil properties so that more realistic geotechnical data can be generated.

Test type	Direction	Property	Correlation Distance (m) Clay	Correlation Distance (m) Silt	Correlation Distance (m) Sand	Standard Dev. (bar) Clay	Standard Dev. (bar) Silt	Standard Dev. (bar) Sand
SPT	Vertical	N	2.1	2.4	2.5	0.5	0.6	0.7
CPT	Vertical	Tip resistance	0.5	0.4	0.6	2.5	4.0	10.0
		Sleeve friction	0.6	0.5	1	0.1	0.2	0.7
		Pore pressure	2	2.16	1.3	0.7	0.5	0.07
DMT	Vertical	P0	1	1.2	1.5	1.5	1.6	1.7
		P1	0.9	1.1	1.4	1.5	1.6	1.7

Use Default Values Check Input Data

Figure 7.3 Correlation distance subordinate tab

The surface topography in Figure 7.4 provides the instructor with the ability to define the ground surface elevation at selected points on a site plan.

X Value	Y Value	Elevation(m)
180	30	40
240	30	41
300	30	42
360	30	43
420	30	44
120	90	42
180	90	44
240	90	45
300	90	46
360	90	53
420	90	45
480	90	44
60	150	42
120	150	44
180	150	46
240	150	47
300	150	47
300	300	48
240	300	49

Use Default Values Check Input Data

Figure 7.4 Surface topography subordinate tab

In the unit cost element of Figure 7.5, the instructor can specify costs for equipment mobilization, borings, soundings, and samples associated with field work as well as laboratory tests for the site investigation simulation of a specific project. Per diem meal and lodging costs for drilling crews also are included. Default values in the program are based on information provided by several geotechnical consulting firms. The cost information is used to calculate the total cost of the simulated site investigation if the instructor wishes to impose a limited budget.

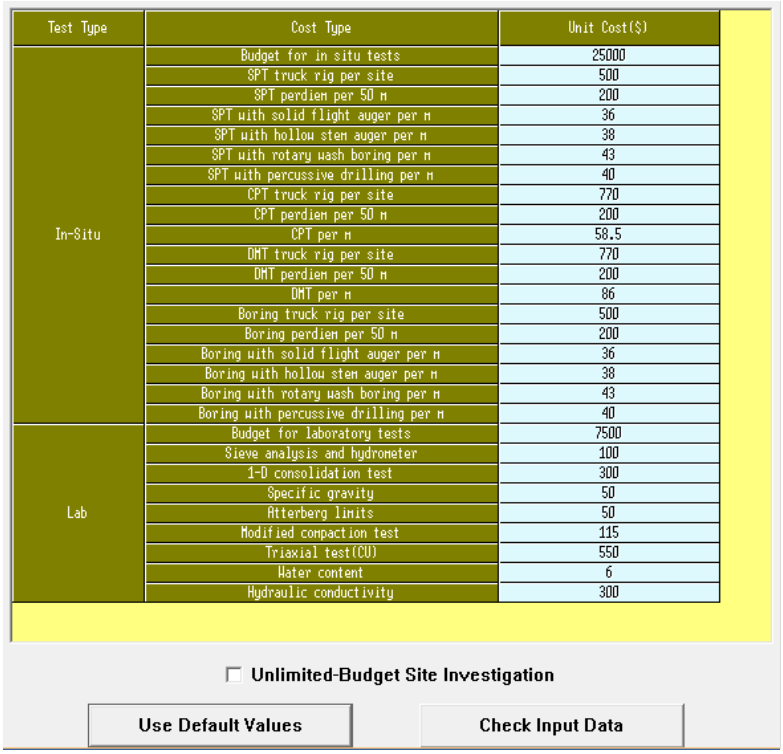

Figure 7.5 Unit cost subordinate tab

The preliminary building footprint element allows the instructor to depict general information for a given project including building type, building dimension, the number

of stories, and structure type. Several basic building footprints such as rectangular, T-shaped, L-shaped, and U-shaped are shown in Figure 7.6. Building structures such as residential structures, commercial structures, industrial structures, educational structures, medical structures, storage structures, and the like represent most of projects in civil engineering. In the case of bridges, in general, it has been known that geotechnical site investigation for bridges is performed at each abutment or pier (Carter and Symons, 1989; U.S. Army Corps of Engineering, 2001). Compared with geotechnical site investigation for structures, geotechnical site investigation for bridges is relatively simpler. The statistical structures of soil properties obtained from geotechnical site investigation performed at a bridge site can be used to simulate soil properties at an unsampled or undersampled building site in the same or a similar area and vice versa.

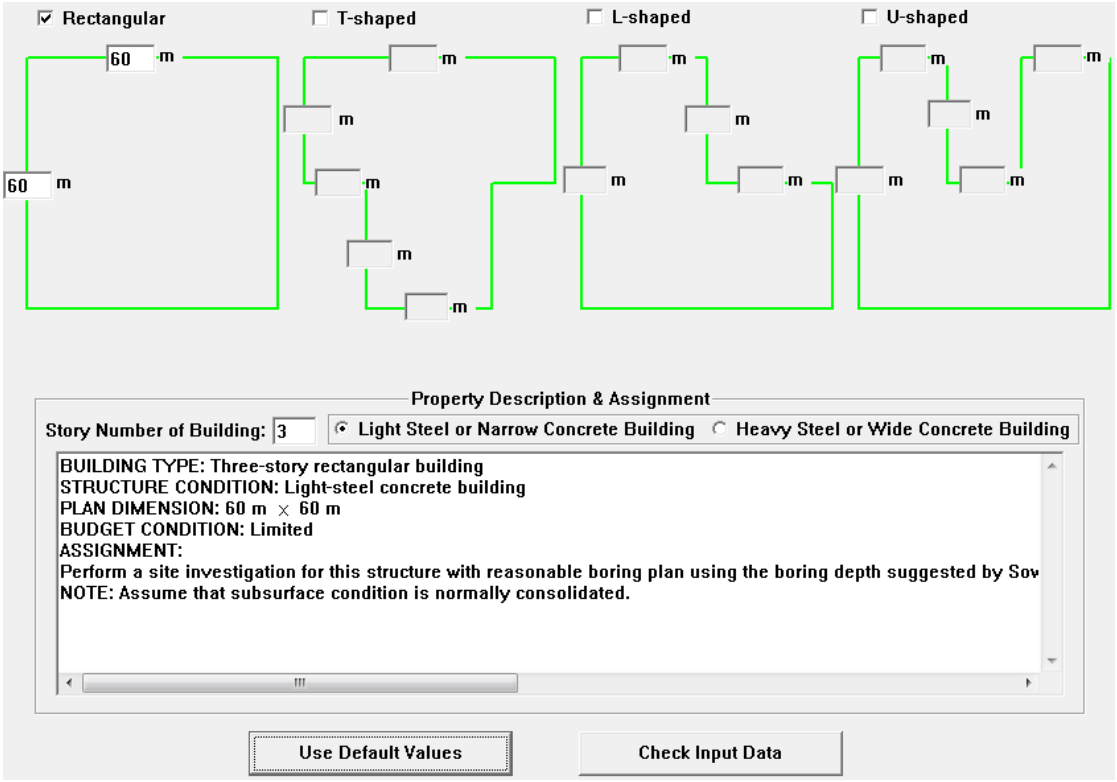

Figure 7.6 Preliminary building footprint subordinate tab

Finally, the evaluation factor element in Figure 7.7 consists of four objectives - expenditures, boring plan, the physical characteristics of each soil layer, and the soil parameters of each soil layer - to evaluate a student's site investigation performance. The instructor can determine the type of evaluation item, weight and allowance of each evaluation item. The rationale for each evaluation item will be explained in detail in the Evaluation Module.

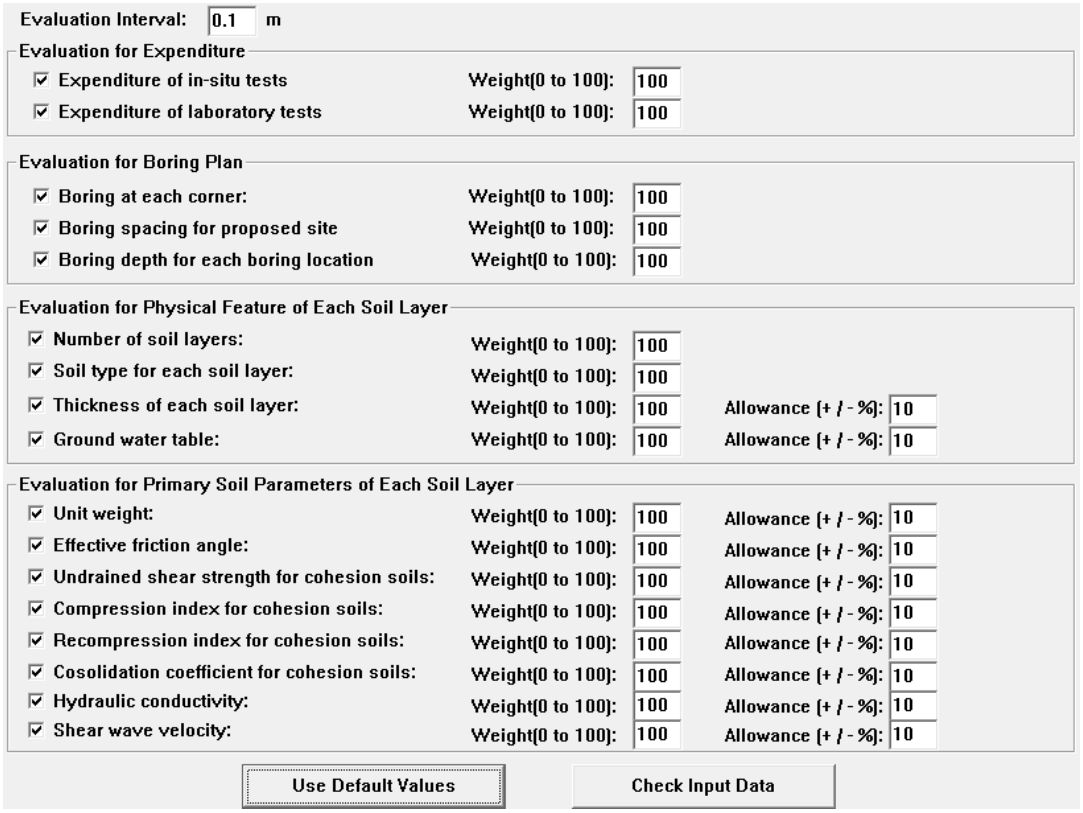

Figure 7.7 Evaluation factor subordinate tab

Figure 7.8 shows an example of encryption and decryption. Input data in the Instructor Input Module are coded via the process of encryption and can be saved as a

distributable input file with a “gsi” extension. The input data are encrypted to prevent a student from viewing the site and soil information entered by the instructor. When a student loads the coded input file, the input data file is decoded by the Student Input Module to perform the site investigation simulation. For convenience, each subordinate element in the Instructor Input Module recalls the default values of input from a template file when the “Use Default Values” button is clicked. Then, each subordinate element allows instructors to edit input values on each subordinate element and generate a distributable input file for students to perform the site investigation simulation.

Figure 7.8 Example of encryption and decryption

7.4.3. Student Input Module

The Student Input Module allows a student to perform a site investigation by specifying an in-situ test type, total boring/sounding number, boring/sounding location, and sampling depth to obtain the relevant subsurface information such as the types and spatial extent of various soils and their engineering properties for a given project. The module provides students with a preliminary site plan including a building type and dimension, structure condition, and budget limitations as defined by the instructor in a graphical interface as illustrated in Figure 7.9.

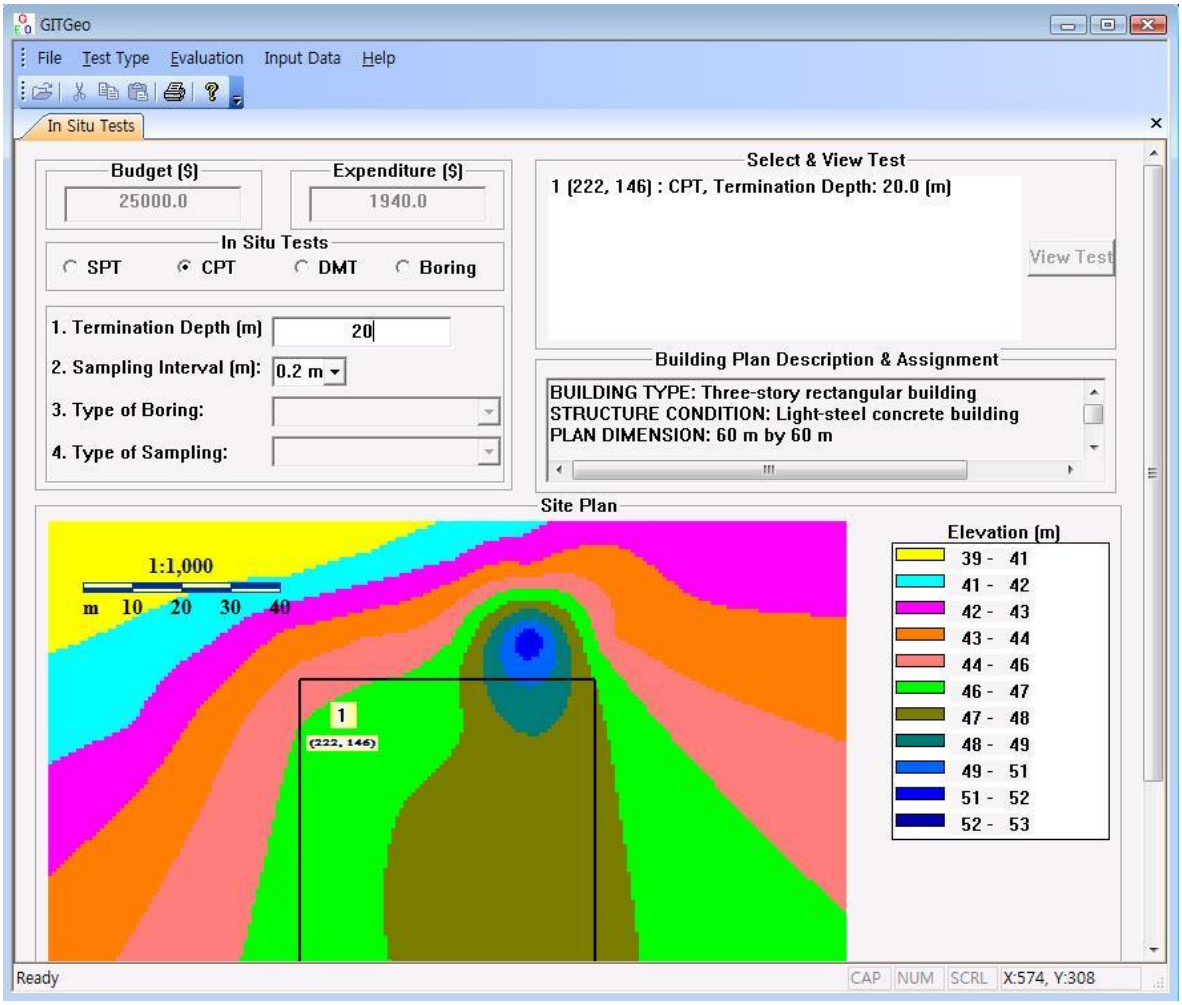

Figure 7.9 Student Input Module

Students may click a specific point on a given site to conduct a new soil boring or test. The options currently available include the type, the depth, and the sampling interval of in-situ tests; the type of boring including rotary wash boring and percussive drilling; the type of sampling; the depth of undisturbed samples obtained from a boring method; and the type of laboratory tests such as a 1-D consolidation test, permeability test, Proctor test, and consolidated-undrained triaxial test performed on each sample. The module will also display a budget for all tests and procedures such as equipment mobilization, borings, soundings, samples, and tests using unit costs provided by the instructor. If a limited budget is specified by the instructor, students must develop their site investigation plan within the budget. Fee information is included to reinforce the idea that site investigations must be designed to yield the necessary information about a site within a limited budget. For example, given that unit costs are defined as:

- Maximum boring/sounding depth per day: 50 m
- SPT truck rig mobilization per site: $500
- SPT with solid flight auger per meter: $36
- SPT per-diem on the daily basis of maximum boring and sounding depth: $200
- CPT truck rig mobilization per site: $770
- CPT per meter: $58.5
- CPT per-diem on the daily basis of maximum boring and sounding depth: $200
- DMT truck rig mobilization per site: $770
- DMT per meter: $86
- DMT per-diem on the daily basis of maximum boring and sounding depth: $200,

in-situ tests at a specific site are carried out as follows:

- SPT with solid flight auger performed to a depth of 10 m at 6 boring locations
- CPT performed to a depth of 10 m at 3 sounding locations
- DMT performed to a depth of 10 m at 3 sounding locations

It is assumed that each in-situ test is performed using different equipment. The per-diem of each in-situ test is calculated on the basis of rounding down to the nearest integer when the accumulated depth of each in-situ test performed exceeds the maximum boring/sounding depth per day because technicians to operate the equipments need to stay in a hotel during only the number of night, which rounds down to the nearest integer, when the number of total days of the per-diem is a floating-point number. For example, if the number of total days of the per-diem of a specific in-situ test based on the maximum boring and sounding depth per day is 1.9 days, it is regarded as 1.0 day. A total expenditure for the above in-situ tests performed is estimated as:

- SPT expenditure = Truck mobilization ($500) + SPT performance (60 m×$36)
  + SPT perdiem ($200) = $2860
- CPT expenditure = Truck mobilization ($770) + CPT performance (30 m×$58.5)
  = $2525
- DMT expenditure = Truck mobilization ($770) + DMT performance (30 m×$86)
  = $3350
- Total expenditure = SPT expenditure + CPT expenditure + DMT expenditure
  = $8735

If an unlimited budget is specified, students can perform a site investigation regardless of the budget. If the student makes an illogical choice, an on-screen tutorial mode will guide the student to make a more appropriate decision using a simple overview of the choice including a brief description of the procedure or test. On the basis of the fundamental site information, which instructors will have already input into the Instructor Input Module, the tutorial mode estimates the essential soil properties such as vertical effective stress, relative density, and friction angle at each depth and the site condition such as soil types, spatial distribution of soils, and the position of the water table. Using its own estimates of soil properties and subsurface conditions, the mode guides students to make a more relevant determination at almost every step of the investigation ranging from the selection of an in-situ test and the determination of the boring termination depth as the first step of site investigation, to the selection of laboratory tests and the determination of sampling depth for a specimen as shown in the following:

- before a student performs in-situ tests, a tutorial mode lets the student know “site plan” to perform site investigation;
- when a student determines a termination depth without selecting any in-situ test, a tutorial mode leads the student to choose one of in-situ tests;
- when a student types an improper boring/sounding termination depth during in-situ tests, a tutorial mode informs the student of the proper range of boring/sounding termination depth;
- when a student select an irrelevant boring/sounding location, a tutorial mode shows a brief description to revise the boring/sounding location;

- when spacing between borings is narrow, a tutorial mode shows a brief description for a proper boring location;
- when “Boring method” is performed, a tutorial mode explains that boring method is a test to perform laboratory tests using undisturbed soil samples;
- when the “Tip” button for depth(s) is pressed, a tutorial mode informs the student of the proper depth(s) and/or depth range(s);
- when a student wants to execute laboratory tests, a tutorial mode gives brief information about how to obtain undisturbed soil samples for laboratory tests;
- when a student performs laboratory tests using undisturbed soil samples, a tutorial provides the student with information including visually-inspected soil type, soil layer thickness, and sounding locations and depths of undisturbed soil samples;
- when a student determine an improper sampling depth for a specimen, a tutorial mode lead the student to correct the sampling depth;
- when a student’s total expense exceeds a given budget, a tutorial mode warns the student of it and informs the student of the rest of the budget;
- when a student types an improper value(s) for soil layer thickness and ground water table, a tutorial mode warn the student of it; and
- when a student select an irrelevant value(s) for soil parameter(s), a tutorial mode informs the student of the location(s) of the irrelevant value(s) for soil parameter(s).

The tutorial mode was designed as an effective learning tool to make it easier for students to perform their own site investigation as well as to guide students to make more

reasonable decisions. Even though new instructors use this site investigation simulation program, this simulation program will not result in poor-quality site investigation performance when instructors follow the manual of the simulation program provided because the simulation program has a system of quality checks that alerts both the student and the professor when faulty or flawed models are being developed.

7.4.4. Test Simulation Module

The Test Simulation Module is designed to simulate results for each in-situ and laboratory test chosen by a student via combining deterministic soil engineering properties derived from existing correlation equations with stochastic random fields to simulate spatial variability. For example, assume that the student has chosen a Cone Penetration Test (CPT) to obtain the relevant subsurface condition such as the soil types and spatial distribution of soils, and engineering properties of soils. Using basic subsurface information at four discrete locations (which the instructor has already input into the Instructor Input Module), the module will first calculate soil properties such as vertical effective stress, relative density, and friction angle at each depth. As an exercise, given that void ratio representative in the clay layer as the first layer is 0.8, saturation degree is 47%, liquid limit is 70%, plastic limit is 33%, specific gravity is 2.6, and overconsolidation ratio (OCR) is 3, plasticity index is calculated as 37%, total unit weight representative in the clay layer is estimated as 16.2 kN/m^3, and vertical effective stress at the depth of 4 meters is 64.9 kPa. Effective preconsolidation stress is estimated as 194.6 kPa by means of vertical effective stress times OCR. By use of the equation presented by

Mesri (1975) in Table 7.2, undrained shear strength at the depth of 4 meters in the clay layer is calculated as 49.5 kPa.

Table 7.2 Correlation equations of undrained shear strength and effective friction angle with each soil type

	Sand	Silt and Clay
Undrained Shear Strength	$s_u = NA$ where s_u = undrained shear strength NA = not applicable	$s_u = \sigma'_p \times (-0.00002314 \cdot PI^2 + 0.00462032 \cdot PI + 0.11522951)$ (Mesri, 1975) where σ'_p = effective preconsolidation stress PI = plasticity index
Effective Friction Angle	$\phi' = 33 + 3 \cdot I_R$ (Bolton, 1986) $I_R = D_r \cdot (10 - \ln P') - 1$ (Bolton, 1986) $D_r = -240.96 \cdot e + 194.98$ (Das, 1997) where ϕ' = effective friction angle I_R = relative dilatancy index D_r = relative density P' = mean effective stress at failure e = void ratio	$\phi' = 0.00147 \cdot PI^2 - 0.2811 \cdot PI + 35.90646)$ (Bjerrum and Simons, 1960)

As the next step, this module interpolates all information necessary to calculate the deterministic engineering properties of CPT at the sounding location selected by the student. The deterministic engineering properties are estimated via the existing correlation equations shown in Table 7.3. In the case that there exist more than two correlation equations to estimate a specific engineering property like cone resistance in sand, the engineering property is estimated as the average of the values obtained from the correlation equations. Correlated random fields generated by the Cholesky decomposition

method (Baecher and Christian, 2003) will be incorporated with the deterministic results obtained by the existing correlation equations to simulate realistic soil properties within individually given homogeneous layers specified by the instructor.

Table 7.3 Correlation equations of CPT deterministic engineering properties with each soil type

	Sand	Silt and Clay
Cone Resistance	1) $\sigma'_{v0} \times 10^{\left[\frac{(\tan\phi' - 0.1)}{0.38}\right]}$ (Robertson and Campanella, 1983) 2) $(\sigma'_{v0} \cdot P_a)^{0.5} \times 10^{\left[\frac{(\phi' - 17.6)}{11.0}\right]}$ (Kulhawy and Mayne, 1990)	$\sigma'_{v0} + 3 \times \left[\left(\frac{2 \times s_u}{\sigma'_{v0} \times \sin\phi'}\right)^{1/0.8} \times \sigma'_{v0}\right]$ (Mayne, 1995)
Sleeve Friction	$\sigma'_{v0} \times \left(\tan(45 + \frac{\phi'}{2})\right)^2 \times \tan(\frac{\phi'}{3})$ (Masood and Mitchell, 1993)	$\sigma'_{v0} \times \left(\tan(45 + \frac{\phi'}{2})\right)^2 \times \tan(\frac{\phi'}{3})$ (Masood and Mitchell, 1993)
Pore Pressure	u_0 where σ'_{v0} = effective vertical stress P_a = atmosphere pressure σ_{v0} = total vertical stress u_0 = steady state pore water pressure	$\frac{1}{0.53} \times \left[\left(\frac{2 \times s_u}{\sigma'_{v0} \times \sin\phi'}\right)^{1/0.8} \times \sigma'_{v0}\right] + u_0$ (Larsson and Mulabdic, 1991)

As a reference, the remainder of the existing correlation equations used in this module is shown in Appendix F-1 for in-situ tests and Appendix F-2 for laboratory tests.

Finally, the test simulation module will display the results for each in-situ test that the student has chosen as shown in Figure 7.10.

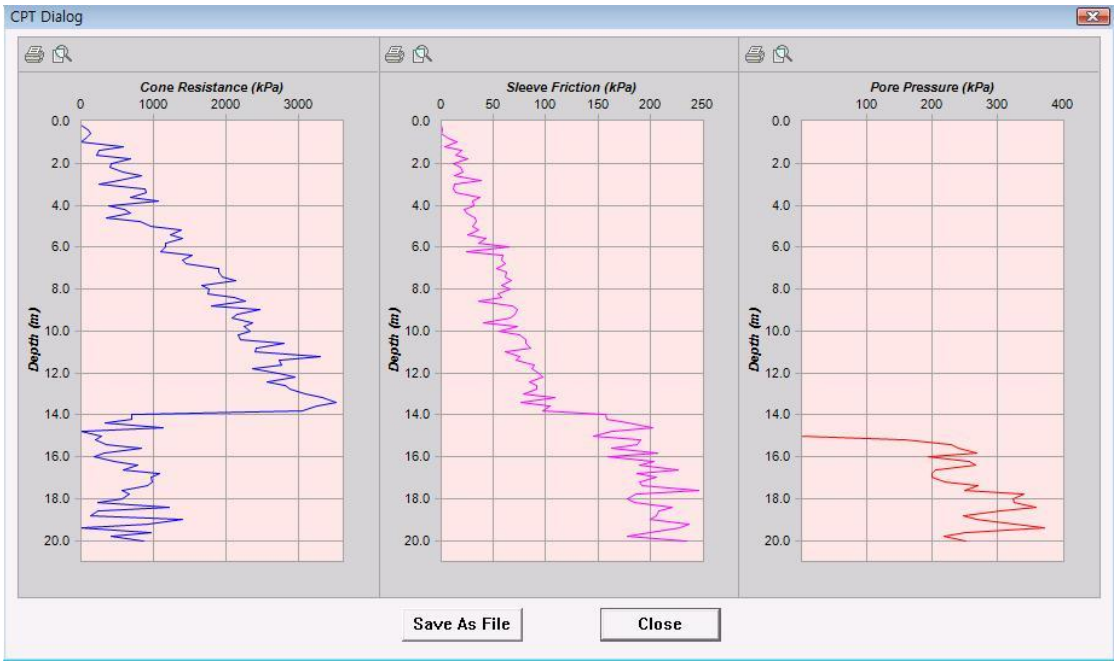

Figure 7.10 Test Simulation Module: CPT results in a silty clay layer

Figure 7.11 displays results of laboratory tests using the undisturbed samples obtained from a boring. The simulation program was developed for a preliminary site investigation to determine the general site conditions and to estimate the basic engineering properties of each soil layer. Furthermore, through the site investigation, students may establish their own plan for site preparation and specific foundation design for a given project. This part is for traditional educational approaches; self-development may be learned using techniques taught by instructors in lectures.

Several authors (Arduino et al., 1997; Bourne and Brodersen, 1995; Bertz, 1998) recommended that simulations should not be used in place of educational approaches taught by teachers in classes. However, as part of a learning regimen that includes first-hand experience, simulations may be incorporated with the traditional educational

approaches in a more meaningful way in order to lead students to a more solid and well-rounded education in engineering theory and practice.

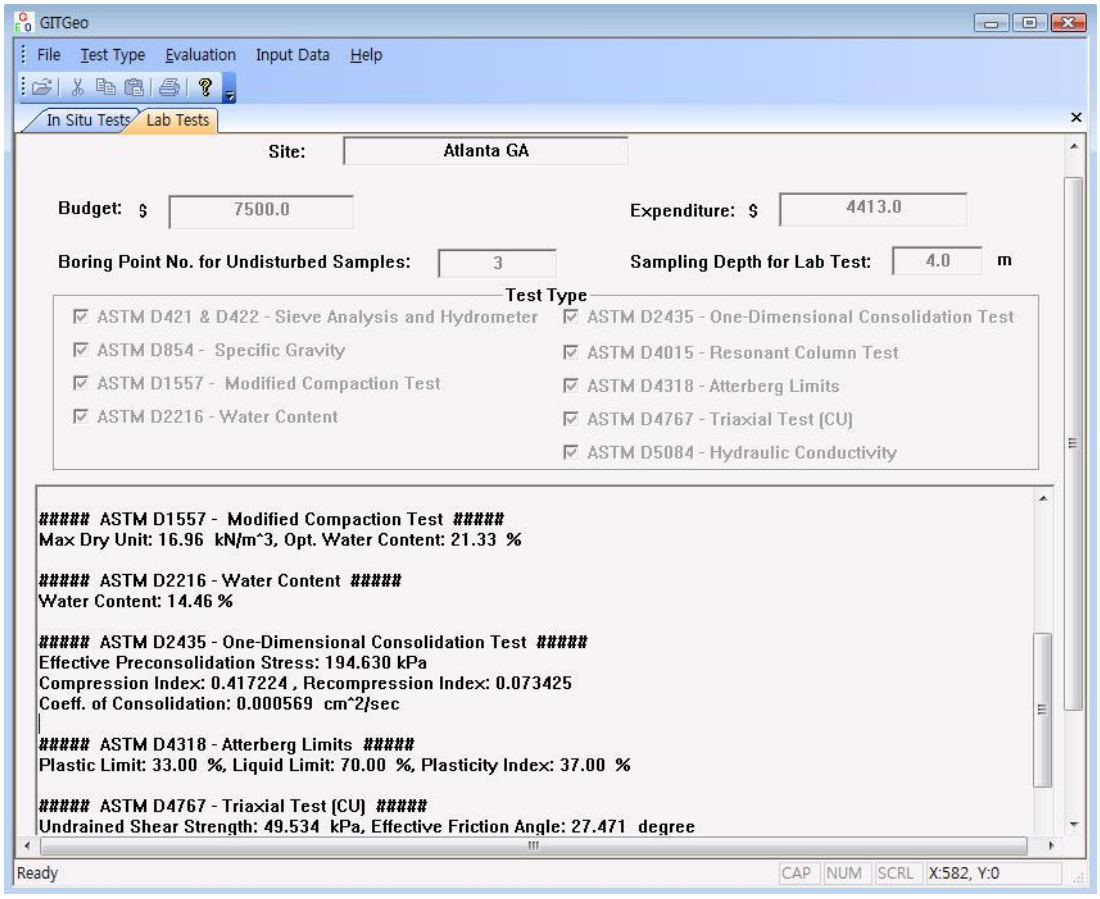

Figure 7.11 Test Simulation Module: results of laboratory tests

7.4.5. Evaluation Module

The Evaluation Module is used to assess and quantify a student's performance based on the cost, boring plan, subsurface conditions, and soil parameters as illustrated in Figure 7.12. In general, the costs, boring plan, subsurface conditions, and soil parameters

determined by student are evaluated by comparing them to the values specified by the instructor in the Instructor Input Module. Through the site investigation simulation program, students can learn how to make an initial boring plan of site investigation within a given budget by determining boring/sounding spacing and depth, understanding the subsurface condition of a proposed construction site via the results of site investigation, estimating the engineering properties of each soil layer necessary for geotechnical design, and determining the position of the water table and poor soils that adversely affect construction.

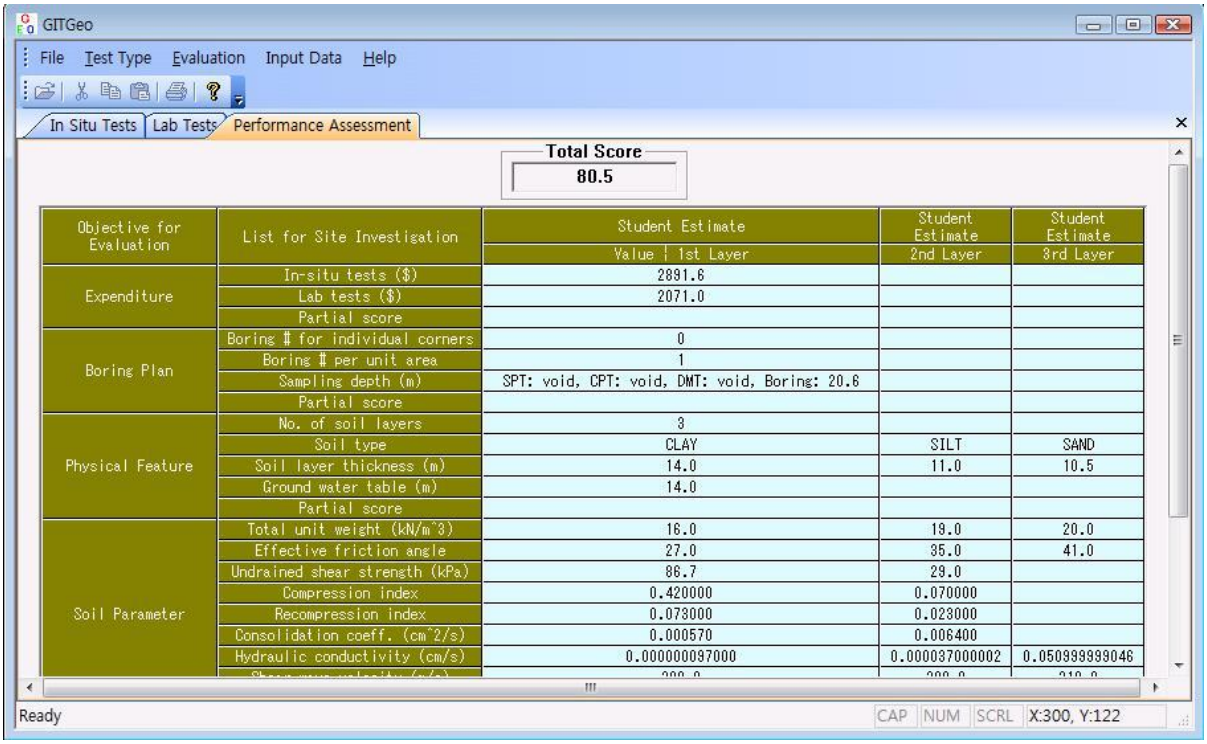

Objective for Evaluation	List for Site Investigation	Student Estimate Value | 1st Layer	Student Estimate 2nd Layer	Student Estimate 3rd Layer
Expenditure	In-situ tests ($)	2891.6		
	Lab tests ($)	2071.0		
	Partial score			
Boring Plan	Boring # for individual corners	0		
	Boring # per unit area	1		
	Sampling depth (m)	SPT: void, CPT: void, DMT: void, Boring: 20.6		
	Partial score			
Physical Feature	No. of soil layers	3		
	Soil type	CLAY	SILT	SAND
	Soil layer thickness (m)	14.0	11.0	10.5
	Ground water table (m)	14.0		
	Partial score			
Soil Parameter	Total unit weight (kN/m^3)	16.0	19.0	20.0
	Effective friction angle	27.0	35.0	41.0
	Undrained shear strength (kPa)	86.7	29.0	
	Compression index	0.420000	0.070000	
	Recompression index	0.073000	0.023000	
	Consolidation coeff. (cm^2/s)	0.000570	0.006400	
	Hydraulic conductivity (cm/s)	0.000000097000	0.000037000002	0.050999999046

Figure 7.12 Evaluation Module

The accuracies of the cost, boring plan, subsurface condition and soil parameters determined by the student are individually quantified as a score. As a result, the instructor may discuss with each student their weak points via analysis of the score obtained by them and suggest to each student a measure to improve the student's performance in the simulated site investigation. If needed, the student can be allowed to conduct additional simulations to supplement existing site investigation information. The measures to estimate the validity of the site investigation model built by the student are described as follows.

Expenditure

As mentioned earlier, cost is one of the measures used to assess a student's performance. The partial score of either in-situ tests or laboratory tests is equal to the ratio of a designated budget to the cost of either in-situ tests or laboratory tests performed by a student. When the partial score exceeds 100 points in calculation, it is adjusted to 100 points because a full score is defined as 100 points. If laboratory tests are not executed, the partial score of the expenditure does not include the part of the laboratory tests. For example, given budgets of $ 25,000 and $ 7,500 for in-situ tests and laboratory tests, respectively, and the individual evaluation weight as 100 (determined by instructors in the Instructor Input Module), the partial scores (P.S.) of in-situ tests, laboratory tests, and expenditure for the following individual cases are estimated as:

(1) total cost ($ 30,000) for in-situ tests and total cost ($ 7,000) for laboratory tests

$$\text{P.S. of in - situ tests} = \frac{25000}{30000} \times 100 = 83.3$$

$$\text{P.S. of laboratory tests} = \frac{7500}{7000} \times 100 = 107.1 \Rightarrow 100$$

$$\text{P.S. of expenditure} = \frac{\textbf{\textit{Sum of the product of each P.S. by each evaluation weight}}}{\textbf{\textit{Total evalution weight}}}$$

$$= \frac{83.3 \times 100 + 100 \times 100}{100 + 100} = 91.7$$

(2) total cost ($ 35,000) for in-situ tests and total cost ($ 0) for laboratory tests

$$\text{P.S. of in - situ tests} = \frac{25000}{35000} \times 100 = 71.4$$

$$\text{P.S. of expenditure} = \frac{\textbf{\textit{Sum of the product of each P.S. by each evaluation weight}}}{\textbf{\textit{Total evalution weight}}}$$

$$= \frac{71.4 \times 100}{100} = 71.4$$

Boring number for each corner

Several authors (Das, 1997; Bowles, 1996; Henry, 1986; NAVFAC DM-7.1, 1982) have suggested that at least one boring at each corner of a proposed multi-story building plan should be performed. Each corner of the proposed building plan is virtually centered at the 30 m square grid as shown in Figure 7.13. When a boring performed by a student is located within this 30 m square grid, this is considered effective for estimating a student's performance number in boring for each corner. The partial score of the boring number for each corner is estimated as the ratio of the boring number performed by the student to a target boring number.

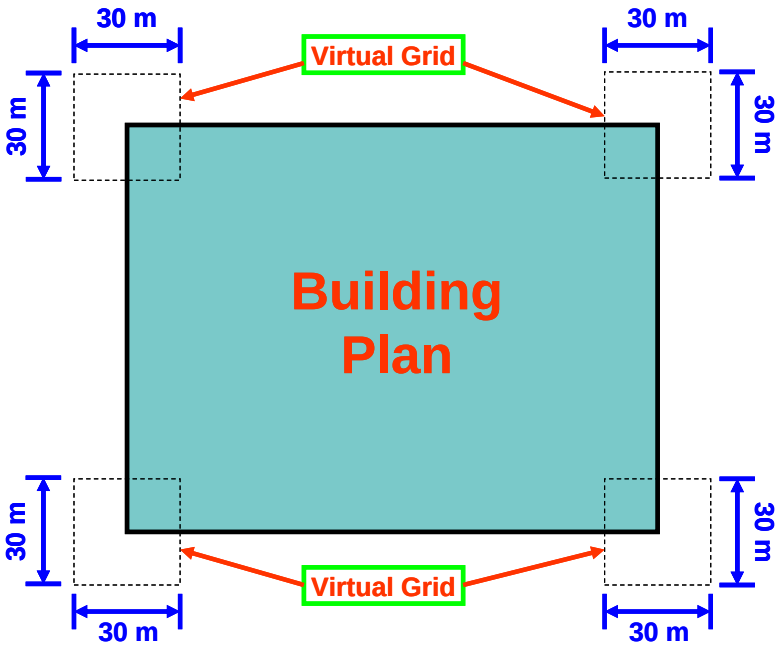

Figure 7.13 30 m square virtual grids at each corner of proposed building plan

Boring number per unit area

Several authors (Sowers and Sowers, 1970; Das, 1997; Bowles, 1996; Henry, 1986; NAVFAC DM-7.1, 1982) have proposed a minimum of 15-meter boring spacing for rigid frame structures. Recently, the U.S. Army Corps of Engineers (2001) suggested one boring per 230 square meters of ground floor for rigid frame structures. This is almost identical to the boring spacing suggested by the other authors in the past. Using this boring spacing formula, a target boring number per unit area for a building area at a specific site can be obtained. A five-meter buffer zone surrounding a proposed building plan is set. It is a virtual area and is not considered for a target boring number per unit area. Borings performed by students within this virtual area, however, are counted as effective to estimate a student's performance in boring numbers per unit area. Hence, the partial score of the boring number per unit area is estimated as the ratio of the boring number per unit area performed by the student to the target boring number per unit area.

Sampling depth

Sowers and Sowers (1970) showed approximate correlations of the minimum sampling depth with story numbers for rigid-frame structures as follows:

- For light steel or narrow concrete buildings,

$$D_b = 3 \cdot S^{0.7} \qquad (7.4.1)$$

where

D_b : depth of boring (meter)

S : number of stories

- For heavy steel or wide concrete buildings,

$$D_b = 6 \cdot S^{0.7} \qquad (7.4.2)$$

The partial score of the sampling depth is estimated as the ratio of the sampling depth performed by the student to the least sampling depth estimated via the above correlations. When the partial score exceeds 100 points in calculation, it is adjusted to 100 points.

Number of soil layers

Corresponding to a total soil layer depth defined by the student for the evaluation of his or her site investigation performance, a target soil layer number is calculated on the basis of the soil stratigraphy specified by the instructor. The total soil layer depth should be at least larger than the minimum sampling depth obtained via the correlations of Sowers and Sowers (1970) introduced above. The partial score of the soil layer number is estimated as the identity of the soil layer number defined by the student with the target soil layer number. When the soil layer number defined by the student is equal to the target soil layer number, the partial score is 100. Otherwise, it is zero. For example, as shown in Figure 7.14, the student's soil layer number is 2. This is identical to the target soil layer number within the total soil layer depth defined by the student. Hence, the partial score (P.S.) of the soil layer number is 100.

Soil type

The identity of the soil types defined by the student with the target soil types specified by the instructor is assessed up to the total soil layer depth defined by the student. The partial score of the soil type is estimated as the ratio of the identical depth of the soil types defined by the student with the target soil types to the total soil layer depth defined by the student. For example, as shown in Figure 7.14, the soil type of the first soil layer defined by the student is identical with the first target soil type of 6 m in thickness. On the other hand, the soil type of the second soil layer defined by the student is identical with the second target soil type of 10 m in thickness. Therefore, the partial score of the soil type is estimated as:

$$\text{P.S.} = \frac{\text{Total identical depth}}{\text{Total depth defined by student}} \times 100 = \frac{16\ \boldsymbol{m}}{17\ \boldsymbol{m}} \times 100 = 94.1$$

Thickness of soil layer

Each layer thickness defined by the student is compared with the target soil layer thickness specified by the instructor in a range of the total soil layer depth defined by the student. An error term, namely allowance, is applied to the target soil layer thickness in order to obtain an allowable range of each target soil layer thickness. When each layer thickness defined by the student is within the allowance of the target soil layer thickness, the partial score of the soil layer thickness is 100. Otherwise, it is zero. For example, Figure 7.14 shows a simple example of stratigraphy. Given that the allowance of the soil layer thickness is 10%, the student's first soil layer thickness (7 m) is outside the allowable range (5.4 m - 6.6 m) of the first target soil layer thickness. On the other hand,

the student's second soil layer thickness (10 m) satisfies the allowable range (9.9 m - 12.1 m) of the second target soil layer thickness. Hence, the partial score (P.S.) of the soil layer thickness is estimated as:

$$\text{P.S.} = \frac{\text{Total layer number within the allowance of target layer thickness}}{\text{Total soil layer number}} \times 100$$

$$= \frac{1}{2} \times 100 = 50.0$$

Ground water table

The ground water table is also estimated as an independent item because this is an important parameter used to calculate effective stresses in the soil profile. When the ground water table defined by the student is within the allowance of the target ground water table specified by the instructor, the partial score of the ground water table is 100. Otherwise, it is zero.

Soil parameters of each soil layer

Soil parameters defined by the student are assessed up to the total soil layer depth defined by the student. An allowance is applied to each target soil parameter in order to obtain an allowable range of each target soil parameter. The identical depth of each soil parameter is accumulatively calculated as long as the soil parameter satisfies the allowance of the target soil parameter. The partial score of each soil parameter is estimated as the ratio of the total identical depth of each soil parameter defined by the student with each target soil parameter to the total soil layer depth specified by the student. For example, as shown in Figure 7.14, given that the allowance of each soil

parameter is 10%, the undrained shear strength (24 kPa) of the first soil layer defined by the student is not within the allowable range (27 kPa - 33 kPa) of the target undrained shear strength of the first soil layer. Hence, the partial score of the undrained shear strength is zero. On the other hand, the effective friction angle of the second soil layer defined by the student is within the allowance (31.5° - 38.5°) of the target effective friction angle of the second soil layer. The partial score (P.S.) of the effective friction angle is calculated as:

$$\text{P.S.} = \frac{\text{Total identical depth}}{\text{Total depth defined by student}} \times 100 = \frac{10\ \boldsymbol{m}}{11\ \boldsymbol{m}} \times 100 = 90.9$$

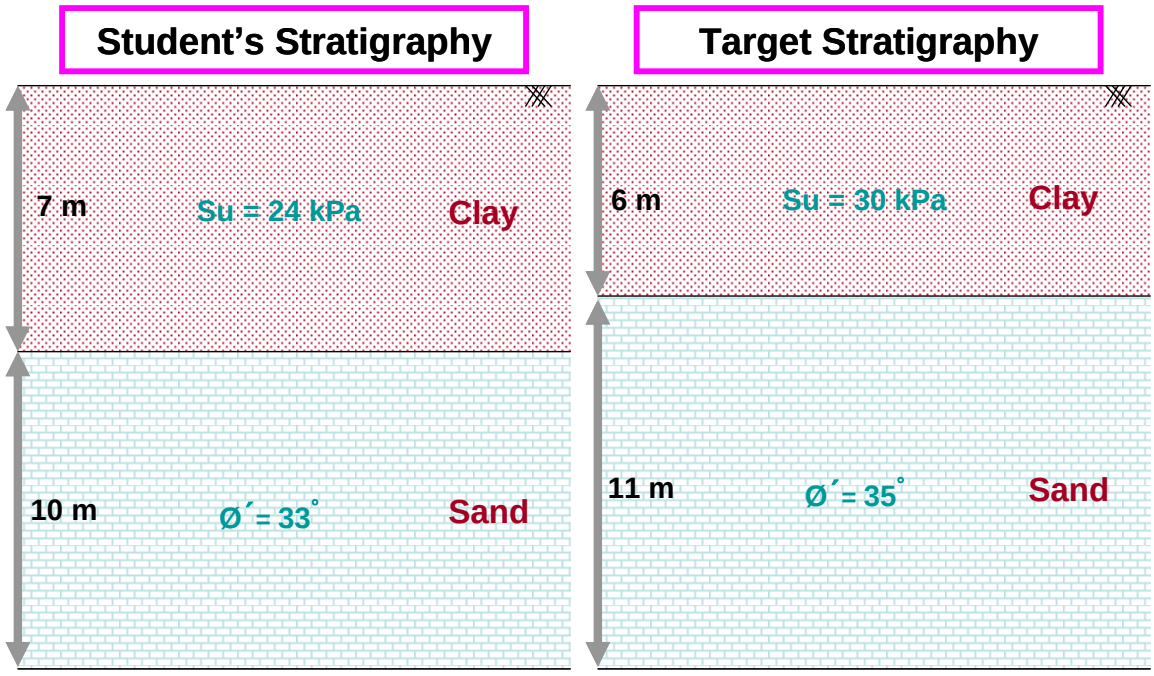

Figure 7.14 Simple example of student's stratigraphy and target stratigraphy

7.4.6. Assessment techniques

The evaluation of the effectiveness of the proposed site investigation simulation program is divided into two parts as follows: (1) a student evaluation of the prototype software by comparing students' knowledge and skills in site investigation with and without using the prototype software; and (2) a survey completed by students who have used prototype software. This evaluation suggested the constructive direction for the proposed site investigation simulation program that results in more effective site investigation learning.

7.4.6.1. Student evaluation for the site investigation simulation program

The effectiveness of the proposed site investigation simulation program as an educational tool was evaluated in the Introduction to Geotechnical Engineering (CEE 4405) class at the Georgia Institute of Technology during the Summer 2008 semester. CEE 4405 is an elective course that is open to all civil majors and is taken by approximately two-thirds of all undergraduate CEE students. The CEE 4405 class was designed for seniors in civil engineering. This course explains the importance of geotechnical engineering to civil engineering and introduced principles and techniques for estimating engineering properties of soil through the theory of soil mechanics and a variety of laboratory and in-situ tests. All students registered for CEE 4405 had to register for lab section A or B during registration period; students have chosen either session A or B that they wanted to take. The first group (Group A) consisted of 22 undergraduate students and the second group (Group B) was composed of 20 undergraduate students. The class instructor confirmed that nobody had previously

enrolled in the course and was repeating it due to a failing grade. The class instructor additionally explained that undergraduate students had already learned the fundamental concepts of site investigation by reading the required material from the class syllabus and from the class instructor's discussion of the required reading prior to running the site investigation simulation program.

The first group seems slightly lower in grade performance than the second group; according to the average GPAs of each group estimated as of the end of the 2008 spring semester, just before the students enrolled in CEE 4405, the first group's average GPA (2.88 of 4.0) was a little lower than the second's average GPA (3.02 of 4.0); in the case of two lab reports (lab report 1 and lab report 2) distributed prior to testing the simulation software, the first group had averages lower approximately two points than the second group as shown in Table 7.4 below; in the case of all lab reports, homeworks, and exams, the first group consistently showed lower averages than the second group by somewhere between 0.3 and 7.5 points with a 95% confidence interval.

Three different methods (assignment, quiz, and survey) were employed. The first group was allowed to run the simulation program installed on each computer in a computer lab along with a brief presentation on the usage of the simulation program.

Table 7.4 Results of a variety of tests

Test Type	Group Type	Average Score	Standard Deviation
Lab report 1	First group	84.85	18.92
	Second group	86.34	19.77
Lab report 2	First group	87.75	19.65
	Second group	90.57	8.73
Lab report 3	First group	91.75	6.76
	Second group	84.82	23.39
Lab report 4	First group	77.90	26.32
	Second group	85.64	18.44
Homework 1	First group	86.26	23.22
	Second group	93.47	5.72
Homework 2	First group	78.50	21.39
	Second group	84.04	13.26
Homework 3	First group	73.50	33.34
	Second group	82.95	23.88
Midterm	First group	86.95	8.81
	Second group	84.00	14.29
Final exam	First group	77.63	14.94
	Second group	80.86	13.75

Simultaneously, an assignment and an instruction for the simulation program were provided. The assignment required students in the first group to solve a site investigation problem using the simulation program before taking a quiz. The detailed assignment is presented in Appendix G. The object of this assignment was to lead students to logically plan and develop their own site investigation and characterization for a given project. After implementing the assignment, students were asked to take a quiz with 26 questions to measure as illustrated in Table 7.5:

- basic knowledge of soil properties obtained from in-situ tests and laboratory tests performed for the purpose of site investigation;

- understanding of basic characteristics of each soil type necessary to perform site investigation;
- basic ability of making initial boring plan of site investigation via determining boring/sounding spacing and depth;
- basic ability of determining unsuitable site condition such as the water table to adversely affect construction using the results of in-situ tests.

The quiz questions are in detail presented in Appendix H. Before running the site investigation simulation program, the second group was tested using the same quiz taken by the first group. As a result, as shown in Table 7.6, for all evaluation types of quiz, the first group had higher scores than the second group; the first group seems to overall better understand the basic theoretical principles and the concepts of geotechnical site investigation than the second group. The grades of the first group, in which students had been allowed to run the site investigation simulation program before taking the quiz, were compared with those of the second group, in which students had been allowed to run the site investigation simulation program only after taking the quiz. That is, to measure the overall effect of the simulation program on the changes in the students' knowledge and skills, an average quiz score of the first group (who had extensively used the site investigation simulation program before taking the quiz) was compared with that of the second group, which was taught the theoretical basics of site investigation in class without running the site investigation simulation program.

Table 7.5 Evaluation types of question and quiz questions

■ Basic knowledge of soil properties obtained from in-situ tests and laboratory tests performed for the purpose of site investigation - Select an in-situ test necessary to obtain “N value”. - Select an in-situ test necessary to obtain “cone resistance”. - Select an in-situ test necessary to obtain “sleeve friction”. - Select an in-situ test necessary to obtain “pore water pressure”. - Select an in-situ test necessary to obtain “lift-off pressure”. - Select an in-situ test necessary to obtain “expansion pressure”. - Select a laboratory test necessary to obtain “maximum dry density”. - Select a laboratory test necessary to obtain “optimum moisture content”. - Select a laboratory test necessary to obtain “coefficient of consolidation”. - Select a laboratory test necessary to obtain “compression index”. - Select a laboratory test necessary to obtain “plastic limit”. - Select a laboratory test necessary to obtain “permeability”. - Select a laboratory test necessary to obtain “shear wave velocity”. - Select a laboratory test necessary to obtain “undrained shear strength”. - Select a laboratory test necessary to obtain “effective friction angle”. - Estimate the minimum sampling interval for SPT. - Estimate the minimum sampling interval for boring - Specify the soil property of CPT directly related to water table.
■ Basic ability of making initial boring plan of site investigation via determining boring/sounding spacing and depth - Specify boring locations based U.S. Army Corps of Engineers (2001)’s method. - Calculate the minimum boring depth based on Sowers and Sowers (1970).
■ Basic ability of determining unsuitable site condition such as the water table to adversely affect construction using the results of in-situ tests - Estimate ground water table. - Calculate hydrostatic water pressure.
■ Understanding of basic characteristics of each soil type necessary to perform site investigation - Specify the general value of plastic limit of sand. - Specify the soil type to have the largest value of liquid limit. - Specify the soil type(s) to show effective friction angle. - Specify the soil type(s) to show undrained shear strength.

Table 7.6 Result of quiz taken by students of each group

Evaluation Type	Group Type	Full Score	Average Score	Standard Deviation of Score
Basic knowledge of soil properties obtained from in-situ tests and laboratory tests performed for the purpose of site investigation	First group	18.0	15.45	1.47
	Second group		7.80	2.38
Basic ability of making initial boring plan of site investigation via determining boring/sounding spacing and depth	First group	2.0	1.77	0.43
	Second group		1.15	0.73
Basic ability of determining unsuitable site condition such as the water table to adversely affect construction using the results of in-situ tests	First group	2.0	1.18	0.66
	Second group		0.85	0.67
Understanding of basic characteristics of each soil type necessary to perform site investigation	First group	4.0	2.59	1.30
	Second group		2.10	1.21

The paired *t* test was employed as a statistical tool for this purpose. The comparison brought about the following results:

Estimated quiz means of the first group and the second group:

$$\bar{Y}_{\text{first}} = 21.0 \; ; \; \bar{Y}_{\text{second}} = 11.9$$

Student numbers of the first group and of the second group:

$$n_{\text{first}} = 22 \qquad n_{\text{second}} = 20$$

Error sum of squares of two groups:

$$\boldsymbol{SSE} = 355.3$$

Mean square error of two groups:

$$\boldsymbol{MSE} = \frac{\boldsymbol{SSE}}{\boldsymbol{n}_{\text{first}} + \boldsymbol{n}_{\text{second}} - \boldsymbol{r}} = \frac{355.3}{22 + 20 - 2} = 8.8825$$

Point estimator of difference between means of two groups:

$$\hat{\boldsymbol{D}} = \overline{\boldsymbol{Y}}_{\text{first}} - \overline{\boldsymbol{Y}}_{\text{second}} = -9.1$$

Estimated variance of point estimator of difference between means of two groups:

$$\boldsymbol{S}^2\left\{\hat{\boldsymbol{D}}\right\} = \boldsymbol{MSE}\left(\frac{1}{\boldsymbol{n}_{\text{first}}} + \frac{1}{\boldsymbol{n}_{\text{second}}}\right) = 0.8479$$

95 percent confidence coefficient:

$$\boldsymbol{t}(0.975;40) = 2.021$$

95 percent confidence interval of difference between means of two groups:

$$\hat{\boldsymbol{D}} - \boldsymbol{t}(0.975;40) \times \boldsymbol{S}\left\{\hat{\boldsymbol{D}}\right\} \le \boldsymbol{\mu}_{\text{second}} - \boldsymbol{\mu}_{\text{first}} \le \hat{\boldsymbol{D}} + \boldsymbol{t}(0.975;40) \times \boldsymbol{S}\left\{\hat{\boldsymbol{D}}\right\}$$

$$-10.96 \le \boldsymbol{\mu}_{\text{second}} - \boldsymbol{\mu}_{\text{first}} \le -7.24$$

Therefore, with 95% confidence interval, the quiz mean of the second group is lower than that of the first group by somewhere between 7.24 and 10.96.

Considering the previous fact that the first group was slightly lower in prior academic performance than the second group, the above results indicate that the simulation program overall improved students' level of understanding regarding many aspects of the site investigation process in geotechnical engineering.

7.4.6.2. Survey for the site investigation simulation program

After all students in the two groups had run the site investigation simulation program, a survey was carried out to obtain their opinions, feelings, and suggestions about the overall function of the site investigation simulation program, as presented in Appendix I. The students' ratings of each question in the survey form were summarized in percentages in Figures 7.15 -7.23, as shown below and on following pages. The 42 students' responses to the questions ranged from 59 to 96 percent positively. They have given high ratings for the functional and logical aspects of the site investigation simulation program such as a graphical user interface and the logical performance of site investigation. In addition, approximately 90% of the students have recommended the simulation program to be used for undergraduate students enrolled in an introductory geotechnical engineering course. As shown in Figure 7.23, for question 9, when evaluating the overall quality of the software, students responded 95% positively.

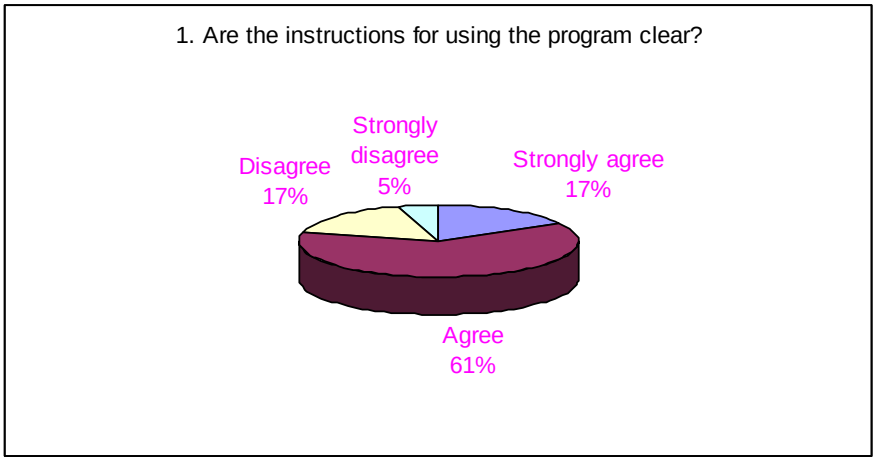

Figure 7.15 Students' rating for question #1, "Are the instructions for using the program clear?"

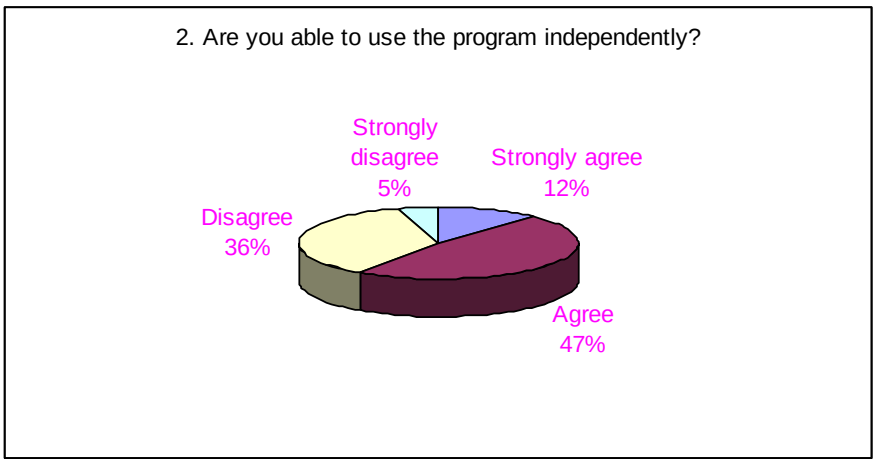

Figure 7.16 Students' rating for question #2, "Are you able to use the program independently?"

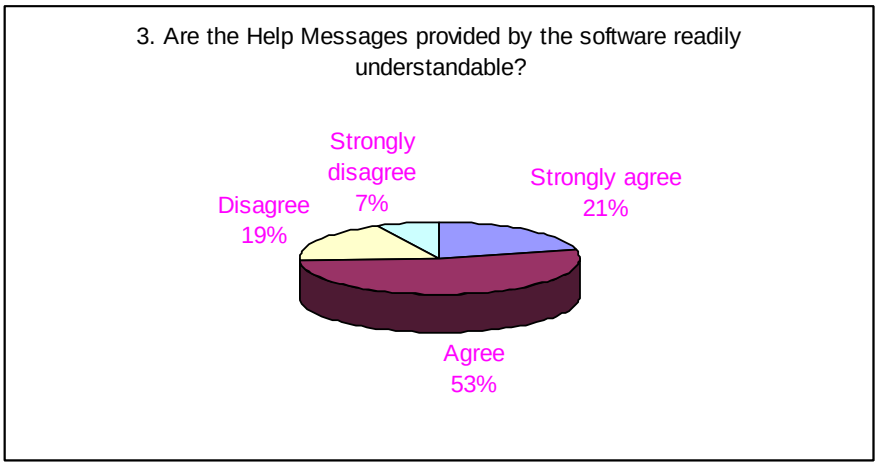

Figure 7.17 Students' rating for question #3, "Are the Help Messages provided by the software readily understandable?"

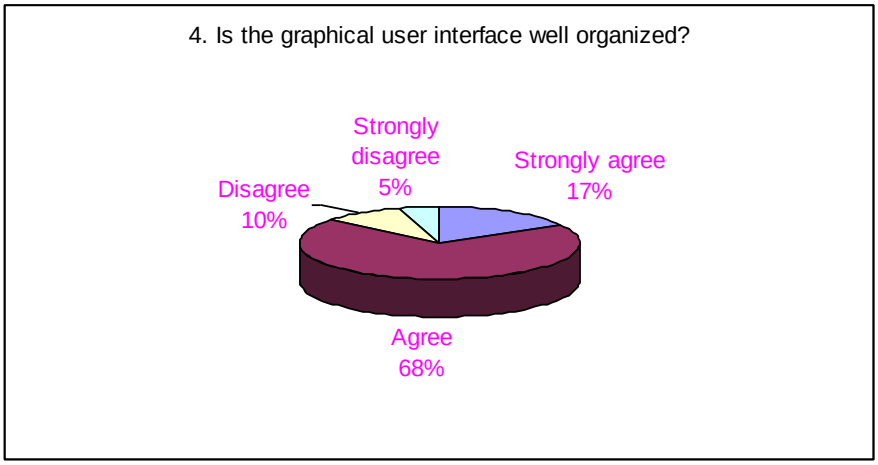

Figure 7.18 Students' rating for question #4, "Is the graphical user interface well organized?"

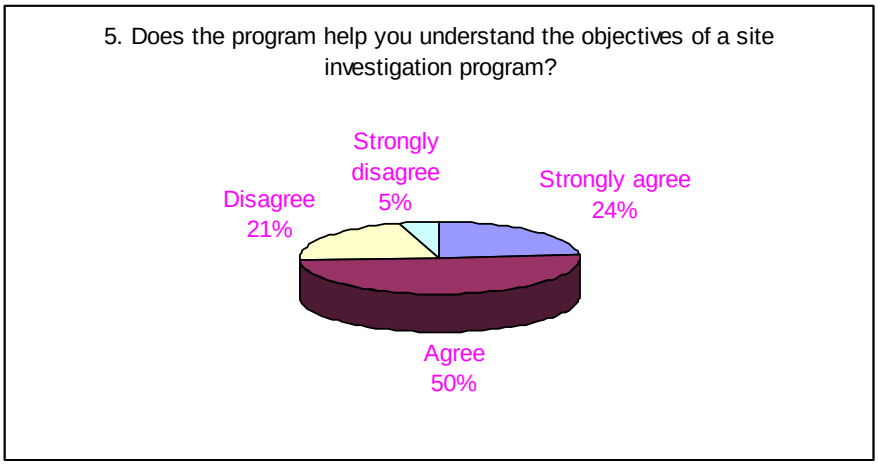

Figure 7.19 Students' rating for question #5, "Does the program help you understand the objectives of a site investigation program?"

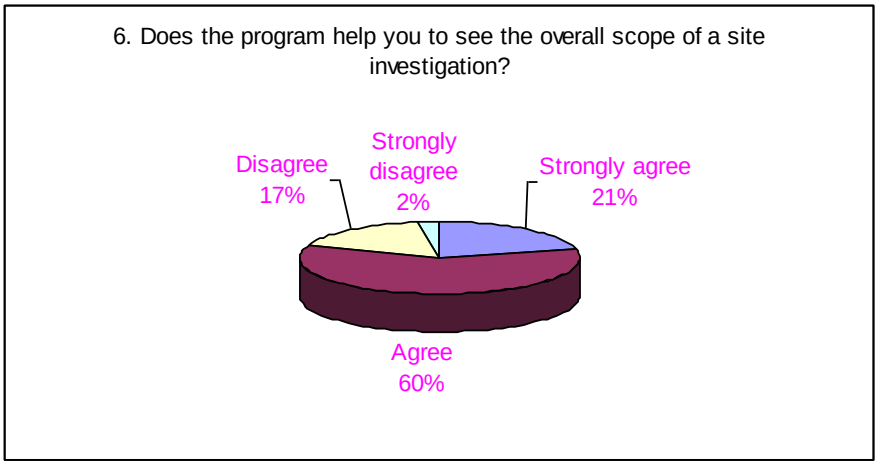

Figure 7.20 Students' rating for question #6, "Does the program help you to see the overall scope of a site investigation?"

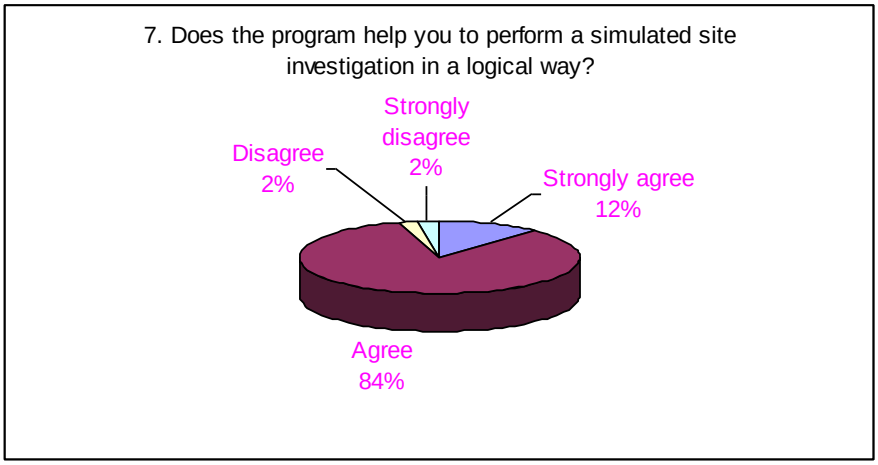

Figure 7.21 Students' rating for question #7, "Does the program help you to perform a simulated site investigation in a logical way?"

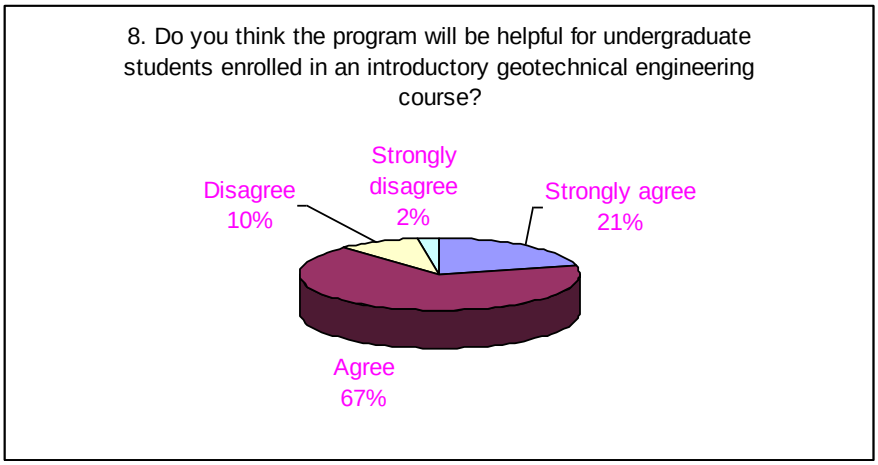

Figure 7.22 Students' rating for question #8, "Do you think the program will be helpful for undergraduate students enrolled in an introductory geotechnical engineering course?"

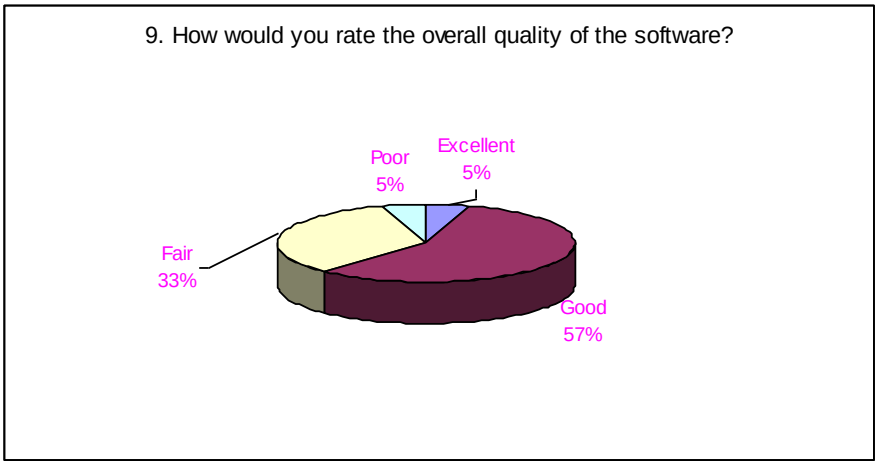

Figure 7.23 Students' rating for question #9, "How would you rate the overall quality of the software?"

Furthermore, the students have provided additional comments and suggestions for the improvement of the site investigation simulation program. Students' additional comments and suggestions have been associated with user-friendly issues. These have been so constructive and complementary that some functions of the simulation program have been changed. Table 7.7 shows corresponding solutions to the comments and suggestions.

Table 7.7 Corresponding solutions to comments and suggestions

Comments and Suggestions	Solutions
Use in the end of semester	Recommending use in the end of semester
Problem with saving data files due to user's permission	Saving data files in "Temp" folder created in C drive
Need of modaless window	Adding function of modaless window

7.4.7. Contributions

It is meaningful to note that the developed site investigation simulation program is not a substitute for traditional educational approaches in geotechnical engineering, but, rather, complements and uses the traditional educational approaches. The simulation contributes to students becoming well-trained engineers with sound education in both theory and practice in geotechnical engineering by means of promoting the self-directed learning, engineering intuition, and skills of decision-making and resource management as employed in the simulation program.

This new site investigation simulation program may be more effective than previous developments of simulation applications for education in geotechnical engineering which placed stress on conducting single laboratory tests. Conversely, emphasis was placed on the development of a site investigation simulation program with a wide variety of tests to perform a comprehensive site investigation program. In addition, the introduction of the site investigation simulation program will help students have a good bridge to their potential future work in the geotechnical industry. Therefore, by using this application that reflects the entire site investigation process, the students can be trained more quickly and successfully in the industry.

7.5. Conclusions

Simulation environments are a useful tool to complement the traditional educational approaches for site investigation and help students connect basic theoretical principles and concepts with their use in practice. The primary objective of the geotechnical site investigation simulation program is to allow students to perform their own site investigation programs and thus gain valuable experience in a critical component of geotechnical engineering projects.

The effectiveness of the proposed site investigation simulation program as an educational tool was evaluated in the Introduction to Geotechnical Engineering (CEE 4405) class at the Georgia Institute of Technology during the Summer 2008 semester.

When comparing the scores of students who used the simulation program with those that did not, the results strongly supported the conclusion that students who used

the simulation did significantly better than those who did not. When employing the paired *t* test, with a 95% confidence interval, the quiz mean of the simulation group is higher than that of the non-simulation group by somewhere between 7.24 and 10.96 points. This means that the simulation program overall improved students' understanding level of entire aspects of site investigation in geotechnical engineering.

In addition to being an effective learning tool, the proposed simulation program was also educationally popular. In the survey carried out to obtain students' opinions, feelings, and suggestions about overall function of the site investigation simulation program, the responses ranged from 59% to 96% positive to each question in the survey form. This indicates that the simulation is likely to be utilized by the students in geotechnical engineering programs. The above evidences support the fact that the proposed simulation program can promote the self-directed learning, engineering intuition, and skills of decision-making and resource management, thereby leading students to become well-trained engineers with sound education in both theory and practice in geotechnical engineering.

The proposed simulation program was also cost-efficient and allowed a greater range of student access in a simulation than in a real on-site visit, where issues of cost, training, and risk of injury limit the students' accessibility to on-site tools. Thus, the simulation program, if properly implemented, may result in increased educational cost-effectiveness as well as in increased student learning.

CHAPTER 8

SUMMARY AND CONCLUSIONS

8.1. Introduction

The main purpose of this dissertation is to improve site investigation in geotechnical engineering via the evaluation and development of statistical approaches for characterizing the spatial variability of soil properties and the development of site investigation simulation software for educational use. The essential points presented in each chapter are described in order below.

Chapter 3 estimated the statistical characteristics of the spatial variability of soil properties with respect to soil formation processes based on the results of common in situ soil tests at three representative areas: the Upper Mississippi Embayment, the Atlantic Coastal Plain Province, and the Piedmont Province. The statistical significance for COV, zero-correlation distance, and scale of fluctuation of soil properties of each soil type in these areas was investigated through hypothesis testing using the two-sample *t* test.

Although not all the COV values of soil properties of each soil type layer were statistically significant, the process of soil formation is to some extent associated with the level of variation of soil properties; in the Memphis subregion, which is mainly formed by sedimentation, the more granular a soil layer becomes, the lower its average COV

value; in the Piedmont Province under the process of the chemical weathering, the more granular a soil layer becomes, the higher its average COV value.

According to the statistical analyses of zero-correlation distance and scale of fluctuation of soil properties, in the Upper Mississippi Embayment and the Coastal Plain Province, granular soil layers have higher levels of correlation of soil properties than do fine soil layers. In the Piedmont Province, fine soil layers have higher levels of correlation of soil properties than do granular soil layers.

The statistical characteristics of soil properties at a potential site in these or similar areas can be approximated via the estimates of the statistical structures of soil properties obtained from the above three areas, so that the estimates offer valuable information for simulation of random fields of soil properties at undersampled or unsampled locations in these areas or similar areas. Obviously, while these three regions may not be sufficient to obtain a comprehensive database, they provide a diversity of physical and statistical characteristics of soil properties due to widely dissimilar soil formation processes.

Chapter 4 employed the aliasing concept to estimate the maximum statistically allowable sampling interval of data obtained from the three zones: it was suggested that this concept be used to derive equivalent wavelengths. A modified model based on extensive statistical estimates of soil properties was suggested for the interpretation of the spatial variability of a soil property in geotechnical engineering; this modified model consists of three elements: the trend, an equivalent wavelength, and a random error. The maximum statistically allowable sampling intervals were estimated from equivalent

wavelengths by use of the aliasing concept. The Upper Mississippi Embayment and the Coastal Plain Province have relatively higher maximum statistically allowable sampling intervals in granular soil layers than in fine soil layers. On the other hand, in the Piedmont Province, fine soil layers have larger maximum statistically allowable sampling intervals than do granular soil layers. Once a maximum sampling interval from the aliasing concept is determined for a specific soil property, then the minimum statistically required number of soundings/borings is calculated to perform an economical site investigation at a specific site.

In Chapter 5, soil strengths, COV values of soil properties, and correlation coefficient functions of soil properties within the same range of sand layers and at the same points at the Embayment Seismic Excitation Experiment project area and the Jebba hydroelectric project area were analyzed in order to obtain the effect of blasting on correlation structures of soil properties. The average values of cone resistances after blasting increased when compared with those of cone resistances measured before blasting. Compared with the results of a single explosion that used a higher amount of explosive charge in the Embayment Seismic Excitation Experiment project area, several subsequent explosions with several small charged holes cumulatively improved the soil strength over the short term.

The analysis results of the change in the COV value and the zero-correlation distance of soil properties after blasting and vibration support the conclusion that dynamic loadings such as vibration and blasting decrease to some extent the deviation and correlation levels of soil properties. That is, dynamic loadings make to some extent

original soil structures more randomized. Thus, it is necessary to estimate consistent changes in the relative deviation and correlation of soil properties caused by blasting using more data sets. It is obvious from the above evidence that dynamic loadings such as blastings and earthquakes break and rearrange the steady-state soil structures, thereby resulting in changes in the statistical characteristics of soil properties in geotechnical engineering. Hence, the history of seismic activities at an area of interest should be considered when estimating its correlation structures because correlation structures are not invariable, but are influenced by past seismic activities.

Chapter 6 presented a simple technique for generating more accurate and more correlated multi-dimensional simulations of soil properties that are consistent with the observed or proposed physical variations and statistical structures of soil properties. The cosine exponential model was employed to best represent the features of the cross-correlation coefficient function with positive and negative values for multi-dimensional simulation.

One of the shortcomings in this simulation technique is the significant dependence on the accuracy of the estimation of correlations between data. The running time of the algorithm of the proposed method increased when the data number of divided individual sections increased. The other drawback of this technique is that it is more applicable to large geotechnical projects with a considerable database. However, taking into consideration the results of the cross-correlation function, the proposed method improved the accuracy in simulation for undersampled areas.

In Chapter 7, for the stochastic simulation of site investigation and characterization, a geotechnical site investigation simulation program with a wide variety of in situ and laboratory tests was developed to allow students to plan and perform their own comprehensive site investigation programs. Spatial variability in soil properties was modeled via correlated random fields, interpolation, and a decomposition method to yield realistic geotechnical data.

The effectiveness of the proposed site investigation simulation program as an educational tool was evaluated in the Introduction to Geotechnical Engineering (CEE 4405) class at Georgia Institute of Technology with 42 students during the Summer 2008 semester. The undergraduate students in the CEE 4405 class were separated into two groups; an average quiz score of the first group that extensively used the site investigation simulation program was compared with that of the second group without running the site investigation simulation program. As a result, the quiz mean of the first group was higher than that of the second group by somewhere between 7 and 11 points with a 95% confidence interval. This means that the simulation program overall improved students' understanding level of entire aspects of site investigation in geotechnical engineering. In addition, the students reported from 59% to 96% positive responses to each question in the survey form to obtain students' opinions, feelings, and suggestions about the overall functions of the site investigation simulation program. Therefore, the proposed site investigation simulation program can promote self-directed learning, engineering intuition, and skills in decision-making and resource management, thereby leading students to become well-trained engineers with sound education in both theory and practice in geotechnical engineering.

8.2. Future directions

The statistical characteristics of soil properties were estimated based on the results of common in situ soil tests at three different geographical areas in the Eastern United States along with the process of soil formation. It was verified that the process of soil formation has an influence on the statistical characteristics of soil properties. However, the effect of the process of soil formation on the statistical characteristics of soil properties should be further investigated using a valid number of raw data points obtained from other areas with a variety of soil formation processes.

From the statistical estimates of soil properties, it has been observed that most soil properties with stationarity in geotechnical engineering can be represented as their own equivalent wavelengths obtained from the correlation coefficient function. In this study, a modified model for soil property was suggested to apply periodicity to analysis of spatial variability of soil properties: the modified model estimates equivalent wavelengths from soil properties. The modified model contributed to the estimation of the maximum statistically allowable sampling intervals and minimum statistically required number of borings/soundings. To develop new simulation methods, further studies based on this modified model of soil properties should be performed.

In the light of the design of geotechnical structures, it is only recently that stochastic approaches have been employed to supplement deterministic approaches. However, since stochastic approaches provide additional information that results in the reduction of risk and higher reliability in geotechnical practice, stochastic approaches in geotechnical practice will be desired to obtain the best and most efficient results. Accordingly, more studies and efforts from a statistical aspect to enhance the

performance of reliability analysis in geotechnical practice as well as to supplement traditional deterministic methods should be carried out.

Finally, it was noted that simulation is a potential technology to improve students' understanding in learning circumstance. The geotechnical site investigation simulation program suggested in this study was developed as a computer-based simulation program to attain the primary objective, which is to allow students to perform their own comprehensive site investigation programs. For a more advanced alternative, the development of web-based site investigation simulation is recommended in order for any learners to perform the simulation as well as to interact with an operator in real time anywhere with a permit.

REFERENCES

AbouRizk, S. M. and Sawhney, A. (1994). "Simulation and Gaming in Construction Engineering Education." *ASEE/C2E2/C2EI Conference*, Edmonton, Alberta.

Alonzo, E. E. and Krizek, R. J. (1975). "Stochastic Formulation of Soil Properties." *Proceedings of the Second Conference on Application of Probability and Statistics to Soil and Structural Engineering*, Aachen, Germany, Vol. 2, 99-32.

Alyamani, M. S., and Sen, Z. (1993). "Determination of Hydraulic Conductivity from Grain-Size Distribution Curves." *Ground Water*, Vol. 31, 551-555.

Andris, J. F. (1996). "The Relationship of Indices of Student Navigational Patterns in a Hypermedia Geology Lab Simulation to Two Measures of Learning Style." *Journal of Educational Multimedia and Hypermedia*, Vol. 5, No. 3, 303-315.

Arduino, P., Op den Bosch, A., and Macari, E. J. (1997). "Geotechnical Triaxial Soil Testing within Virtual Environment." *Journal of Computing in Civil Engineering*, ASCE, Vo. 11, No. 1, 44-47.

Asaoka, A. and A-Grivas, D. (1982). "Spatial Variability of the Undrained Strength of Clays." *Journal of Geotechnical Engineering*, ASCE, Vol. 108, No. GT5, 743-756.

Azzouz, A. S., Krizek, R. J., and Corotis, R. B. (1976). "Regression Analysis of Soil Compressibility." *Soils & Foundations*, Vol. 16, No. 2, 19-29.

Baecher, G. B. (1982). "Simplified Geotechnical Data Analysis." *Reliability theory and its applications in structural and soil engineering*, P. Thoft-Christensen, Ed. D. Reidal Publishing, Dordrecht, The Netherlands.

Baecher, G. B. (1986). "Geotechnical Error Analysis." *Transportation Research Record* 1105, 23-31.

Baecher, G. B. (1987). *Statistical Analysis of Geotechnical Data*, Final Report No. GL-87-1, USACE Waterways Experiment Station, Wicksburg, MI.

Baecher, G. B. and Christian, J. T. (2003). *Reliability and Statistics in Geotechnical Engineering*, John Wiley and Sons Ltd, Chichester, England.

Barab, S. A., Hay, K. E., Barnett, M., and Squire, K. (2001). "Constructing Virtual Worlds: Tracing the Historical Development of Learner Practices." *Cognition and Instruction*, Vol. 19, No. 1, 47-94.

Bendat, J. S. and Piersol, A. G. (1986). *Random Data: Analysis and Measurement Procedures*, John Wiley and Sons, New York.

Benson, C. (1991). "Predicting Excursions Beyond Regulatory Thresholds of Hydraulic Conductivity Using Quality Control Measurements." *Proceedings of the 1st Canadian Conference on Environmental Geotechnics*, Canadian Geotechnical Society, Montreal, Quebec, 447-454.

Bertz, M. D. (1998). *Situated Learning Methodologies and Assessment in Civil Engineering Structures Education,* Ph D. Thesis, Georgia Institute of Technology, Atlanta, GA.

Bjerg, P. L., Hinsby, K. Christensen, T. H., and Gravesen, P. (1992). "Spatial Variability of Hydraulic Conductivity of an Unconfined Sandy Aquifer Determined by a Mini Slug Test." *Journal of Hydrology*, Vol. 136, 107-122.

Bjerrum, L. and Simons, N. E. (1960). "Comparison of Shear Strength Characteristics of Normally Consolidated Clays." *Proceedings of the ASCE Research Conference on the Shear Strength of Cohesive Soils*, Boulder, CO, 711-726.

Blight, G. E. (1997). *Mechanics of Residual Soils*, Balkema: Rotterdam.

Blotz, L., Benson, C., and Boutwell, G. (1998). "Estimating Optimum Water Content and Maximum Dry Unit Weight for Compacted Clays." *Journal of Geotechnical and Geoenvironmental Engineering*, ASCE, Vol. 124, No. 9, 907-912.

Bolton M. D. (1986). "The Strength and Dilatancy of Sands." *Géotechnique*, Vol. 36, No. 1, 65–78.

Bouchlaghem, N., Sher, W., and Beacham, N. (2000). "Computer Imagery and Visualization in Civil Engineering Education." *Journal of Computing in Civil Engineering*, Vol. 14, No. 2, 134–140.

Bourne, J. R. and Brodersen, A. J. (1995). "The Impact of Computer and Communications Technology on Engineering Education." *The Influence of Technology on Engineering Education*, CRC Press, Boca Raton, FL, 178-201.

Bowles, J. E. (1996). *Foundation Analysis and Design*, McGraw-Hill.

Box, G. E. P. and Jenkins, G. M. (1970). *Time Series Analysis: Forecastinq and Control*, San Francisco: Holden Day.

Brockwell, P. J. and Davis, R. A. (1987). *Time Series: Theory and Methods*, Springer-Verlang.

Brown, J. S., Collins, A., and Duguid, P. (1989). "Situated Cognition and the Culture of Learning." *Education Resources*, Vol. 18, No. 1, 32–42.

Budhu, M. (2000). *Soil Mechanics and Foundations*, John Wiley & Sons, NY.

Camara, A. S., Neves, J. N., Muchaxo, J., Fernandes, J. P., Sousa, I., Nobre, E., Costa, M., Mil-Homens, J., Webster, E. M., and Archer, G. C. (2001). "Exploration of Structural Stability: A Computer Implementation." *Computer Applications in Engineering Education*, Vol. 9, No. 2, 122-135.

Campanella, R.G. & Robertson, P.K. (1991). "Use and Interpretation of a Research Dilatometer." *Canadian Geotechnical Journal*, Vol. 28, 113-126.

Carman, P. C. (1956). *Flow of Gases through Porous Media*, Butterworths Scientific Publications, London.

Carter, M. and Symons, M. V. (1989). *Site Investigations and Foundations Explained,* American Society of Civil Engineers, Reston, VA.

Charlie, W. A., Martin, J., Blouin, S. and Melzer, S. (1980). "Blast Induced Soil Liquefaction Phenomena and Evaluation." *International Symposium on Soils Under Cyclic and Transient Loading*, Swansea, UK, 533-542.

Chiasson, P., Lafleur, J., Soulie, M., and Law, K. T. (1995). "Characterizing Spatial Variability of a Clay by Geostatistics." *Canadian Geotechnical Journal*, Vol. 32, 1-10.

Christian, J. T. and Swinger, W. F. (1975). "Statistics of Liquefaction and SPT Results." *Journal of Geotechnical Engineering*, ASCE, Vol. 101, No. GT11, 1135-1150.

Collofello, J. S. (2000). "University/Industry Collaboration in Developing a Simulation Based Software Project Management Training Course In." *Proceedings of the*

Thirteenth Conference on Software Engineering Education and Training, IEEE Computer Society: Austin, TX, 161–168.

Das, B. M. (1997). *Principles of Geotechnical Engineering*, Prindle, Weber and Schmidt.

Davey-Wilson, I. E. G. (1991). "Geotechnical Laboratory Test Simulation Using AI Techniques." *Artificial Intelligence and Civil Engineering*, Civil-Comp Press, 119-124.

Davis, M. W. (1987). "Production of Conditional Simulations via the LU Triangular Decomposition of the Covariance Matrix." *Mathematical Geology*, Vol. 19, No. 2, 91-98.

DeGroot, D.J. and Baecher, G.B. (1993). "Estimating Autocovariance of In Situ Soil Properties." *Journal of Geotechnical Engineering*, ASCE, Vol. 119, No. 1, 147-166.

DeGroot, D. J. (1996). "Analyzing Spatial Variability of In Situ Soil Properties." *Uncertainty in the Geologic Environment: From Theory to Practice, Geotechnical Special Publication No. 58*, ASCE, Vol. 1, 210-238.

Dowding, C. H. and Hryciw, R. D. (1986). "A Labortory Study of Blast Densification of Saturated Sands." *Journal of Geotechnical Engineering*, ASCE, Vol. 112, No. 2, 187-199.

Dowling, C. (1997). "Simulations: New 'Worlds' for Learning?" *Journal of Educational Multimedia and Hypermedia*, Vol. 6, No. 3, 321-337.

Drappa, A. and Ludewig, J. (2000). "Simulation in Software Engineering Training." *Proceedings of the 22nd International Conference on Software Engineering*, ACM: Limerick, Ireland, 199–208.

Echeverry, D. (1996). "Multimedia-Based Instruction of Building Construction." *Proceedings of 3rd Congress on Computing in Civil Engineering*, ASCE, Reston, VA, 972–977.

El Shamy, U. (2007). "DEM-Based Computational Lab for Geotechnical Engineering Education." *Geotechnical Special Publication*, ASCE, Reston, VA, n 166.

Fenton, G.A. (1994). "Error Evaluation of Three Random Field Generators," *Journal of Engineering Mechanics,* ASCE, Vol.120, No. 12, 2478–2497.

Fenton, G. A. (1999). "Random Field Modeling of CPT Data." *Journal of Geotechnical and Geoenvironmental Engineering,* ASCE, Vol.125, No.6, 486-498.

Fu, T. T. (2003). "Applications of Computer Simulation in Mechanism Teaching." *Computer Applications in Engineering Education*, Vol. 11, 156-165.

Garcia, S. R. (1991). *Interrelationship Between the Initial Liftoff and Extended Pressure Readings of the Marchetti Flat Blade Dilatometer in Soils,* Master's degree thesis, Georgia Institute of Technology, Atlanta, GA

Gidigasu, D. D. (1976). *Laterite Soil Engineering,* Elsevier: Amsterdam.

Hadipriono, F. C., Larew, R. E., and Tsay, T. C. (1996). "Interactive and Immersive Training in a Virtual Environment for Construction Students." *Proceedings of the 1996 ASEE Annual Conference and Exposition,* Washington D. C.

Haldar, A. and Miller, F. (1984). "Statistical Evaluation of Cyclic Strength of Sand." *Journal of Geotechnical Engineering,* ASCE, Vol. 110, No. 12, 1785-1802.

Haldar A, Tang W. H. (1979). "Probabilistic Evaluation of Liquefaction Potential." *Journal of Geotechnical Engineering,* ASCE, Vol. 105, No. 2, 145-163.

Hall, C. R., Stiles, R. J., and Horwitz, C. D. (1998). "Virtual Reality for Training: Evaluating Knowledge Retention." *Proceedings of the 1998 IEEE Virtual Reality Annual International Symposium,* IEEE Computer Society, Atlanta, GA, 184-188.

Halpin, D. W., Jen, H., and Kim, J. W. (2003). "A Construction Process Simulation Web Service." *Proceedings of the 2003 Winter Simulation Conference,* 1503-1509.

Hamel, C. J. and Ryan-Jones, D. L. (1997). "Using Three-Dimensional Interactive Graphics to Teach Equipment Procedures." *Educational Technology Research and Development,* AECT, Vol. 45, No. 4, 77-87.

Hardin, B.O. (1978). "The Nature of Stress-Strain Behaviour for Soils." *Proceedings of Specialty Conference on Earthquake Engineering and Soil Dynamics,* ASCE, Pasadena, California, 3-90.

Hashash, Y.M.A., Wotring, D., Yao, J.I.-C., Lee, J.-S., and Fu, Q. (2002). Visual Framework for Development and use of Constitutive Models. *International Journal for Numerical and Analytical Methods in Geomechanics*, Vol. 26, 1493-1513.

Hatanaka, M. and Uchida, A. (1996). "Empirical Correlation Between Penetration Resistance and Effective Friction of Sandy Soil." *Soils & Foundations*, Japanese Geotechnical Society, Vol. 36, No. 4, 1-9.

Hazen, A. (1911). Discussion of "Dams on Sand Foundations." By A. C. Koenig, *Transactions*, ASCE, Vol. 73, 199-203.

Henning, G. A. and Higuchi, H. (1995). "Virtual Aerospace Engineering laboratory." *Proceedings of the 1995 ASEE Annual Conference and Exposition*, Anaheim, CA.

Henry, F. D. C. (1986). *The Design and Construction of Engineering Foundations*, J. W. Arrowsmith Ltd.

Hicks, M. A. (2005). "Risk and Variability in Geotechnical Engineering." *Geotechnique*, Vol. 55, No. 1. 1-2.

Hilldale-Cunningham, C. (1971). *A Probabilistic Approach to Estimating Differential Settlement*, M.S. Thesis, Massachusetts Institute of Technology, Cambridge, MA.

Hoeg, K. and Tang, W. (1976). "Probabilisic Consolidations in the Foundation Engineering of Off shore Structures." *Proceedings of the 2nd ICOSSAR*, Aachen, Germany, 29.

Holtz, R. D. and Kovacs, W. D. (1981). *An Introduction to Geotechnical Engineering*, Prentice-Hall, Inc., Englewood Cliffs, N.J.

Hwang, H., Chien, M. C., and Lin, Y. W., (1999). "Investigation of Soil Conditions in Memphis, Tennessee." USGS Award No. 1434-HQ-98-GR-00002.

Jaksa, M. B. (1995). *The Influence of Spatial Variability on the Geotechnical Design Properties of a Stiff, Overconsolidated Clay*, Ph.D. Thesis, Faculty of Engineering, The University of Adelaide, Australia.

Jaksa, M. B., and Kaggwa, W. S., and Brooker, P. I. (1993). "Geostatistical Modelling of the Undrained Shear Strength of a Stiff, Overconsolidated, Clay." *Proceedings of*

Conference of Probalilistic Methods in Geotechnical Engineering, Canberra, A. A. Balkema, Rotterdam, 185-194.

Jaksa, M. B., Brooker, P. I., and Kaggwa, W. S. (1997). "Inaccuracies Associated with Estimating Random Measurement Errors." *Journal of Geotechnical and Geoenvironmental Engineering*, ASCE, Vol. 123, No. 5, 393-401.

Jaksa, M. B. and Kaggwa, W. S. (1992). "Degree of Saturation of the Keswick Clay Within the Adelaide City Area Above the General Groundwater Table." *Proceedings 6th Australia New Zealand Conf. on Geomechanics*, Christchurch, 336-341.

Keaveny, J. M., Nadim, F., and Lacasse, S. (1989). "Autocorrelation Functions for Offshore Geotechnical Data." *Proceedings of the Fifth International Conference on Structural Safety and Reliability*, Vancouver, B. C., Vol. 1, 263-270.

Konya, C. J. and Water, E. J. (1990). *Surface Blast Design*, Prentice Hall, Inc., Englewood Cliffs, NJ.

Kulatilake, P. H. S. W. and Ghosh, A. (1988). "An Investigation into Accuracy of Spatial Variation Estimation Using Static Cone Penetrometer Data." *Proceedings of the First International Conference on Penetration Testing*, Orlando, FL, 815-821.

Kulathilake, P. H. S. W. and Um, J. G. (2003). "Spatial Variation of Cone Tip Resistance for the Clay Site at Texas A&M University." *Geotechnical and Geological Engineering*, Vol. 21, 149–165.

Kulhawy, F. H., Birgisson, B., and Grigoriu, M. D. (1992). *Reliability-based Foundation Design for Transmission Line Structures: Transformation Models for In Situ Tests*, Electric Power Research Institute, Palo Alto, California, Report EL-5507(4).

Kulhawy, F. H. and Mayne, P. W. (1990). *Manual for Estimating Soil Properties for Foundation Design*, Report EL-6800, EPRI, Palo Alto.

Kulhawy, H., Roth, N. J. S., and Grigoriu, N. B. (1991). "Some Statistical Evaluations of Geotechnical Properties." *Proceedings of the 6th International Conference on Applications of Statistics and Probability in Soil and Structural Engineering VI ICASP*, Mexico City, 705-712.

Kulhawy, F. H. and Trautmann, C. H. (1996). "Estimation of In-Situ Test Uncertainty."

Uncertainty in the Geologic Environment: From Theory to Practice, C. D. Shackelford, P. P. Nelson, M. J. S. Roth, eds. ASCE, 269-286.

Lacasse, S. and de Lamballerie, J. Y. N. (1995), "Statistical Treatment of CPT Data." *International Symposium on Cone Penetration Testing, Linkoping*, Sweden, 369-380.

Lacasse, S., and Nadim, F. (1996), "Uncertainties in Characterizing Soil Properties." *Uncertainty in the Geologic Environment, From Theory to Practice, Proceeding of Uncertainty '96*, Geotechnical Special Publication No. 58.

Larsson, R. and Mulabdic, M. (1991). *Piezocone Tests in Clay*, Report No. 42, Swedish Geotechnical Institute, AB Ostgotatryck, Linkoping.

Law, J. (1944). "A Statistical Approach to the Interstitial Heterogeneity of Sand Reservoirs." *Transactions of the AIME*, Vol. 155, 202-222.

Lumb, P. (1966). "The Variability of Natural Soils." *Canadian Getechnical Journal*, Vol. 3, No. 2, 74-97.

McCord, J. T., Stephens, D. B., and Wilson, J. L. (1991). "Toward Validating State-Dependent Macroscopic Anisotropy in Unsaturated Media: Field Experiments and Modeling Condiderations." *Journal of Contaminant Hydrology*, Vol. 7, No. 1-2, 145-175.

Masood, T. and Mitchell, J. K. (1993). "Estimation of In-Situ Lateral Stresses in Soils by Cone Penetration Test." *Journal of Geotechnical Engineering*, ASCE, Vol. 119, No. 10, 1624-1639.

Marr, S. A., Gilbert, R. B., and Rauch, A. F. (2004). "A Practical Method for Predicting Expansive Soil Behavior." *Geotechnical Special Publication*, No. 126 I, Geotechnical Engineering for Transportation Projects: Proceedings of Geo-Trans 2004 1144-1152.

Masala, S. and Biggar, K. (2003). "Geotechnical Virtual Laboratory: I. Permeability." *Computer Applications in Engineering Education*, Vol. 11, 132-143.

Matheron, G. (1963). "Principles of Geostatistics." *Economic Geology*, Vol. 58, 1246-1266.

Matheron, G. (1973). “The Intrinsic Random Functions and Their Applications.” Advances in Applied Probability, Vol. 5, 439-468.

Mantoglu, A. and Wilson, J. L. (1981). “Simulation of Random Fields with the Turning Bands Method.” Report No. 264, Department of Civil Engineering, MIT, Cambridge, MA.

Mayne, P.W. (1995). "Profiling Yield Stress in Clays by In-Situ Tests." *Transportation Research Record 1479*, National Academy Press, Washington, D.C, 43-50.

Mayne, P. W. and Kemper, J. B., Jr. (1988). "Profiling OCR in Stiff Clays by CPT and SPT." *Geotechnical Testing Journal*, ASTM, Vol. 11, No. 2, 139-147.

Mesri, G. (1975). Discussion of “New Design Procedures for Stability of Soft Clays.” *Journal of Geotechnical Engineering*, ASCE, Vol. 99, No. SM1, 123-137.

Morineau, T., Gorzerino, P, and Papin, J. P. (1997). “Virtual Environment: for Learning or for Training? A Cognitive Approach.” in *Virtual Reality, Training’s Future? Perspectives on Virtual Reality and Related Emerging Technologies*, Proceedings of a NATO Defense Research Group Panel 8, Research Study Group 16 Workshop on Advanced Technologies Applied to Training Design, Portsmouth, England.

Nadim, F. (1988). “Geotechnical Site Description Using Stochastic Interpolation.” *Norwegian Geotechnical Institute*, No. 176, 1-4.

Nagaraj, T. and Murty, B. R. S. (1985). “Prediction of the Preconsolidation Pressure and Recompression Index of Soils.” *Geotechnical Testing Journal*, Vol. 8, No. 4, 199-202.

Narin van Court, W. A. and Mitchell, J. K. (1994). “Soil Improvement by Blasting.” *Journal of Explosives Engineering*, Vol. 12, No. 3, 34-41.

Navarro, E. O. and van der Hoek, A. (2005). “Software Process Modeling for an Educational Software Engineering Simulation Game.” *Software Process: Improvement Practice*, Vol. 10, 311–325.

NAVFAC DM-7.1 (1982). *Soil Mechanics Design Manual 7.1*, Department of the Navy, Naval Facilities Engineering Command, Alexandria, Virginia.

Ng, K. W., Chang, T. S., and Hwang, H. M. (1989). “Subsurface Conditions of Memphis and Shelby County.” *NCEER technical report NCEER-89-0021*.

Novak, G. A. (1999). "Virtual Courseware for Geoscience Education: Virtual Earthquake and Virtual Dating." *Computers and Geosciences*, Vol. 25, 475-488.

Olsen, P. E., Froelich , A. J., Daniels, D. L., Smoot, J. P., and Gore, P. J. W. (1991). "Rift Basins of Early Mesozoic Age." *The Geology of the Carolinas*, The University of Tennessee Press:Knoxville, Tennessee, 42-170.

Op den Bosch, A. and Baker, N. (1994). "Simulation of Construction Operations in Virtual Interactive Environments." *Journal of Computing in Civil Engineering*, 1435-1442.

Parsons, R. L. and Frost, J. D. (2002). "Evaluating Site Investigation Quality Using GIS and Geostatistics." *Journal of Geotechnical and Geoenvironmental Engineering*, ASCE. Vol. 128, No. 6. 451-461.

Pennell, R., Durham, M., Ozog, C., and Spark, A. (1997). "Writing in Context: Situated Learning on the Web." *Proceedings of 14th Annual ASCILITE Conference*, The Australasian Society for Computers in Learning in Tertiary Education, Perth, Western Australia, 463–469.

Penumadu, D., Zhao, R., and Frost, D. (1997). "Geotechnical Test Simulator." *Proceedings of 14th International Conference on Soil Mechanics and Foundation Engineering*, Hamburg, Vol. 3, 2109-2022.

Petersen, M., Brand, S., Roldan, R., and Sommerfeld, G. (1999). "Residual Soil Characterization for a Power Plant." *Geotechnical Special Publication*, ASCE, No. 92, 26-42.

Phoon, K. K. and Kulhawy, F. H. (1996). "On Quantifying Inherent Soil Variability." *Uncertainty in the Geologic Environment (GSP58)*, ASCE, New York, 326–340..

Phoon, K. K. and Kulhawy, F. H. (1999a). "Characterization of Geotechnical Variability." *Canadian Geotechnical Journal*, Vol. 36, 612-624.

Phoon, K. K. and Kulhawy, F. H. (1999b). "Evaluation of Geotechnical Property Variability." *Canadian Geotechnical Journal*, Vol. 36, 625-639.

Phoon, K. K., Quek, S. T., and An, P. (2003). "Identification of Statistically Homogeneous Soil Layers Using Modified Bartlett Statistics." *Journal of*

Geotechnical and Geoenvironmental Engineering, ASCE, Vol. 129, No. 7, 649-659.

Rendon-Herrero, O. (1983). Discusstion of "Universal Compression Index Equation." *Journal of Geotechnical Engineering*, ASCE, Vol. 109, No. 10, 1349.

Rendu, J. M. (1981). "An Introduction to Geostatistical Methods of Mineral Exploration." *South African Institute of Mineral and Metallurgy*, Johannesburg, South Africa.

Reyna, F. and Chameau, J. L. (1991). "Dilatometer Based Liquefaction Potential of Sites in the Imperial Valley." *Proc. 2nd Int. Conf. on Recent Adv. in Geot. Earthquake Engrg. and Soil Dyn.*, St. Louis, 385-392.

Rezaei, A. and Katz, L. (1998). "A Cognitive Model for Conceptual Change in Science Instruction with a Focus on Educational Software Development." *Journal of Educational Computing Research*, Vol. 19, No. 2, 155-174.

Rix, G. J. and Romero-Hudock, S. (2006). "Liquefaction Potential Mapping in Memphis and Shelby County, Tennessee." *Earthquake Spectra*, p27.

Robertson, P.K. and Campanella, R.G. (1983). "Interpretation of Cone Penetration Tests: Part I - Sands; Part II – Clays." *Canadian Geotechnical Journal*, Vol. 20, No. 4, 719-745.

Robertson, P. K., Campanella, R. G., Gillespie, D., and Greig, J. (1986). "Use of Piezometer Cone Data: Use of In-Situ Tests in Geotechnical Engineering." *Geotechnical Special Publication No. 6*, ASCE, Reston, VA., 1263-1280.

Rojas, E. M. and Mukherjee, A. (2005). "General-Purpose Situational Simulation Environment for Construction Education." *Journal of Construction Engineering and Management*, Vol. 131, No. 3, 319–329.

Santamarina, J. C. and Fratta, D. (1998). *Introduction to Discrete Signals and Inverse Problems in Civil Engineering*, ASCE Press, Reston, VA.

Schmertmann, J. H. (1975). "Measurement of In Situ Shear Strength: State of the Art Report." *Proceedings of ASCE Conf. on In Situ Measurements of Soil Properties*, Raleigh, North Carolina, Vol. 2, 57-138.

Sharma, S. and Hardcastle, J. H. (2001). "Computer Based Instruction for Consolidation Testing." *Proceedings, 36th Annual Symposium on Engineering Geology and Geotechnical Engineering*, Las Vegas, Nevada, March 28-30.

Sharp, H. and Hall, P. (2000). "An Interactive Multimedia Software House Simulation for Postgraduate Software Engineers." *Proceedings of the 22nd International Conference on Software Engineering*, ACM, Limerick, Ireland, 688–691.

Shimobe, S. and Moroto, N. (1995). "A New Classification Chart for Sand Liquefaction." *Proceedings of 1st International Conference on Earthquake Geotechnical Engineering*, Tokyo, Vol. 1, 315-320.

Solymar, Z.V. (1984). "Compaction of Alluvial Sands by Deep Blasting," *Canadian Geotechnical Journal*, Vol. 21, No. 2, 305-321.

Soulie, M., Montes, P., and Silvestri, V. (1990). "Modelling Spatial Variability of Soil Parameters." *Canadian Geotechnical Journal*, Vol. 27, 617-630.

South Carolina Emergency Preparedness Division (2001). *Comprehensive Seismic Risk and Vulnerability Study for the State of South Carolina*, 51-D0111027.00.

South Carolina Emergency Preparedness Division (2007). *South Carolina Hazard Mitigation Plan: Section 3: State Profile* (http://www.scemd.org/Plans/miti_plan.html)

Sowers, G. F. (1963). "Engineering Properties of Residual Soils Derived from Igneous and Metamorphic Rocks." *Proceedings of 2nd Panamerican Conference on Soil Mechanics And Foundation Engineering*, San Paulo, Brazil.

Sowers, G. B. and Sowers, G. F. (1970). *Introductory Soil Mechanics and Foundations*, Macmillan, New York.

Sowers, G. F. (1979). *Introductory Soil Mechanics and Foundations: Geotechnical Engineering*, Macmillan, New York.

Sowers, G. F., and Richardson, T. L. (1983). "Residual Soils of Piedmont and Blue Ridge." *Transportation Research Record 919*, Transportation Research Board, Wanshington, D. C.

Studer, J. and Kok, L. (1980). "Blast-Induced Excess Porewater Pressure and Liquefaction. Experience and Application." *Microstructural Science*, Vol. 2, 581-593.

Tang, W. H. (1979). "Probabilistic Evaluation of Penetration Resistance." *Journal of Geotechnical Engineering*, ASCE, Vol. 105, No. 10, 1173-1191.

Terzaghi, K. and Peck, R. B. (1967). *Soil Mechanics in Engineering Practice*, John Wiley & Sons, Inc., New York.

Townsend, F. C. (1985). "Geotechnical Characteristics of Residual Soils." *Journal of Geotechnical Engineering*, ASCE, Vol. 111, No. 1, 77-94.

Ural, D. N. (1996). "Spatial Variability of Soil Parameters." *Uncertainty in the Geologic Environment: from Theory to Practice, Proceedings of Uncertainty '96*, Madison, Wisconsin, 341-352.

U.S. Navy (1971). *Soil Mechanics, Foundations, and Earth Structures*, NAVFAC Design Manual DM-7, Washington, D.C.

U.S. Army Corps of Engineers (2001*). Engineering and Design: Geotechnical Investigations*, Department of the Army. Washington, D.C.

Uzielli, M., Vannucchi, G., and Phoon, K. K. (2005). "Random Field Characterisation of Stress-Normalised Cone Penetration Testing Parameters." *Geotechnique*, Vol. 55, No. 1, 3-20.

Vanmarcke, E. H. (1983). *Random Fields: Analysis and Synthesis*, MIT Press.

Vanmarcke, E. H. (1977). "Probabilistic Modeling of Soil Profiles." *Journal of Geotechnical Engineering*, ASCE, Vo. 103, No. 11, 1227-1246.

Willmer, J. L., Futrell, G. E., and Langfelder, J. (1982). "Settlement Predictions in Piedmont Residual Soils." *Proceedings of Conference on Engineering and Construction in Tropical and Residual Soils*, Honolulu, Hawaii, 629-646.

Winkler, T., Mitchell, R., and Venegas, J. G. (2005). "Computer Simulation and a Realistic Simulator in Conjunction with the New Educational Style How People Learn (HPL) to Improve Learning Achievements." *Proceedings of the 2005 ASEE Annual Conference and Exposition*, 2087-2092.

Wu, T. H. (1974). "Uncertainty, Safety, and Decision in Soil Engineering." *Journal of Geotechnical Engineering*, ASCE, Vol. 100, No. 3, 329-348.

Wyatt, T. R. and Macari, E. J. (1998). "Learner-Centered Educational Software for Constitutive Modeling of Soils." *Proceedings of the 1999 ASEE Annual Conference and Exposition*, Charlotte, NC.